

**NOVEL SUSTAINABLE SOLVENTS FOR BIOPROCESSING  
APPLICATIONS**

A Thesis  
Presented to  
The Academic Faculty

by

Michelle Kimberly Kassner

In Partial Fulfillment  
of the Requirements for the Degree  
Doctor of Philosophy in the  
School of Chemical and Biomolecular Engineering

Georgia Institute of Technology  
December 2008

# NOVEL SUSTAINABLE SOLVENTS FOR BIOPROCESSING APPLICATIONS

Approved by:

Dr. Charles A. Eckert, Co-Advisor  
School of Chemical and Biomolecular  
Engineering  
*Georgia Institute of Technology*

Dr. Charles L. Liotta, Co-Advisor  
School of Chemistry and Biochemistry  
*Georgia Institute of Technology*

Dr. Andreas S. Bommarius  
School of Chemical and Biomolecular  
Engineering  
*Georgia Institute of Technology*

Dr. Facundo M. Fernández  
School of Chemistry and Biochemistry  
*Georgia Institute of Technology*

Dr. Hang Lu  
School of Chemical and Biomolecular  
Engineering  
*Georgia Institute of Technology*

Date Approved: November 5, 2008

*To my parents, who have always led by example, and who have taught me that every goal is achievable when you give your best effort.*

*To Jimmy, for making my world a better place.*

## ACKNOWLEDGEMENTS

I would like first to thank my advisors, Dr. Charles Eckert and Dr. Charles Liotta. My research skills and professional development have been invaluable influenced by their guidance and contributions. Dr. Eckert gave me the opportunity to focus on research that specifically interested me, whether funded or not. Dr. Liotta's enthusiasm for research is unparalleled, and I appreciate the opportunities I had to work closely with the chemists. I would also like to thank my other committee members: Dr. Andreas Bommarius, Dr. Facundo Fernández, and Dr. Hang Lu. Collaborating with Dr. Bommarius and Dr. Fernández enhanced my knowledge of other fields and improved my laboratory skills. Additionally, I would like to thank the American Pacific Corporation, and specifically Kent Richman, for funding and research guidance.

This research group is highly collaborative and my successes belong in part to each person in the group influencing my research and being a wonderful friend. I would like to thank all members of the Eckert-Liotta research group, both past and present. Specifically, I would like to thank Dr. Reagan Charney for sharing an office and working on two projects with me. I would also like to thank Dr. Liz Hill for helping me join the group, Dr. Megan Donaldson for her constant advice, Tori Blasucci for her assistance through our shared experiences as classmates, and Deborah Babykin for all of her administrative help.

Our post-docs, including Dr. Pam Pollet, Dr. Beth Cope, Dr. Veronica Llopis-Mestre, Dr. Jie Lu, Dr. Jason Hallett, and Dr. Chris Kitchens, provided me with invaluable assistance over the years. I would also like to thank Dr. Mélanie Hall from the

Bommarius group and Wai Keen Chung from Rensselaer Polytechnic Institute for his advice with instrumentation. I was also fortunate to work with talented undergraduates at Georgia Tech. Special thanks to them for their excellent research and contributions to this thesis: Stuart Terrett, Kierston Shill, Paul Nielsen, Anne Talley, Raymond Oxendine, Megan Shenstone, Sarah Lencenski, and Kyle Manning.

Many friends outside the group have always been there for me. I would like to thank Janna Blum, Krystle Chavez, Dr. Stephanie Barthe, and Angel Olivera-Toro for their friendship while at Georgia Tech. Special thanks to Melanie Webb, Dr. Scott McAllister, Dr. Alison Gillies, and Dr. Barclay Satterfield for continued friendship and support after my Princeton years. Additional thanks to Jennifer Servi, Courtney Pearce, Jonathan Vroom, Patrick Renckly, Dr. D’Arcy Collins, Peter Ercius, Siân Kleindienst, and Dr. Carrie Bedient for long years of friendship and support.

I am most thankful, however, for the amazing support of my family. Their faith and love never wavered, even during difficult times. Thank you so much Mom, Dad, Amy, Kevin, Grandma and Grandpa Underhill, Grandma and Grandpa Kassner, and all of my aunts, uncles, cousins, and extended family. Finally, I would like to thank my fiancé Jimmy Young for his constant love, companionship, and support. His presence in my life is more special than I can describe. I love you all dearly.

# TABLE OF CONTENTS

ACKNOWLEDGEMENTS .....	IV
LIST OF TABLES .....	XII
LIST OF FIGURES .....	XIII
LIST OF ABBREVIATIONS .....	XX
LIST OF SYMBOLS .....	XXIV
SUMMARY .....	XXV
CHAPTER 1: INTRODUCTION .....	1
CHAPTER 2: APPLICATION OF A KINETIC STUDY TO A SMALL SCALE CONTINUOUS REACTOR TO PRODUCE (1-BENZYL-3-DIAZO-2-OXO- PROPYL)-CARBAMIC ACID ISOPROPYL ESTER, A DIAZOKETONE PHARMACEUTICAL INTERMEDIATE .....	5
INTRODUCTION .....	5
BACKGROUND .....	6
Benefits of Using Continuous Flow Reactors .....	6
Potential Applications of (1-Benzyl-3-chloro-2-hydroxy-propyl)-carbamic acid tert-butyl ester .....	7
Trimethylsilyl Diazomethane .....	8
EXPERIMENTAL .....	9
Materials .....	9
Methods .....	15
RESULTS AND DISCUSSION .....	40
Optimize Model Reaction for Use in Continuous Flow Reactor .....	40
Calibration for Batch Reaction Results .....	42
Design and Use of 1 <sup>st</sup> Generation Continuous Flow Reactor .....	44
Design and Use of 2 <sup>nd</sup> Generation Continuous Flow Reactor .....	46
Design and Use of 3 <sup>rd</sup> Generation Continuous Flow Reactor .....	53
Coiled Continuous Flow Reactor .....	67
CONCLUSIONS AND RECOMMENDATIONS .....	75
REFERENCES .....	77

CHAPTER 3: SWITCHABLE SOLVENTS FOR THE PRETREATMENT OF LIGNOCELLULOSIC BIOMASS .....	79
INTRODUCTION .....	79
BACKGROUND.....	79
Lignocellulosic Biomass.....	79
Pretreatment Rationale.....	83
Near-Critical Water with CO <sub>2</sub> .....	84
Organic Acid-Enhanced CO <sub>2</sub> .....	86
Sulfones (Piperylene Sulfone and Butadiene Sulfone).....	89
Experimental Considerations for Each Pretreatment.....	93
EXPERIMENTAL.....	94
Materials .....	94
Instrumentation .....	96
Methods.....	96
RESULTS AND DISCUSSION.....	106
CO <sub>2</sub> -Enhanced Near Critical Water .....	106
Organic Acid-Enhanced CO <sub>2</sub> .....	110
Sulfone .....	113
CONCLUSIONS AND RECOMMENDATIONS.....	118
CO <sub>2</sub> -Enhanced NCW .....	119
Organic Acid-Enhanced scCO <sub>2</sub> .....	120
Sulfone .....	121
REFERENCES .....	122
CHAPTER 4: EMPLOYING SUPERCRITICAL FLUID CHROMATOGRAPHY FOR GREEN METABOLOMICS .....	125
INTRODUCTION .....	125
BACKGROUND.....	126
Metabolites.....	126
SFC .....	126
Improving SFC for Metabolomics.....	127
Project Goals.....	129

EXPERIMENTAL.....	130
Materials .....	130
Analysis.....	138
RESULTS AND DISCUSSION.....	139
Rebuilding the SFC.....	139
Silylation of Amino Acids .....	143
Preliminary Results.....	147
Co-solvents in scCO <sub>2</sub> .....	158
CONCLUSIONS AND RECOMMENDATIONS.....	164
REFERENCES .....	166
CHAPTER 5: CONCLUSIONS AND RECOMMENDATIONS.....	168
INTRODUCTION .....	168
CONTINUOUS FLOW REACTOR .....	168
Hydrochloric Acid Hydrolysis.....	169
Carbohydrate Reactions in Continuous Flow Reactors .....	170
BIOMASS PRETREATMENT.....	171
CO <sub>2</sub> -Enhanced NCW .....	171
Piperylene Sulfone.....	172
SUPERCRITICAL FLUID CHROMATOGRAPHY FOR METABOLOMICS.....	173
ALTERNATIVE SOLVENTS FOR CELLULOSE DISSOLUTION.....	173
Designing New Cellulose Solvents.....	174
Enhancing Enzymatic Stability in Alternative Solvents.....	174
COFACTOR STABILITY IN ORGANIC-AQUEOUS SOLVENTS .....	175
REFERENCES .....	176
APPENDIX A: CELLULOSE SOLUBILITY AND IMPACT ON CRYSTALLINITY IN ALTERNATIVE SOLVENTS.....	178
INTRODUCTION .....	178
BACKGROUND.....	179
Enzymatic Hydrolysis of Cellulose to Glucose .....	179
Importance of Cellulose Dissolution .....	180
Ionic Liquids .....	181
Deep Eutectic Solvents .....	182
Tetra-Alkyl Ammonium Ionic Liquids.....	185



EXPERIMENTAL.....	187
Materials .....	187
Methods.....	192
RESULTS AND DISCUSSION.....	195
Improved Hydrolysis of Amorphous Cellulose .....	195
DES Studies .....	197
IL Studies.....	202
Path Forward.....	205
CONCLUSIONS AND RECOMMENDATIONS.....	205
REFERENCES .....	207
APPENDIX B: COFACTOR STABILITY IN ORGANIC-AQUEOUS SOLVENTS..	209
INTRODUCTION .....	209
BACKGROUND.....	209
Benefits of Biocatalysis .....	209
Organic-Aqueous Tunable Solvents (OATS).....	210
Enzymatic Cofactors.....	213
OATS with Cofactors .....	215
Cofactor Stability .....	216
Capillary Electrophoresis.....	218
EXPERIMENTAL.....	220
Materials .....	220
Method .....	221
RESULTS AND DISCUSSION.....	223
Cofactor Stability in MOPS pH 7.0 .....	223
Cofactor Stability in Phosphate Buffer pH 7.8 .....	227
Cofactor Stability in a Acetonitrile / Phosphate Buffer pH 7.8 Mixture .....	231
CONCLUSIONS.....	234
REFERENCES .....	235
APPENDIX C: PRODUCTION OF HIGH VALUE-ADDED CHEMICALS FROM CARBOHYDRATES USING PIPERYLENE SUFLONE.....	237
INTRODUCTION .....	237
BACKGROUND.....	238

EXPERIMENTAL.....	241
Materials .....	241
Methods.....	241
RESULTS AND DISCUSSION.....	241
Fructose.....	242
CONCLUSIONS AND RECOMMENDATIONS.....	243
REFERENCES .....	244
<b>APPENDIX D: OXIDATION OF CARBOHYDRATE STARTING MATERIALS TO GLUCARIC ACID AND OTHER TARGET OXIDATION PRODUCTS.....</b>	
INTRODUCTION .....	245
BACKGROUND.....	245
EXPERIMENTAL.....	250
Materials .....	250
Method .....	250
RESULTS AND DISCUSSION .....	251
Glucose Oxidation .....	251
Additional Monosaccharide Oxidation.....	251
CONCLUSIONS AND RECOMMENDATIONS.....	252
REFERENCES .....	253
<b>APPENDIX E: EXAMINING GAS-EXPANDED LIQUIDS AS A POSSIBLE LIGNOCELLUSIC PRETREATMENT .....</b>	
INTRODUCTION .....	254
BACKGROUND.....	255
Gas-Expanded Liquids.....	255
Biomass Extractives.....	257
EXPERIMENTAL.....	258
Materials .....	258
Methods.....	258
RESULTS AND DISCUSSION.....	261
Woodchip Extractives.....	261
Biomass Pretreatments.....	264
CONCLUSIONS AND RECOMMENDATIONS.....	269
REFERENCES .....	270

APPENDIX F: ACID-CATALYZED BIODIESEL PRODUCTION USING GAS- EXPANDED LIQUIDS .....	272
INTRODUCTION .....	272
BACKGROUND.....	273
EXPERIMENTAL.....	276
Materials .....	276
Methods.....	276
RESULTS AND DISCUSSION.....	277
CONCLUSIONS AND RECOMMENDATIONS.....	281
REFERENCES .....	281
VITA.....	282

## LIST OF TABLES

Table 2.1: Pump settings and reactant ratios using hydrocarbon trace.....	25
Table 2.2: Flow rate optimization for the two-tubular reactor system. ....	32
Table 2.3: Flow rate optimization for the four-tubular reactor system.....	33
Table 2.4: Temperature optimization for the four-tubular reactor system.....	34
Table 2.5: Excess isobutylchloroformate optimization for the four-tubular reactor system. ....	35
Table 2.6: Experimental paramters for 2 <sup>nd</sup> generation continuous flow reactor (Runs 1-5). ....	48
Table 2.7: Experimental conditions for 2 <sup>nd</sup> generation continuous flow reactor. The best result provided 2% isolated yield (583 cm length). ....	52
Table 2.8: Variables changed during optimization of the diazoketone reaction.....	70
Table 3.1: Solvent characterization and comparison of DMSO and PS. <sup>24</sup> .....	91
Table 3.2: Dry weight composition (%) of selected lignocellulosic biomass feedstock <i>Note:</i> Numbers do not sum to 100% because minor components are not listed.....	94
Table A.1: Molar ratios of DES mixtures.....	193
Table B.1: Results of cofactor stability studies completed by Liz Hill using UV spectrometry (results not published).....	217
Table D.1: Top 12 building blocks identified by the US DOE. <sup>2</sup> .....	246
Table E.1: Extractive components recovered from wood chips with GX-MeOH (40 °C, 17.4 bar, 3 days), MeOH only (ambient temperature and pressure, 3 days) and GX-MeOH (40 °C, 17.4 bar, 24 hours).....	262
Table E.2: Dry weight composition (%) of selected lignocellulosic biomass feedstock as reported by Mosier et al. <sup>19</sup> .....	265
Table E.3: Comparison of extractive composition as reported in literature and compared to chemical analysis completed in lab for three different treatments.....	268
Table F.1: Reaction conditions for each set of experiments.....	277

## LIST OF FIGURES

Figure 2.1: Synthetic route previously used in industry. <sup>8</sup> .....	8
Figure 2.2: Diazoketone synthesis from L-boc-phenylalanine. <sup>11</sup> .....	9
Figure 2.3: Reaction using triethylamine as the HCl scavenger followed by a benzylamine quench.....	11
Figure 2.4: Modified reaction using a benzylamine quench instead of continuing to the diazomethane second step.....	41
Figure 2.5: GC-MS spectrum of the sample containing a decane standard, benzylamine, and (1-benzylcarbamoyl-2-phenyl-ethyl)-carbamic acid tert-butyl ester product.....	43
Figure 2.6: Picture of the 1st generation continuous flow reactor.....	45
Figure 2.7: Picture of the 2nd generation continuous flow reactor.....	47
Figure 2.8: Specifications of the 2nd generation continuous flow reactor. ....	47
Figure 2.9: Batch reaction product appearance and starting material disappearance over time (-30 °C, 0.04 M reactants).....	51
Figure 2.10: Batch reaction isolated yields obtained over time (0.75M, -30 °C). ....	51
Figure 2.11: Photo of 3rd generation continuous flow reactor. ....	54
Figure 2.12: Schematic of the initial 3rd generation continuous flow reactor.....	54
Figure 2.13: 3rd generation continuous flow reactor isolated yield results at various temperatures (5 second residence time).....	56
Figure 2.14: Schematic of the 3rd generation continuous flow reactor with increased tubing length to 720 cm. ....	57
Figure 2.15: Optimize pumps by flow rate ratios using a hydrocarbon trace.....	58
Figure 2.16: Schematic of the one-tubular reactor 3rd generation continuous flow reactor. ....	60
Figure 2.17: Schematic of the two-tubular reactor 3rd generation continuous flow reactor. ....	62

Figure 2.18: Effect of flow rate on isolated yield in two-tubular reactors continuous flow reactor system at room temperature.....	63
Figure 2.19: Schematic of the four-tubular reactor 3rd generation continuous flow reactor. ....	64
Figure 2.20: Effect of flow rate on isolated yield with four-tubular reactor continuous flow reactor system at room temperature. ....	65
Figure 2.21: Effect of temperature on the isolated yield with four-tubular reactor continuous flow reactor system at 0.2 mL/min flow rate. ....	65
Figure 2.22: Schematic of coiled continuous flow reactor using propylamine quench.....	68
Figure 2.23: Photograph of the coiled continuous flow reactor.....	68
Figure 2.24: Diazoketone synthesis using trimethylsilyl diazomethane.....	69
Figure 2.25: Diazoketone synthesis with reactants used for batch reactions.....	71
Figure 2.26: Diazoketone reaction over time for 0.2 M reactant concentration. Results analyzed by LC-UV. ....	73
Figure 2.27: Schematic of the two-coiled continuous flow reactor system. The diazoketone product is formed in the second reactor.....	74
Figure 3.1: Cellulose structure.....	81
Figure 3.2: Representative structure of hemicellulose.....	81
Figure 3.3: Representative structure of lignin.....	82
Figure 3.4: Schematic of pretreatment goals. <sup>5</sup> ....	84
Figure 3.5: Reaction of CO <sub>2</sub> with water to form carbonic acid. ....	85
Figure 3.6: Effect of CO <sub>2</sub> on the pH of water. <sup>15</sup> ....	86
Figure 3.7: Structures of formic acid (left) and acetic acid (right). ....	87
Figure 3.8: Supercritical phase boundary for a binary mixture of CO <sub>2</sub> and acetic acid. <sup>22</sup> ....	88
Figure 3.9: Supercritical phase boundary for a binary mixture of CO <sub>2</sub> and formic acid. <sup>22</sup> ....	88
Figure 3.10: Retro-chelotropic reaction of piperylene sulfone. ....	89
Figure 3.11: In-situ formation of sulfurous acid. ....	90

Figure 3.12: Retro-chelotropic reaction of butadiene sulfone. ....	91
Figure 3.13: Methylol cellulose formation in DMSO/formaldehyde solvent. ....	92
Figure 3.14: Titanium reactor setup with heating block apparatus. Illustration modified from E. Newton M.S. thesis. <sup>30</sup> .....	97
Figure 3.15: Experimental setup of Parr high-pressure reactor. Modified from L. Draucker Ph.D. thesis. <sup>34</sup> .....	100
Figure 3.16: Flowchart for full analysis of lignocellulosic biomass.....	104
Figure 3.17: % Monosaccharides recovered from pure cellulose and xylan (NCW at 200 °C).....	107
Figure 3.18: Change in carbohydrate concentration between NCW and NCW+CO <sub>2</sub> for pine wood chips (150 °C, 1000 psi, 20 min).....	109
Figure 3.19: Change in carbohydrate concentration between NCW and NCW+CO <sub>2</sub> for switchgrass (200 °C, 2000 psi, 30 min).....	109
Figure 3.20: SEM images (400x) of untreated corn stover (left) and acetic acid-enhanced scCO <sub>2</sub> pretreated corn stover (right). ....	112
Figure 3.21: HPLC analysis of corn stover liquid process fraction after pretreatment with the formic acid-enhanced scCO <sub>2</sub> process (1500 psi, 1 h, 40 °C). ....	112
Figure 3.22: SEM images of untreated corn stover (left) and butadiene sulfone pretreated corn stover (right). ....	115
Figure 3.23: Frins reaction of piperylene and formaldehyde. <sup>38</sup> .....	117
Figure 3.24: Predicted solid product formation from the reaction of TBAF and PS.....	118
Figure 4.1: Synthesis of 1-[2-(4-chloromethyl-phenyl)-ethyl]-1,1,3,3,3- pentamethyldisiloxane with both isomers shown. ....	131
Figure 4.2: Reaction of cysteine with benzylchloride disiloxane. ....	132
Figure 4.3: Reaction of lysine with benzylchloride disiloxane.....	133
Figure 4.4: Synthesis of 2-amino-3-(methyl-diphenyl-silanyloxy)- propionic acid.....	134
Figure 4.5: Synthesis of 2-amino-3-(4-trimethylsilanyloxy-phenyl)-propionic acid methyl ester. ....	136
Figure 4.6: Synthesis of 3-[4-(tert-butyl-dimethyl-silanyloxy)-phenyl]-2- formylamino-propionic acid methyl ester.....	137

Figure 4.7: Initial reconstituted flow path of the SFC. ....	141
Figure 4.8: Structures of toluene (left), benzyl chloride (center), and acetophenone (right). ....	147
Figure 4.9: Structures of silylated tyrosine (left) and neutralized tryptophan (right). ....	149
Figure 4.10: Density and phase behavior of carbon dioxide at 40 °C. <sup>16</sup> .....	150
Figure 4.11: Schematic of the fiber optic UV-Vis flow cell. Design provided by Dr. Frank Bright (SUNY-Buffalo). ....	152
Figure 4.12: Structure of boc-phenylalanine. ....	153
Figure 4.13: UV-Vis spectrum of silylated tyrosine, boc-phenylalanine, and tryptophan in scCO <sub>2</sub> at 215 nm and 225 nm (2465 psi, 40 °C). ....	154
Figure 4.14: UV-Vis spectra of saturated silylated tyrosine in MeOH at 215 nm (2464 psi, 40 °C). ....	155
Figure 4.15: UV-Vis spectra of neutralized tryptophan (0.06 g/mL) in MeOH at 215 nm (2466 psi, 40 °C). ....	155
Figure 4.16: UV-Vis spectra of saturated boc-phenylalanine in MeOH at 215 nm (2468 psi, 40 °C). ....	156
Figure 4.17: UV-Vis spectra of concentrated silylated tyrosine (0.07 g/mL) in MeOH, and the first MeOH wash, at 225 nm (2467 psi, 40 °C). ....	157
Figure 4.18: UV-Vis spectra of diluted silylated tyrosine (0.035 g/mL) in MeOH, and two MeOH washes, at 225 nm (2465 psi, 40 °C). ....	158
Figure 4.19: Initial tryptophan peak (neutralized) followed by MeOH washes in scCO <sub>2</sub> and 20% MeOH co-solvent. ....	160
Figure 4.20: Initial tryptophan peak (neutralized) followed by MeOH washes in scCO <sub>2</sub> and 20% EtOH co-solvent. ....	161
Figure 4.21: Initial tryptophan peak (neutralized) followed by MeOH washes in scCO <sub>2</sub> and 20% trifluoroethanol co-solvent. ....	162
Figure 4.22: Hangover spectrum after trifluoroethanol co-solvent runs. ....	163
Figure A.1: Ionic liquid structures of [Bmim]Cl (top left), [Amim]Cl (top center), [Amim][OAc] (top right), [Bmpy]Cl (bottom left), and [Emim][OAc] (bottom right). ....	181
Figure A.2: Structures of choline chloride (left) and ethylammonium chloride (right). ....	183



Figure A.3: Structures of acetamide (top left), ethylene glycol (top middle), glycerol (top right), malonic acid (bottom left), and urea (bottom right).	184
Figure A.4: Structure of [Et <sub>3</sub> N-Glycol][acetate].	186
Figure A.5: Total synthesis of triethyl (2-(2-methoxyethoxy)ethoxy) ethylammonium acetate).	191
Figure A.6: Enzymatic hydrolysis of untreated and amorphous cellulose to glucose over 3.5 hours.	196
Figure A.7: Enzymatic hydrolysis of untreated and amorphous cellulose to glucose over 4 days.	196
Figure A.8: Crystallinity index of cellulose pretreated in choline chloride DESs.	198
Figure A.9: Crystallinity index of cellulose pretreated in ethylammonium chloride DESs.	200
Figure A.10: Enzymatic hydrolysis of untreated and EAC:U treated (120 °C) cellulose to glucose over 20 hours.	201
Figure A.11: Enzymatic hydrolysis of untreated and EAC:EG (80 °C) treated cellulose to glucose over 30 minutes.	201
Figure A.12: IR spectrum of solid formed from IL-cellulose mixture.	204
Figure B.1: OATS process schematic as depicted by E. Hill. <sup>6</sup>	211
Figure B.2: Model reaction for CAL B ester hydrolysis.	212
Figure B.3: Model chiral reaction for CAL B ester hydrolysis.	213
Figure B.4: Structures of the nicotinamide cofactors NAD <sup>+</sup> (left) and NADH (right).	214
Figure B.5: Ketoreductase reaction of 2-benzoylpyridine (2BP) to phenylpyridin-2-yl methanol (PPM) using KRED 101, coupled with GDH 103 to regenerate the cofactors.	215
Figure B.6: Calibration curve of NAD <sup>+</sup> in 100 mM MOPS pH 7.0 (254 nm). Concentrations range from 125 μM to 1 mM.	224
Figure B.7: Variation in peak area observed for NAD <sup>+</sup> in 100 mM MOPS pH 7.0 (254 nm). The data shows six subsequent samples taken within a 2 hour time span.	224
Figure B.8: Change in the ratio of NADH to thiourea over time.	227

Figure B.9: Separation of nicotinamide, NAD <sup>+</sup> , and NADH in 50 mM phosphate pH 7.8 (254 nm) using 20 kV applied voltage.....	228
Figure B.10: Decomposition of NAD <sup>+</sup> over time (50 mM phosphate pH 7.8, 25 °C). .....	229
Figure B.11: Decomposition of NADH over time (50 mM phosphate pH 7.8, 25 °C). .....	230
Figure B.12: Electropherogram of NAD <sup>+</sup> in a 50/50 vol mixture of acetonitrile (ACN) and 100 mM phosphate pH 7.8. ....	233
Figure C.1: HMF production from fructose.....	238
Figure C.2: Oxidation reaction of HMF to form to 2,5-furandicarboxylic acid. ....	238
Figure C.3: Production of HMF derivates from carbohydrate feedstock. ....	239
Figure C.4: Condensation reaction of HMF to form oxo-bis(5-methylfurfuraldehyde). ....	242
Figure D.1: Derivatives of Glucaric Acid. <sup>2</sup> .....	247
Figure D.2: Reactions of CO <sub>2</sub> with hydrogen peroxide.....	248
Figure D.3: Ionization Equilibrium of Peroxycarbonic Acid .....	249
Figure E.1: Qualitative comparison of GXLs to other solvent classes.....	255
Figure E.2: Two equilibria reactions of alkylcarbonic acids.....	256
Figure E.3: Percentage of components over time extracted from wood chips by GX-MeOH (40 °C, 26.6 bar).....	264
Figure E.4: Mass percent removed by GX-MeOH pretreatment for wood chips, corn stover, and switchgrass (60 °C, 30 bar, 24 h).....	265
Figure E.5: Solid wood chip composition after no treatment, treatment with GX-MeOH (60 °C, 30 bar, 24 hours), and treatment with GX-MeOH (30 °C, 40 bar, 3 hours). ....	266
Figure E.6: Solid corn stover composition after no treatment, treatment with GX-MeOH (60 °C, 30 bar, 24 hours), and treatment with GX-MeOH (30 °C, 40 bar, 3 hours). ....	266
Figure E.7: Solid switchgrass composition after no treatment, treatment with GX-MeOH (60 °C, 30 bar, 24 hours), and treatment with GX-MeOH (30 °C, 40 bar, 3 hours). ....	267

Figure F.1: Percent conversion of vinyl palmitate to methyl palmitate after 48 hours using differing amounts of CO <sub>2</sub> (75 °C, 15:1 molar ratio methanol to vinyl palmitate).....	279
Figure F.2: Percent conversion of vinyl palmitate to methyl palmitate after 4 hours using differing amounts of CO <sub>2</sub> (75 °C, 15:1 molar ratio methanol to vinyl palmitate).....	280

## LIST OF ABBREVIATIONS

A	Acetamide
ACN	Acetonitrile
AIDS	Acquired immune deficiency syndrome
AMPAC	American Pacific Corporation
<i>AMUSE</i>	Array of Micromachined UltraSonic ElectroSprays
BnNH <sub>2</sub>	Benzylamine
BS	Butadiene sulfone
(i)CAL A, B	<i>Candida antarctica</i> lipase A, B (immobilized)
<sup>13</sup> C NMR	Carbon-13 nuclear magnetic resonance spectroscopy
CE	Capillary electrophoresis
ChCl	Choline chloride
CMK	Chloromethylketone
CrI	Crystallinity index
CTFE	Chlorotrifluoroethylene
DCM	Dichloromethane
DES	Deep eutectic solvents
diH <sub>2</sub> O	Deionized water
DMF	<i>N-N</i> -Dimethyl formamide
DMSO	Dimethylsulfoxide
DNS	Dinitrosalicylic acid
DP	Degree of polymerization

DSC	Differential scanning calorimeter
DVDS-Pt	Platinum (0)-1,3-divinyl-1,1,3,3-tetramethyldisiloxane
EA	Elemental analysis
EAC	Ethylammonium chloride
EG	Ethylene glycol
ESI	Electrospray ionization
EtOAc	Ethyl Acetate
EtOH	Ethanol
FDCA	2,5-furandicarboxylic acid
FID	Flame ionization detector
G	Glycerol
GC	Gas chromatography
GDH	Glucose dehydrogenase
GPC	Gel permeation chromatography
GXL / GX-MeOH	Gas-expanded liquid / Gas-expanded methanol
<sup>1</sup> H NMR	Proton nuclear magnetic resonance spectroscopy
HMF	5-Hydroxymethylfurfural
HEPES	(2-hydroxyethyl)-1-piperazineethanesulfonic acid
HIV	Human immunodeficiency virus
HP	Hewlett-Packard
HPLC	High performance liquid chromatography
ILs	Ionic Liquids
IPA	Isopropyl alcohol

IR	Infrared spectroscopy
KRED	Ketoreductase
LC	Liquid chromatography
MA	Malonic acid
MeOH	Methanol
MMGBS	2-(2-(2-methoxyethoxy)ethyl benzenesulfonate
mp	Melting point
MOPS	3-morpholinopropane-1-sulfonic acid
MS	Mass spectrometer
NAD <sup>+</sup>	Nicotinamide adenine dinucleotide
NADH	Nicotinamide adenine dinucleotide disodium salt
NADP	Nicotinamide adenine dinucleotide phosphate
NADPH	Nicotinamide adenine dinucleotide phosphate-oxidase tetrasodium salt
NCW	Near critical water
NPT	Normal pipe threading
NREL	National Renewable Energy Laboratory
PASC	Phosphoric acid swollen cellulose
PS	Piperylene sulfone
psi	Pound per square inch
RID	Refractive index detector
RSD	Relative standard deviation
RT	Room temperature
scCO <sub>2</sub>	Supercritical carbon dioxide

SCFs	Supercritical fluids
SEM	Scanning electron microscopy
SFC	Supercritical fluid chromatography
SRS	Sugar recovery standard
TBAF	Tetrabutylammonium fluoride
TEA-HCl	Triethylamine-hydrochloride salt
TGA	Thermogravimetric analyze
THF	Tetrahydrofuran
TLC	Thin layer chromatography
Tris	Tris (hydroxymethyl) aminomethane
U	Urea
UV-Vis	Ultraviolet-visible spectroscopy

## LIST OF SYMBOLS

$\alpha$	H-bond donating ability
$\beta$	H-bond accepting ability
$\Delta P$	Pressure drop
$\epsilon$	Polarity measurement
$\mu$	Viscosity
$\pi^*$	Polarity/polarizability
$\Phi_s$	Sphericity of packing material
$D_p$	Diameter of packing material
$E_T(30)$	Polarity measurement
$L$	Length
$\bar{V}_o$	Linear fluid velocity



## SUMMARY

Bioprocessing applications are gaining importance in the traditional chemical industries. With environmental, political, and economical concerns growing, research efforts have recently focused on the substitution of petroleum-derived transportation fuels and materials. As possible products and feedstocks are being investigated, it is important to ensure the new processes are also sustainable. There are several aspects to developing sustainable processes: minimize waste, use environmentally-benign chemicals, find renewable feedstocks, and limit the number of processing steps.

This thesis examines ways to enhance the sustainability of bioprocesses. Novel, alternative solvent systems are studied and applied to a variety of bioprocesses. Downstream processing steps and waste can be minimized by designing systems that combine reactions and separations into one process unit. This is accomplished by designing new reactor systems and by replacing currently used solvents. Additional studies, involving analytical techniques that reduce the use of organic solvents, are tested and applied to industrial problems. Finally, new solvent systems are examined for potential processes using renewable carbohydrate feedstock.

## **CHAPTER 1: INTRODUCTION**

The priorities of traditional chemical industries have been shifting rapidly over the past decade. While profit is still the primary goal, a new emphasis has also been placed on the environmental impacts, political implications, and safety concerns of all processes. In order to alleviate negative environmental effects, focus has turned to minimizing waste, reducing energy consumption, and removing process units whenever possible. The dwindling petroleum resources, environmental concerns, and political implications have forced a closer examination of sustainable materials, such as carbohydrates from plant materials, as feedstock for the production of transportation fuels, plastics, synthetic fibers, lubricants, dyes, and other every day materials. The emphasis placed on safety in the workplace has also caused many processes to be redeveloped in order to use less hazardous materials, substitute toxic solvents, and employ more environmentally benign chemicals.

Bioprocesses are becoming more common as the traditional chemical processes are redeveloped. Bioprocessing applications, which combine knowledge from chemistry, chemical engineering, biochemistry, and biology, are widespread. They include the production of biofuels, the design and operation of enzymatic or fermentation systems, the manufacture of pharmaceuticals, and the development of new analytical techniques for identifying biological compounds. Many new processes, and ones being modified to meet more stringent environmental and safety requirements, incorporate at least one aspect of bioprocessing. This thesis examines several novel solvents that could potentially be used in a variety of bioprocesses.

The pharmaceutical industry uses a combination of synthetic chemical processes and bioprocesses. Traditionally, the industry has employed batch reactions instead of implementing continuous flow processes. For many reactions, however, the use of continuous flow reactors provides many advantages. The high heat transfer capability allows better temperature control, which in turn can improve product quality, reduce waste, and minimize safety concerns. In Chapter 2, a continuous process is examined for the production of a HIV pharmaceutical precursor. The synthesis has a temperature-sensitive intermediate, uses the hazardous chemical diazomethane, and one reaction has an exotherm. A combination of chemical engineering and chemistry principles was used to successfully design, build, and optimize a continuous flow reactor.

The production of biofuels from lignocellulosic feedstock is currently a major bioprocessing field. Ethanol production has grown substantially in the United States in the past five years because its production from corn is straightforward. The price of corn, dairy, and meat has dramatically risen, however, as food sources are used to make transportation fuels. Thus lignocellulosic biomass, including trees, grasses, agricultural discards, and municipal wastes, will need to be the feedstock in order for the production to be sustainable both economically and environmentally. New technologies need to be developed in order to maximize sugar yields from the cellulose and hemicellulose components while removing lignin and extractives. Chapter 3 determines the effectiveness of several possible lignocellulosic pretreatment methods. Each method involves the use of an alternative solvent developed and used previously in our lab.

Chapter 4 focuses on the development of new analytical processes for the determination of biological compounds. The separation and quantification of metabolites, the end products of cellular processes, from physiological fluids can aid in the detection of disease. Additionally, metabolites can provide new drug targets. In this chapter, supercritical fluid chromatography (SFC) is examined as a possible analytical technique for metabolite detection. SFC can reduce both solvent waste and processing time when compared to more traditional analyses such as high performance liquid chromatography (HPLC) or gas chromatography (GC). A SFC was rebuilt and modified, and several chemical modifications attempted on amino acids, to improve the performance of SFC in metabolomic separation and identification.

In Appendix A, ionic liquids (ILs) and deep eutectic solvents (DESs) were studied as possible cellulose dissolution solvents. Sustainable solvents able to dissolve a substantial amount of cellulose have many applications in biofuels and biomaterials. The solubility of cellulose was tested in several known DESs. New ionic liquids were designed and synthesized to improve cellulose dissolution and enzymatic activity. These quaternary ammonium ionic liquids are capable of dissolving cellulose, and are expected to be more environmentally friendly than imidazolium-based ILs.

Many bioprocesses require enzymes to catalyze reactions of interest. The use of biocatalysis for reactions involving hydrophobic substrates, however, has typically been limited only to substrates soluble in aqueous environments. Although alternative solvents such as ILs have been used successfully, the enzymes must be immobilized or suffer from limited enzymatic activity. In the past, our lab has shown that Organic-Aqueous Tunable Solvents (OATS) can be successfully employed for simple enzymatic catalysis.

One research goal is to develop the system to work with enzymes requiring cofactors. Before cofactors can be incorporated into the system, however, it is important to understand their stability in mixed organic-aqueous solvents. Appendix B discusses the use of capillary electrophoresis (CE) to determine the stability of several cofactors under various experimental conditions.

Appendices C and D investigate the use of alternative solvents for the production of value-added chemicals from lignocellulosic feedstock. In Appendix C, a process involving piperylene sulfone (PS) is developed to create 5-hydroxymethylfurfural, a biological precursor for several alternative fuels and biomaterials, from fructose. Although pure HMF has not yet been made, other possibly important compounds derived from HMF are studied in this appendix. In Appendix D, peroxycarbonic acid is examined as a possible oxidation route for the production of glucaric acid. Glucaric acid, also called saccharic acid, has been identified as one of the 12 most important biological building blocks derived from carbohydrates.

Bioprocesses developed for the production of alternative fuels are again explored in Appendices E and F. In both appendices, gas-expanded methanol (GX-MeOH), a specific gas-expanded liquid (GXL) created by adding CO<sub>2</sub> to methanol, is applied to biofuels processes. GX-MeOH is known to form the in-situ acid methylcarbonic acid. The study of methylcarbonic acid for the acid-catalyzed hydrolysis of lignocellulosic biomass during pretreatment is detailed in Appendix E. The possibility of removing extractives from the biomass with the GX-MeOH was also examined. Finally, Appendix F examines the feasibility of using the methylcarbonic acid created in GX-MeOH to facilitate the acid-catalyzed production of biodiesel.

# **CHAPTER 2: APPLICATION OF A KINETIC STUDY TO A SMALL SCALE CONTINUOUS REACTOR TO PRODUCE (1-BENZYL-3-DIAZO-2-OXO-PROPYL)-CARBAMIC ACID ISOPROPYL ESTER, A DIAZOKETONE PHARMACEUTICAL INTERMEDIATE**

## **INTRODUCTION**

Although the pharmaceutical industry has been traditionally dominated by batch processes, continuous flow reactors are becoming more common due to their superior heat transfer capabilities, which can lead to reduced waste, improved product quality, and enhanced safety. This project focused on part of a multi-step synthetic sequence for the preparation of an active ingredient of a HIV drug. The sequence of interest for this project involved three reactions: the formation of a mixed anhydride, the formation of the corresponding diazoketone, and the subsequent HCl hydrolysis to yield the  $\alpha$ -chloroketone. The initial aspect of this project focused on optimization of the mixed anhydride formed in the first step. To make the analysis more facile, the temperature-sensitive mixed anhydride was quenched with an amine to form the corresponding amide. The second part of the project, the formation of the diazoketone, was accomplished by reacting the mixed anhydride intermediate with trimethylsilyl diazomethane.

This project also involved optimizing the reaction conditions for the development of a continuous flow process. Several continuous flow reactor configurations were designed, built, and tested in order to optimize the conditions of this specific synthesis.

## **BACKGROUND**

### **Benefits of Using Continuous Flow Reactors**

Using a continuous flow process instead of the batch process can have many benefits. Although continuous flow reactors are commonly used for large scale processes, they can vary drastically in size. Recent research has focused on small reactors either on the microreactor scale or slightly larger. In the literature, small continuous flow reactors have been shown to maintain several desirable characteristics of microreactors including improved heat exchange, safety, and scale-out ability.<sup>1, 2</sup> Microreactors are usually defined as small reaction systems that have dimensions in the sub-micrometer to the sub-millimeter range.<sup>3</sup> Small scale continuous flow reactors, as defined here, are slightly larger and reside in the millimeter range, but still have many positive attributes.

Micro- and small-scale reactors have a high surface area to volume ratio due to their reduced size.<sup>3</sup> The high surface area provides a high heat-exchange efficiency, which results in rapid heating or cooling and allows for better temperature control.<sup>4</sup> The small volumes also decrease the potential hazard of explosive or extremely exothermic reactions. Additionally, the small dimensions of these reactors prevent common mechanistic explosion pathways by suppressing radical chains and thermal build up.<sup>4, 5</sup> Continuous flow reactors are often built from stainless steel, an improvement over the glass (the material of construction usually used in batch reactions) because it can contain potential explosions and the heat transfer is significantly better.<sup>5</sup> This improved safety is desirable for any reactions that use diazomethane or other highly explosive compounds.<sup>6</sup>

Finally, the scale-out ability means that additional reactors can be added to increase production instead of scaling up the reaction and reactor.<sup>1</sup> This aspect of small-scale continuous flow reactors saves time and money because it makes the process easier to adapt to production needs without requiring additional research or pilot plant testing. Continuous flow processes can also be more desirable because they tend to be less labor intensive, and can occur much faster, than batch processes.<sup>7</sup>

As the reaction sequence in this project involved a temperature-sensitive intermediate, a potentially explosive reagent (diazomethane), and reactions that can be highly exothermic, this process was an ideal candidate for conversion to a continuous flow process. The advantages of continuous flow reactors can overcome these unfavorable reaction characteristics by significantly increasing heat transfer, mass transfer, safety and overall performances.

### **Potential Applications of (1-Benzyl-3-chloro-2-hydroxy-propyl)-carbamic acid tert-butyl ester**

Inhibiting the three enzymes encoded by Human Immunodeficiency Virus (HIV) is a possible pathway for treating Acquired Immunodeficiency Syndrome (AIDS). The product depicted in Figure 2.1 is a precursor for the pharmaceutically active compound Ro 31-8959, which is a possible HIV protease inhibitor.<sup>8</sup> Modern HIV inhibitors use a central three-carbon piece that contains two chiral carbons.<sup>8,9</sup> This synthesis uses L-boc-phenylalanine to set the chirality of the first carbon center, then symmetrically reduces the ketone to provide the other chiral center.



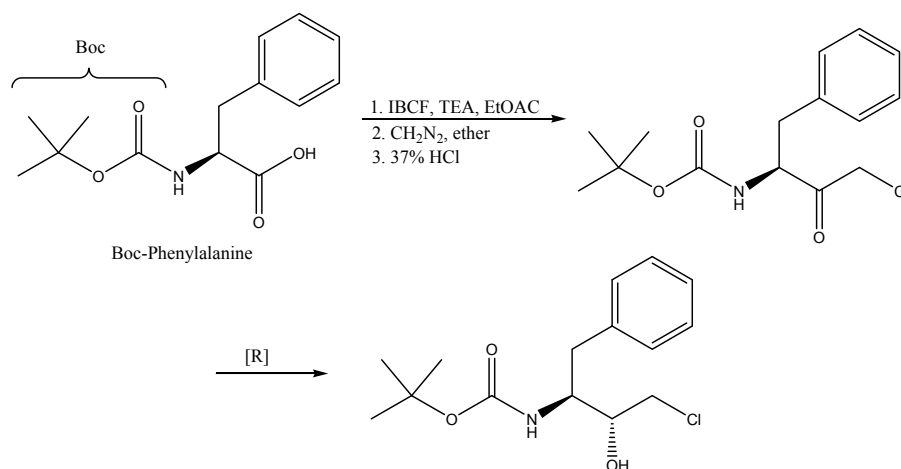


Figure 2.1: Synthetic route previously used in industry.<sup>8</sup>

### Trimethylsilyl Diazomethane

Our synthesis of interest originally used diazomethane as a reactant in the second step. Diazomethane is not a desirable reactant, however, because it is extremely reactive, highly toxic, thermally labile, and potentially explosive. In contrast, trimethylsilyl diazomethane is an attractive substitute for diazomethane because it is non-explosive, non-mutagenic, and can be used by industry without hazard.<sup>10</sup> It has also been used as a diazomethane substitute in several reactions.<sup>11</sup> The substitution has been made successfully before in an Arndt–Eistert synthesis, which involves the conversion of activated carboxylic acids to diazoketones by diazomethane, followed by a Wolff rearrangement.<sup>12</sup> Cesar et al. has used trimethylsilyl diazomethane in the synthesis depicted in Figure 2.2.<sup>11</sup> In their reaction, a 78% isolated yield was obtained by using trimethylsilyl diazomethane, compared to 76% isolated yield using diazomethane. This example illustrates that trimethylsilyl diazomethane can actually outperform diazomethane in some applications.

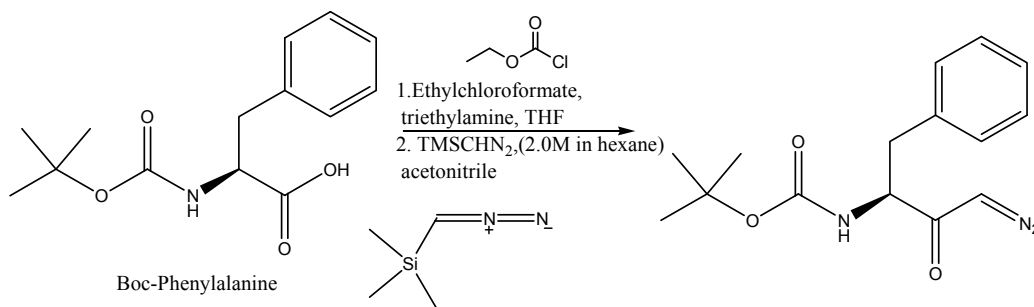


Figure 2.2: Diazoketone synthesis from L-boc-phenylalanine.<sup>11</sup>

## EXPERIMENTAL

### Materials

All chemicals were ordered from Aldrich or VWR and used as received, unless noted. <sup>1</sup>H and <sup>13</sup>C NMR spectra were recorded using a Varian Mercury Vx 400 spectrometer with a residual CDCl<sub>3</sub> peak used as an internal reference. Mass spectrometry samples were submitted to the mass spectrometry lab and used ESI-MS. GC-MS analysis was done on a HP GC 6890/ HP MS 5973. GC-FID analysis was done on a HP GC 6890 with FID detector, equipped with a HP-5MS (Agilent, 5% phenylmethylpolysilane) column. Elemental analyses were submitted to Atlantic Microlabs, Inc. Melting points were determined on Mettler-Toledo capillary apparatus and were uncorrected. LC-UV analysis was done on an Agilent 1100 Series LC equipped with a Luna C18 column (150 cm, 4.6 mm ID, 5 μM pore, 100Å), and the UV-visible spectra were recorded on a Hewlett-Packard 8453 spectrometer.

Synthesis of (1-benzylcarbamoyl-2-phenyl-ethyl)-carbamic acid tert-butyl ester using triethylamine (Figure 2.3)

L-Boc-phenylalanine (3.0 g, 0.0114 mol, 1 equiv) was added to dry ethyl acetate (15 mL, 20% wt solution). The solution was put under nitrogen and in a CaCl<sub>2</sub>/ice/water bath kept at -30 °C. Isobutylchloroformate (1.8 g, 0.015 mol, 1.3 equiv) was added to the cold solution. Triethylamine (1.5 g, 0.015 mol, 1.3 equiv) was then added drop-wise and a white precipitate (TEA-HCl salt) formed during the addition. The reaction was stirred for 1 hour at -30 °C. Then benzylamine (1.5 mL, 1.2 equiv) was added to quench the reaction. The reaction was allowed to warm to room temperature overnight. To work up the reaction, the TEA-HCl salt was removed by filtration and washed with cold ethyl acetate. The ethyl acetate solution was washed with saturated aqueous NaHCO<sub>3</sub>, water, and saturated aqueous NaCl. The solution was dried over magnesium sulfate and the solvent was removed under reduced pressure. The white solid was characterized, and a calibration curve was made from it for the continuous flow reactor.

*(1-Benzylcarbamoyl-2-phenyl-ethyl)-carbamic acid tert-butyl ester*: <sup>1</sup>H NMR (CDCl<sub>3</sub>) ppm: 1.39 (9, s), 3.06 (2, m), 4.37 (3, d), 5.02 (1, s), 6.01 (1, s), 7.10 (10, m). <sup>13</sup>C NMR (CDCl<sub>3</sub>, ppm): 28.24, 38.52, 43.47, 44.73, 56.05, 126.96, 127.48, 127.46, 127.67, 128.61, 128.73, 129.34, 137.62, 170.94. GC-MS analysis was done on a HP GC 6890/ HP MS 5973. MS(m/z): 281 (loss O-C(CH<sub>3</sub>)<sub>3</sub>). EA: calculated C, 71.16%, H, 7.39%, N, 7.90%. Found C, 71.27%, H, 7.46%, N, 7.84%.

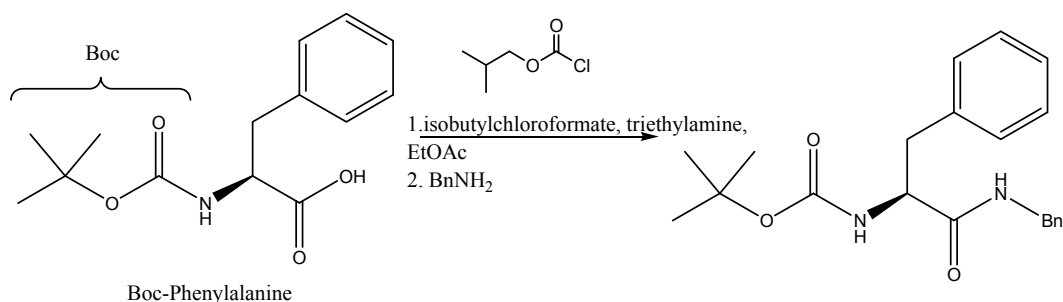


Figure 2.3: Reaction using triethylamine as the HCl scavenger followed by a benzylamine quench.

### Solubility test of amines

Pyridine, DBU, piperidine, tripropylamine, and tributylamine were tested to determine if a visible precipitate was formed upon the addition of HCl (37% reagent grade). For all amines, 1 g was added to 10 mL of ethyl acetate. Then 1 mL of HCl was added drop wise and compared visibly to a control of triethylamine (1g), ethyl acetate (10 mL), and HCl (1 mL). Pyridine, DBU, and piperidine all showed significant precipitate. Tripropylamine and tributylamine did not precipitate upon the addition of HCl.

### *Synthesis of (1-benzylcarbamoyl-2-phenyl-ethyl)-carbamic acid tert-butyl ester using tripropylamine*

L-Boc-phenylalanine (0.5 g, 0.0019 mol) was dissolved in ethyl acetate (2.5 mL) to make a 20 wt% solution. The solution was put under nitrogen and cooled in a CaCl<sub>2</sub>/H<sub>2</sub>O/ice bath kept at -30 °C. Isobutylchloroformate (0.3 g, 0.0025 mol) was added to the solution. Then tripropylamine (0.36 g, 0.0025 mol) was added to the solution. A white precipitate formed, however, upon the addition of the tripropylamine, so this synthetic method was not pursued further.

*Synthesis of (1-benzylcarbamoyl-2-phenyl-ethyl)-carbamic acid tert-butyl ester using tributylamine*

L-Boc-phenylalanine (0.5 g, 0.0019 mol) was dissolved in ethyl acetate (2.5 mL) to make a 20 wt% solution. The solution was put under nitrogen and cooled in a CaCl<sub>2</sub>/ice/water bath kept at -30 °C. Isobutylchloroformate (0.3 g, 0.0025 mol) was added to this solution. Tributylamine (0.46 g, 0.0025 mol) was added, and a precipitate did not form. The reaction was allowed to continue for one hour, and then 7 mL of a 5 wt% solution of benzylamine in ethyl acetate (1.0 g in 20 mL) was added to the reaction solution. The reaction was allowed to warm to room temperature overnight. No starting material was observed in <sup>1</sup>H NMR. The product was not purified because the goal was to confirm that a precipitate did not form in the first step.

Synthesis of (2-phenyl-1-propylcarbamoyl-ethyl)-carbamic acid tert-butyl ester using triethylamine

L-Boc-phenylalanine (3 g) was added to dry ethyl acetate (15 mL) to make a 20 wt% solution. The solution was put under nitrogen and in a CaCl<sub>2</sub>/water/ice bath kept at -30 °C. Triethylamine (2 mL, 1.3 equiv) and isobutylchloroformate (1.8 mL, 1.3 equiv) were added to the solution. The solution was stirred for 1 hour, propylamine (1.4 mL, 1.5 equiv) was added, and the solution was stirred for another hour. The reaction was filtered and the solid, TEA-HCl salt, was washed with ethyl acetate. The organic phase was washed with saturated aqueous NaHCO<sub>3</sub>, water twice, and saturated aqueous NaCl. It was then dried over magnesium sulfate. The solvent was removed under reduced pressure. The white solid was stirred with cold hexane and filtered, providing 76% yield.

*(2-Phenyl-1-propylcarbamoyl-ethyl)-carbamic acid tert-butyl ester using tributylamine:*  
<sup>1</sup>H NMR (CDCl<sub>3</sub>) ppm: 0.88 (3, m), 1.34 (11, m), 3.05 (4, m), 4.25 (1, m), 5.11 (1, s),  
5.74 (1, s), 7.25 (5, m). <sup>13</sup>C NMR (CDCl<sub>3</sub>) ppm: 11.215, 22.56, 28.25, 38.76, 41.11,  
56.09, 80.10, 136.89, 128.63, 129.30, 136.86, 155.370, 170.94. EA: calculated C,  
66.64%, H, 8.55%, N, 9.14%. Found C, 66.76%, H, 8.61%, N, 9.12%.

Synthesis of (2-phenyl-1-propylcarbamoyl-ethyl)-carbamic acid tert-butyl ester using  
tributylamine

L-Boc-phenylalanine (0.5 g, 0.0019 mol) was dissolved in dry ethyl acetate (2.5 mL) to make a 20 wt% solution. The solution was put under nitrogen and cooled in a CaCl<sub>2</sub>/ice/water bath kept at -30 °C. Isobutylchloroformate (0.3 g, 0.0025 mol) was added to this solution, followed by dry tributylamine (0.46 g, 0.0025 mol). The reaction proceeded for one hour. Dry propylamine (0.23 mL, 0.0029 mol, 1.5 equiv) in dry ethyl acetate (1 mL) was added to the solution. The reaction was allowed to warm to room temperature overnight. The reaction solution was washed with saturated aqueous NaHCO<sub>3</sub>, water, and saturated aqueous NaCl solution. The ethyl acetate layer was dried over magnesium sulfate, and the solvent was reduced under pressure. The resulting white solid (76% yield) was characterized.

*(2-Phenyl-1-propylcarbamoyl-ethyl)-carbamic acid tert-butyl ester using tributylamine:*  
<sup>1</sup>H NMR (CDCl<sub>3</sub>) ppm: 0.88 (3, m), 1.34 (11, m), 3.05 (4, m), 4.25 (1, m), 5.11 (1, s),  
5.74 (1, s), 7.25 (5, m). <sup>13</sup>C NMR (CDCl<sub>3</sub>) ppm: 11.215, 22.56, 28.25, 38.76, 41.11,  
56.09, 80.10, 136.89, 128.63, 129.30, 136.86, 155.370, 170.94. EA: calculated C,  
66.64%, H, 8.55%, N, 9.14%. Found C, 66.76%, H, 8.61%, N, 9.12%.

Synthesis of Diazoketone ((1-benzyl-3-diazo-2-oxo-propyl)-carbamic acid tert-butyl ester) Using Isobutylchloroformate

L-Boc-phenylalanine (0.8 g, 3 mmol) was dissolved in anhydrous THF (15 mL), cooled to -15 °C, and put under argon. Triethylamine (0.43 mL, 3.1 mmol) was added. Isobutylchloroformate (0.4 mL, 3.1 mmol) was combined with 2.5 mL anhydrous THF and added slowly to the solution. The reaction was allowed to react for 30 minutes. The triethylamine hydrochloride salt was filtered while keeping the filtrate cold. The trimethylsilyl diazomethane (2.0 M in hexane, 3 mL, 6 mmol) was combined with anhydrous acetonitrile (10 mL) and added slowly to the reaction solution. The reaction was warmed to 4 °C and allowed to react for 24 hours. The reaction was worked up by adding diethyl ether (40 mL), washing with 10% aqueous citric acid (30 mL), saturated aqueous NaHCO<sub>3</sub> (30 mL), and saturated aqueous NaCl (30 mL), then dried over magnesium sulfate. The solvent was removed under reduced pressure. The product was purified by a silica gel column was run using 1/2=ethyl acetate/ hexane giving a yellow solid (32% yield). These results were repeated and gave the same yield.

*(1-Benzyl-3-diazo-2-oxo-propyl)-carbamic acid tert-butyl ester:*

<sup>1</sup>H NMR (CDCl<sub>3</sub>) ppm: 1.398 (s, 9H), 3.05 (m, 2H), 4.40 (br s, 1H), 5.10 (br s, 1H), 5.20 (br s, 1H), 7.27 (m, 5H). <sup>13</sup>C NMR (CDCl<sub>3</sub>) ppm: 28.2, 38.5, 54.4, 58.4, 80.0, 126.9, 128.6, 129.3, 136.3, 155.1, 193.3. MS(m/z) 290 (M+1) EA: calculated C, 62.27%, H, 6.62%, N, 14.52%. Found C, 62.25%, H, 6.65%, N, 14.32%.

Synthesis of Diazoketone ((1-benzyl-3-diazo-2-oxo-propyl)-carbamic acid tert-butyl ester) Using Ethylchloroformate<sup>11</sup>

L-Boc-phenylalanine (0.8 g, 3 mmol) was dissolved in anhydrous THF (15 mL), cooled to -15 °C, and put under argon. Triethylamine (0.43 mL, 3.1 mmol) was added. Ethylchloroformate (0.3 mL, 3.1 mmol) was combined with 2.5 mL anhydrous THF and added slowly. The reaction was allowed to run for 30 minutes. The triethylamine hydrochloride salt was filtered while keeping the filtrate cold. The trimethylsilyl diazomethane (2.0 M in hexane, 4.5 mL, 9 mmol) was combined with anhydrous acetonitrile (10 mL) and added slowly. The reaction was warmed to 4 °C and allowed to react for 24 hours. The reaction was worked up by adding diethyl ether (40 mL), washing with 10% aqueous citric acid (30 mL), saturated aqueous NaHCO<sub>3</sub> (30 mL), and saturated aqueous NaCl (30 mL), then dried over magnesium sulfate. The solvent was removed under reduced pressure. The product was purified by a silica gel column was run using 1/2 ethyl acetate/ hexane giving a yellow solid (75+/-3% yield).

**Methods**

Calibration Curve of L-Boc-phenylalanine

Five different amounts (0.0152 g, 0.0422 g, 0.0740 g, 0.1107 g, 0.1418 g) of L-boc-phenylalanine were used to make a calibration curve on the LC-UV at 230 nm wavelength. The L-boc-phenylalanine was dissolved in 1 mL of methanol. A standard of 0.0646 g L-boc-phenylalanine in 1 mL of methanol was used to test the calibration curve. The LC calibration curve gave 0.0687 g, which is approximately 6% error.



### Calibration Curve of (2-Phenyl-1-propylcarbamoyl-ethyl)-carbamic acid tert-butyl ester

The LC-UV (229 nm) was used to make a calibration curve of the product. Different amounts of product (0.356 g, 0.0527 g, 0.1028 g, 0.0744 g, 0.0148 g) were added to five vials, and 0.5 mL of methanol was added to each. The concentrations (0.2324 M, 0.3440 M, 0.6710 M, 0.4856 M, and 0.0966 M) were calculated and used to make the calibration curve. The calibration curve was tested using a standard of 0.2304 M. The calibration curve gave 0.231 M, which was within error to the known standard concentration.

### 1<sup>st</sup> Generation Continuous Flow Reactor

The continuous flow reactor was run using 0.04 M solutions. The L-boc-phenylalanine solution was prepared by combining L-boc-phenylalanine (0.75 g) and dry tributylamine (0.7 mL) in dry ethyl acetate (75 mL). This solution was pumped into the system using an HPLC pump from a round bottom in the chiller. The isobutylchloroformate (2.4 mL) solution was in ethyl acetate (450 mL) and was pumped into the system using an Isco syringe pump. The propylamine solution was made by adding propylamine (0.16 mL) in ethyl acetate (5 mL), which was based on having 1.5 equiv of propylamine after a 10 min run at 3.3 mL/min. The chiller was set at -20 °C. The L-boc-phenylalanine solution alone was run through the system for 2 minutes, giving a reading of -7.8 °C on the thermocouple. The Isco syringe pump was set for 3.3 mL/min to match the flow rate of the HPLC pump.

All the reactants were run through the continuous flow reactor for 2 min to flush the system. The reactant solution was then dripped into the flask containing the propylamine solution for 10 min. The thermocouple reading increased to -7.3 °C during the run. The propylamine solution containing the reactants was put into a round bottom, and the solvent was removed under reduced pressure, which resulted in an oil. The NMR peaks and the LC-UV retention time did not correlate with the product. The experiment was repeated with the same results.

## 2<sup>nd</sup> Generation Continuous Flow Reactor

### *Specifications*

The cross fitting and tee fittings were HIP fittings made of stainless steel (SS 314). The tubing had a 7 mm ID and was also SS 314. The HPLC pumps were from Eldex. The tubing lengths can be seen in Figure 2.8.

## 2<sup>nd</sup> Generation Continuous Flow Reactor (0.04M)

### *Runs 2-3 (Pump failed during Run 1)*

L-Boc-phenylalanine (0.75 g) and dry tributylamine (0.7 mL) were added to dry ethyl acetate (75 mL), and isobutylchloroformate (0.6 mL) was added to dry ethyl acetate (112 mL), to make a 0.04 M solutions. Dry propylamine (2 mL) was added to dry methanol (75 mL) to make a 0.3 M solution (in excess). The chiller was set to -20 °C and the thermocouple read -19.7 °C. The reactants were collected for 6 minutes for Run 2 and for 20 minutes for Run 3. The solvent was removed under reduced pressure, giving an oil. The NMR did not show any product formation.

#### *Run 4*

The L-boc-phenylalanine solution and the isobutylchloroformate solution were the same as for Runs 1-3. Propylamine (0.44 mL) was added to dry methanol (75 mL), providing 1.5 equiv, which was 0.072 M when corrected for the slower flow rate of the quench pump. The system was flushed with all the reactants for 1 minute. The solution was collected for 20 min and the solvent was removed under reduced pressure. The NMR did not show any product formation.

#### *Run 5*

The solutions were prepared as described for Run 4. The system was flushed for 1 minute, and then the product stream was collected for 20 min. The solution was then worked up the same way as the batch reaction: first the solution was washed with water, then saturated aqueous NaHCO<sub>3</sub>, and finally saturated aqueous NaCl. The organic phase was dried over magnesium sulfate and solvent was removed under reduced pressure. The resulting oil did not show any product by NMR.

#### Batch Reaction at 0.04 M

L-Boc-phenylalanine (0.75 g) was dissolved in dry ethyl acetate (75 mL). The reaction was put under nitrogen and in a CaCl<sub>2</sub>/water/ice bath kept at -30°C. Tributylamine (0.7 mL) and isobutylchloroformate (0.4mL) were added to make a 0.04 M solution. The reaction was stirred for 1 hour. Then dry methanol (20 mL) and propylamine (0.1 mL) were added, providing a 0.06 M solution of propylamine, and the reaction was stirred at room temperature overnight. To workup the reaction mixture, the

organic phase was washed with saturated aqueous NaCO<sub>3</sub>, water twice, and saturated aqueous NaCl. The organic phase was dried over magnesium sulfate and the solvent was removed under reduced pressure. To purify the resulting white solid, the solid was washed with cold hexane and filtered. The solid was pure by <sup>1</sup>H NMR with a 62% yield.

#### Batch Reaction at 0.04 M (with stainless steel)

The reaction conditions were the same as above, except a small piece of stainless steel tubing was added to the round bottom. This was done to determine if the stainless steel was hindering the reaction in the continuous flow reactor. The product was pure by <sup>1</sup>H NMR with a 52% yield.

#### Reaction Time Determination Using 0.04 M Batch Reactions

L-Boc-phenylalanine (0.75 g) was dissolved in dry ethyl acetate (75 mL). The solution was put under argon and placed in a CaCl<sub>2</sub>/water/ice bath kept at -30 °C. Tributylamine (0.7 mL) and isobutylchloroformate (0.4 mL) were added to the solution to form a concentration of 0.04 M. A separate propylamine solution was made with propylamine (0.1 mL) in dry methanol (20 mL) to form a 0.06 M concentration, which resulted in 1.5 equiv of propylamine. Vials were made with the propylamine solution (0.5 mL) and placed in an ice bath. The reaction was started, and at 1, 2, 3, 4, 5, 10, 15, 20, 25, 30, 45, 60 minute intervals, samples of the L-boc-phenylalanine solution (0.5 mL) were removed and put into a vial containing the propylamine quench. All the samples were run on the LC-UV. The samples taken at 4 minutes and 30 minutes were also tested by <sup>1</sup>H NMR. The sample at 4 minutes showed partial conversion to the product, and the sample at 30 minutes showed only product peaks in the <sup>1</sup>H NMR.

#### Reaction Time Determination Using 0.75 M Batch Reactions (LC-UV)

L-Boc-phenylalanine (5 g) was dissolved in dry ethyl acetate (25 mL). The solution was put under argon and placed in a CaCl<sub>2</sub>/water/ice bath kept at -30 °C. Tributylamine (3.0 mL) and isobutylchloroformate (1.5 mL) were added to the solution to form a 0.75 M concentration. A separate propylamine solution was made with propylamine (1.8 mL) in dry methanol (20 mL), forming a 1.1 M concentration, which results in 1.5 equiv of propylamine. Vials were made containing the propylamine solution (0.5 mL) and placed in an ice bath. . The reaction was started, and at 1, 2, 3, 4, 5, 10, 15, 20, 25, 30, 45, 60 minute intervals, samples of the L-boc-phenylalanine solution (0.5 mL) were removed and put into a vial containing the propylamine quench. All the samples were run on the LC-UV. Product had already appeared in the 1 minute sample analyzed by LC-UV.

#### Reaction Time Determination Using 0.75 M Batch Reactions (Isolated Yield)

A stock solution was made with L-boc-phenylalanine (5 g), tributylamine (6 mL), and dry ethyl acetate (50 mL). Each test used 2.8 mL of stock solution. A separate solution of the quench was made with propylamine (2.4 mL) and dry methanol (26 mL). For each test, 1.4 mL of the quench stock solution was used. Isobutylchloroformate (0.15 mL) was added to the 2.8 mL of stock solution, forming a 0.75 M concentration. The quench was added at 5, 15, and 30 seconds, as well as 1, 5, 10, and 20 minutes. Each reaction time was done in triplicate. The solutions were worked up by washing with saturated aqueous NaHCO<sub>3</sub>, twice with water, and saturated aqueous NaCl. The solutions were dried over magnesium sulfate and the solvent was removed under reduced

pressure. The 5 second time sample did not show any product formation by  $^1\text{H}$  NMR. The 15 and 30 second time sample gave 20% and 30% isolated yield, respectively. Any time after 1 minute gave the maximum possible isolated yield of 76 $\pm$ 5%.

## 2<sup>nd</sup> Generation Continuous Flow Reactor 0.75 M

### *Run 1*

L-Boc-phenylalanine (14.9 g) and tributylamine (13.3 mL) were added to dry ethyl acetate (75 mL) to make a 0.75 M solution. Isobutylchloroformate (7.3 mL) was added to dry ethyl acetate (75 mL) to make a second 0.75 M solution. Propylamine (8.3 mL) was added to dry methanol (75 mL) to make a 1.35 M solution, so there were 1.5 equiv of propylamine in solution from the slower pump. The dials on both HPLC pumps were set to 1, and the Isco syringe pump, containing the isobutylchloroformate, was set to 2.4 mL/min. The chiller was set to -20 °C. The residence time was 1 min. Three runs were performed with a 2 min flush of reactants, followed by 5 min collecting the exit stream for each run. The thermocouple read -20.3 °C during the runs. The three runs were then worked up using the same procedure as the batch reactions. Only trace amounts of product was seen by  $^1\text{H}$  NMR analysis.

### *Run 2 -3*

The solutions were made the same way as with Run 1. The flow rates were reduced to 0.8 mL/min for the HPLC pumps, and the Isco was set to 0.8 mL/min. The residence time was 3.4 minutes. The chiller was set to -20 °C for Run 2 and -10 °C for Run 3. Each run was collected in duplicate for each temperature. The continuous flow

reactor was flushed with reactants for 5 min, and the exit stream was collected for 5 min for each run. All of the runs were worked up using the same procedure as the batch reaction. In Run 2, 2% isolated yield for the product was obtained. Only trace product was observed by  $^1\text{H}$  NMR for Run 3.

### 3<sup>rd</sup> Generation Continuous Flow Reactor

#### *Specifications*

The HPLC mixer (Agilent, G1312-87330) was 6 cm long, and the purchasing specifications stated that its volume was 420  $\mu\text{L}$ , and it contained stainless steel beads. The HPLC tubing was purchased from Agilent. Each piece was 80 cm in length, had an inner diameter of 0.17 mm, and was made of stainless steel (SS 314). The cross fitting and tee fitting were HIP fittings made of SS 314. HPLC pumps were used to pump the reactants through the continuous flow reactor. Three Eldex Recipro Model AA stainless steel pumps were used until partway through the 3<sup>rd</sup> generation system. At this point, two Eldex Recipro Optos 2SM pumps were used for the reactant streams and an Eldex Recipro Model A pump was used for the quench. For the continuous flow reactor, an Eldex Recipro A pump made from CTFE was used for the isobutylchloroformate stream, and the two Optos pumps were utilized for the other streams.

#### *Flow Rates*

All pumps were tested individually to determine individual flow rates. The final settings, with all three pumps combined, gave a 15% pressure drop. At the 0.01 setting, the boc-phenylalanine pump should provide 0.6 mL/min, and at the 0.25 setting the

isobutylchloroformate pump should provide 0.6 mL/min. Finally, the propylamine quench pump should provide at 1 mL/min. Various flow rates were tested to determine optimal settings for the experiments.

### 3<sup>rd</sup> Generation Continuous Flow Reactor (400 cm Tubing)

L-Boc-phenylalanine (6 g) and tributylamine (5.4 mL) were added to dry ethyl acetate (15 mL) to make a 1.5 M solution. The isobutylchloroformate (2.9 mL) was added to dry ethyl acetate (15 mL) to make a 1.5 M solution. The two solutions combined inside the reactor to make a 0.75 M solution of all the reactants. Propylamine (2.8 mL) was added to dry methanol (30 mL) to make a 1.125 M solution, which was 1.5 equiv of propylamine compared to the L-boc-phenylalanine. The L-boc-phenylalanine pump was set at 0.01, which correlated to a flow rate of 0.6 mL/min. The isobutylchloroformate pump was set at 0.25, which correlated to a flow rate of 0.6 mL/min. The propylamine pump was set at 0.25, which correlated to a flow rate of 1.0 mL/min. With the inherent pressure drop, the overall flow rate should be 1.7 mL/min. The chiller was set to -20 °C, -10 °C, 0 °C, 10 °C, 20 °C, 25 °C, and 50 °C with the thermocouple respectively reading -20.4 °C, -10.5 °C, -0.5 °C, 10.0 °C, 19.7 °C, 24.8 °C, and 49.9 °C.

The reactants were flushed in the continuous flow reactor for 2 minutes before each temperature change. For each temperature, the exit stream was collected in duplicate 2 min runs at -20 °C, -10 °C, and 0 °C. The runs, still collected in duplicate, were increased to 3 min at 10 °C, 20 °C, 25 °C and 50 °C. The samples were worked up as previously described. The product was isolated, and the melting point determined for each sample and compared to the product melting point of 111.4 °C. The -20 °C



produced an oil, but showed trace amounts of product. The isolated yield of the -10 °C was 6 +/-5%, for 0 °C was 10+/-5%, for 10 °C was 17+/-5%, for 20 °C was 20 +/-5%, for 25 °C was 23+/-5%, and for 50 °C was 25 +/-5%. The results are depicted in Figure 2.13.

### 3<sup>rd</sup> Generation Continuous Flow Reactor (720 cm Tubing)

#### *Optimize Flow Rates for Pressure Drop*

The same reactant quantities used for the 400 cm tubing length continuous flow reactor were used for this experiment. The L-boc-phenylalanine pump was set to 0.01 for a flow rate of 0.6mL/min, and the isobutylchloroformate pump was set to 0.25 for a flow rate of 0.6 mL/min. The propylamine pump was set to 0.50 for a flow rate of 1.2 mL/min. All of these flows should have provided a total flow rate of 1.8 mL/min after the 15% flow rate reduction. The continuous flow reactor was flushed with reactants for 2 minutes before each temperature change, and the reactants were collected in duplicate for 3 minutes at each temperature. The chiller was set to 10 °C, 25 °C, and 50 °C with the thermocouple respectively reading 10.1 °C, 25.2 °C, and 50.3 °C. The exit stream was collected and worked up the same way as the batch reaction. The isolated yield at 10 °C was 6+/-5%, at 25 °C was 16+/-5%, and at 50 °C was 18+/-5%.

#### *Flow Ratios Using Hydrocarbon Trace*

For the hydrocarbon trace, L-boc-phenylalanine (6 g), tributylamine (5.4 mL), and octane (0.15 mL, 1% vol) were added to dry ethyl acetate (15 mL). Isobutylchloroformate (2.9 mL) and nonane (0.15 mL, 1% vol) were added to dry ethyl acetate (15 mL). Propylamine (2.8 mL) and decane (0.30 mL, 1% vol) were added to dry

methanol (30 mL). The continuous flow reactor was flushed for 2 min before each collection, and two 1 mL samples from the exit stream were collected and run on the GC-FID to determine the ratios by the peak area. The results are shown in Table 2.1.

Table 2.1: Pump settings and reactant ratios using hydrocarbon trace.

<b>Reactants with 1% vol Hydrocarbons (at 25 °C)</b>					
Pump Settings			Hydrocarbon Ratios (average of 2 runs)		
Boc	Iso	Propyl	Octane	Nonane	Decane
0.01	0.23	0.09	11	32.5	56.5
0.01	0.2	0.09	10.5	30.5	59
0.03	0.2	0.09	17	32	51
0.05	0.2	0.09	24.5	35	40.5
0.04	0.2	0.09	27.5	39.5	33

#### *Optimizing Pumps with Hydrocarbon Trace*

L-Boc-phenylalanine (6 g), tributylamine (5.4 mL), and octane (0.15 mL, 1% vol) were added to dry ethyl acetate (15 mL). Isobutylchloroformate (2.9 mL) and nonane (0.15 mL, 1% vol) were added to dry ethyl acetate (15 mL). Propylamine (2.8 mL) and decane (0.30 mL, 1% vol) were added to dry methanol (30 mL). The chiller temperature was set to 25 °C. The L-boc-phenylalanine pump was set to 0.04, the isobutylchloroformate pump was set to 0.15, and the propylamine pump was set to 0.09. The reactor was flushed with reactants for 3 minutes, and 5 mL of the exit stream was collected in duplicate. The residence time was measured to be 19.2 sec. The ratios of the octane, nonane, and decane were measured at 26%, 27%, and 47%, respectively, on the GC-FID. The duplicate runs were worked up like the batch reaction. The isolated yield was 30+/-5%. The product purity was measured by melting point and <sup>1</sup>H NMR.

### *Mixing with the Sonicator*

L-Boc-phenylalanine (6 g), tributylamine (5.4 mL), and octane (0.15 mL, 1% vol) were added to dry ethyl acetate (15 mL). Isobutylchloroformate (2.9 mL) and nonane (0.15 mL, 1% vol) were added to dry ethyl acetate (15 mL). Propylamine (2.8 mL) and decane (0.30 mL, 1% vol) were added to dry methanol (30 mL). The L-boc-phenylalanine pump was set to 0.04, the isobutylchloroformate pump was set to 0.15, and the propylamine pump was set to 0.09.

The continuous flow reactor was placed in a VWR Aquasonic 75HT sonicator for this run. The sonicator temperature was measured using a thermocouple, and was maintained between 24-27 °C by adding ice as needed. The reactants were flushed through the continuous flow reactor for 5 min, and then 7 mL of the exit stream was collected in duplicate. The ratios of the octane, nonane, and decane were 19%, 28%, and 53%, respectively, as measured on the GC-FID. The duplicate runs were worked up using the same procedure as the batch reaction. The isolated yield was 30+/-5%. Melting point and <sup>1</sup>H NMR were used to verify purity.

### *One-Tubular Reactor System*

L-Boc-phenylalanine (6 g), tributylamine (5.4 mL), and octane (0.15 mL, 1% vol) were added to dry ethyl acetate (15 mL). Isobutylchloroformate (2.9 mL) and nonane (0.15 mL, 1% vol) were added to dry ethyl acetate (15 mL). Propylamine (2.8 mL) and decane (0.30 mL, 1% vol) were added to dry methanol (30 mL). The L-boc-phenylalanine pump was set to 0.04, the isobutylchloroformate pump was set to 0.15, and the propylamine pump was set to 0.09. The chiller was set to 25 °C.

The stripped HPLC column was repacked with 3 mm glass beads, and placed after four 80 cm tubing lengths. The HPLC column was 25 cm long with a 4.6 mm ID. The reactor was flushed with reactants for 5 min, and 8 mL of the exit stream was collected in duplicate. The ratios of the octane, nonane, and decane were measured to be 15%, 20%, and 65%, respectively, on the GC-FID. The residence time was measured to be 10.2 sec. The duplicate runs were worked up using the same procedure as the batch reaction. The isolated yield was 40+/-5%. Melting point and <sup>1</sup>H NMR were used to verify purity.

#### *Mixing with Beads in Cross Fitting*

Glass beads (0.5 mm) were added inside the cross fitting that combined the reactant streams. These beads were supposed to improve mixing at the fitting, improving the yield. The beads clogged the system, however, so the option was abandoned.

#### *Mixing Improvement by Using Smaller Beads in the Tubular Reactor*

The 3 mm glass beads were removed and the tubular reactor was repacked with 0.5 mm glass beads. The L-boc-phenylalanine and isobutylchloroformate pumps were set to 0.3 mL/min. The propylamine pump was optimized using the GC-FID and hydrocarbon trace. The system worked the best when the pump dial was kept at the 0.03 mark. L-Boc-phenylalanine (6 g), tributylamine (5.4 mL), and octane (0.15 mL, 1% vol) were added to dry ethyl acetate (15 mL). Isobutylchloroformate (2.9 mL) and nonane (0.15 mL, 1% vol) were added to dry ethyl acetate (15 mL). Propylamine (2.8 mL) and decane (0.30 mL, 1% vol) were added to dry methanol (30 mL). The chiller temperature was not set and was left at room temperature. The thermocouple read 21.3 °C.

The continuous flow reactor was flushed with all three streams for 7 minutes. Three samples of 5 mL were collected for each run. Each sample took between 4 min and 4.5 min to collect. One mL was removed from each sample and run on the GC-FID to determine the percentage of octane, nonane, and decane. The percentages for all samples were 19% octane, 27% nonane, and 54% decane. The remaining four mL of the product stream was worked up the next day the same way as the batch reaction. The white solid was dried in a vacuum oven overnight and purity was confirmed by melting point and  $^1\text{H}$  NMR. The average isolated yield was 47 +/-5%.

#### *Mixing with Bent Tubing*

The tubular reactor packed with 0.5 mm glass beads was left in the system. An 80 cm piece of 0.17 mm ID HPLC tubing was bent sharply to provide 1 cm angles in order to induce chaotic mixing. The bent tubing replaced the third 80 cm section of HPLC tubing in the reactor.

The L-boc-phenylalanine and isobutylchloroformate pumps were set to 0.3 mL/min. The propylamine pump was optimized using the GC-FID and hydrocarbon trace, which resulted in setting the propylamine pump at 0.03. L-Boc-phenylalanine (6 g), tributylamine (5.4 mL), and octane (0.15 mL, 1% vol) were added to dry ethyl acetate (15 mL). Isobutylchloroformate (2.9 mL) and nonane (0.15 mL, 1% vol) were added to dry ethyl acetate (15 mL). Propylamine (2.8 mL) and decane (0.30 mL, 1% vol) were added to dry methanol (30 mL). The chiller temperature was not set and was left at room temperature. The thermocouple read 21.5 °C.

The continuous flow reactor was flushed with the three streams for 7 minutes. Three samples of 5 mL were collected for each run. The samples took between 4 min and 4.5 min to collect. One mL was removed from each sample and run on the GC-FID to determine the percentage of octane, nonane, and decane. The percentages for all samples were 21% octane, 28 $\pm$ 2% nonane, and 51 $\pm$ 2% decane. The remaining four mL of the product stream was worked up the same way as the batch reaction. The white solid was dried in a vacuum oven overnight and purity was confirmed by melting point and  $^1\text{H}$  NMR. The average isolated yield was 47  $\pm$ 5%.

#### *Reduced Flow Rate*

The bent tubing was removed and replaced with the original non-bent HPLC. The tubular reactor packed with 0.5 mm glass beads remained. The L-boc-phenylalanine and isobutylchloroformate pumps were set to 0.1, 0.01, and 0.05 mL/min during the experiments. The propylamine pump was set to its lowest setting of 0.01. Since the propylamine pump pumps faster than the other two pumps at this setting, this resulted in a larger percentage of the propylamine stream.

The first test was to ensure that the quench propylamine stream would not overwhelm the other two streams. L-Boc-phenylalanine (6 g), tributylamine (5.4 mL), and octane (0.15 mL, 1% vol) were added to dry ethyl acetate (15 mL). Isobutylchloroformate (2.9 mL) and nonane (0.15 mL, 1% vol) were added to dry ethyl acetate (15 mL). Propylamine (2.8 mL) and decane (0.30 mL, 1% vol) were added to dry methanol (30 mL). The chiller temperature was not set and was left at room temperature. The thermocouple read 20.9°C. The continuous flow reactor was flushed with all three streams for 4 minutes. Two samples of one mL each were collected to be run on the GC-

FID. For the 0.01 mL/min, the octane and nonane were not observed by GC-FID. For the 0.05 mL/min, the percentages were 4% octane, 2% nonane, and 94% decane. For the 0.1 mL/min, the percentages were 10% octane, 12% nonane, and 78% decane.

Since the 0.1 mL/min flow rate seemed to give acceptable percentages of the hydrocarbon trace, the system was run using these flow rate. The continuous flow reactor was flushed with the three streams for 20 minutes. Triplicate samples of 10 mL were collected, with each sample taking between 14.5 to 15 min to collect. One mL was removed from each sample to be run on the GC-FID to determine the percentage of octane, nonane, and decane. The percentages for the first sample were 10% octane, 9% nonane, and 81% decane. The percentages for the second and third samples were 11% octane, 15 $\pm$ 1% nonane, and 74 $\pm$ 1% decane. The percentages were not acceptable for the first sample, so that sample was not worked up. The remaining nine mL of the product stream was worked up the next day the same way as the batch reaction. The white solid was dried in a vacuum oven overnight and purity was confirmed by melting point and  $^1\text{H}$  NMR. The average isolated yield was 48  $\pm$ 5%.

#### *Adding a Second Tubular Reactor: Two-Tubular Reactor System*

A second HPLC column was stripped of its silica and repacked with 0.5 mm glass beads. The HPLC column was 15 cm long with a 4 mm ID. This tubular reactor was added between the 3<sup>rd</sup> and 4<sup>th</sup> HPLC tubing in the continuous flow reactor, placing it after 240 cm of HPLC tubing.

The L-boc-phenylalanine and isobutylchloroformate pumps were set to 0.3 mL/min for the first run, and 0.1 mL/min for the second run. The propylamine pump was put at the lowest setting of 0.01. L-Boc-phenylalanine (6 g), tributylamine (5.4 mL), and

octane (0.15 mL, 1% vol) were added to dry ethyl acetate (15 mL). Isobutylchloroformate (2.9 mL) and nonane (0.15 mL, 1% vol) were added to dry ethyl acetate (15 mL). Propylamine (2.8 mL) and decane (0.30 mL, 1% vol) were added to dry methanol (30 mL). The chiller was not set and left at room temperature. The thermocouple read 21.2 °C.

The continuous flow reactor was flushed with all three streams for 20 minutes. Three samples of 5 mL each at the 0.3 mL/min and three samples of 10 mL each for the 0.1 mL/min each were collected. The samples took approximately 4.5 min to collect for the 0.3 mL/min and 15.75 min for the 0.1 mL/min. One mL was removed from each sample and run on the GC-FID to determine the percentage of octane, nonane, and decane. The percentages at 0.3 mL/min were 19% octane, 29% nonane, and 51% decane. The percentages at 0.1 mL/min were 10% octane, 16% nonane, and 74% decane. The remaining four or nine mL of the product stream samples were worked up the same way as the batch reaction. The white solid was dried in a vacuum oven overnight and purity was confirmed by melting point and <sup>1</sup>H NMR. The average isolated yield was 51 +/-5% for the 0.3 mL/min and 60+/-5% for the 0.1 mL/min.

#### *Mixing with Bent Tubing for the 2-Tubular Reactor System*

The bent tubing was again substituted for the third piece of normal HPLC tubing. The L-boc-phenylalanine and isobutylchloroformate pumps were set at 0.3 mL/min and the propylamine pump was set at 0.01. All other reaction conditions were the same as above. Duplicate 4 mL samples were collected and worked up as described previously. The GC-FID percentages were 17+/-1% octane, 29+/-2% nonane, and 54+/-3% decane. The isolated yield from this system was 56+/-5%. This represents an improvement over



the 51+/-5% isolated yield achieved without the bent tubing. The difference, however, is not necessarily significant considering the inherent analysis error. It was decided at this point not to continue pursuing the bent tubing option.

#### *Optimizing Flow Rates for the Two-Tubular Reactor System*

L-Boc-phenylalanine (6 g), tributylamine (5.4 mL), and octane (0.15 mL, 1% vol) were added to dry ethyl acetate (15 mL). Isobutylchloroformate (2.9 mL) and nonane (0.15 mL, 1% vol) were added to dry ethyl acetate (15 mL). Propylamine (2.8 mL) and decane (0.30 mL, 1% vol) were added to dry methanol (30 mL). The chiller temperature was not set and was left at room temperature. The L-boc-phenylalanine and isobutylchloroformate pumps were set using the flow rates below. The propylamine pump was set at 0.01. The various experimental parameters (flush times, amount of exit stream worked up, collection times, hydrocarbon percentages from the GC-FID, and isolated yield) are presented in Figure 2-38. The change in isolated yield with different of flow rates can also be seen in Figure 2.18. The product stream was worked up and purified using the method described previously. The purity was confirmed using melting point and <sup>1</sup>H NMR.

Table 2.2: Flow rate optimization for the two-tubular reactor system.

Flow Rate (mL/min)	Flush (min)	Workup (mL)	Collect Time (min)	Octane (%)	Nonane (%)	Decane (%)	Isolated Yield
0.05	60	25	60	8	9+/-2	83+/-2	48+/-5
0.15	45	9	13:45-15	12	18	70	57+/-5
0.125	45	9	14:16-14:58	11	17	72	57+/-5
0.075	60	9	16:43-17:09	8	12	80	55 +/-5

### *Adding Two More Tubular Reactors: Four-Tubular Reactor System*

Two additional tubular reactors were built out of Swagelok SS 314 tubing with ¼ in. OD and 4.6 mm ID. Both tubular reactors were 20 cm long and were packed with 0.5 mm glass beads. The glass beads were packed using a VWR Fixed Speed Vortex mixer (150 watts). One tubular reactor was added after 320 cm of HPLC tubing, and the other tubular reactor was added after 560 cm of tubing. All the other reaction conditions were maintained. The propylamine pump was set at 0.01, and the L-boc-phenylalanine and isobutylchloroformate pumps were set at the same flow rate. The chiller was left at room temperature and the thermocouple read 23.2 °C throughout the experiment.

The first tubular reactor (after 320 cm) was added and run at 0.1 mL/min giving an isolated yield of 49+/-5%. Then the second tubular reactor (after 560 cm) was added and run at 0.1 mL/min, giving an isolated yield of 57+/-5%. The flow rates were then optimized. Reaction specifications are presented in Table 2.3, and the results can be seen in Figure 2.20. The product stream was worked up and purified using the method described previously. The purity was confirmed using melting point and <sup>1</sup>H NMR.

Table 2.3: Flow rate optimization for the four-tubular reactor system.

Flow Rate (mL/min)	Flush (min)	Workup (mL)	Collect Time (min)	Octane (%)	Nonane (%)	Decane (%)	Isolated Yield
0.1	60 m	9 mL	15:39	10	11	78	49+/-5
0.1	60 m	9.5 mL	8:46	6	7	87	44+/-5
0.2	60 m	9.5 mL	7:37	10	13	77	53+/-5
0.3	30 m	9.5 mL	7:08	8	19	73	51+/-5
0.4	30 m	9.5 mL	6:10	15	21	64	50+/-5

### *Optimizing Temperatures for the Four-Tubular Reactor System*

The next step involved optimizing the temperature of the four-tubular reactor system. All the reaction conditions and reagents were the same as previously used. The propylamine pump was set at 0.01. The L-boc-phenylalanine and isobutylchloroformate pumps were both set at 0.2 mL/min. The chiller was set to -20 °C and to 0 °C. The exit stream was collected, worked up, and purified using the method described previously. The purity was confirmed using melting point and <sup>1</sup>H NMR. The details are listed in Table 2.4, and the results are depicted in Figure 2.21.

Table 2.4: Temperature optimization for the four-tubular reactor system.

Temperature (°C)	Flush (min)	Workup (mL)	Collect Time (min)	Octane (%)	Nonane (%)	Decane (%)	Isolated Yield
-20	35 min	9.5 mL	7:20	7	11	82	53+/-5
0	35 min	9.5 mL	7:28	8	10	82	60+/-5

### *Different Equivalents of Isobutylchloroformate*

Different equivalents of isobutylchloroformate were tested with the-four tubular reactor system. The L-boc-phenylalanine, tributylamine, and octane in ethyl acetate, and the propylamine in methanol, were prepared in the same concentrations as the previous experiments (1.5 M). Both reactant pumps were set at 0.2 mL/min and the propylamine pump was set at 0.01. The chiller was left at room temperature and the thermocouple read 21.2 °C. The isobutylchloroformate equivalents were done in both 2x excess and 3x excess (based on the concentration of L-boc-phenylalanine). The product stream was

worked up and purified using the method described previously. The purity was confirmed using melting point and  $^1\text{H}$  NMR. The reaction details for this experiment are shown in Table 2.5.

Table 2.5: Excess isobutylchloroformate optimization for the four-tubular reactor system.

Equivalents	Flush (min)	Workup (mL)	Collect Time (min)	Octane (%)	Nonane (%)	Decane (%)	Isolated Yield
2x excess	35	9.5 mL	7:53	8	9	83	54+/-5
3x excess	35	9.5 mL	7:23	9	9	82	48+/-5

#### *Batch Studies of Propylamine Quench at Room Temperature*

The same solutions were used as in the continuous flow reactor: L-boc-phenylalanine and tributylamine in ethyl acetate (1.5 M), isobutylchloroformate in ethyl acetate (1.5 M), and propylamine in methanol (1.2 M). The L-boc-phenylalanine solution (2 mL) and isobutylchloroformate solution (2 mL) were combined. The quench solution (4 mL) was added after 16 minutes and 1 hour. Each time was done in triplicate. The product was worked up and purified using the method described previously. Product purity was confirmed using melting point and  $^1\text{H}$  NMR. The 16 min quench time gave an isolated yield of 37+/-5%, and the 1 hour quench time gave an isolated yield of 27+/-5%.

#### Calibration Curve of Diazoketone ((1-benzyl-3-diazo-2-oxo-propyl)-carbamic acid tert-butyl ester)

Pure diazoketone, (1-benzyl-3-diazo-2-oxo-propyl)-carbamic acid tert-butyl ester, was dissolved in methanol at various concentrations. These solutions were run on the LC-UV to create a calibration curve. The calibration curve had  $R^2 = 0.9997$ .

### Calibration Curve of 2-Phenyl-1-propylcarbamoyl-ethyl)-carbamic acid tert-butyl ester

Pure 2-phenyl-1-propylcarbamoyl-ethyl)-carbamic acid tert-butyl ester was dissolved in methanol at various concentrations. These solutions were run on the LC-UV to create a calibration curve. The calibration curve had  $R^2 = 0.9901$ .

### Batch Reaction of 2-Phenyl-1-propylcarbamoyl-ethyl)-carbamic acid tert-butyl ester

#### Using Ethylchloroformate

A stock solution was made with L-boc-phenylalanine (2.5 g), tributylamine (1.5 mL), and dry ethyl acetate (12.5 mL). Each test used 2.8 mL of stock solution. A separate stock solution of quench solution was made with propylamine (1.2 mL) and dry methanol (13 mL). For each test, 1.4 mL of the quench stock solution was used. Ethylchloroformate (0.2 mL) was added to the 2.8 mL solution, forming a 0.75 M concentration. The reaction times tested were 1, 16, and 30 minutes. The reaction solutions were run on the LC-UV, and concentrations were determined using the calibration curve of 2-phenyl-1-propylcarbamoyl-ethyl)-carbamic acid tert-butyl ester. The LC-UV showed 100% yield for both 16 and 30 minutes. The 30 minute sample was worked up by adding ethyl acetate, then washing with aqueous saturated  $\text{NaHCO}_3$ , water, and brine. The reaction solution was dried over magnesium sulfate and the solvent removed under reduced pressure. The product was isolated using a silica gel column (2/1: hexane/ethyl acetate), giving a white solid (49% yield).

Monitoring the Reaction Rate of Diazoketone, (1-benzyl-3-diazo-2-oxo-propyl)-carbamic acid tert-butyl ester)

L-Boc-phenylalanine (0.8 g, 3 mmol) was dissolved in anhydrous ethyl acetate (15 mL), cooled to -8 °C, and put under argon. Tributylamine (0.7 mL, 3.1 mmol) was added. Ethylchloroformate (0.3 mL, 3.1 mmol) was combined with 2.5 mL anhydrous ethyl acetate and added slowly to the solution. The reaction was warmed to -5 °C and allowed to react for 30 minutes. The trimethylsilyl diazomethane (2.0 M in hexane, 3 mL, 6 mmol) was combined with anhydrous acetonitrile (10 mL) and added slowly to the reaction solution. The reaction was warmed to 4 °C and was sampled at 15, 30, 45, and 60 min, as well as 2, 4, and 22 hours. A 50 µL sample was removed from the reaction solution and combined with 1.3 mL of methanol. The samples were run on the LC-UV, and the calibration curve of the diazoketone was used to determine the product concentration at various time intervals. For this system, quantitative yield was obtained after 2 hours and then reached a plateau. These results are shown in Figure 2.26. The points after two hours were within error of the maximum yield.

Monitoring the Reaction Rate of Diazoketone, (1-Benzyl-3-diazo-2-oxo-propyl)-carbamic acid tert-butyl ester) at 0.75 M

L-Boc-phenylalanine (0.8 g, 3 mmol) was dissolved in anhydrous ethyl acetate (4 mL), cooled to -8 °C, and put under argon. Tributylamine (0.7 mL, 3.1 mmol) and ethylchloroformate (0.3 mL, 3.1 mmol) were added. The reaction was warmed to -5 °C and allowed to react for 30 minutes. The trimethylsilyl diazomethane (2.0 M in hexane, 3

mL, 6 mmol) was combined with anhydrous acetonitrile (10 mL) and added slowly to the reaction solution. Anisole (1.6 mL, 0.75 M) was added as an internal standard. The reaction was warmed to 4 °C, and samples were taken at 10, 20, 30, 45, 60, 90, and 120 minutes. A 15 µL sample was removed from the reaction solution and combined with 1 mL of methanol. The samples were run on the LC-UV, and the calibration curve of the diazoketone was used to determine the product concentration at various time intervals. For this system, all samples provided quantitative yield via LC-UV. Times shorter than 10 minutes were not tested.

### Coiled Continuous Flow Reactor System

#### *Specifications*

A continuous flow reactor was constructed using of 45 cm length of SS 314 tubing with a ¼ in. OD and a 4.6 mm ID. The tubing was packed with glass beads (0.5 mm) using a VWR Fixed Speed Vortex mixer. The coil was achieved by bending the tubing around a pump pulley with a diameter of 3 inches. The ends were carefully bent with a tube bender. A schematic of the single coiled continuous flow reactor system is shown in Figure 2.22.

#### *Single Coiled Continuous Flow Reactor Using Ethylchloroformate*

L-Boc-phenylalanine (18 g), tributylamine (16.2 mL), and octane (0.45 mL, 1% vol) were dissolved in dry ethyl acetate (45 mL) to make a 1.5 M solution. Ethylchloroformate (12.76 mL), anisole (4.4 mL), and nonane (0.66 mL, 1% vol) were added to dry ethyl acetate (30 mL) to make a 3.3 M solution, which compensated for the

slower pump. Propylamine (5.6 mL) and decane (0.6 mL, 1% vol) were added to dry methanol to make a 1.5 M solution. The L-boc-phenylalanine pump and propylamine pumps were set at 0.2 mL/min, and the ethylchloroformate pump was set at 1.0. The chiller was set at 0 °C and the thermocouple read 0.2 °C. The system was flushed with reactants for 30 minutes, and then 3 samples (3.5 mL) were collected. For the GC-FID analysis, 0.5 mL of sample was added to 0.5 mL methanol. For the LC-UV, 10 µL of sample was added to 1 mL of methanol. The hydrocarbon trace from the GC-FID was used to calculate the maximum concentration of product. The LC-UV showed that the yield was quantitative for this system.

#### *Continuous Flow Reactor Using Trimethylsilyl Diazomethane*

A second continuous flow reactor, identical to the first continuous flow reactor, was added after the tee fitting to add the trimethylsilyl diazomethane. The schematic is shown in Figure 2.27. The first reactor was still used for the first step of the reaction. The same concentrations of the L-boc-phenylalanine and ethylchloroformate solutions were used. The propylamine solution was replaced with trimethylsilyl diazomethane (9 mL) and decane (0.3 mL, 1 % vol) in dry acetonitrile (30 mL) for a 0.6 M solution. The flow rates used were the same and the chiller was set to 0 °C.

The system was flushed with reactants for 30 minutes, and then three 2.5 mL samples were collected. For the GC-FID, 0.5 mL sample was added to 0.5 mL methanol. For the LC-UV, 10 µL of sample was added to 1 mL of methanol. The hydrocarbon trace from the GC-FID was used to calculate the maximum concentration of product. The LC-UV showed that the yield was quantitative for this system.



## RESULTS AND DISCUSSION

### Optimize Model Reaction for Use in Continuous Flow Reactor

The synthesis of interest was divided into two reactions before testing the continuous flow reactor. The mixed anhydride formed from L-boc-phenylalanine and isobutylchloroformate, in the presence of triethylamine in ethyl acetate, was the first reaction optimized. This reaction is illustrated in Figure 2.4. Instead of reacting the mixed anhydride with diazomethane to form the diazoketone as depicted in Figure 2.1, however, the mixed anhydride was quenched with a primary amine in our studies.

In our reaction, benzylamine was the primary amine used to quench the mixed anhydride. This primary amine reacted with the mixed anhydride intermediate to form (1-benzylcarbamoyl-2-phenyl-ethyl)-carbamic acid tert-butyl ester, which is also depicted in Figure 2.4. The reaction used triethylamine as an HCl scavenger to determine the maximum yield of the mixed anhydride. A 20 wt % solution of L-boc-phenylalanine (1 equiv) in ethyl acetate was cooled to -30 °C. Isobutylchloroformate (1.3 equiv) and triethylamine (1.3 equiv) were added and stirred at -30 °C for 1 hour, which is analogous to the industrial procedure used currently.<sup>9</sup> The benzylamine (1.3 equiv) was then added to quench the solution. The product was characterized by <sup>1</sup>H and <sup>13</sup>C NMR, MS, and elemental analysis.

In this reaction, triethylamine acts as an HCl scavenger and forms a salt that precipitates out of the reaction. In a batch reaction, a salt that can be filtered is desirable because the purification is facile. Any precipitate could clog a small-scale continuous flow reactor, however, because of the small tubing. Thus a secondary or tertiary amine was needed that would act as an HCl scavenger, but would not precipitate out of the solution and would not quench the reaction. Pyridine, 1,8-diazabicyclo[5.4.0]undec-7-ene (DBU), piperidine, tripropylamine, tributylamine were tested by adding one mL of HCl (37% reagent grade) to a solution of the amine (1 g) in ethyl acetate (10 mL). All the amines except tripropylamine and tributylamine formed a visible precipitate.

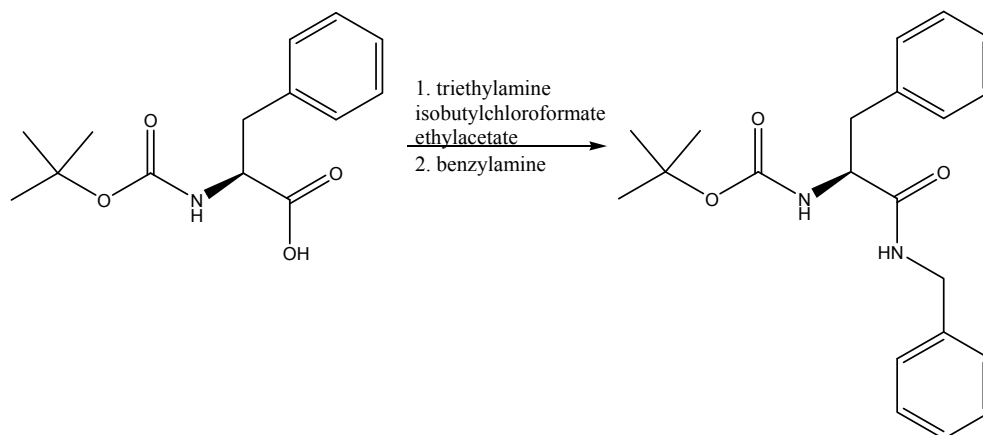


Figure 2.4: Modified reaction using a benzylamine quench instead of continuing to the diazomethane second step.

Triethylamine was replaced with tripropylamine in the reaction shown in Figure 2.4 to make (1-benzylcarbamoyl-2-phenyl-ethyl)-carbamic acid tert-butyl ester, followed by a benzylamine quench. All other conditions remained as previously mentioned except for this amine substitution (1.3 equiv). Under the actual reaction conditions, however, the tripropylamine formed a visible precipitate.

This same reaction was repeated using tributylamine instead of tripropylamine. All the conditions were the same as previously mentioned except for the substitution of the triethylamine with the tributylamine (1.3 equiv). With this substitution, no precipitate was formed. Additionally, the starting material was not observed when an aliquot of the reaction solution was analyzed by  $^1\text{H}$  NMR.

### **Calibration for Batch Reaction Results**

The reaction in the continuous flow reactor was monitored by LC-UV to determine conversions. In the batch reaction, the reaction was allowed to proceed for one hour. Calibration curves were prepared for the starting material, L-boc-phenylalanine, and for the product, (1-benzylcarbamoyl-2-phenyl-ethyl)-carbamic acid tert-butyl ester.

The calibration curve for the L-boc-phenylalanine was made without issue. The LC-UV spectrum of the pure product, (1-benzylcarbamoyl-2-phenyl-ethyl)-carbamic acid tert-butyl ester, however, had no peak at similar concentrations. The UV maximum for (1-benzylcarbamoyl-2-phenyl-ethyl)-carbamic acid tert-butyl ester was checked and determined to be 229 nm, which was the wavelength programmed into the diode array detector. Still no peak was observed for the (1-benzylcarbamoyl-2-phenyl-ethyl)-carbamic acid tert-butyl ester.

The analytical procedure was changed to use GC-MS. A sample of the pure product, (1-benzylcarbamoyl-2-phenyl-ethyl)-carbamic acid tert-butyl ester, benzylamine, and a decane standard [4:4:1 molar ratio] was run through the GC-MS. The GC-MS analysis, however, showed the product to decane ratio was 1:12, and the benzylamine to decane ratio was 1:5. These results are illustrated in Figure 2.5. These incorrect ratios suggest that the product was decomposing in the GC-MS.

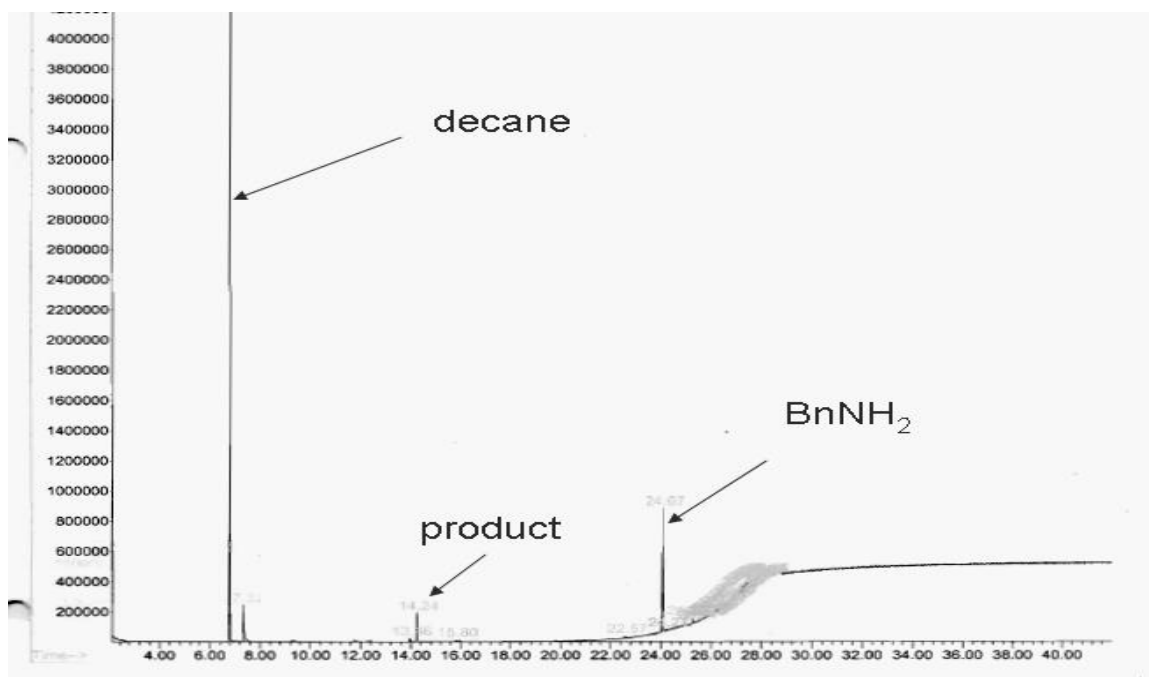


Figure 2.5: GC-MS spectrum of the sample containing a decane standard, benzylamine, and (1-benzylcarbamoyl-2-phenyl-ethyl)-carbamic acid tert-butyl ester product.

The benzylamine quench was replaced by propylamine (1.5 equiv) to form (2-phenyl-1-propylcarbamoyl-ethyl)-carbamic acid tert-butyl ester under the same reaction conditions. The TEA-HCl salt was filtered and the product was purified and isolated. The (2-phenyl-1-propylcarbamoyl-ethyl)-carbamic acid tert-butyl ester was characterized using  $^1\text{H}$  NMR,  $^{13}\text{C}$  NMR, and elemental analysis. A product peak in the LC (at 229 nm wavelength) was easily detected, so propylamine was used as the quench amine for the remainder of the project. The (2-phenyl-1-propylcarbamoyl-ethyl)-carbamic acid tert-butyl ester was then synthesized using tributylamine, rather than triethylamine, as the HCl scavenger. The product was isolated, purified and characterized using  $^1\text{H}$  NMR,  $^{13}\text{C}$  NMR, and elemental analysis. The characterization results of the (2-phenyl-1-propylcarbamoyl-ethyl)-carbamic acid tert-butyl ester produced using triethylamine and the tributylamine were the same.

### **Design and Use of 1<sup>st</sup> Generation Continuous Flow Reactor**

The first continuous flow reactor was built using parts already available in the laboratory. Two product streams entered the continuous flow reactor, mixed at a tee fitting, and combined to form a third stream. This product stream then dripped into a propylamine quench flask in an ice bath. The first reactant stream (L-boc-phenylalanine and tributylamine in ethyl acetate) was pumped into the continuous flow reactor using an Eldex HPLC pump. L-boc-phenylalanine (0.75 g) and dry tributylamine (0.7 mL) were combined in dry ethyl acetate (75 mL) to make a 0.04 M solution. The second reactant stream (isobutylchloroformate in ethyl acetate) was pumped into the continuous flow reactor using an Isco 500D syringe pump. The isobutylchloroformate (2.4 mL) was

added to dry ethyl acetate (450 mL) to make a 0.04 M solution. The reagents, Isco syringe pump, and continuous flow reactor were kept at temperature by a refrigerated constant temperature circulator (VWR 115) set at -20 °C. The same chiller was used throughout the project.

The continuous flow reactor itself was 6 ft long, with an inner diameter of 0.06 inches, and a thermocouple was used to measure the temperature at the exit. A picture of the 1<sup>st</sup> generation continuous flow reactor is shown in Figure 2.6. The concentration of the reactant streams was 0.04 M, chosen instead of the 0.75 M used in the batch reaction, to reduce the concerns of an exotherm formed upon the formation of the mixed anhydride. The quench solution, containing propylamine (0.16 mL) in ethyl acetate (5 mL), was chosen in order to have 1.5 equiv after a 10 min run with a flow rate of 3.3 mL/min. The flow rate for the Isco syringe pump was set at 3.3 mL/min to match the flow rate measured for the HPLC pump.

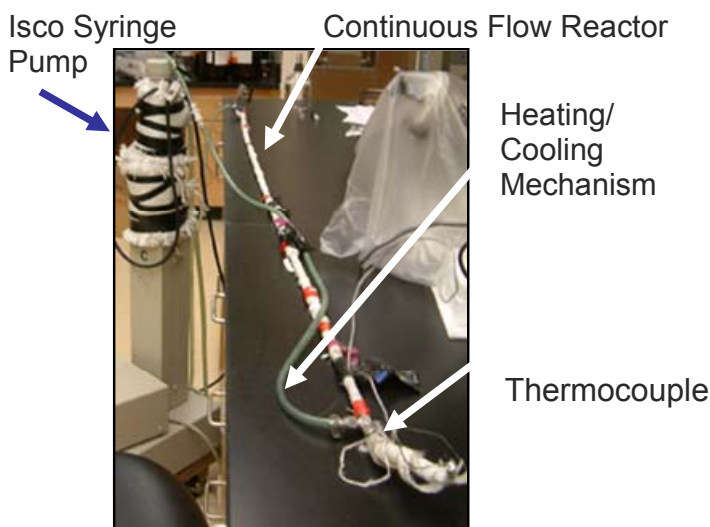


Figure 2.6: Picture of the 1st generation continuous flow reactor.

The product stream from the reactor was analyzed using LC-UV and  $^1\text{H}$  NMR, but no product was observed with either. The thermocouple placed at the end of the continuous flow reactor read  $-7.3\text{ }^\circ\text{C}$ , compared to the initial temperature of  $-20\text{ }^\circ\text{C}$ . Back of the envelope calculations confirmed that the exotherm from the reaction should not be this drastic, suggesting that the cooling mechanism of the continuous flow reactor was not sufficient. It was originally hypothesized that product was not observed due to inefficient cooling of the reactor.

### **Design and Use of 2<sup>nd</sup> Generation Continuous Flow Reactor**

The goal of the 2<sup>nd</sup> generation continuous flow reactor was to improve the heat transfer characteristics. A more compact continuous flow reactor was designed and built from  $1/16$  inch OD stainless steel (SS 314) tubing with a 7 mm ID. The entire reactor was coiled to enhance mixing and to fit inside the chiller. Keeping the entire reactor in the chiller provided better temperature control. Another significant change in this generation was that the use of a second Eldex HPLC pump, which added the quench stream directly to the reactor. The pump provided better control over the rate of the addition of the quench stream. Additionally, the thermocouple was added to the mixing point of the two reagent streams via a cross fitting, providing a more accurate understanding of any potential exotherms created during the reaction. The tubing lengths of the reactant streams were chosen by calculating how long it would take to cool a liquid from room temperature to  $-20\text{ }^\circ\text{C}$ . A picture of the 2<sup>nd</sup> generation continuous flow reactor can be seen in Figure 2.7, and a detailed schematic is depicted in Figure 2.8.

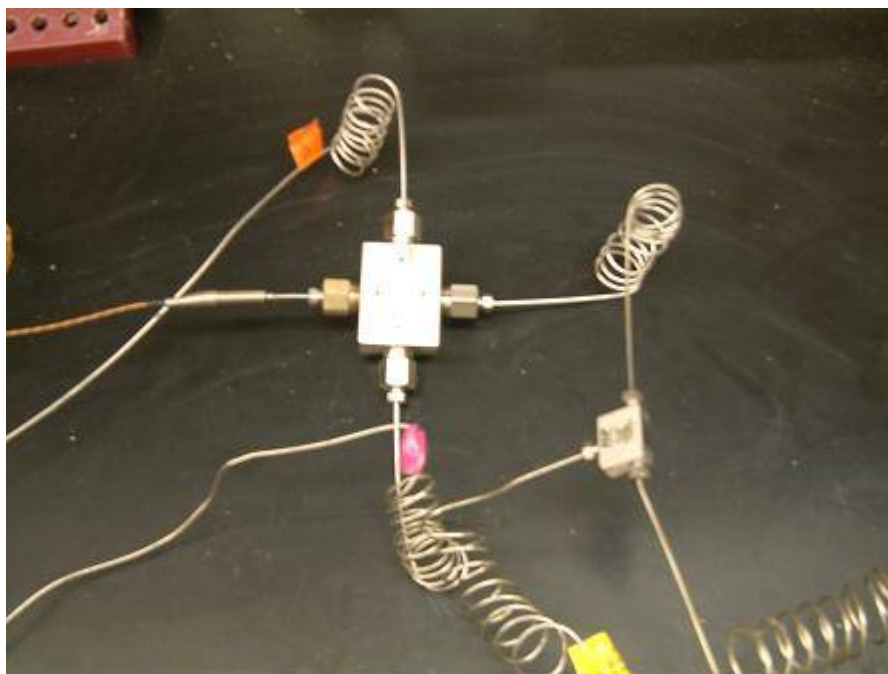


Figure 2.7: Picture of the 2nd generation continuous flow reactor.

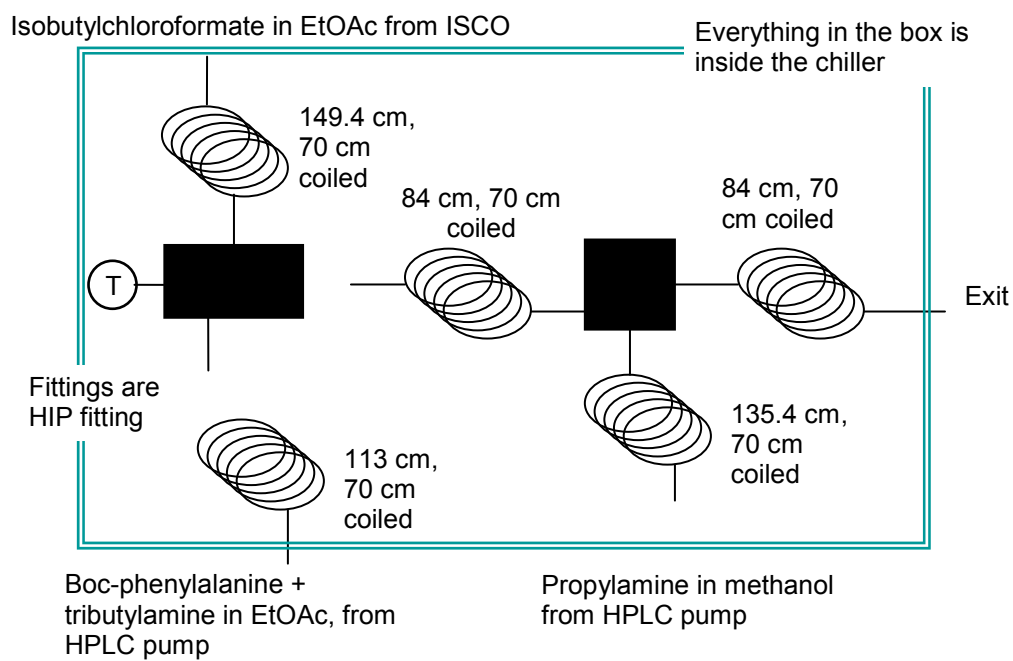


Figure 2.8: Specifications of the 2nd generation continuous flow reactor.



Another difference between the 1<sup>st</sup> and 2<sup>nd</sup> generation continuous flow reactors involved a solvent change. Previously during the batch reaction, a white precipitate formed upon the addition of the propylamine in ethyl acetate. Since the quench stream was added into the reactor directly with the 2<sup>nd</sup> generation, the propylamine was dissolved in MeOH instead of ethyl acetate. The product was soluble in MeOH, so the precipitate was avoided and the chance of clogging reduced.

The 2<sup>nd</sup> generation continuous flow reactor was run five times using the conditions summarized in Table 2.6. All experiments were run with the 2<sup>nd</sup> generation continuous flow reactor kept the chiller, which was set at -20 °C. The two reactant streams (L-boc-phenylalanine and tributylamine in ethyl acetate, and isobutylchloroformate in ethyl acetate) had concentration of 0.04 M. The propylamine quench was added in excess (0.3 M) for the first three runs, and at 1.5 equiv for the other two, with the concentrations adjusted for the different flow rates. Runs 2-4 were rotavapped after they were collected and analyzed using <sup>1</sup>H NMR. Run 5 was the only run that was worked up like the batch reactions with a saturated aqueous sodium bicarbonate wash, followed by a water wash and subsequent brine wash.

Table 2.6: Experimental parameters for 2<sup>nd</sup> generation continuous flow reactor (Runs 1-5).

Run	Concentration (M)				Flow Rate (mL/min)			Temp (°C)	Time (min)
	B-PA	TBA	IBCF	P-Amine	B-PA+TBA	IBCF	P-Amine		
1	0.04	0.04	0.04	0.3	2.4	2.4	2.0	-19.6	Pump broke
2	0.04	0.04	0.04	0.3	2.4	2.4	2.0	-19.7	6
3	0.04	0.04	0.04	0.3	2.4	2.4	2.0	-19.7	20
4	0.04	0.04	0.04	0.072	2.4	2.4	2.0	-19.9	20
5	0.04	0.04	0.04	0.072	2.4	2.4	2.0	-20.2	20

The flow rates of the two reactant streams were set at 2.4 mL/min, and the propylamine quench in MeOH was 2.0 mL/min. During Run 2, the product stream was collected at the outlet for six minutes. During Runs 3-5, the product stream was collected for 20 minutes. Regardless of the reactant flow rates, the temperature at the mixing point of the two reactant streams did not change.

The desired amide product was not seen by  $^1\text{H}$  NMR for any of the 2<sup>nd</sup> generation runs; all the  $^1\text{H}$  NMR spectra were consistent, however, from batch to batch. It was hypothesized that the continuous flow reactor and batch results were different due to the MOC since the batch was run in glassware and the reactor was SS. The batch reaction was completed in SS tubing, with a yield of 52% for the 0.04 M concentration. This compared favorably to the optimal isolated yield of 62% for the 0.04 M concentration done in glassware, suggesting that the stainless steel probably did not interfere with the reaction's reagents and/or intermediates. Another possibility considered was that the residence time in the continuous flow reactor might have been too short, not providing enough time for the reaction to take place. The reaction time was studied closely using batch reactions with the 0.04 M reaction concentration.

For the batch study, 0.04 M solutions were made by adding L-boc-phenylalanine (0.75 g), tributylamine (0.7 mL), isobutylchloroformate (0.4 mL) to dry ethyl acetate (75 mL). The solution was cooled in a -30 °C bath under argon gas. A separate solution of propylamine (0.1 mL, 1.5 equiv) was made in dry methanol (20 mL), providing a 0.06 M concentration. From this stock propylamine solution, 0.5 mL was added to 12 vials all kept in an ice bath. After the reaction started, 0.5 mL aliquots of the reaction solution were removed at various time intervals [1, 2, 3, 4, 5, 10, 15, 20, 25, 30, 45, 60 minutes]

and added to the propylamine vials. The quenched aliquots were analyzed on the LC-UV, and the previously determined calibration curves were used to determine the ratio of product to starting material. The 4 minute and 30 minutes samples were also analyzed by  $^1\text{H}$  NMR to confirm the LC-UV results. The results can be seen in Figure 2.9.

As shown in Figure 2.9, all the starting material had reacted and only product was observed after 30 minutes when the reaction was 0.04 M. Both the LC-UV and NMR analyses showed only starting material for all samples prior to the 5 minute sample. Since the residence time in the continuous reactor was estimated to be less than four minutes, it is possible that the reaction did not have sufficient time to occur. The reaction time was studied again using solutions at a concentration of 0.75 M instead of 0.04 M. The reaction was monitored as described previously. The product appeared after only 15 seconds. For subsequent runs, the reaction was still monitored by LC-UV, but the isolated yields were also determined for each reaction time.

For the isolated yield batch experiments, a 0.75 M stock solution of L-boc-phenylalanine and tributylamine was made in dry ethyl acetate. Each reaction used 2.8 mL of stock solution. Isobutylchloroformate (0.15 mL) was added to each reaction, and the reactions were allowed to proceed for 5, 15, and 30 seconds, and 1, 5, 10, and 20 minutes before the quench solution was added. All experiments were run in triplicate, and the isolated yield was determined for each. Melting point analysis and  $^1\text{H}$  NMR were used to confirm product purity. No product formation was observed at 5 seconds, and incomplete reactions at 15 and 30 seconds respectively provided a 20% and 30% isolated yield. The maximum yield of 76% was obtained after 1 minute of reaction time, as shown in Figure 2.10.

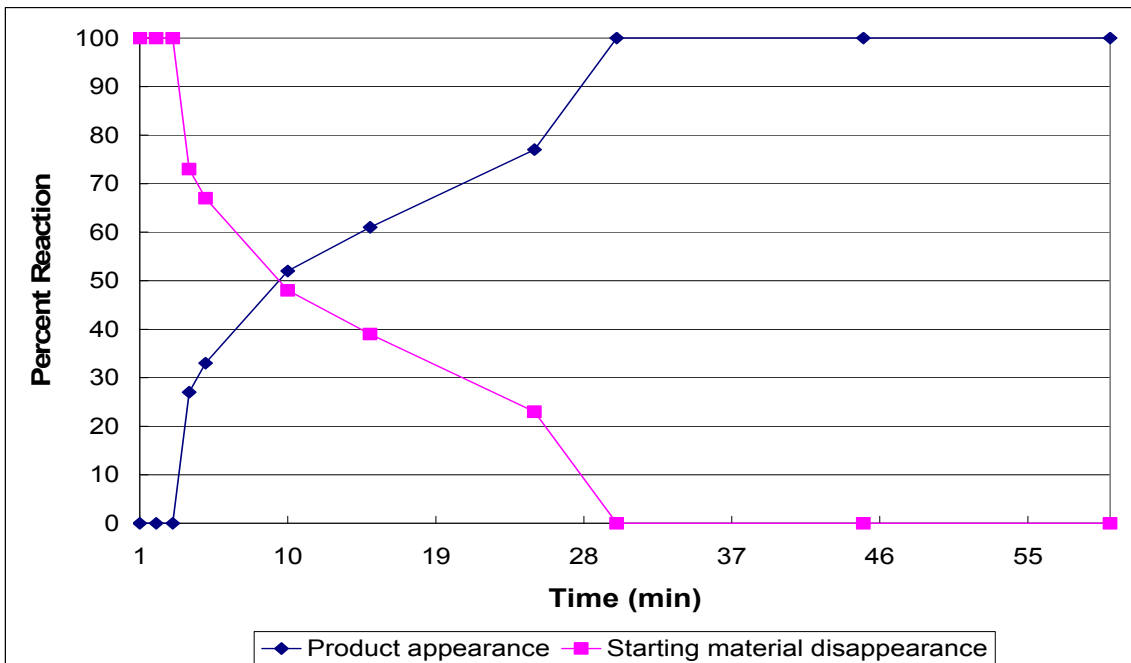


Figure 2.9: Batch reaction product appearance and starting material disappearance over time (-30 °C, 0.04 M reactants).

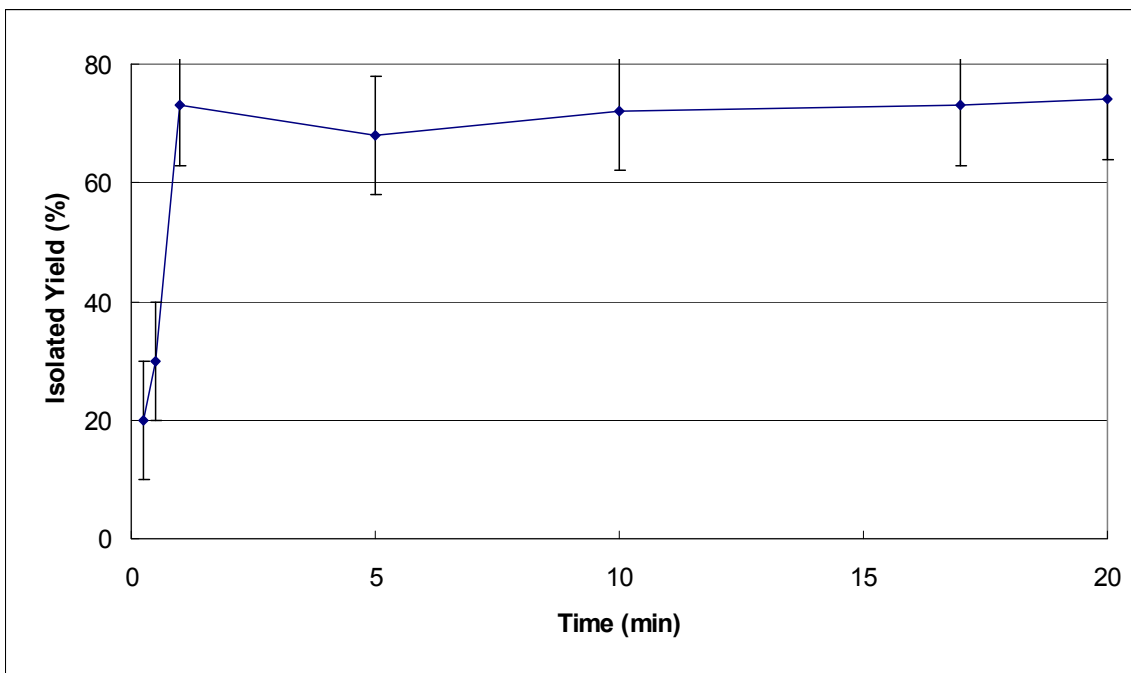


Figure 2.10: Batch reaction isolated yields obtained over time (0.75M, -30 °C).

A calculation showed that 526 cm tubing length was needed to provide 1 minute of residence time with the current continuous flow reactor configuration and conditions. The tubing length was increased to 583 cm to ensure full reaction, and three runs were performed. For each run, one reactant stream (0.75 M L-boc-phenylalanine and 0.75 M tributylamine in dry ethyl acetate) was added by an Eldex Recipro HPLC pump. The other reactant stream (0.75 M isobutylchloroformate in dry ethyl acetate) was added by a second Eldex Recipro HPLC pump. The concentration of the propylamine in dry methanol (1.35 M) was adjusted for the different flow rate, and was added downstream in the continuous flow reactor as the quench stream by a third Eldex Recipro HPLC pump.

The reactants streams were run for 2 minutes through the continuous flow reactor before beginning collection in order to avoid startup effects. The reaction mixture was then collected at the exit for 5 minutes. During the experiments, the chiller was set at -20 °C for Runs 1 and 2, and increased to -10 °C for Run 3. After Run 1, the flow rate was decreased to 0.8 mL/min, from 2.4 mL/min used previously, for the reactant streams. This flow rate change increased the residence time from 1 min to 3.4 min. With these changes, product was detected for the first time by <sup>1</sup>H NMR for all three runs. The isolated yield was 2% with Run 2. The reaction conditions are summarized in Table 2.7.

Table 2.7: Experimental conditions for 2<sup>nd</sup> generation continuous flow reactor. The best result provided 2% isolated yield (583 cm length).

Run	Flow Rate (mL/min)	Temp (°C)	Residence Time (min)
1	2.4	-20	1
2	0.8	-20	3.4
3	0.8	-10	3.4

After reviewing these results, two options were considered for improvement: increase the tubing length and decrease the tubing ID. The first option would increase the residence time, and the second could place the continuous flow reactor in a microreactor regime and thus hopefully improve the mixing. With these options in mind, a 3<sup>rd</sup> generation continuous flow reactor incorporating both ideas was built.

### **Design and Use of 3<sup>rd</sup> Generation Continuous Flow Reactor**

The 3<sup>rd</sup> generation continuous flow reactor was built from HPLC tubing containing a 0.17 mm ID. HPLC tubing offered several advantages over standard HIP tubing. First, the ID is guaranteed by the manufacturer. The tubing is also flexible and is cleaned of any particles prior to being sold, which helps minimize potential clogging. Agilent also offered a standard HPLC cleaning kit in case clogging did occur. A picture of the 3<sup>rd</sup> generation continuous flow reactor is shown in Figure 2.11. The blue tape on the reactor was used to label and distinguish different parts.

As depicted in Figure 2.12, the basic schematic of the 2<sup>nd</sup> generation reactor was retained. The reactor still had two streams: L-boc-phenylalanine and tributylamine in ethyl acetate, and isobutylchloroformate in ethyl acetate. The streams were pumped into the reactor individually; the reactants mixed at the cross fitting that contained a thermocouple to measure any possible exotherms occurring during the reaction. The propylamine quench in methanol was added by a third pump through a tee fitting. The original configuration used 400 cm of HPLC tubing between the cross fitting and the tee fitting. To further improve mixing, a HPLC mixer, containing stainless steel beads, was placed at the beginning of the reactant stream tubing.

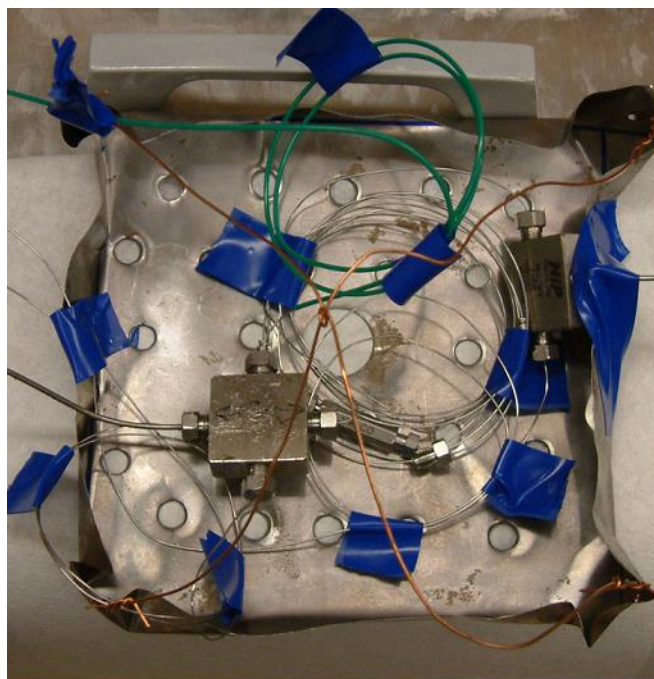


Figure 2.11: Photo of 3rd generation continuous flow reactor.

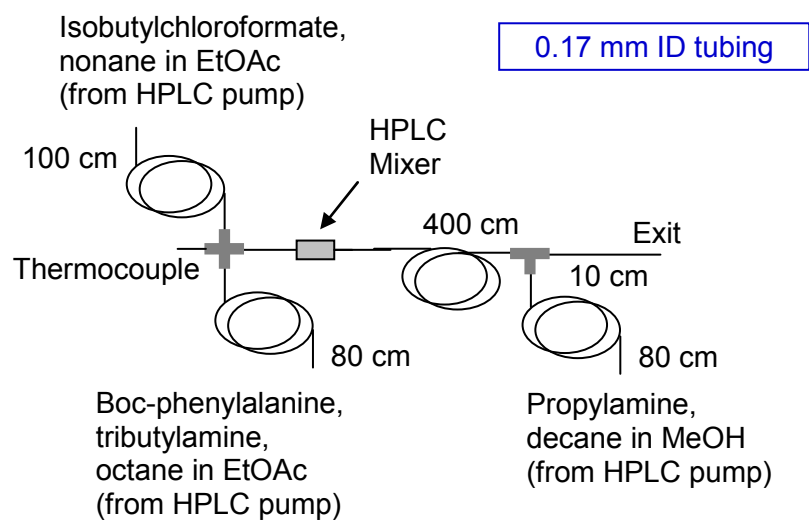


Figure 2.12: Schematic of the initial 3rd generation continuous flow reactor.

The HPLC pumps had a dial with numeral settings that do not correlate well with the flow rate. To control process parameters better, the flow rates of the three HPLC pumps were calibrated. After the calibration, the flow rate of both reactant pumps was set to 0.6 mL/min. The flow rate of the quench pump was set to 1.0 mL/min. The inherent system pressure drop, however, dropped the measured overall flow rate to 1.7 mL/min, which corresponded to a 5.4 second residence time.

The next continuous flow reactor study was done to determine the effect of temperature on the product yield. The reactor was run using a 0.75 M combined concentration of the L-boc-phenylalanine, tributylamine, and isobutylchloroformate in dry ethyl acetate. The propylamine in dry methanol quench stream was 1.5 M. The chiller was set at seven different temperatures for the experimental runs: -20 °C, -10 °C, 0 °C, 10 °C, 20 °C, 25 °C, and 50 °C. The reactants and quench were pumped through the reactor for 2 minutes before each temperature change to flush the reactor and avoid startup effects. For each temperature, the product stream was collected in duplicate. The purity of the isolated product was confirmed using both melting point analysis and <sup>1</sup>H NMR. The -20 °C showed only trace amounts of product in the <sup>1</sup>H NMR, but the rest of the temperatures had measurable isolated yield. The results are illustrated in Figure 2.13. These results demonstrate that, for this continuous flow reactor configuration, isolated yield improves with increasing temperature.



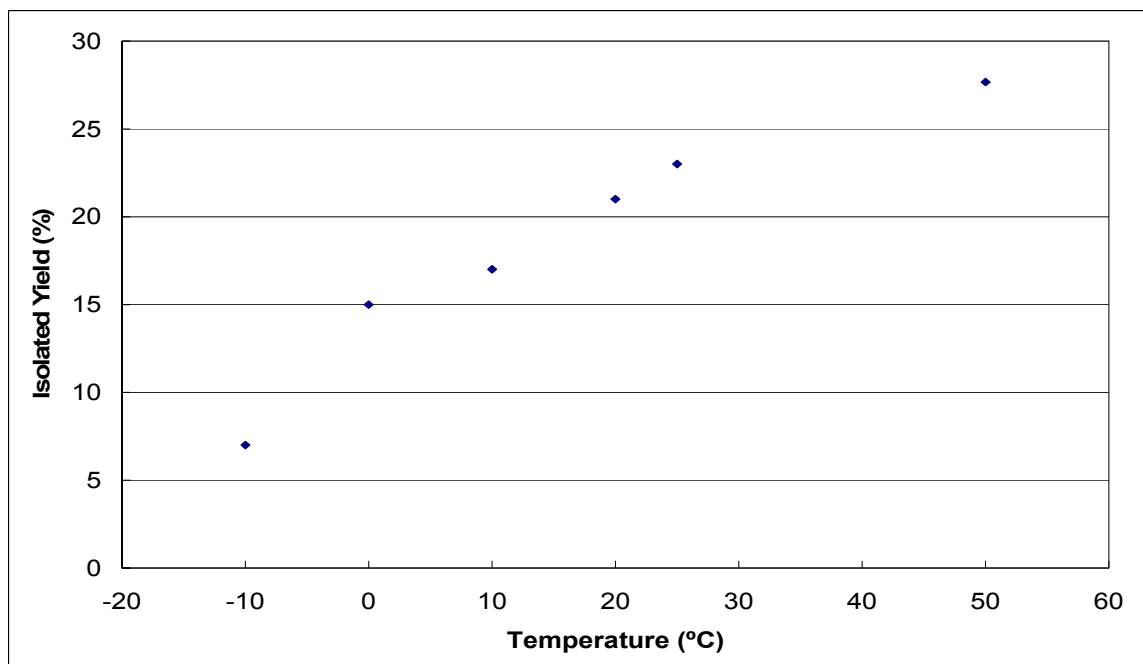


Figure 2.13: 3rd generation continuous flow reactor isolated yield results at various temperatures (5 second residence time).

Increasing the temperature from 25 to 50 °C increased the yield only within error, while increasing in temperature from -20 to 25 °C resulted in a definitive improvement in yield. The ability to run this reaction above -20 °C in the continuous flow reactor is significant. In batch mode, the optimal temperature for this reaction is -20 °C, which is attributed to the temperature sensitive nature of the mixed anhydride intermediate. With the improved heat transfer of the continuous flow reactor, however, the intermediate can be run at higher ambient conditions. Performing this reaction at room temperature could drastically reduce energy costs. Additionally, the 3<sup>rd</sup> generation continuous flow reactor yields were significantly better than the 2<sup>nd</sup> generation continuous flow reactor yields (25% compared to 2%). The low yield, however, clearly indicated that the process was not fully optimized. The length of the tubing was increased to allow longer reaction time.

The 3<sup>rd</sup> generation continuous flow reactor was modified to increase the length of tubing from 400 cm to 720 cm. The new schematic can be seen in Figure 2.14. Another temperature study was conducted in the continuous flow reactor at 10 °C, 25 °C, and 50 °C with the 0.75 M concentration. All results were analyzed by isolating the yields. The two reactant streams and the product stream were flushed through the continuous flow reactor for 2 minutes for each temperature. The product stream was collected at the end of the reactor for three minutes at each temperature, and each temperature was tested in duplicate. The isolated yields for the 720 cm continuous flow reactor were significantly lower, however, than the isolated yield for the 400 cm continuous flow reactor. One example is the yields for 50 °C. At this temperature, the 720 cm reactor provided 18+/-5% isolated yield, compared to the 400 cm reactor giving 28+/-% isolated yield. These results suggested that other factors were influencing the yield.

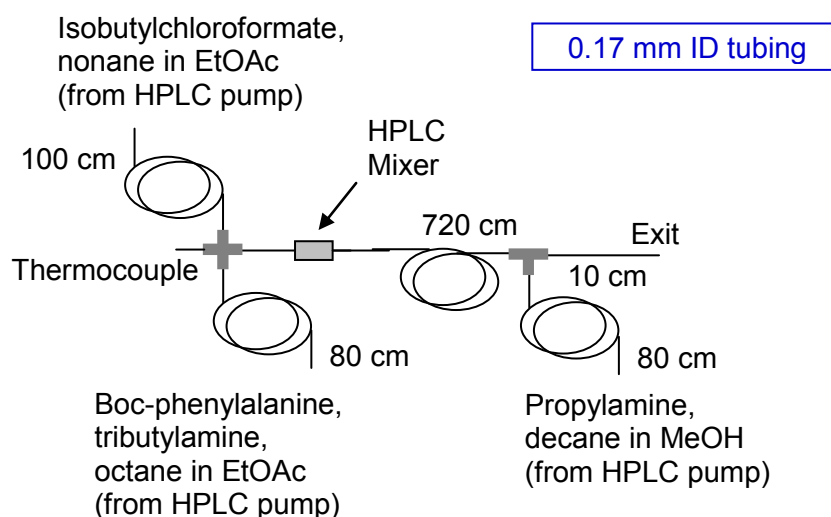


Figure 2.14: Schematic of the 3<sup>rd</sup> generation continuous flow reactor with increased tubing length to 720 cm.

One concern was that the flow rates were not actually the expected amounts. A detailed study was undertaken to ensure the proper ratios of starting material were being pumped into the reactor. An analysis method using GC-MS was devised to ensure the streams were mixing in the proper ratios. Alkanes (octane, nonane, and decane) were added to each stream (1%) as a trace. Octane was added to one reactant stream, nonane to the second reactant stream, and decane to the quench stream. The exit stream from the continuous flow reactor was then analyzed using GC-MS, and the area of the hydrocarbon peaks was used to determine the reactant ratios. Since the reactant streams are added in a 1:1 ratio and the quench stream is added at double the flow, the relative ratio of the alkane peaks should be 25:25:50 for octane, nonane, and decane.

For subsequent experiments, octane (1%) was added to the first reactant stream (L-boc-phenylalanine and tributylamine in dry ethyl acetate) and nonane (1%) was added to the other reactant stream (isobutylchloroformate in dry ethyl acetate). When combined, these streams provided a concentration of 0.75 M for all reactants. Decane (1%) was added to the 1.5 M quench stream (propylamine in methanol). The configuration can be seen in Figure 2.15. The residence time of this system was measured at 19.2 seconds.

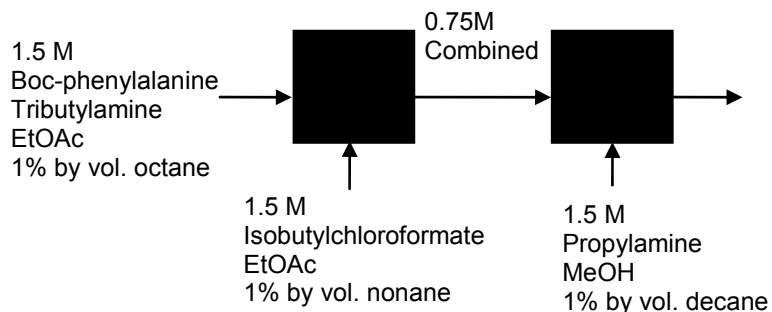


Figure 2.15: Optimize pumps by flow rate ratios using a hydrocarbon trace.

To compensate for the increased residence time, the continuous flow reactor was flushed with the reactant and quench streams for 3 minutes. During the experimental runs, 5 mL of the product stream was collected in duplicate. The hydrocarbon ratios were systematically monitored by GC-FID, and determined to be 26% (octane), 27% (nonane), and 47% (decane). With the trace system implemented to know when pumps were malfunctioning, the actual isolated yield for the 720 cm tubing was 30+/-5% (compared to 20+/-5% for the 400 cm tubing) at 25 °C. The residence time of 19.2 seconds, however, was nearly 4x the residence time of the 400 cm reactor (5.4 seconds). Although the residence time was 4x greater, the yield only increased by 50%, so residence time could not be the only issue. These results strongly suggested that the limiting factor was mixing.

In order to improve the mixing, a HPLC column (25 cm) was stripped of its original packing material and repacked with 3 mm glass beads. This tubular reactor was added after 320 cm of tubing, placing it approximately in the middle of the system. The schematic of this continuous flow system is shown in Figure 2.16. The continuous flow reactor was run using the same concentrations, flow rates, and experimental procedures mentioned previously. The hydrocarbon trace portrayed a flow rate profile of 17% octane, 23% nonane, and 60% decane. The isolated yield was 40+/-5%, comparing favorably to the previous 30+/-5%.

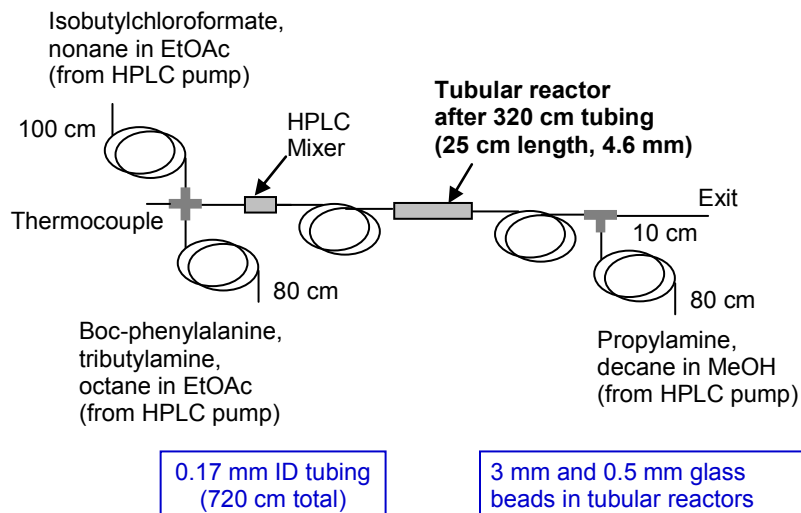


Figure 2.16: Schematic of the one-tubular reactor 3rd generation continuous flow reactor.

Other mixing options were also examined. Literature results had shown that sonication can increase mixing in microreactors.<sup>13</sup> To test the effect on our system, the continuous flow reactor was placed in a sonicator. Identical experiments were run with and without turning on the sonicator. The isolated yield from the sonicator run was 30+/-5%, which was not an improvement. This alternative was not investigated further. Another idea to improve mixing had been to add 0.5 mm glass beads in the cross fitting to enhance mixing at the point of contact of the reaction streams. The beads added to the cross fitting clogged the system, however, so this route was also abandoned.

Another mixing option tested was to replace the 3 mm packing beads with smaller diameter beads (0.5 mm) in the tubular reactor. Packing the reactor with smaller beads could induce more turbulence, and therefore better mixing. The isolated yield increased to 47+/-5% at room temperature, which was approximately a 5% improvement over the 3 mm glass beads.

At this juncture, the pumping inconsistencies became significantly worse. Using the hydrocarbon trace allowed us to determine quality experimental runs from erroneous ones, but the unsuitable runs became more frequent. It was decided to purchase two new Eldex HPLC pumps. This time, Eldex Recipro Optos 2SM pumps were chosen for the system. These pumps provided digital flow rate settings, allowing the pumps to be more closely controlled. Additionally, the pump flow rates could go to the minimum 0.1 mL/min, which was substantially lower than the previous pumps.

Since the tubular reactor filled with glass beads had the most impact on yield, a second tubular reactor was added to the system. This tubular reactor was 15 cm long with a 4 mm ID. The silica packing inside an HPLC column was again removed, and the column was repacked with 0.5 mm glass beads. This tubular reactor was added after 240 cm of tubing, and the first tubular reactor was moved to after 480 cm of tubing, as seen in Figure 2.17. Experiments were run with the same concentrations, flow rates, and experimental procedures mentioned previously. The flow rates were then optimized for the system at room temperature, and the best isolated yield of 60 $\pm$ 5% was obtained using a 0.1 mL/min flow rate. The impact of various flow rates on the isolated yield is shown in Figure 2.18. The significant improvement gained by changing the flow rate from 0.3 mL/min to 0.1 mL/min was probably due to the longer residence time with the slower flow rate. Conversely, the improvement from 0.05 mL/min to 0.1 mL/min is likely due to improved mixing with the faster flow rate. The balance between these two factors demonstrated the need to optimize both flow rate and mixing.

Bends have also been shown to induce chaotic mixing in systems with laminar flow.<sup>14</sup> To test this option, sharp bends (approximately 1 cm) were induced in an 80 cm piece of HPLC tubing. The length of bent tubing was added after 160 cm of tubing (replacing the regular 80 cm length of tubing already there), and a reactant flow rate of 0.3 mL/min was used. Experiments in the continuous flow reactor were run using the same concentrations and experimental procedures. The isolated yield was 55+/-5% compared to 51+/-5% without the bent tubing at room temperature. The slight improvement in yields was probably not significant because it was within the expected experimental error.

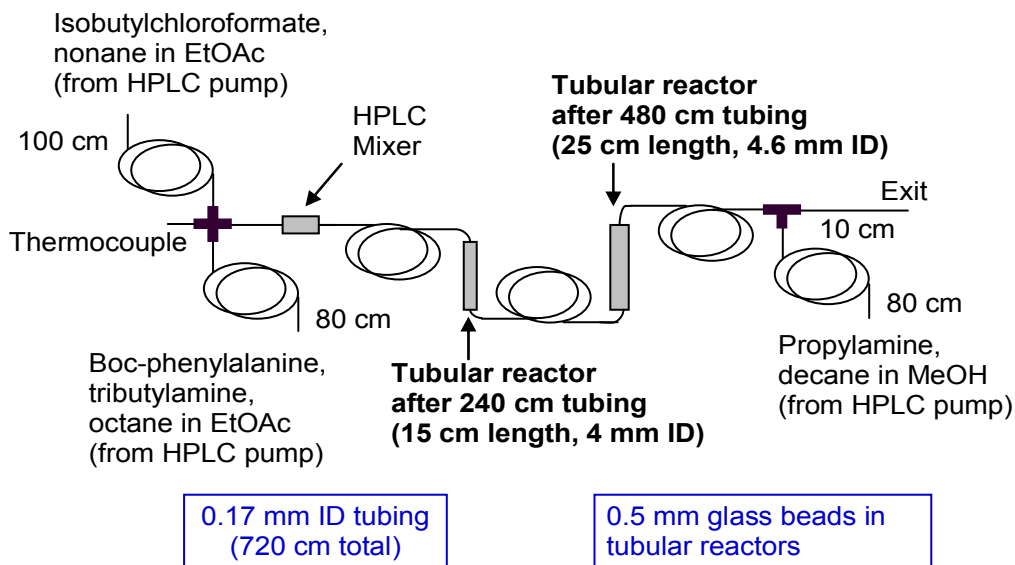


Figure 2.17: Schematic of the two-tubular reactor 3rd generation continuous flow reactor.

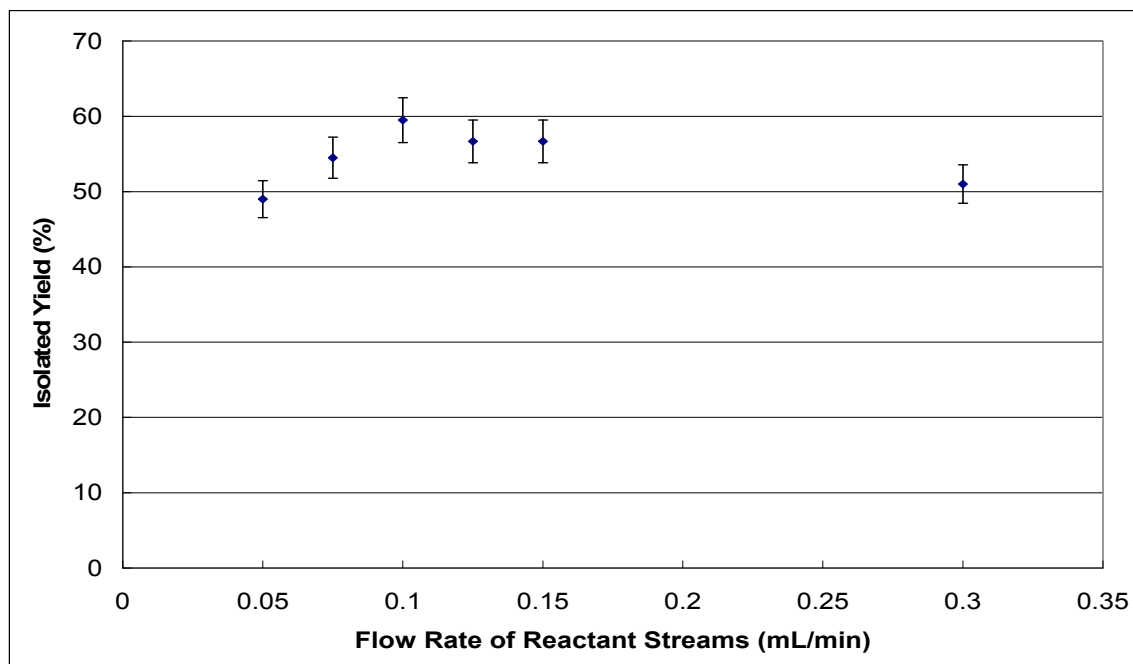


Figure 2.18: Effect of flow rate on isolated yield in two-tubular reactors continuous flow reactor system at room temperature.

With the success of the two tubular reactor system, two additional tubular reactors were built, packed with 0.5 mm glass beads, and added to the system. Both new tubular reactors were 20 cm long with a 4.6 mm ID. Each reactor was filled with 0.5 mm glass beads, and the beads were packed using a VWR vortex mixer. One tubular reactor was added after 320 cm of tubing, and the other tubular reactor was added after 560 cm of tubing. The original two tubular reactors were left in their previous position, providing a four-tubular reactor continuous flow reactor system. The schematic of the four-tubular reactor system is depicted in Figure 2.19.



The reactor configuration change meant the flow rates needed to be optimized again. Various flow rates between 0.1 mL/min and 0.4 mL/min were tested, and the isolated yield was determined for each flow rate. As can be seen in Figure 2.20, the best flow rate was 0.2 mL/min and provided an isolated yield of 53+/-5% at room temperature. It had not been expected that the yield would decrease with extended residence time and increased mixing. With a longer residence time, however, the product can start degrading because the intermediate is not stable at room temperature. When the experiments were repeated at the lower temperatures of -20 °C and 0 °C, the isolated yields increased. This result, seen in Figure 2.21, further confirmed that the decomposition of the unstable intermediate is minimized at lower temperatures.

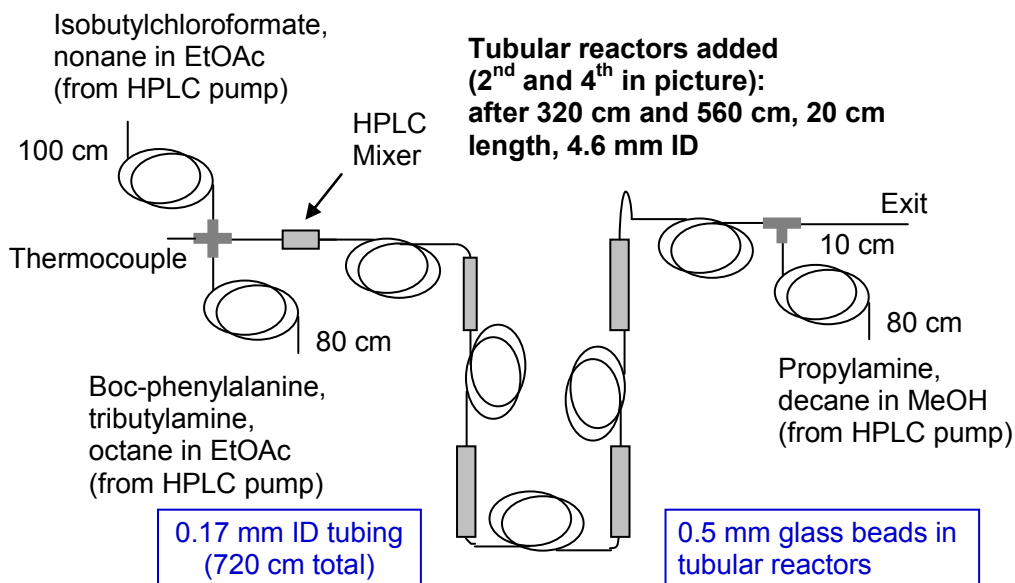


Figure 2.19: Schematic of the four-tubular reactor 3rd generation continuous flow reactor.

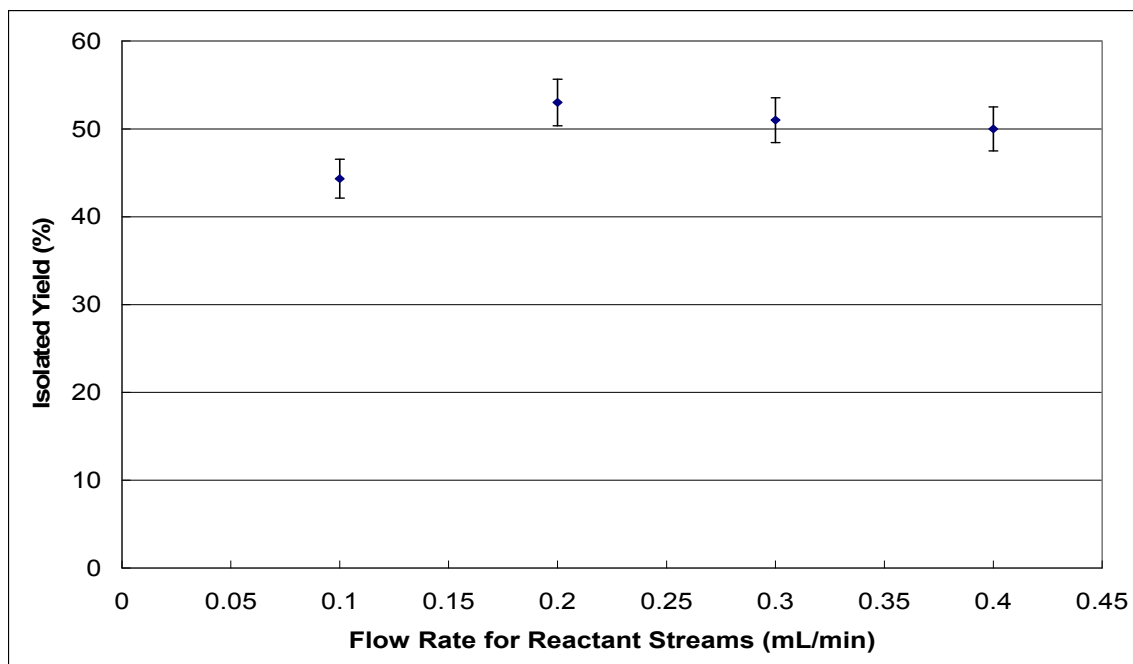


Figure 2.20: Effect of flow rate on isolated yield with four-tubular reactor continuous flow reactor system at room temperature.

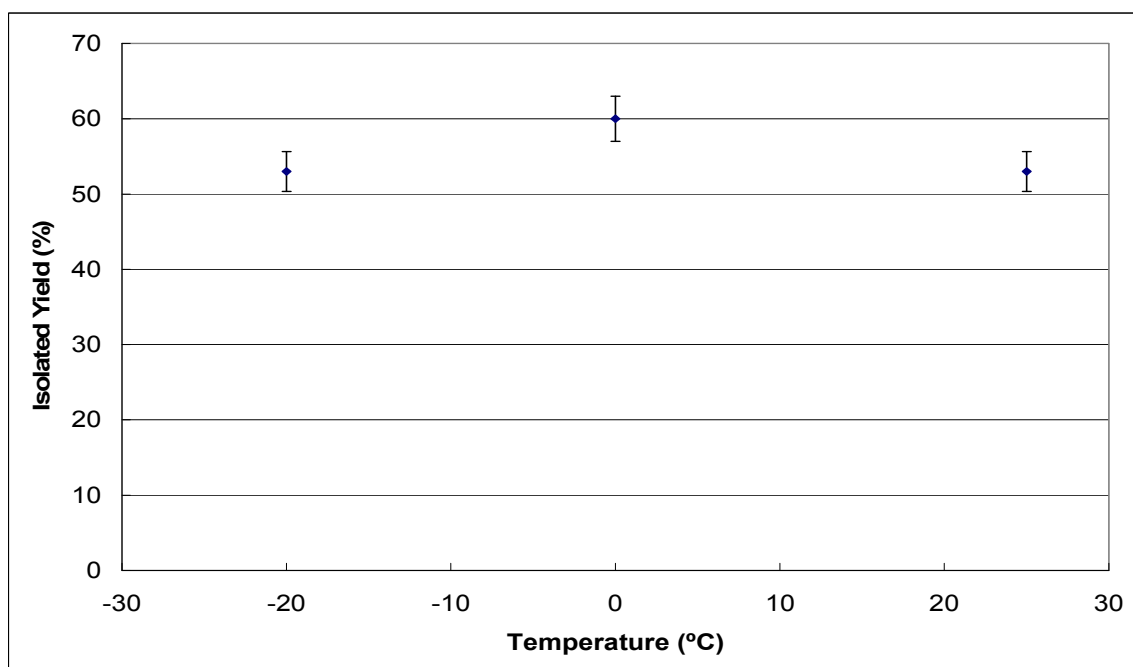


Figure 2.21: Effect of temperature on the isolated yield with four-tubular reactor continuous flow reactor system at 0.2 mL/min flow rate.

The best isolated yield obtained from the four-tubular reactor system was 60+/-5% at 0 °C. This result was unexpected because, as shown in Figure 2.13, increased temperature improved the yield in the 1<sup>st</sup> generation continuous flow reactor. This trend was attributed to the excellent heat transfer capabilities and mixing of the continuous flow reactor. One interpretation of the differing results in Figure 2.21, however, is that the residence time of this continuous flow reactor configuration is too long for the unstable mixed anhydride intermediate to remain at room temperature. To test this hypothesis, the batch reaction was tested at room temperature instead of its original temperature of -20 °C.

The first reaction was quenched after 16 minutes to mimic the residence time of the two-tubular reactor continuous flow reactor and gave an isolated yield of 37+/-5%. The second reaction was quenched after 1 hour, like the original batch reaction conditions, and gave an isolated yield of 27+/-5%. The drop in isolated yield between these two reaction times confirmed that the mixed anhydride intermediate decomposed over time at room temperature. The instability of the mixed anhydride intermediate meant that the two-tubular reactor configuration is superior to the four-tubular reactor due to shorter residence times.

The batch experiment done at 25 °C also clearly demonstrated that the two-tubular reactor continuous flow reactor was superior to the batch reaction at the same temperature. The continuous flow reactor gave an isolated yield of 60+/-5%, while the batch reaction was only 37+/-5%. The excellent heat transfer capabilities of the continuous flow reactor clearly make a difference with the reaction performances when compared to a batch-mode process.

One additional modification was made to try improving the yield of the continuous flow reactor. Increasing the equivalents of isobutylchloroformate (2x and 3x excess) had no significant effect on the isolated yield. At this juncture, it was decided enough information had been learned 3<sup>rd</sup> generation continuous flow reactor to design and build a new, more effective system.

### **Coiled Continuous Flow Reactor**

Although the 3<sup>rd</sup> generation continuous flow reactor performed, well, it had become quite complex throughout its development. Additionally, during the various tests of the 3<sup>rd</sup> generation continuous flow reactor, it became obvious that the HPLC tubing was playing only a minimal role and could be eliminated. The resulting design, called the coiled continuous flow reactor, was expected to have similar performance yet greatly simplify the system. Besides keeping the advantages of excellent heat transfer and improved safety, other benefits, such cost reduction and chance of clogging, were gained by implementing this system. The coiled continuous flow reactor was constructed of stainless steel (314 SS) tubing, was 45 cm long, and had a 4.6 mm ID. The reactor was again packed with 0.5 mm diameter glass beads. A schematic of the continuous flow reactor is depicted in Figure 2.22, and a photograph can be seen in Figure 2.23.

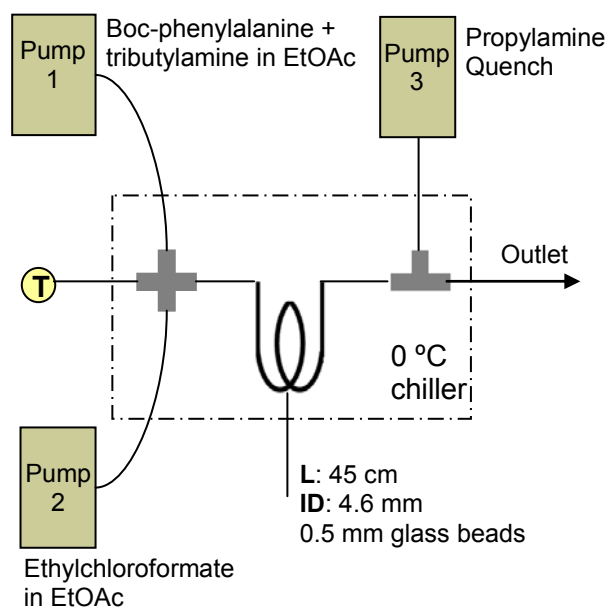


Figure 2.22: Schematic of coiled continuous flow reactor using propylamine quench.



Figure 2.23: Photograph of the coiled continuous flow reactor.

It became apparent while switching to the coiled continuous flow reactor that the isobutylchloroformate pump was corroding, despite the vendor's claims that the stainless steel pump was compatible with the chemical. We hypothesized that despite using dry solvents, enough water was still available to form hydrochloric acid from the isobutylchloroformate. A third pump was ordered, an Eldex Recipro A-60-SF, which contained only chlorotrifluoroethylene (CTFE) wetted parts. CTFE is known to be highly resistant to hydrochloric acid. The Optos pump was cleaned and used instead of the final Eldex Recipro AA pump.

At this point, it was also decided to complete the second step of the synthesis, the formation of the diazoketone, in the continuous flow reactor. Before running any experiments in the continuous reactor, the reaction of the mixed anhydride with trimethylsilyl diazomethane was completed in the batch process. As shown in Figure 2.1, the original synthesis used diazomethane. We decided to change this reactant, however, and use trimethylsilyl diazomethane instead, which is a safer alternative to diazomethane. For our reaction, a procedure analogous to one reported in the literature was chosen. The mixed anhydride was formed first, and then was reacted with trimethylsilyl diazomethane to form a diazoketone. This reaction is illustrated in Figure 2.24.<sup>11</sup>

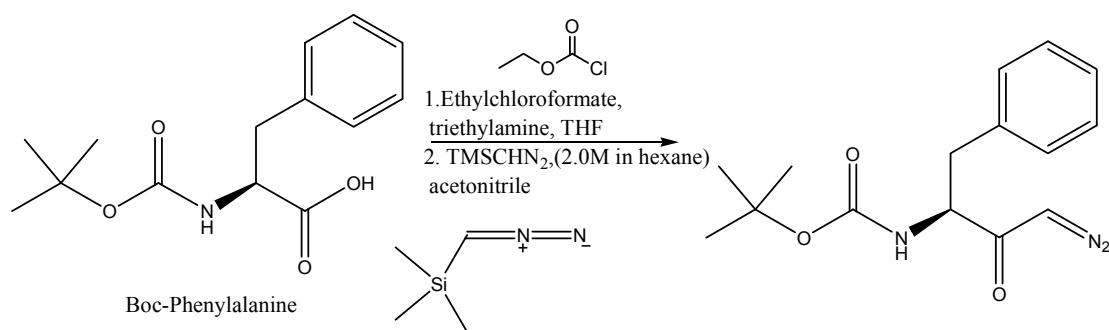


Figure 2.24: Diazoketone synthesis using trimethylsilyl diazomethane.

The synthesis was first performed using L-boc-phenylalanine (1 equiv), isobutylchloroformate (1.3 equiv), and tributylamine (1.3 equiv) in THF (0.2 M), followed by trimethylsilyl diazomethane (3 mL of 2.0 M solution in hexane) in acetonitrile (0.6 M). This provided a 32% isolated yield of the 1-(benzyl-3-diazo-2-oxopropyl)-carbamic acid tert-butyl ester. The reaction conditions were varied to optimize the system, as shown in Table 2.8. The biggest effect came from switching isobutylchloroformate to ethylchloroformate, resulting in a nearly double isolated yield (78%). It was hypothesized that the increased yield was due to the smaller size of the ethyl group compared to the isobutyl group, reducing the steric hindrance and allowing easier addition from the trimethylsilyl diazomethane.

After obtaining a similar yield as reported in the literature, the reaction was then optimized for use in a coiled continuous flow reactor. Tributylamine was again substituted for triethylamine to keep the hydrochloride salt from crashing out of the reaction mixture. The solvent was also changed to ethyl acetate, since that is what was used for the previous mixed anhydride synthesis. The final reaction for the continuous flow reactor is shown in Figure 2.25.

Table 2.8: Variables changed during optimization of the diazoketone reaction.

Isolated Yield	Variable Changed
32%	Standard reaction using isobutylchloroformate
23%	Trimethylsilyl diazomethane purchased as 2.0 M in diethyl ether
25%	Trimethylsilyl diazomethane - 3 equivalents (9 mmol)
78%	Ethylchloroformate
66%	Tributylamine with ethylchloroformate
61%	Ethyl acetate (instead of THF) with ethylchloroformate

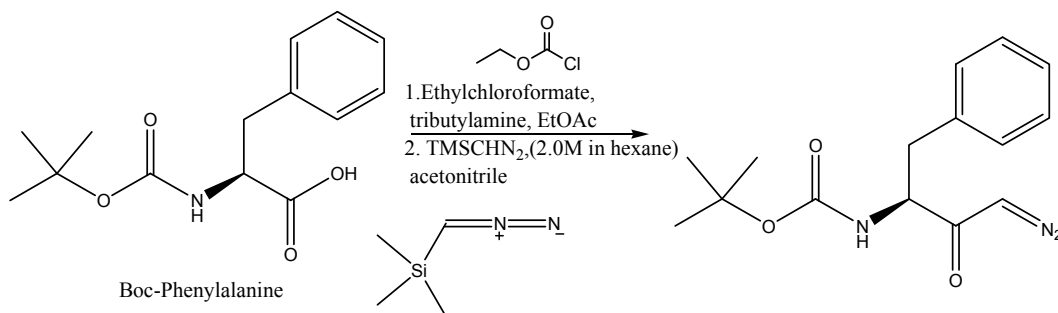


Figure 2.25: Diazoketone synthesis with reactants used for batch reactions.

Before running the reaction in the coiled continuous flow reactor, an estimation of the optimal reaction time was required to set up flow rates. The first step of the reaction now used isobutylchloroformate instead of ethylchloroformate, so it needed to be monitored with the propylamine quench. Additionally, the second step involving the addition of the trimethylsilyl diazomethane needed to be understood before setting up another continuous flow reactor for that reaction.

As before, calibration curves of the propylamine quench product, (2-phenyl-1-propylcarbamoylethyl)-carbamic acid tert-butyl ester, and the diazoketone, (1-benzyl-3-diazo-2-oxo-propyl)-carbamic acid tert-butyl ester were prepared on the LC-UV. Once the calibration curve was completed, the batch reaction was tested with ethylchloroformate and the propylamine quench for 16 and 30 minutes. Both reactions gave a peak on the LC-UV correlating to 100% yield. This batch test proved that the reactants only needed to be in the continuous flow reactor for 16 minutes.



The first step of the synthesis was then run in the coiled continuous flow reactor. The new Eldex Recipro CTFE pump added a 1.5 M solution of ethylchloroformate, anisole (the internal standard), and nonane in ethyl acetate. The 1.5 M L-boc-phenylalanine and tributylamine solution was added by an Eldex Optos pump. The quench stream was added by the second Eldex Optos pump. The coiled continuous flow reactor was run using 1.5 M concentrations, and the entire continuous flow reactor was kept in a chiller set at 0 °C. The results were monitored by LC-UV, and the theoretical concentration was determined using the hydrocarbon trace ratios measured by GC-FID. The residence time of the coiled continuous flow reactor was estimated to be 16 minutes, which matched the time determined from the batch experiments. The continuous flow reactor provided quantitative yield of the quench product, as measured by LC-UV.

With these results, the design of the continuous flow reactor for the first step of the synthesis was deemed successful. All focus then turned to optimizing the second synthetic step as well. Batch reactions were again run to determine the necessary experimental conditions for this step.

The diazoketone reaction time was monitored by sampling at time intervals, and running the samples through the LC-UV. The maximum yield of 100% was obtained after 2 hours, although the concentration reached a plateau after this point (within error). The results can be seen in Figure 2.26. These results, however, were obtained using the literature concentration (2.0 M) for the reactants. The reaction was accelerated by increasing the reactant concentrations of the first step to 0.75 M, the concentration used in previous continuous flow reactor experiments. The concentration of the trimethylsilyl diazomethane in acetonitrile, however, remained the same for safety considerations.

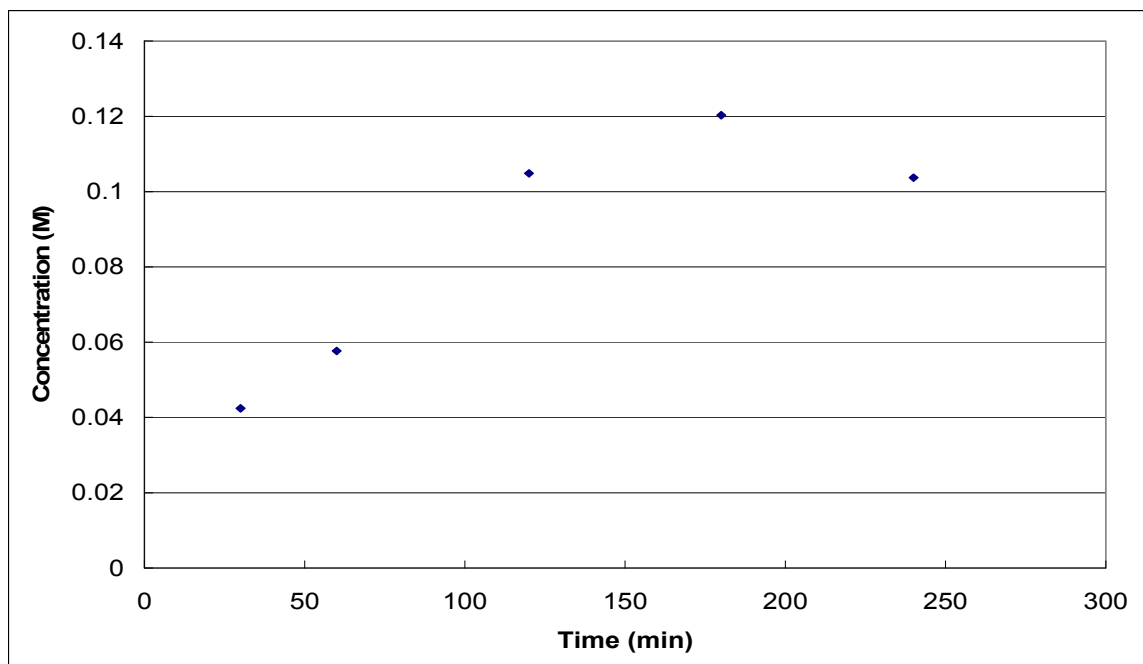


Figure 2.26: Diazoketone reaction over time for 0.2 M reactant concentration. Results analyzed by LC-UV.

Batch reaction studies were completed with the concentration of the reagents increased to 0.75 M. Aliquots were taken at 10, 20, 30, 45, 90, and 120 minutes, and the samples were analyzed by LC-UV. An internal standard, anisole, was added to improve analysis accuracy. Quantitative yield of the diazoketone product, within the inherent 3% analytical error, was obtained after as little as 10 minutes.

Since there was no appreciable difference between the 10 and 20 minute batch reactions, it was decided to add a second continuous flow reactor identical to the first one. The overall design has the product from the first reactor entered a tee fitting, where it mixes with the trimethylsilyl diazomethane stream. The diazoketone is formed in the second reactor. This experimental setup is shown in Figure 2.27.

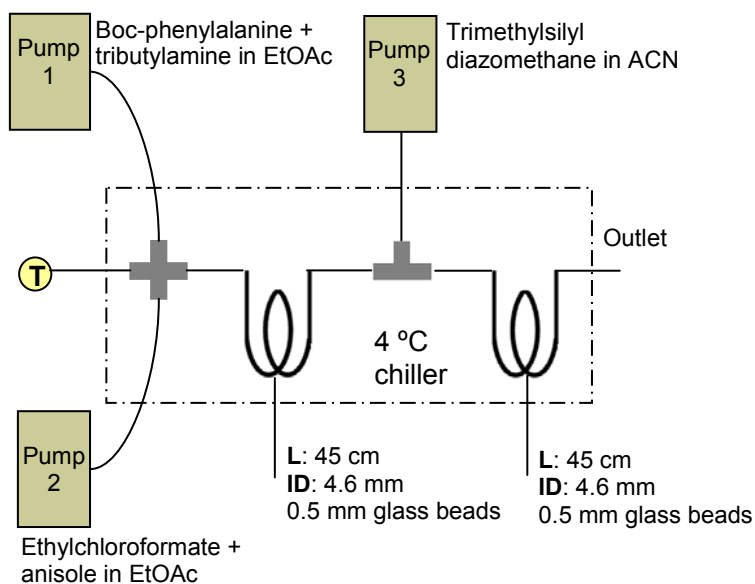


Figure 2.27: Schematic of the two-coiled continuous flow reactor system. The diazoketone product is formed in the second reactor.

In the two-coiled continuous flow reactor system, both coiled reactors were placed in the chiller set at 4 °C. The 1.5 M solution of L-boc-phenylalanine and tributylamine in ethyl acetate (with 1% octane, the hydrocarbon trace) were added to the cross fitting by an Eldex Optos pump. The 1.5 M solution of ethylchloroformate in ethyl acetate (with anisole, the internal standard, and 1% nonane) was added to the same cross fitting by the Eldex CTFE pump. The 0.6 M solution of trimethylsilyl diazomethane in acetonitrile (with 1% decane) was added to the tee fitting placed between reactors by the other Eldex Optos pump.

The results were monitored by LC-UV, and the theoretical concentration was determined using the hydrocarbon trace ratios measured by GC-FID. The residence time of each continuous flow reactor was estimated to be 16 minutes, for a total reaction time of 32 minutes. With this system, the diazoketone was produced in quantitative yield. This remarkable success means that the simple design of two coiled continuous flow reactors allows a two step synthesis, involving a very temperature-sensitive intermediate, to be carried out at quantitative yield.

## **CONCLUSIONS AND RECOMMENDATIONS**

The reaction of L-boc-phenylalanine with an alkylchloroformate to form a mixed anhydride, followed by reaction with trimethylsilyl diazomethane, was explored in a continuous flow reactor. In the batch mode, the optimal temperature of the first step of the reaction is -20 °C because the mixed anhydride is temperature sensitive and decomposes readily above 0 °C. The best overall yield reported in the literature for this sequence was 78%. During the course of this research project, several continuous flow reactor configurations were designed and built. The final configuration, which involved two coiled continuous flow reactors packed with glass beads, is both simple and extremely efficient.

The two-step reaction sequence was carried out at 4 °C with quantitative yield obtained for the diazoketone product. This remarkable result clearly demonstrates that a continuous flow process can not only improve yields (and product quality) over a batch process, but it can also utilize cheaper and safer reagents. For example, our system

utilized the cheaper reagent ethylchloroformate instead of isobutylchloroformate. Trimethylsilyl diazomethane, a safe substitute for diazomethane, was also used successfully. Finally, energy requirements can be reduced by eliminating the need for low reaction temperatures.

Although this project was considered a complete success, there are improvements that could be made. The final continuous flow reactor design was not fully optimized; instead, the second reactor was built identical to the first. It probably could have been a shorter length, which would have lessened the residence time but also decreased the overall cost. While the difference of a few inches is not significant for one single reactor, if many of these were to be made (scale-out), then it could be important.

Several aspects of the continuous flow reactors have not been fully characterized. While a rough Reynolds number was calculated to ensure the system was in the laminar regime, many flow characteristics are unknown for the system. A full understanding of the axial dispersion effects, mixing, and the temperature profile would help design the next generation of continuous flow reactors.

The incompatibility of the stainless steel pump with the isobutylchloroformate is a concern because most of the reactor is also stainless steel. This issue, however, is easily addressed. The final step of this synthesis requires HCl, which is also incompatible with stainless steel. Thus it will likely be necessary to use hastelloy, Inconel, or use a protective coating, such as Restek Silcosteel CR, inside of the reactor. Should stainless steel continue to be used, the reactor itself would have to be replaced occasionally for safety reasons.

An economic analysis should also be undertaken to assess the impact this reactor design can have on the anticipated reaction, as well as other reactions. Depending on the scale that the desired product needs to be manufactured at, using small reactors may not be advantageous from a cost perspective. Additionally, using a more expensive material of construction will reduce the cost-effectiveness of this reactor. Batch reactions typically require more man-hours, however, so this may balance out.

The simplicity of this design, however, suggests that this type of continuous flow reactor could be applied to a wide variety of future projects. Temperature-sensitive reactions, highly exo- or endothermic reactions, and reactions involving unsafe compounds are good candidates for our continuous flow reactor system.

## REFERENCES

1. D. Yang, L. A. Le, R. J. Martinez, R. P. Currier, D. F. Spencer and G. Deppe, *Energy & Fuels*, 2008, **22**, 2649-2659.
2. D. I. C. Wang, A. E. Humphrey and L. C. Eagleton, *Biotechnology and Bioengineering*, 1964, **6**, 367-&.
3. W. Ehrfeld, Hessel, V., and Lowe, H., *Microreactors: New Technology for Modern Chemistry*, Wiley-VCH, Weinheim, 2000.
4. K. Jahnisch, Hessel, V., Lowe, H., and Baerns, M., *Angew. Chem. Int. Ed.*, 2004, **43**, 406-446.
5. L. D. Proctor and A. J. Warr, *Organic Process Research & Development*, 2002, **6**, 884-892.
6. B. Mason, Price, K, Steinbacher, J., Bogdan, A., and McQuade, D., *Chemical Reviews*, 2007, **107**, 2300-2318.
7. I. R. Baxendale, S. V. Ley, C. D. Smith and G. K. Tranmer, *Chemical Communications*, 2006, 4835-4837.

8. K. E. B. Parkes, D. J. Bushnell, P. H. Crackett, S. J. Dunsdon, A. C. Freeman, M. P. Gunn, R. A. Hopkins, R. W. Lambert, J. A. Martin, and et al., *J. Org. Chem.*, 1994, **59**, 3656-3664.
9. A. A. Malik, T. E. Clement, H. Palandoken, J. Robinson III and J. A. Stringer, ed. USPTO, United States, 2003.
10. T. Aoyama and T. Shioiri, *Chemical & Pharmaceutical Bulletin*, 1981, **29**, 3249-3255.
11. J. Cesar and M. S. Dolenc, *Tetrahedron Letters*, 2001, **42**, 7099-7102.
12. F. Arndt, B. Eistert and W. Partale, *Ber. Dtsch. Chem. Ges.*, 1927, **60**, 1364.
13. B. Ahmed-Omer, D. Barrow and T. Wirth, 2008, pp. S280-S283.
14. H. Song, M. R. Bringer, J. D. Tice, C. J. Gerds and R. F. Ismagilov, *Applied Physics Letters*, 2003, **83**, 4664-4666.

## **CHAPTER 3: SWITCHABLE SOLVENTS FOR THE PRETREATMENT OF LIGNOCELLULOSIC BIOMASS**

### **INTRODUCTION**

Environmental, economic, and political issues have renewed significant interest in finding a sustainable energy source for transportation fuels. During the past few years, bioethanol has emerged as a promising alternative fuel that can be produced from renewable resources. Recent research has focused on lignocellulosic biomass, not food sources such as corn and sugarcane, due to its low cost and availability. Our lab is examining several promising sustainable biomass pretreatment methods including near-critical water, supercritical fluids, and novel switchable solvents. These sustainable methods improve current biomass pretreatment strategies by eliminating the need for acid or base neutralization, which lowers the overall cost and can allow industrial ethanol production to become a more economically viable process.

### **BACKGROUND**

#### **Lignocellulosic Biomass**

With the supply of fossil fuels diminishing and concerns over CO<sub>2</sub> production rising, the development of alternative fuels from sustainable resources has become a focus of national and international research. Many developing countries are quickly becoming technologically advanced, and energy production is expected to increase by at least 50% by 2025.<sup>1</sup> Bioethanol has emerged during the past few years as a viable fuel



alternative derived from renewable resources. In 2005, bioethanol comprised only 2% of transportation fuels in the United States.<sup>2</sup> A combination of tax incentives and public awareness, partially caused by the recent promotion of alternative fuels by the automotive industry, has caused ethanol production to increase by nearly 40% from 2005 to 2007.<sup>3</sup> In the United States, bioethanol is produced mainly from corn, resulting in the “food vs. fuels” debate. The U.S. Deputy Energy Secretary declared in March 2007 that “...the future of biofuels is not based on corn” after the price of corn more than doubled within a year from government incentives intended to boost ethanol production.<sup>4</sup>

Many experts believe that if bioethanol is to become a realistic sustainable fuel, it must be produced from lignocellulosic biomass. This category includes not only trees and grass, but also municipal waste, such as wood pulp, and agricultural discards, such as corn stover. Lignocellulosic biomass is more complicated than food as a feedstock. For example, corn is primarily made from starch, which is pure glucose. Lignocellulosic biomass, however, is comprised of three major components: cellulose, hemicellulose, and lignin. Cellulose is a polymer of glucose molecules linked together by  $\beta$  (1-4) glycosidic bonds. Hemicellulose is a branched polymer formed primarily from the five-carbon sugar xylose, but also from the pentose arabinose and the hexoses glucose, galactose, and mannose. Lignin is a complex polymer of phenylpropane units that is difficult to characterize because the monomers are cross-linked with a variety of different chemical bonds. Figures 3.1 - 3.3 depict representative structures of these biopolymers.

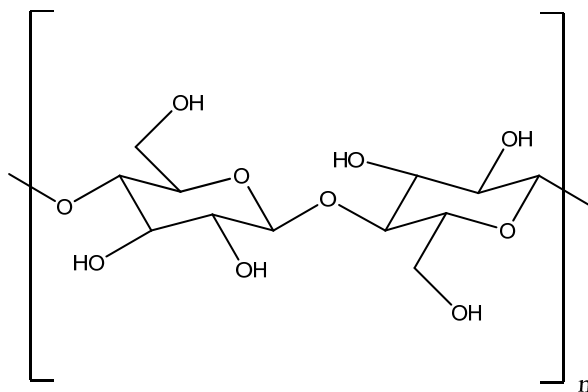


Figure 3.1: Cellulose structure.

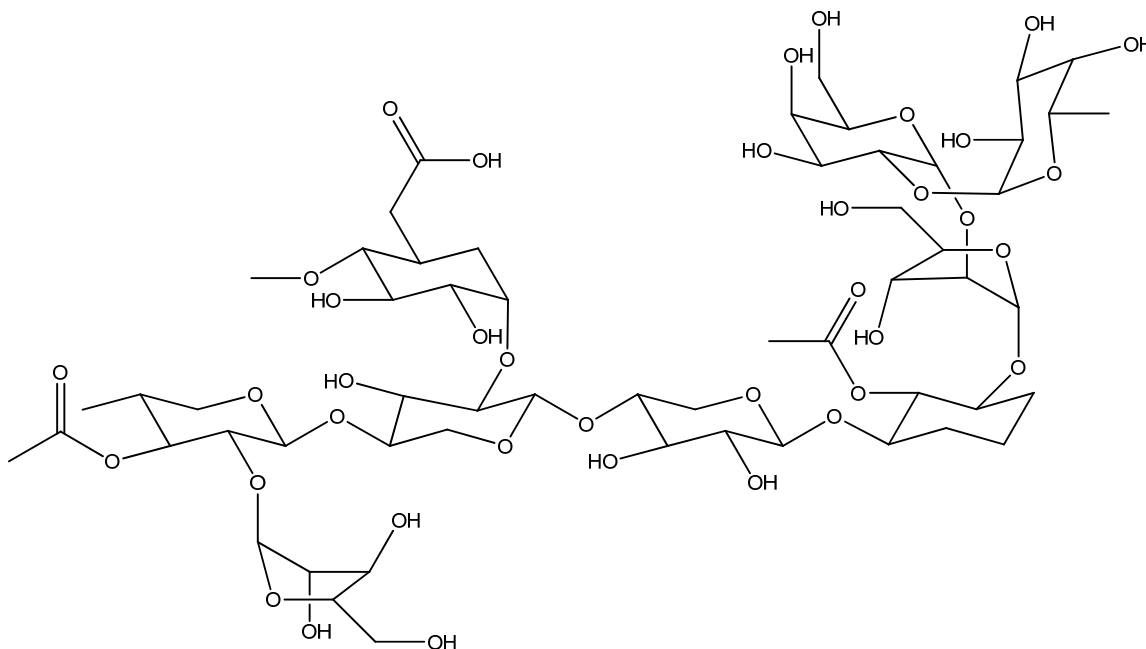


Figure 3.2: Representative structure of hemicellulose.

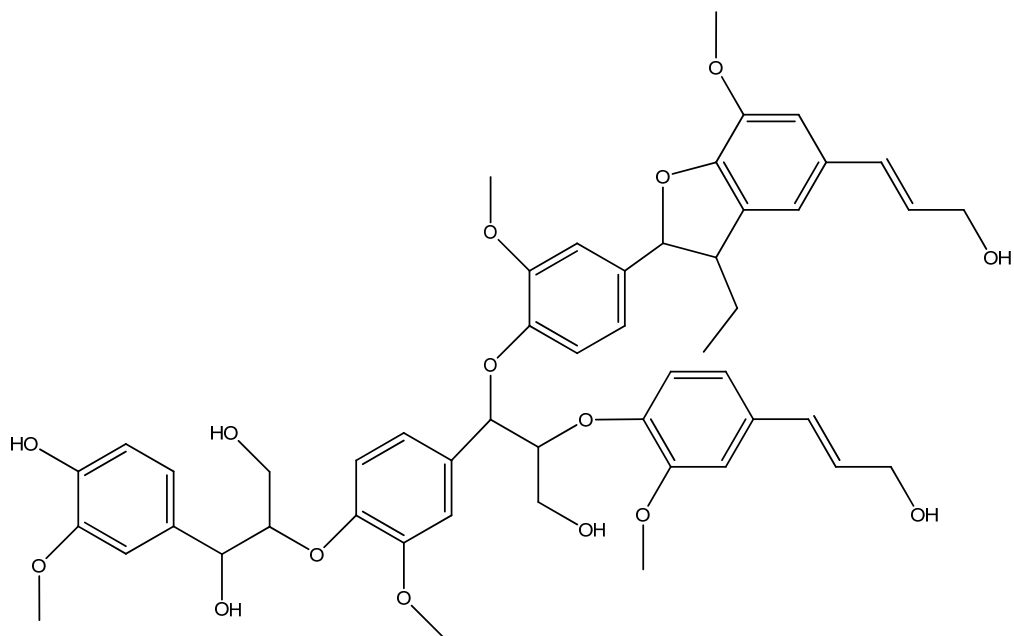


Figure 3.3: Representative structure of lignin.

The cellulose and hemicellulose components of lignocellulosic biomass can be broken down to glucose and other monosaccharides for fermentation to ethanol. There are two standard ways to achieve the depolymerization: chemical hydrolysis and enzymatic hydrolysis. The rigid structure of lignin, however, blocks microbial access to the cellulose and hemicellulose components of lignocellulosic biomass. This prevents efficient enzymatic hydrolysis of starting materials. Finding a cost-effective method to open up the lignocellulosic structure, reduce cellulose and hemicellulose to monomeric sugars, and ferment these monosaccharides to bioethanol is a high priority in alternative fuel research.

## Pretreatment Rationale

Biomass pretreatment prior to fermentation has become a standard way to open up the rigid structure of lignocellulosic material and allow enzymes to access the cellulose and hemicellulose. A successful pretreatment method ideally should rupture the lignin barrier and interrupt the cellulose crystallinity, as can be seen in Figure 3.4.<sup>5</sup> At present, the most common pretreatment technologies include uncatalyzed steam explosion, liquid hot water, flow-through acid, lime, and ammonium. Acid- and base-catalyzed pretreatments are currently the most effective methods, but these procedures require neutralization and subsequent waste disposal.<sup>6</sup> The other methods also have drawbacks, including high energy consumption, sugar degradation, expensive solvents, and material of construction demands. As a result, current lignocellulosic biomass pretreatment methods cost \$0.30 per gallon of ethanol.<sup>5</sup> Any new methods should minimize costs, be sustainable, and include the following criteria for effective pretreatment strategies:

- Avoid the need to reduce biomass size
- Reduce cellulose crystallinity
- Preserve hemicellulose components
- Minimize energy demands and costs
- Limit degradation products
- Reduce production of fermentation inhibitors
- Lower catalyst cost and enhance recycle
- Minimize waste production<sup>5</sup>

Although effective, the harsh techniques previously mentioned require neutralization and subsequent waste disposal. This waste consists of salts, many of which are contaminated, creating a challenge for proper disposal. For these reasons, such processes are detrimental both economically and environmentally. The high processing

costs, however, provide significant opportunities to enhance efficiency and reduce the overall expense of current pretreatment methods. This research project involved examining three different sustainable pretreatment options: CO<sub>2</sub>-enhanced near critical water, organic acid-enhanced supercritical CO<sub>2</sub>, and sulfones.

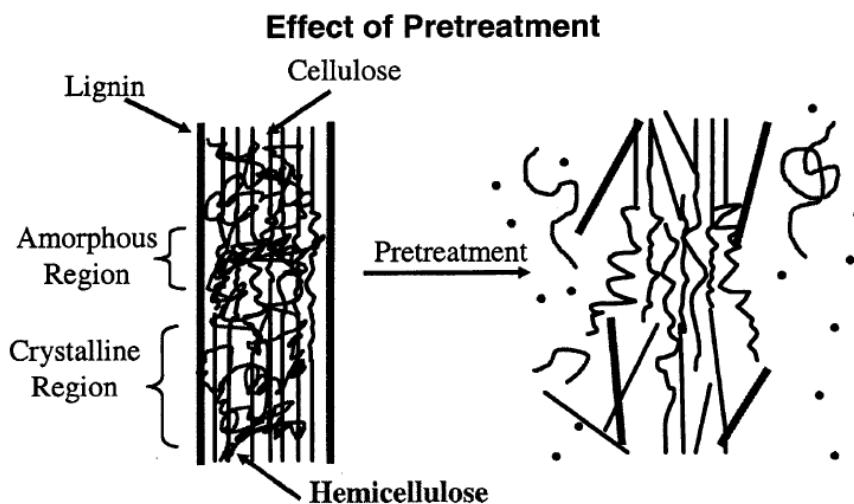


Figure 3.4: Schematic of pretreatment goals.<sup>5</sup>

### Near-Critical Water with CO<sub>2</sub>

Near-critical water (NCW) shows promise as a sustainable biomass pretreatment method. As water is heated to near its critical region, the fluid dilates and assumes many useful properties.<sup>7, 8</sup> It dissolves salts and organic chemicals, providing a homogeneous aqueous/organic phase for reactions.<sup>8-12</sup> The dissociation constant of water,  $K_w$ , increases by several orders of magnitude as the temperature rises from room temperature to several hundred degrees C. At these high temperatures, a substantial percentage of the water dissociates into hydronium and hydroxide ions, and can facilitate both acid- and base-

catalyzed reactions.<sup>13</sup> More importantly, however, the acid or base is negated by simple cooling. The formation of *in-situ* catalysis avoids the need for neutralization and salt disposal, significantly reducing processing costs.

Although hot water as a pretreatment method has been tried before, the considerable water consumption and sugar degradation at high temperatures limited the effectiveness of this process.<sup>14</sup> The addition of CO<sub>2</sub>, however, is known to accelerate acid-catalyzed reactions in hot water.<sup>15, 16</sup> As seen in Figure 3.5, CO<sub>2</sub> will dissolve in water and form carbonic acid, which has a pKa of 6.37. The presence of carbonic acid thus drops the pH of NCW,<sup>15</sup> allowing the acid-catalyzed hydrolysis of lignocellulose to occur at lower temperatures and decreasing the energy costs. This pH decrease can be seen in Figure 3.6. More importantly, the acid is simply reversed by depressurization so there are no downstream neutralization requirements. Thus, adding CO<sub>2</sub> to NCW can provide a stronger acid at lower temperatures, aiding in the breakdown of lignocellulosic biomass without requiring the high temperatures that are detrimental due to energy consumption and sugar degradation.

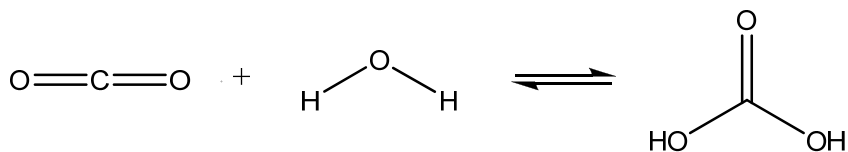


Figure 3.5: Reaction of CO<sub>2</sub> with water to form carbonic acid.

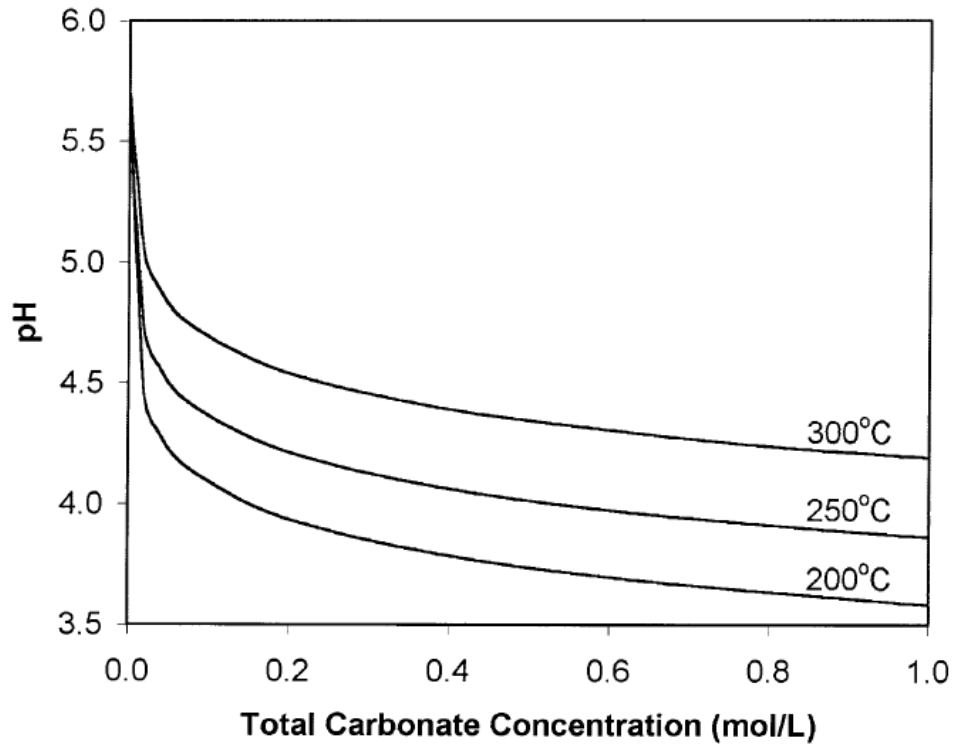


Figure 3.6: Effect of CO<sub>2</sub> on the pH of water.<sup>15</sup>

### Organic Acid-Enhanced CO<sub>2</sub>

Supercritical fluids (SCFs) are often used in processes requiring exceptional transport properties. Current industrial applications of supercritical CO<sub>2</sub> (scCO<sub>2</sub>) include the extraction of natural products requiring low temperature, high mass-transfer rates, and minimal solvent carried to the next processing stage.<sup>17</sup> Since SCFs have nearly nonexistent surface tension, negligible viscosity, and high diffusivity, they are able to penetrate materials with low porosity. The biomass field has already taken advantage of these properties by applying scCO<sub>2</sub> to extract compounds such as fermentation inhibitors and organic acids from lignocellulosic material.<sup>18</sup>

While scCO<sub>2</sub> can penetrate the rigid lignocellulosic matrix, the use of scCO<sub>2</sub> is not by itself a suitable technique for biomass pretreatment because it does not have direct chemical effects on the biopolymer components. This proposed strategy overcomes that limitation by adding small amounts of an organic acid, such as acetic acid or formic acid, as a co-solvent to promote acid-catalyzed hydrolysis. These two acids, which can be seen in Figure 3.7, were chosen because they are fairly benign and cheap organic acids. Additionally, acetic acid has been used previously to fractionate biomass.<sup>19</sup> The scCO<sub>2</sub>-organic acid system has the capability to remove extractive material from the biomass as well as hydrolyzing bonds between the biopolymers. As the phase behavior of carbon dioxide and both of these organic acids are well-known,<sup>20, 21</sup> designing a monophasic pretreatment system is straightforward. Most importantly, this process may offer a facile separation mechanism by simple depressurization of CO<sub>2</sub>. A significant amount of the organic acid co-solvent should be purged along with the CO<sub>2</sub>, leaving the remaining solid biomass suitable for further downstream processing.



Figure 3.7: Structures of formic acid (left) and acetic acid (right).



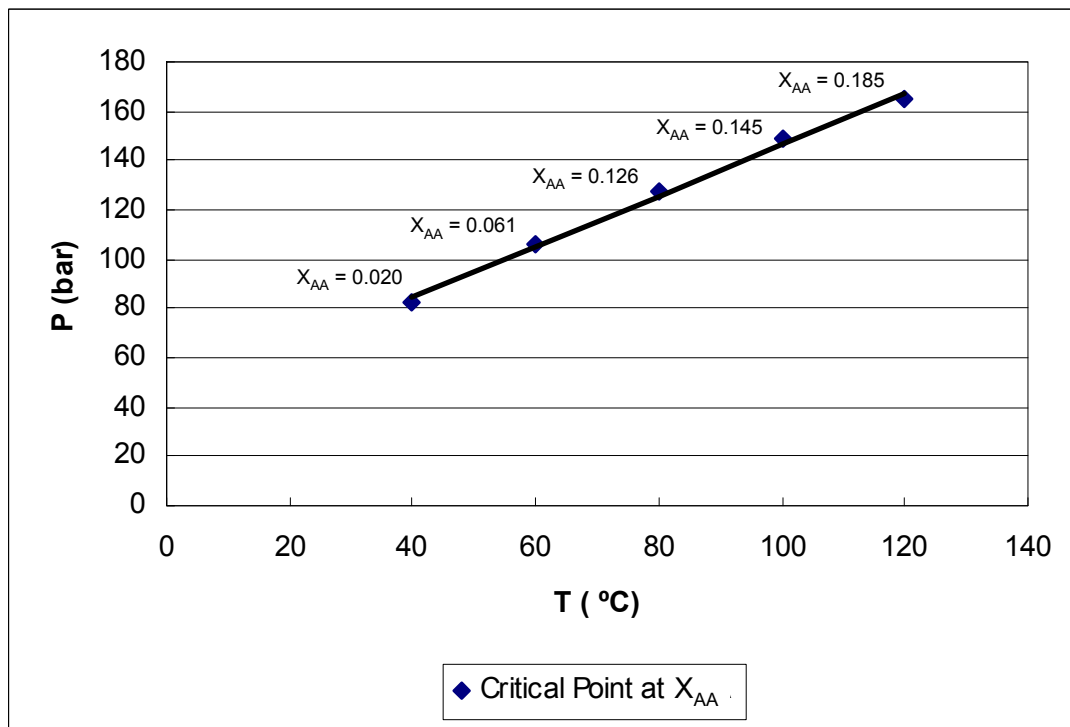


Figure 3.8: Supercritical phase boundary for a binary mixture of CO<sub>2</sub> and acetic acid.<sup>22</sup>

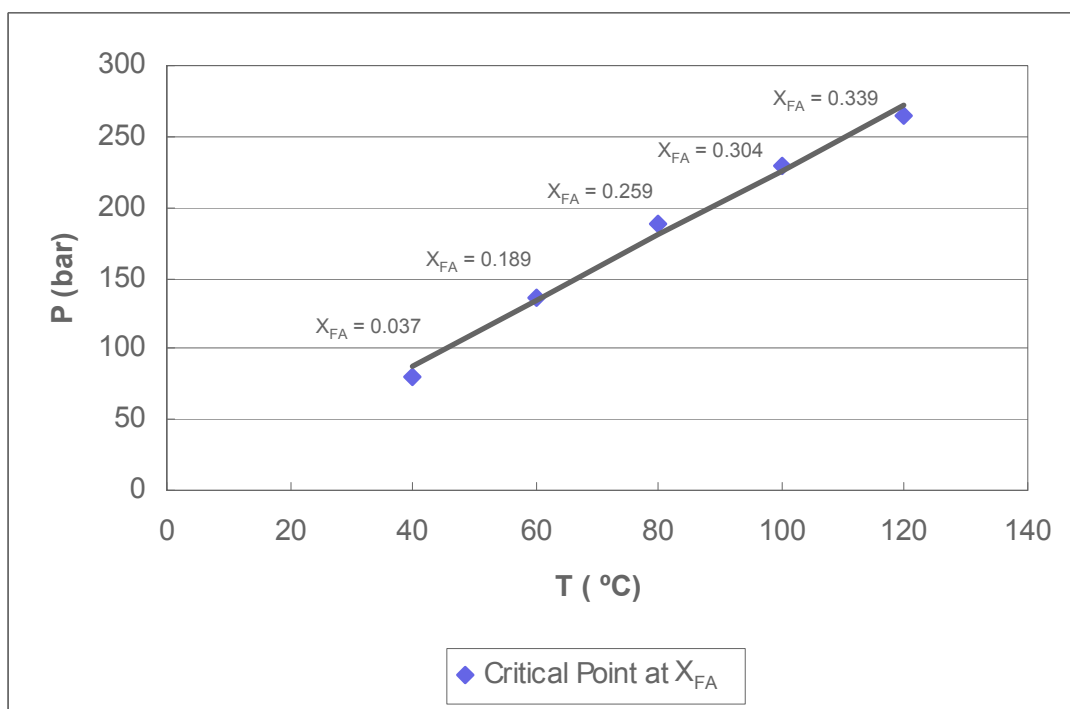


Figure 3.9: Supercritical phase boundary for a binary mixture of CO<sub>2</sub> and formic acid.<sup>22</sup>

## Sulfones (Piperylene Sulfone and Butadiene Sulfone)

### Biomass Pretreatment

Many solvents have been examined for use in pretreatment strategies. Solvents known to dissolve cellulose include ozone, glycerol, dioxane, phenol, and ethylene glycol. Additionally, other solvents have properties that can be exploited during pretreatment processes. For example, dimethyl sulfoxide (DMSO) is a dipolar, aprotic solvent capable of dissolving hemicellulose, breaking apart the association between lignin and cellulose, and decreasing cellulose crystallinity.<sup>5</sup> DMSO, however, has a boiling point of 189 °C, making solvent recycle difficult by traditional means such as distillation. Thus, while solvents can be effective pretreatment strategies, they are rarely practical due to the high cost of both the solvent and subsequent separation techniques.

Our lab has developed a “switchable” dipolar, aprotic solvent called piperylene sulfone (PS). PS is a nonvolatile liquid with similar medium properties to DMSO, but also is easily converted to the volatile substances *trans*-1,3-pentadiene and sulfur dioxide. These volatile species can be collected and then recombined to form PS, allowing for complete recovery of the original solvent. The unique physical properties of PS (melting point of -12 °C and full decomposition at 100 °C) provide a simple temperature switch for facile product separation and solvent recycle.<sup>23</sup> The reaction can be seen in Figure 3.10.

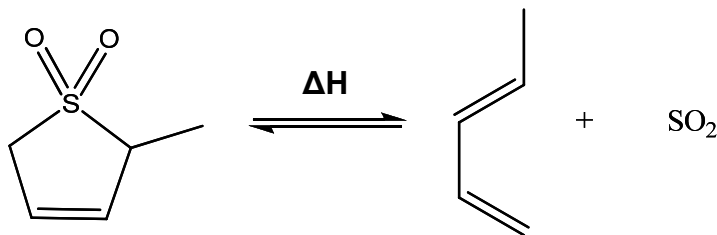


Figure 3.10: Retro-chelotropic reaction of piperylene sulfone.

Recent research in our lab has shown that PS, at moderately high temperatures, also creates an *in-situ* acid with the addition of water. The partial decomposition of PS into the gaseous species begins at ~65 °C. If water is present, the SO<sub>2</sub> dissolves into it, forming sulfurous acid (pKa 1.81) in the reaction shown in Figure 3.11. While sulfurous acid is somewhat weaker than sulfuric acid (pKa -3.0), it can still be quite effective for acid-catalyzed reactions. For example, this acidic PS solution has proven to be an excellent medium for the acid-catalyzed hydrolysis of β-pinene.<sup>24</sup>



Figure 3.11: In-situ formation of sulfurous acid.

Previous experiments have shown that PS is capable of dissolving lignin and swelling cellulose. These initial results led to the decision to determine the effectiveness of PS as a pretreatment solvent for lignocellulosic biomass. Since PS must be synthesized in the lab, however, it is easier to use butadiene sulfone (BS) for preliminary experiments. BS is an inexpensive, commercially-available analog with a structure similar to PS. It also undergoes a retro-chelotropic reaction to produce butadiene and sulfur dioxide, which can be seen in Figure 3.12. BS has similar physical properties to PS, but does not decompose until significantly higher temperatures (>120 °C). All pretreatment experiments with real biomass to date have used BS instead of PS.

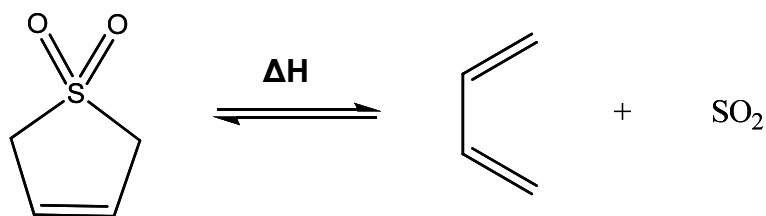


Figure 3.12: Retro-chelotropic reaction of butadiene sulfone.

### Cellulose Solvent

Additional consideration was accorded PS as a possible cellulose solvent because this ability would significantly enhance its applications in the field of carbohydrate chemistry. As mentioned previously, DMSO and other dipolar, aprotic solvents are able to dissolve cellulose.<sup>25</sup> Table 3.1 illustrates the similarities between DMSO and PS by comparing five solvent parameters. Four of the five measured experimental parameters are similar for DMSO and PS, suggesting that PS might be a cellulose solvent that could be removed easily. Each parameter measures a different aspect of a solvent's properties. Thus  $\alpha$  is a measure of its ability as a hydrogen bond donator,  $\beta$  is its ability as a hydrogen bond acceptor,  $\pi^*$  measures its polarity and polarizability, and finally ET(30) and  $\epsilon$  measure its polarity.

Table 3.1: Solvent characterization and comparison of DMSO and PS.<sup>24</sup>

Parameter	Property	DMSO	PS
$\alpha$	H-bond donating ability	0.0	0.0
$\beta$	H-bond accepting ability	0.76	0.46
$\pi^*$	Polarity/polarizability	1	0.87
ET(30)	Polarity	189.0 kJ/mol	189.0 kJ/mol
$\epsilon$	Polarity	46.7	42.6

Although DMSO itself can dissolve cellulose, it becomes a more effective solvent upon the addition of formaldehyde. In DMSO alone, cellulose tends to have between 1-2 wt % solubility at 80 °C. There are two literature methods used to add formaldehyde to DMSO. One is by adding a stream of formaldehyde gas directly to the system; the optimal temperature for cellulose dissolution in this case is 95-100 °C. The second is by adding paraformaldehyde directly to DMSO and heating the entire reaction mixture to 120-125 °C. The higher temperature is needed to decompose the paraformaldehyde to formaldehyde.<sup>26</sup>

By adding up to 5 wt% paraformaldehyde, cellulose solubility can be greatly increased. Cellulose with high degrees of polymerization (ranging from 16 to over 8,000) has all been dissolved in DMSO/formaldehyde mixtures. By increasing the solvent temperature to 125 °C, up to 5 wt% cellulose cotton linters and 10 wt% of cellulose with a lower degree of polymerization (D.P. 275) can dissolve in solution.<sup>25</sup> The DMSO/formaldehyde mixture dissolves cellulose effectively because the formaldehyde reacts with the hydroxyl groups on cellulose, usually with the primary hydroxyl group on the C6 carbon, to form methylol cellulose, as shown in Figure 3.13.

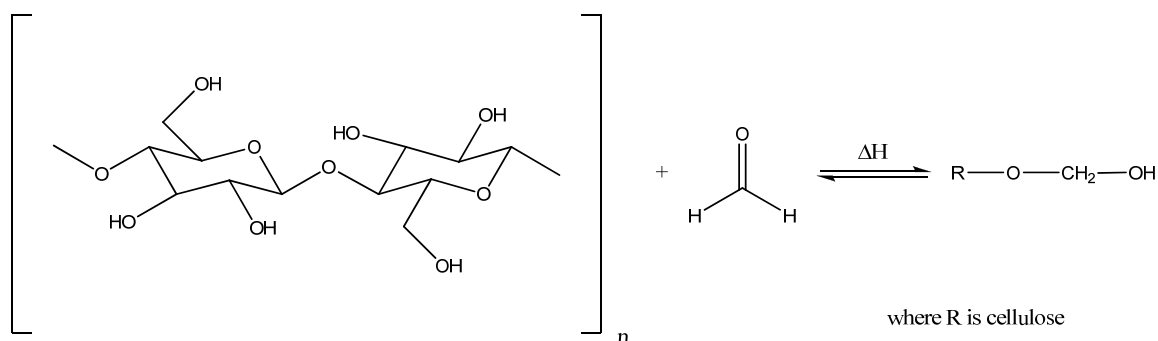


Figure 3.13: Methylol cellulose formation in DMSO/formaldehyde solvent.

Formaldehyde is not the only additive to DMSO that enhances cellulose solubility. Previous research has shown that tetrabutylammonium fluoride trihydrate (TBAF) added to DMSO in a 16.6 wt% ratio dissolved 2.9% Avicel cellulose at room temperature within 15 minutes. Analysis via  $^{13}\text{C}$  NMR spectroscopy showed that the solution dissolves cellulose without derivatizing the cellulose, making it a non-derivatizing cellulose solvent.<sup>27</sup> The DMSO/TBAF system described above was able to dissolve cellulose with a D.P. as high as 650 in 15 minutes.<sup>28</sup>

Due to the inherent similarities between DMSO and PS, it was decided to test cellulose dissolution in PS. PS by itself, PS + formaldehyde, and PS + TBAF were all examined as possible cellulose dissolution solvents.

### **Experimental Considerations for Each Pretreatment**

For the  $\text{CO}_2$ -enhanced NCW system, fundamental studies of pure materials (cellulose and xylan, a simple polysaccharide to model hemicellulose) were undertaken at a variety of conditions. After the initial studies, real biomass samples were also tested under control and  $\text{CO}_2$  conditions. For the organic-acid enhanced  $\text{CO}_2$  system, formic acid and acetic acid were compared to each other as possible organic acid additives. The system was tested on real biomass samples. In the sulfone system, the percent mass loss during the BS pretreatment was examined for real biomass samples. Studies were also done to determine the effectiveness of PS, PS + formaldehyde, and PS + TBAF as cellulose solvents. Since each type of biomass has a different composition, it is important to have at least a basic understanding of the composition of each type prior to analysis. A representative composition of several types of biomass can be seen below.

Table 3.2: Dry weight composition (%) of selected lignocellulosic biomass feedstock.

*Note:* Numbers do not sum to 100% because minor components are not listed.

<b>Feedstock</b>	<b>Cellulose</b>	<b>Hemicellulose</b>	<b>Lignin</b>
Corn stover	37.5	22.4	17.6
Corn fiber	14.28	16.8	8.4
Pine wood	46.4	8.8	29.4
Wheat straw	38.2	21.2	23.4
Switchgrass	31.0	20.4	17.6

## **EXPERIMENTAL**

### **Materials**

#### Common Materials Used for all Three Pretreatment Methods

All experiments used water distilled in the Unit Operations laboratory at the Georgia Institute of Technology (Georgia Tech). All real biomass samples (pine chips, corn stover, and switchgrass) were obtained from the research group of Dr. Art Ragauskas (School of Chemistry and Biochemistry, Georgia Tech). To reduce the biomass size for experimentation, the biomass samples were ground with a Wiley mill and then sifted through a #4 sieve.

#### CO<sub>2</sub>-Enhanced Near Critical Water

The following materials were used as received: cellulose (Fluka cellulose powder, ash ~0.1%, length of fibers: 0.02 – 0.15 mm), xylan (Sigma, from beechwood, >90% with xylose residues), and carbon dioxide gas (Air Gas, SFC grade, 99.99%).

### Organic Acid-Enhanced scCO<sub>2</sub>

All materials were used as received: acetic acid (Aldrich, glacial, 99.8%), formic acid (EMD, 98%, ACS grade), and carbon dioxide gas (Air Gas, SFC grade, 99.99%).

### Sulfone

The following chemicals were used as received from Aldrich: butadiene sulfone (98%), formaldehyde (Aldrich, 37 wt% in H<sub>2</sub>O, ACS Reagent – contains 10-15% MeOH), and TBAF (98%). Cellulose (Fluka cellulose powder, ash ~0.1%, length of fibers: 0.02 – 0.15 mm or Fluka, Avicel PH-101, 60% crystallinity) was used as received. Piperylene sulfone was synthesized in our lab by the procedure explained in Vinci et al.<sup>23</sup>

### Analytical

The following materials were used as received: sulfuric acid (Acros Organics, fuming, ~20% free SO<sub>3</sub>), calcium carbonate (EMD, ACS grade), glucose (D-(+)-glucose Sigma, 99.5% or dextrose, BDH, anhydrous, ACS reagent), arabinose (Aldrich, 98%), xylose (Sigma-Aldrich, Sigma ultra >99%), mannose (Sigma, >99%), galactose (Sigma-Aldrich, 99%, contains <0.01% glucose), and fructose (Sigma, min 99%). Whatman P5 medium porosity filter paper was used to separate the solid biomass from the filtrate. Whatman disposable filter devices (PVDF, 13 mm, 0.2 µm pore size) or Pall Life Sciences Acrodisc syringe filters (nylon, 13 mm, 0.2 µm pore size) were used to filter all samples before analysis via HPLC-RID. Autoclavable plastic vials (BioMed) were used during sulfuric acid induced hydrolysis and workup. Water (Sigma-Aldrich, HPLC grade, >99%) was used as received for the mobile phase in the HPLC and deuterated DMSO (d-DMSO, Aldrich, 99.9 atom % D) was used for NMR analysis.



## **Instrumentation**

Samples that needed to be autoclaved were placed in a Cuisinart CPC-600 1000-Watt 6-Quart Electric Pressure Cooker. After filtration, all samples were analyzed in a Hewlett-Packard (HP) Series 1100 High Performance Liquid Chromatograph (HPLC) equipped with an Agilent Technologies 1200 Series Refractive Index Detector (RID). The HPLC method achieved separation in a BioRad Aminex HPX-87P column (lead resin, sulfonated divinyl benzene-styrene copolymer, 300 x 7.8 mm), preceded by a BioRad De-Ashing cartridge. Scanning electron microscope (SEM) images were taken with a Hitachi S-800 SEM. All samples were coated with gold using an Electro Microscopy Services sputter coater (EMS350) prior to imaging.  $^1\text{H}$  and  $^{13}\text{C}$  NMR spectra were recorded using a Varian Mercury Vx 400 spectrometer using residual d-DMSO peak as an internal reference. Solid-state  $^{13}\text{C}$ -NMR was performed on a Bruker Avance/DSX-400 spectrometer using a Bruker 4-mm MAS probe to measure temperature.

## **Methods**

### CO<sub>2</sub>-Enhanced Near Critical Water

#### *NCW Control Studies*

Samples of cellulose, xylan, or actual biomass were placed in a 3 mL titanium tubular reactor and filled with 1.25 - 2 mL H<sub>2</sub>O. The NPT reactor plug was wrapped with Teflon tape and tightly secured on the reactor. For each experiment, the reactors were all placed at the same time in the aluminum heating block, which was heated by four cartridge heaters (Omega Technologies Co.) using a temperature controller (Omega

Technologies Co., Model CN9000A) equipped with an over-temperature controller (Omega CN355). Calibrations for the thermocouples used in the heating block were made by testing against an external thermocouple placed within one of the titanium tubes. This experimental setup is illustrated in Figure 3.14. To determine the effect of time at different experimental conditions (T, P), several reactors prepared identically were removed at various time intervals. This experimental setup has been used successfully many times in the past by Eckert-Liotta group members to obtain kinetic data in a batch system.<sup>29-33</sup> It should be noted that the titanium reactors should never be filled with more than 2 mL of liquid due to the expansion of water as temperature increases.

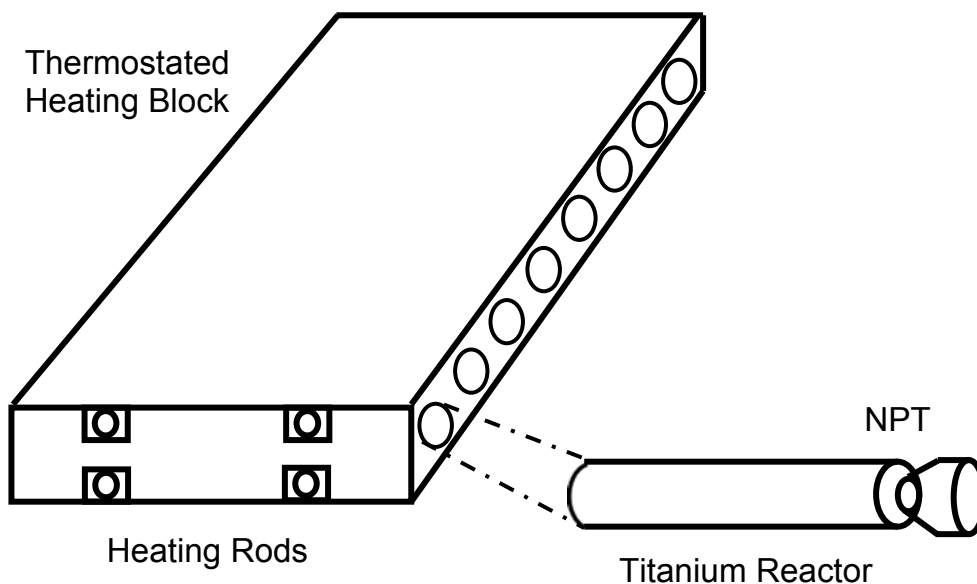


Figure 3.14: Titanium reactor setup with heating block apparatus. Illustration modified from E. Newton M.S. thesis.<sup>30</sup>

After the allotted experimental time, the reactor was removed from the aluminum heating block and placed in a room-temperature water bath to quench the reaction. After sitting for several minutes in the water bath, the reactor contents were emptied into a plastic autoclave vial. The reactor was rinsed with 5 mL of H<sub>2</sub>O to ensure all contents were removed. The rinse H<sub>2</sub>O was also dumped into the plastic autoclave vial. If the experiment involved a real biomass sample, then the autoclave vial was centrifuged (Sargent CL centrifuge) for two minutes to consolidate the solid biomass. A 1.5 mL sample from each vial was taken and filtered for HPLC analysis; no additional workup was required because the samples were already at nearly neutral pH. The remaining liquid fraction was worked up as described in the Sulfuric Acid Hydrolysis of Liquid Fraction Samples section.

#### *NCW + CO<sub>2</sub> Studies*

For experiments involving CO<sub>2</sub>, the reactors were allowed to sit in the aluminum block for 10-15 minutes in order to reach the desired temperature. The CO<sub>2</sub> was then added with an Isco D500 syringe pump (set at constant pressure) through a valve built into modified reactor caps. For these CO<sub>2</sub>-enhanced NCW experiments, experimental time began upon the addition of CO<sub>2</sub> to the titanium reactors. The pressure was monitored using a pressure transducer and indicator (Druck, Model 400019).

The CO<sub>2</sub> was released from the reactor by a vent line into a flask filled with H<sub>2</sub>O. This keeps any volatile chemical species in the reactor from venting into the atmosphere with CO<sub>2</sub>; the chemicals will be trapped in the H<sub>2</sub>O. The samples then underwent the same procedure described in the previous section.

### Organic Acid-Enhanced scCO<sub>2</sub>

Two grams of biomass were placed in a 300 mL high-pressure Parr reactor (Parr Instrument Co.). The temperature and agitation were kept constant by a heating jacket and tachometer controlled by a Parr Model 4842 controller. 10 mL of acetic or formic acid was added to the reactor and the Parr was sealed shut by closing the bolts in a star pattern. The reactor was allowed to heat to the desired temperature, then the CO<sub>2</sub> was added with an Isco 500D syringe pump (set at constant pressure). The reactor pressure was also displayed on the Parr controller via a pressure transducer hooked into the reactor. The experimental setup of the Parr reactor can be seen in Figure 3.15. Control experiments involving only CO<sub>2</sub> (no acid) were also conducted.

After the desired reaction time, the heat was turned off and the CO<sub>2</sub> vented into a flask filled with MeOH. As before, the MeOH flask for this experiment was also designed to trap any possible volatile chemicals in the reaction mixture. The reactor was rinsed with H<sub>2</sub>O and the slurry filtered via vacuum filtration. The biomass was rinsed with H<sub>2</sub>O until the filtrate came off the biomass clear. The total liquid volume of the filtrate was measured. An aliquot was taken for HPLC analysis as described in “Initial Liquid Fraction Sample Workup”, and the rest underwent the workup described in “Sulfuric Acid Hydrolysis of Liquid Fraction Samples” before undergoing analysis via HPLC-RID.

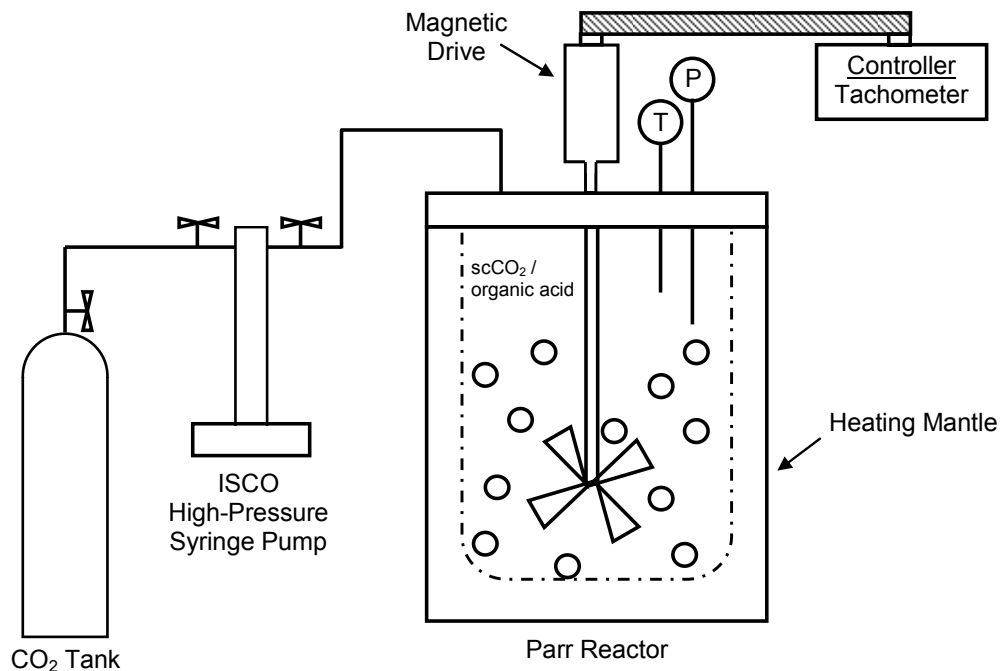


Figure 3.15: Experimental setup of Parr high-pressure reactor. Modified from L. Draucker Ph.D. thesis.<sup>34</sup>

## Sulfones

### *Biomass Pretreatment*

A 100 mL roundbottom flask was filled with 10 g BS, 2 mL H<sub>2</sub>O, and 0.5 g corn stover. The flask was placed in an oil bath maintained at 70 °C with a heated stir plate. Continuous mixing at 400 rpm was provided by a stir bar in the flask. After 24 hours, the resulting slurry was filtered and rinsed thoroughly with water. A heat gun was pointed at the funnel throughout the filtration to keep the BS hot enough to be in its liquid state. The resulting solid biomass residue was rinsed multiple times with water to remove residual BS. The final solid biomass residue was dried overnight in a vacuum oven (30 torr) kept at 80 °C.

### *Cellulose Dissolution*

Cellulose (either Avicel or Sigma) was added (10 wt%) to PS in a roundbottom flask. A dry ice condenser was filled with dry ice and acetone. This setup was used for all cellulose dissolution experiments to prevent the escape of any piperylene or SO<sub>2</sub> formed at the high temperature. For dissolution studies involving an additive, the proper amount of the additive (5 vol% formaldehyde or 16.6 wt% TBAF) was also added to the PS. The mixture was stirred at 400 rpm and heated between 80-120 °C in an oil bath maintained by a heated stir plate. After the solution was allowed to sit overnight, the solution was filtered via vacuum filtration. The PS was removed from the filtrate by keeping it under nitrogen for 24 hours, which forces decomposition to piperylene and SO<sub>2</sub>. Analysis was completed by NMR or by a modification of the workup described in the section “Sulfuric Acid Hydrolysis of Liquid Fraction Samples.”

After the PS was removed from the reaction flask as described above, d-DMSO was added to the flask and the entire mixture transferred to a NMR tube. The NMR was completed at 80 °C to ensure that any cellulose left in the filtrate would dissolve in the d-DMSO during analysis. The solid cellulose on the filter was also analyzed via solid-state NMR by the research lab of Andreas Bommaris (School of Chemical and Biomolecular Engineering, Georgia Tech) to determine the crystallinity index.<sup>35, 36</sup> The solid-state cross polarization/magic angle spinning (CP/MAS) <sup>13</sup>C-NMR experiments were operated at frequencies of 100.55 MHz for <sup>13</sup>C. All experiments were carried out at ambient temperature. The samples (~ 35% moisture content) were packed in 4 mm zirconium dioxide rotors and spun at 10 kHz. Acquisition was carried out with a CP pulse sequence using 5 μs pulse and 2.0 ms contact pulse.

For the modified sulfuric acid hydrolysis, the filtrate was first diluted by adding 5 mL H<sub>2</sub>O. The diluted filtrate was then transferred to a plastic autoclave vial and 174 μL of 72% sulfuric acid was added. The sample was autoclaved for an hour, allowed to cool to room temperature, and neutralized to pH 6 with calcium carbonate. After neutralization, the sample was centrifuged, filtered through a 0.2 μm syringe filter, and put into a HPLC vial. The analysis occurred via HPLC using the method outlined in the section entitled “HPLC-RID Method.”

#### Determination of Mass Loss

Lignocellulosic biomass samples were weighed and placed in a Thelco (Thermo Electronic Company) thermostated oven (105 °C) overnight. The next day, the samples were quickly removed from the oven and weighed again. The difference in mass was assumed to be the initial water mass of the real biomass samples. Thus, the percent moisture of the biomass samples was calculated as seen in Equation 1. For subsequent experiments, a corrected (dry) mass was calculated by multiplying the starting mass of the biomass sample and the % moisture, with the resulting number used as the initial mass of the biomass samples.

$$\% \text{ Moisture} = \frac{[1 - (mass_{dry} - mass_{initial})]}{mass_{initial}} \times 100 \quad (\text{Equation 1})$$

During the pretreatment experiments, the biomass was weighed and subjected to the pretreatment conditions. After undergoing each pretreatment, the real biomass samples were rinsed thoroughly with water and dried in the oven overnight. The next day, the samples were quickly removed from the oven and weighed again. The difference between the corrected mass and the final mass is the mass removed during the pretreatment. Equation 2 shows the equation used to calculate the % mass loss due to the pretreatment process.

$$\% \text{ Mass Loss} = \frac{[1 - (mass_{corrected} - mass_{final})]}{mass_{corrected}} \times 100 \quad (\text{Equation 2})$$

#### Workup and Analysis via HPLC-RID

Each experiment involved two different HPLC analyses. The exact analytical procedure was conducted as outlined for biomass liquid process samples by the National Renewable Energy Laboratory (NREL).<sup>37</sup> Calibration curves for each sugar of interest were created to determine experimental results. One HPLC sample came directly from the liquid process fraction of the experiment. It underwent the basic procedure described in the Sample Workup section. The second sample underwent the workup procedure described below in "Sulfuric Acid Hydrolysis of Liquid Fraction Samples" before undergoing analysis via HPLC-RID. All analyses for this chapter focused on the liquid phase fraction of the biomass after pretreatment. As can be seen in Figure 3.16, there are many additional aspects that must be examined and studied to determine completely an optimal pretreatment. The analysis of the liquid phase fraction, however, does give significant indication as to whether or not the pretreatment is achieving the desired goals.



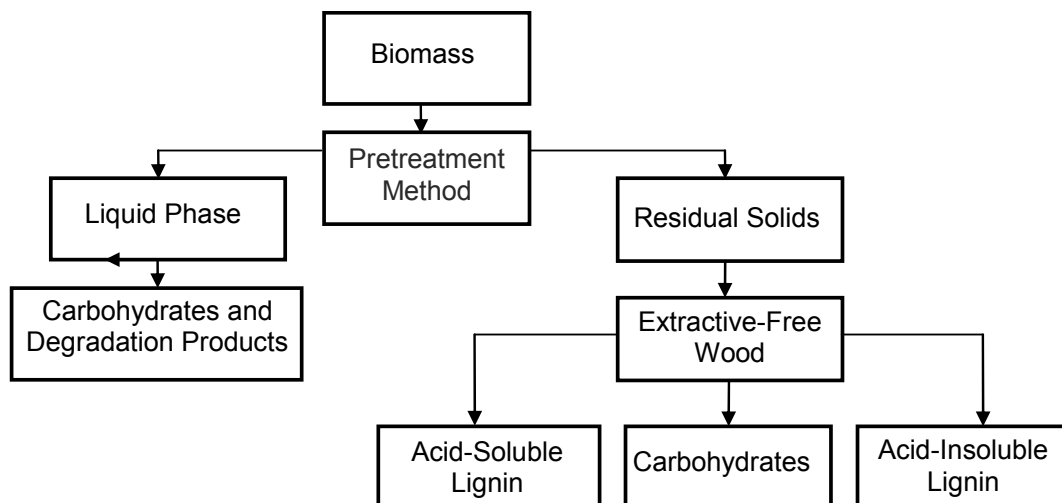


Figure 3.16: Flowchart for full analysis of lignocellulosic biomass.

#### *HPLC-RID Calibration Curves*

Calibration curves were made for the following sugar samples: cellobiose, glucose, xylose, galactose, arabinose, and mannose. The calibration samples were tested at concentrations of 0.1, 0.5, 1.0, 5.0, and 10.0 mg/mL. Each concentration was tested twice to ensure accuracy. The RI absorbances of all sugar concentrations were linear with  $R^2 \geq 0.98$  for all samples, and  $\geq 0.99$  for all but arabinose.

#### *Initial Liquid Fraction Sample Workup*

A 5 mL aliquot of the liquid process fraction was placed in a plastic autoclave vial. The pH was measured using pH paper, and the sample was neutralized using calcium carbonate until the pH reached 5-6. The sample was centrifuged, and 1.5 mL of the supernatant was collected and filtered into a HPLC vial for analysis.

### *Sulfuric Acid Hydrolysis of Liquid Fraction Samples*

Liquid fraction aliquots of 5 or 10 mL were taken from each experiment and placed in a plastic autoclave vial. The pH of each sample was measured using pH paper, and the appropriate amount of 72 wt% sulfuric acid was added to each tube. For a pH of 2.43 and higher, which includes all samples tested during the course of these experiments, 174  $\mu\text{L}$  must be added for 5 mL aliquots and 348  $\mu\text{L}$  must be added for 10 mL aliquots.<sup>37</sup> Individual sugar recovery standards (SRSs) were also made in the plastic autoclave vials. They consisted of 0.25 g of glucose and 0.25 g cellulose, or xylose and xylan, for CO<sub>2</sub>-enhanced NCW experiments. SRSs of all six calibration sugars were made for the Organic Acid-Enhanced scCO<sub>2</sub> experiments.

The liquid process samples and SRSs were autoclaved for 1 hour at 121 °C and 2 atm. The vials were allowed to cool to near room temperature before they were neutralized with calcium carbonate. The pH of each sample was checked regularly with pH paper until all samples and SRSs reached a pH of 5-6. After neutralization, 1.5 mL of each sample and SRS was filtered and put in HPLC vials for analysis.

### *HPLC-RID Method*

The HPLC-RID method used during analysis was obtained from the Department of Energy's laboratory procedure for the analysis of liquid biomass fractions.<sup>37</sup> 10  $\mu\text{L}$  of sample was injected into the HPLC running an AMINEX 87-P column. The mobile phase was pure H<sub>2</sub>O, degassed and 0.2  $\mu\text{m}$  filtered. The flow rate was 0.6 mL/min and the column temperature was 80 °C. The run time was approximately 20 minutes, and a sample of pure H<sub>2</sub>O was run between samples to clean the column.

## **RESULTS AND DISCUSSION**

### **CO<sub>2</sub>-Enhanced Near Critical Water**

The first studies were done in order to determine the effects of NCW on the pure components cellulose and xylan. A range of temperatures from 150 °C to 250 °C was studied and the sugar yields calculated for various conditions. The best conditions for differentiation of NCW pretreatment between cellulose and hemicellulose were 200 °C and 30 min. Temperatures below 200 °C produced minimal xylose and glucose. At higher T, the cellulose was still converted to glucose, but the overall glucose yields decreased at longer times. Additionally, xylan became highly viscous at, and was difficult to filter and analyze properly for, reaction temperatures higher than 200 °C. This can probably be attributed to the formation of degradation products.

The success of the pretreatment method was determined by comparing the glucose or xylose recovered from the experimental liquid process fraction to the SRSs comprised of the same amount of starting material that underwent sulfuric acid hydrolysis. The sulfuric acid hydrolysis method should completely hydrolyze the pure polymer (cellulose or xylan), providing the maximum amount of sugar available from the starting material. Thus the pretreatment method will recover a certain percentage of the available sugars. Figure 3.17 depicts the effectiveness of the NCW pretreatment method at 200 °C for a variety of reaction times. As illustrated, xylose production from hemicellulose became limited after exposed to NCW for 30 minutes.

Some preliminary studies have been run to determine the difference between NCW and NCW+CO<sub>2</sub>. Initial results have been promising, but more reaction conditions need to be studied before trends and conclusions can be made about the ideal reaction conditions for NCW+CO<sub>2</sub> on the pure polymers cellulose and xylan. Several more series of experiments are planned for this phase, and will be discussed later in the chapter.

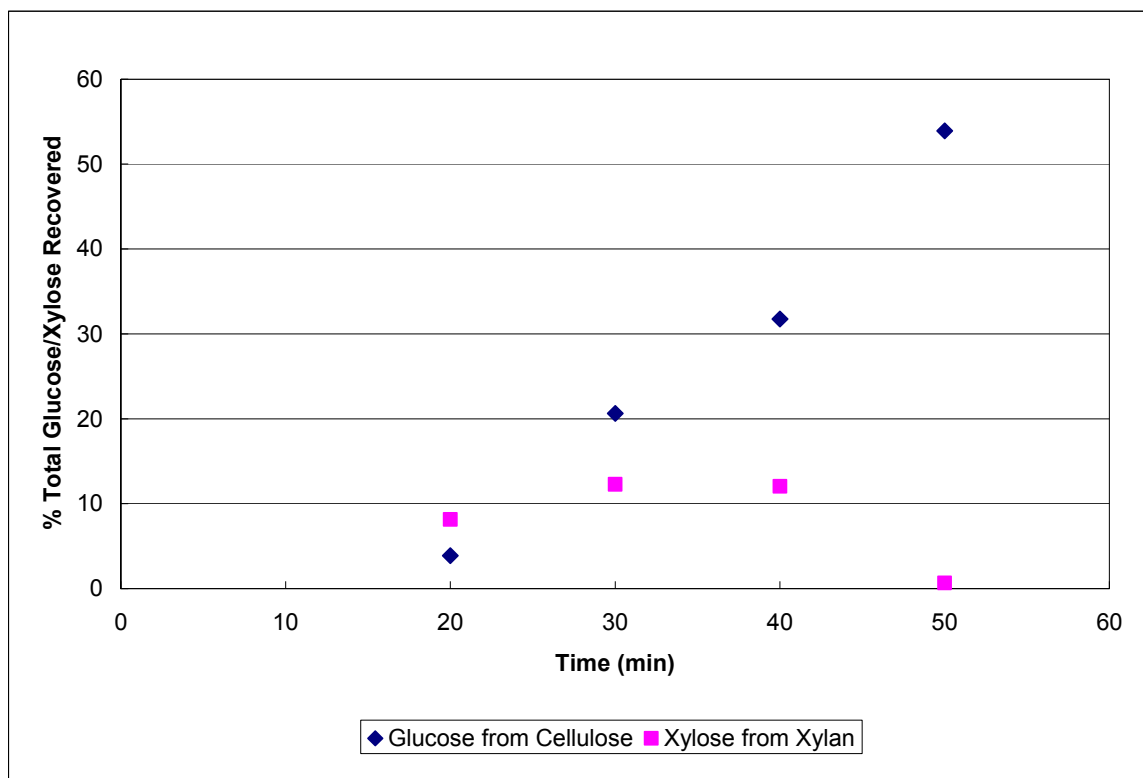


Figure 3.17: Percent monosaccharides recovered from pure cellulose and xylan (NCW at 200 °C).

## Real Biomass

Several test cases for real biomass (pine wood chips and switchgrass) were examined to demonstrate the effectiveness of the CO<sub>2</sub>-Enhanced NCW pretreatment. The first initial study involved pine wood chips pretreated with NCW and NCW+CO<sub>2</sub>, respectively, for 20 min at 150 °C. CO<sub>2</sub> was added at 2000 psi using an Isco syringe pump after 10 minutes, so the NCW+CO<sub>2</sub> reactor was pressurized for a total of 10 min. The total concentrations of carbohydrates found in the liquid process fraction were compared. The results are depicted in Figure 3.18.

As can be seen, the addition of CO<sub>2</sub> significantly affected the concentration of the monosaccharides recovered from the wood chips. In every case except mannose, the addition of CO<sub>2</sub> provided a better sugar recovery. The oligomers reported are not yet identified, but from the HPLC elution time they are expected to be either disaccharides or trisaccharides. The decrease in mannose concentration is most likely due to the formation of degradation products. While no degradation products have yet been identified in this series of experiments, it is the next planned segment of the project.

An examination of switchgrass yielded similar results. The overall concentration of xylose and arabinose, two major components of the hemicellulose fraction of switchgrass, increased drastically. The concentration of Oligomer B, again probably a di- or trisaccharide, also significantly increased. The change in glucose is within experimental error and not considered significant. As for as the decrease in Oligomer A, it is likely that the addition of CO<sub>2</sub> to the NCW allowed it to be broken down further, which can also partially account for the increased concentration of xylose and arabinose.

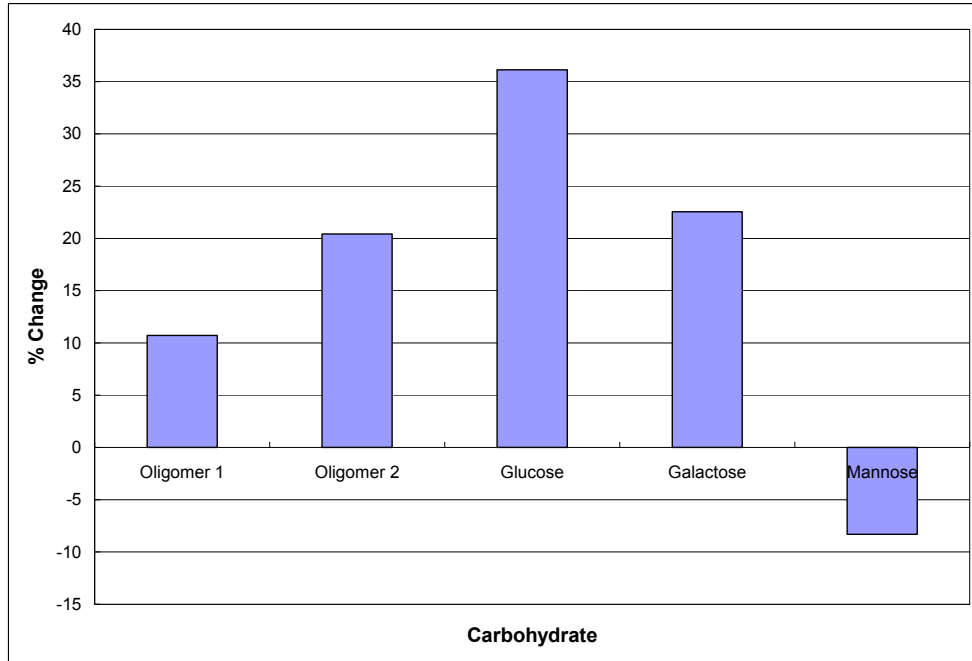


Figure 3.18: Change in carbohydrate concentration between NCW and NCW+CO<sub>2</sub> for pine wood chips (150 °C, 1000 psi, 20 min).

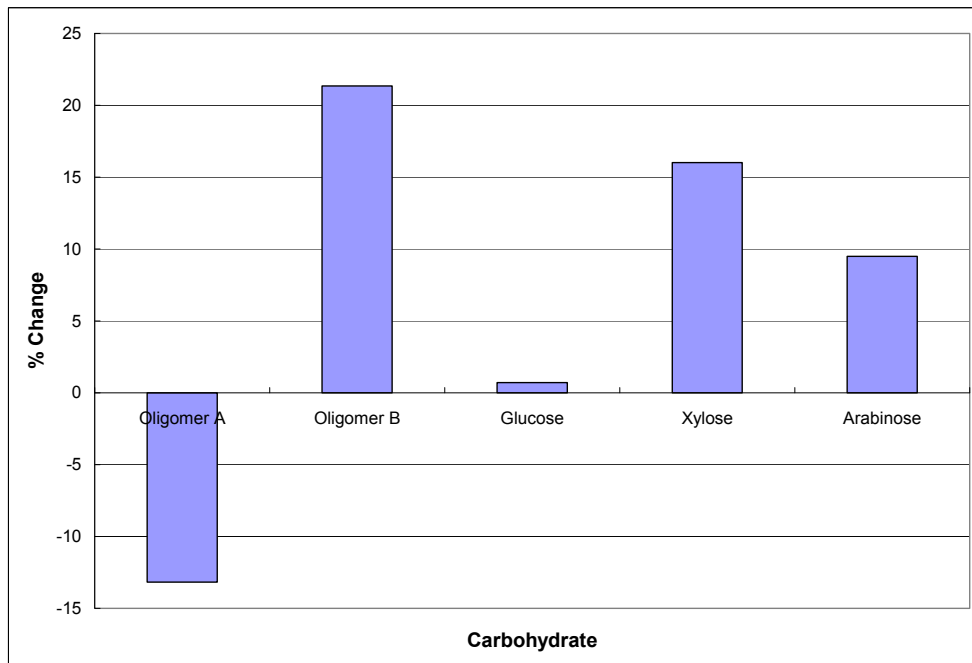


Figure 3.19: Change in carbohydrate concentration between NCW and NCW+CO<sub>2</sub> for switchgrass (200 °C, 2000 psi, 30 min).

These results are promising, but the method needs to be modified before more analysis occurs. The titanium reactors are useful because they allow small amounts of material to be tested at one time, but conversely, the small amount of material can lead to significant experimental error. Due to the complex nature of biomass, it was difficult to keep experimental volumes consistent through the course of the experiments while working up the liquid fraction after pretreatment according to the method described in “Sulfuric Acid Hydrolysis of Liquid Fraction Samples.”

A significant limitation in this experimental procedure is the lack of mixing in the small titanium reactors. One way to circumvent the mixing and volume issues would be to use the Parr reactor for future experiments involving CO<sub>2</sub>-Enhanced NCW. The larger volume available in the Parr reactor reduces the significance of any small volume losses during the workup procedure. Additionally, the larger experimental volume means that no additional H<sub>2</sub>O will need to be added to the sample in order to make it large enough for HPLC analysis. Concentrated samples will also alleviate some experimental error as the signal to noise ratio of the HPLC-RID peaks will improve significantly.

### **Organic Acid-Enhanced CO<sub>2</sub>**

Initial studies for this pretreatment involved examining the mass loss during the pretreatment process. Corn stover was pretreated in just scCO<sub>2</sub>, in acetic acid-enhanced scCO<sub>2</sub>, and in formic acid-enhanced scCO<sub>2</sub>. For all pretreatments, the experimental conditions were 1450 psi, 40 °C, and 1 hour. These conditions are supercritical for only CO<sub>2</sub>, and just outside of supercritical conditions for the mixtures. This means the organic acid-enhanced scCO<sub>2</sub> pretreatments occurred in a gas-expanded liquid (GXL). There was no mass loss for only scCO<sub>2</sub>, supporting the hypothesis that the addition of organic acids

is necessary to facilitate hydrolysis. The mass loss for both acid pretreatments (30% for acetic acid and 28% for formic acid) was within experimental error. These values for the two pretreatment experiments initially suggest that the specific organic acid used may not be significant. Further studies would be needed to see whether formic acid or acetic acid is a better choice, and the specific degradation products formed would probably be the contributing factor in the decision.

A qualitative analysis was completed using Scanning Electron Microscopy (SEM). Samples of untreated corn stover and corn stover pretreated in the acetic acid-enhanced CO<sub>2</sub> system were compared at 400x magnification. As can be seen in Figure 3.20, acetic acid-CO<sub>2</sub> system appreciably altered the physical characteristics of the corn stover sample. Portions of the sample have been fragmented and some parts removed completely. These images provide visual confirmation that an organic acid / CO<sub>2</sub> mixture can have a significant physical effect on the biomass samples.

More detailed studies were undertaken on corn stover pretreated with formic acid-enhanced CO<sub>2</sub>. After the biomass was rinsed with H<sub>2</sub>O and filtered, the carbohydrate concentration of the filtrate was examined. The HPLC-RID chromatograph in Figure 3.21 depicts that a sizeable amount of glucose (elution time 13.176 minutes) was obtained from the pretreated corn stover. A surprising result, however, was the presence of a nearly equal peak of a compound eluting at 20.196 min. This is later than the standard expected monosaccharides (glucose, galactose, arabinose, xylose, and mannose) should elute.



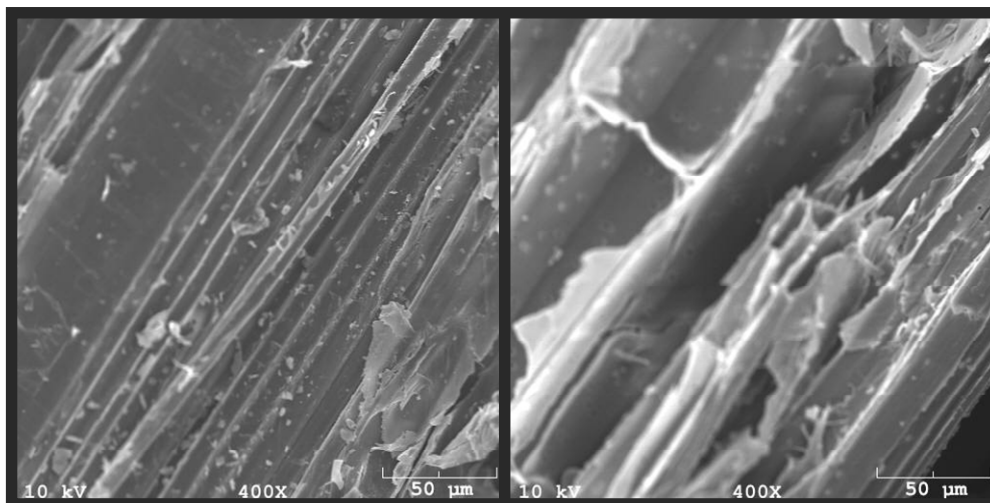


Figure 3.20: SEM images (400x) of untreated corn stover (left) and acetic acid-enhanced  $\text{scCO}_2$  pretreated corn stover (right).

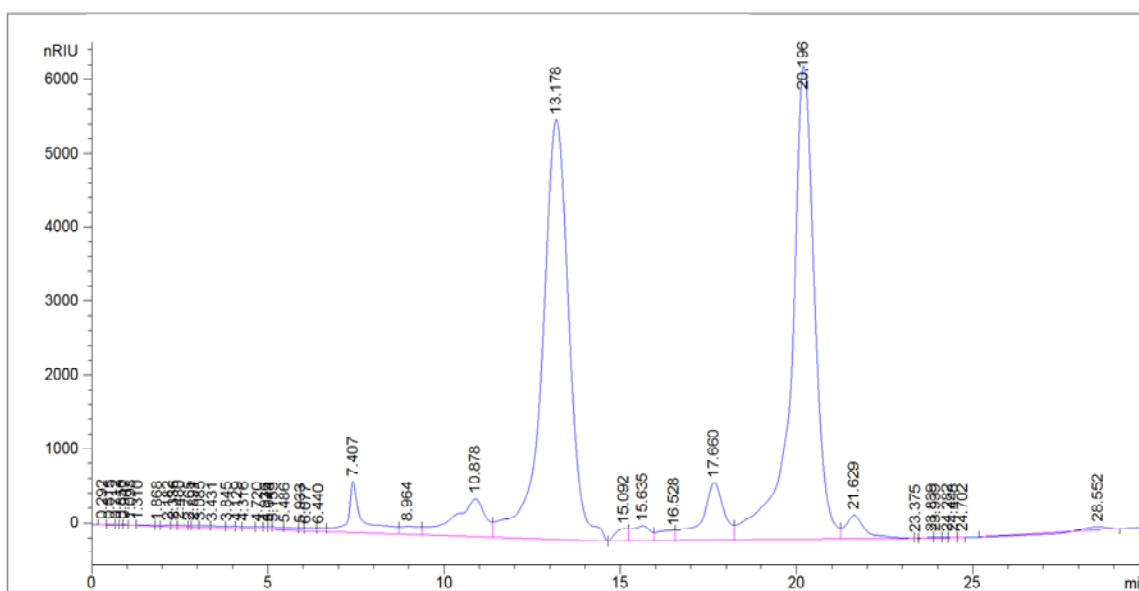


Figure 3.21: HPLC analysis of corn stover liquid process fraction after pretreatment with the formic acid-enhanced  $\text{scCO}_2$  process (1500 psi, 1 h, 40 °C).

It was hypothesized that the glucose might be undergoing an isomerization to fructose during either the pretreatment experiment itself or the workup required before HPLC-RID analysis. Running a standard fructose solution through the HPLC-RID confirmed that the unexpected peak in our process sample elutes at the same time as fructose. As fructose is not a component of either cellulose or hemicellulose, the presence of the peak suggests that our isomerization theory may be correct. The isomerization conditions need to be better understood, however, before further experimentation and analysis can occur. Some ideas for future study for this project will be discussed later.

One significant issue with using the Parr reactor for these experiments is the long heating time required. The heating element often overshoots the desired temperature, so it takes 30 minutes for the Parr to stabilize at 40 °C. This means that before the scCO<sub>2</sub> is even added, the biomass has been sitting in the organic acid for a substantial amount of time. If any experiments were to go higher in temperature, such as the high temperatures required for the NCW+CO<sub>2</sub> system ( $\geq 150$  °C), the heating situation would be more of a problem. Should future NCW+CO<sub>2</sub> experiments be conducted in a Parr reactor, additional measures will have to be taken to decrease the time it takes for the reactor to reach temperature.

## **Sulfone**

### BS for Biomass Pretreatment

Initial studies for this pretreatment also involved examining the mass lost during the pretreatment process. Corn stover was pretreated in butadiene sulfone at 70 °C for 1 hour and for 24 hours. While BS is easier to work with since it is commercially-

available, its higher decomposition temperature makes it difficult to analyze its effectiveness as a pretreatment option. It does not easily decompose into its volatile components, so any efforts to remove the solvent via heat lead to charring of the biomass. Attempts to crystallize BS by dropping the temperature below its freezing point resulted in crystallization not only of butadiene sulfone, but also the liquid fraction of biomass that needed to be analyzed. The procedure eventually used, which involved keeping a heat gun on the BS to keep it a liquid during vacuum filtration of the biomass sample, did not remove the entire amount of BS. Even with copious rinses with H<sub>2</sub>O, enough BS remained on the biomass (visual confirmation due to biomass clumping) that the mass loss measurement was not fully accurate. Thus, the initial mass loss measurement of 35% (1 hour, 70 °C) is likely significantly less than the actual value.

SEM images were also taken of corn stover pretreated in BS and compared to the images of untreated corn stover at 400x magnification. As can be seen in Figure 3.22, the butadiene sulfone pretreatment also drastically altered the physical characteristics of the corn stover sample. The structure has been significantly damaged, suggesting that the sulfurous acid has eroded part of the sample. These images provide visual confirmation that the butadiene sulfone pretreatment also has an impact on the physical structure of the biomass sample.

Considering the difficulties faced when separating the BS from the liquid fraction of the biomass sample after pretreatment, it would make sense to run further pretreatment studies in PS. The following section, however, will discuss why the PS has not been fully studied as a pretreatment option at this juncture.

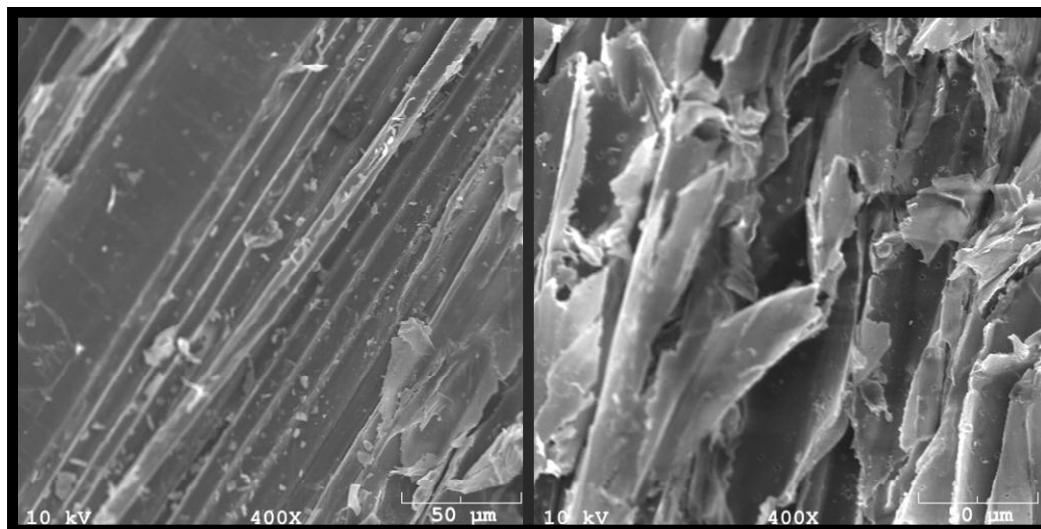


Figure 3.22: SEM images of untreated corn stover (left) and butadiene sulfone pretreated corn stover (right).

### PS as a Cellulose Solvent

#### *PS Only*

PS was first examined by itself as a cellulose solvent. Two different analytical techniques were tried. The first involved  $^1\text{H}$  NMR and  $^{13}\text{C}$  NMR in d-DMSO. The NMRs were attempted at 80 °C to ensure that any cellulose in the NMR sample would be dissolved in the d-DMSO. Neither the  $^1\text{H}$  NMR or  $^{13}\text{C}$  NMR showed any peaks, however, suggesting that there was no cellulose dissolved in the PS. The attempt was then made to modify the sulfuric acid hydrolysis method for cellulose solubility.

The HPLC-RID analysis did not have peaks in the expected elution times for carbohydrates. Near the end of the 30 minute run, however, a large, broad peak began to elute. The method was changed to run for 45 minutes and the sample was run again. The same large, broad peak appeared at approximately 30 minutes and lasted until the method ended at 45 minutes. No peaks appeared in the expected carbohydrate elution time range.

The lack of peaks in the  $^1\text{H}$ -NMR and  $^{13}\text{C}$ -NMR spectra, as well as in the HPLC-RID chromatograph, suggest that there was minimal, if any, cellulose dissolved in the PS at the given conditions. It is important, however, to note the large peak that appeared during the HPLC-RID method. The presence of a large, broad peak late in a method can suggest column degradation. The next several experiments run on the HPLC also gave poor results, so the AMINEX 87-P column had to be washed with copious amounts of 30% acetonitrile/70%  $\text{H}_2\text{O}$  to regenerate it. The observed drop in performance suggests that even if PS proves to be an excellent pretreatment option, the workup procedure and/or analysis must be changed in order to protect the HPLC column and provide accurate results.

The crystallinity index (CrI) of cellulose treated in PS was also examined. Our measurements showed that Avicel cellulose has a starting CrI of approximately 62. The cellulose left in PS overnight at 80 °C had a CrI of 60. Although this is a decrease in the overall crystallinity, this is still possibly within error of the solid-state  $^{13}\text{C}$ -NMR analysis used to determine the CrI. A further discussion of the crystallinity index, and the significance of any decrease in the index, can be found in Appendix A.

#### *PS + Formaldehyde*

Formaldehyde was next examined as a possible PS additive to enhance solubility. It was decided initially to test a 37 wt% formaldehyde solution (in  $\text{H}_2\text{O}$ ) already available in lab before going to the additional effort required to decompose paraformaldehyde into formaldehyde. Previous studies in our lab have shown that adding up to 10 wt%  $\text{H}_2\text{O}$  does not significantly change the solvent properties of PS, and adding 5 wt% of the above formaldehyde solution meant that 8.5%  $\text{H}_2\text{O}$  would be present. Cellulose (10 wt%) was

placed in a formaldehyde/PS (5 wt% formaldehyde, 8.5% H<sub>2</sub>O) solution at 80 °C overnight. The <sup>1</sup>H-NMR spectrum of the solution contained multiple unexpected peaks, suggesting the formation of side products during the attempted cellulose dissolution.

A literature review revealed that formaldehyde is known to undergo a Frins reaction with piperylene. The 80 °C experimental condition was hot enough to decompose some PS to piperylene and SO<sub>2</sub>, so it is possible that the piperylene either reacted with formaldehyde or with both formaldehyde and H<sub>2</sub>O to yield the two products shown in Figure 3.23.<sup>38</sup>

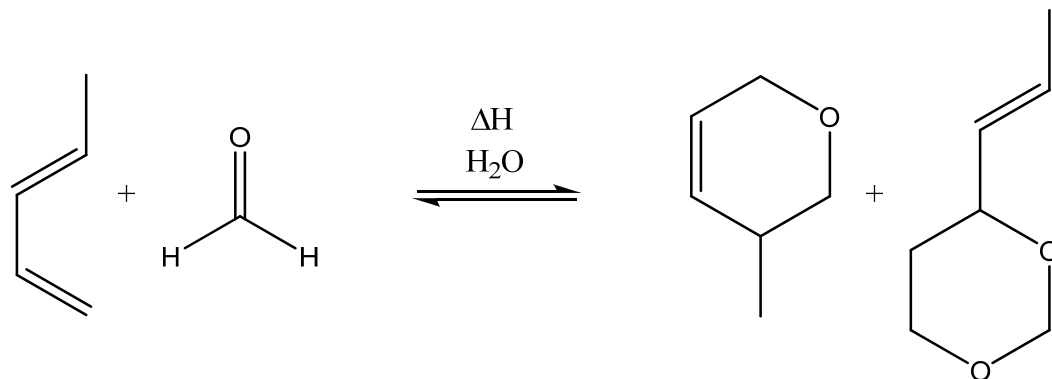


Figure 3.23: Frins reaction of piperylene and formaldehyde.<sup>38</sup>

These products were not confirmed in any way; rather, the reaction is given as a possible explanation as to why products formed while attempting to dissolve cellulose under these conditions. The actual products were never analyzed because there was no interest in pursuing this dissolution path.

## *PS + TBAF*

TBAF was also tested as a possible additive to enhance cellulose solubility in PS. Cellulose (10 wt%) and TBAF (16.6 wt%) were added to PS and left overnight at 80 °C. By the following morning, the entire contents of the flask had changed to an orange solid. A similar situation had occurred previously in our lab when NaOH was added to piperylene sulfone (results not published). It is expected that the TBAF caused a similar reaction to occur, resulting in the formation of a solid. The possible reaction scheme is shown below. The product was again not confirmed by any analytical methods since the experiment was dropped after the solid formation.

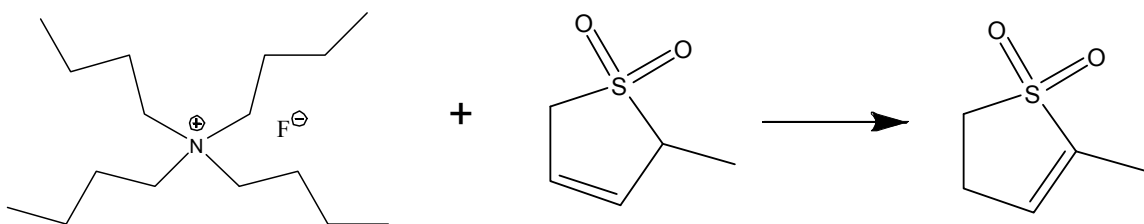


Figure 3.24: Predicted solid product formation from the reaction of TBAF and PS.

## **CONCLUSIONS AND RECOMMENDATIONS**

This chapter discussed an assortment of alternative novel solvents capable of pretreating lignocellulosic biomass. While the different methods had varying degrees of success, all of them were successful in completing at least one of the pretreatment goals mentioned. This section will cover my conclusions and recommendations for each alternative pretreatment system.

## **CO<sub>2</sub>-Enhanced NCW**

The overall results of the NCW+CO<sub>2</sub> pretreatment are encouraging to date. We have a fundamental understanding of the effects of NCW on pure cellulose and hemicellulose. Our knowledge involving NCW+CO<sub>2</sub> and these carbohydrates is increasing as more experimental conditions are tested. When using the NCW+CO<sub>2</sub> pretreatment method on pure biomass, improvements are detected for many monosaccharides and oligosaccharides.

Future work with NCW+CO<sub>2</sub> will focus on determining the percentage of the total available sugars that is recovered during the pretreatment process. We will also identify and minimize the degradation products that occur from our pretreatment process. This will allow us to better optimize the NCW+CO<sub>2</sub> pretreatment system. An AMINEX 87-H HPLC column (Agilent) has been ordered to conduct the degradation product analysis. A more quantitative analysis of the pretreatment method can be undertaken once the total sugar concentrations and degradation product concentrations are known. It is impossible to close the mass balance with our current analysis method, but our results still indicate that the pretreatment has been at least moderately successful.

This method is the most facile and most “green” method discussed in the chapter. It would be difficult to find a possible pretreatment that is more sustainable than H<sub>2</sub>O and CO<sub>2</sub>, which are both cheap and benign. As the production of alternative fuels becomes more prominent, the ability to do it sustainably and at low cost will be paramount. While the materials of construction (MOC) costs might increase due to the pressure requirements, overall this process still offers a relatively cheap method for the pretreatment of lignocellulosic biomass.



## **Organic Acid-Enhanced scCO<sub>2</sub>**

This pretreatment method, while yielding monosaccharides in the initial studies, is the most complicated of the pretreatment methods studied. First of all, the downstream separation of the organic acid from the biomass sample is uncertain. While it is believed that most of the acid will purge from the reaction vessel along with the scCO<sub>2</sub>, this has not yet been validated in an experiment. Too much organic acid left in the liquid fraction will inhibit any downstream fermentation of the sugars to ethanol, so the degree of separation is important for the validity of this option as a pretreatment method.

The results for this pretreatment are uncertain due to the HPLC peak believed to be fructose. Providing independent verification of fructose would provide needed insight into the chemistry occurring during the pretreatment. It is also important to determine whether the fructose is forming during the pretreatment itself, or during the sulfuric acid hydrolysis used to analyze the liquid fraction. Several experiments have been planned to begin this determination. GC/MS has been used in the past by ASTM International as an alternative technique to analyze sugar concentrations. ASTM Standard E 1821 uses an Agilent DB-225 gas chromatography column (or equivalent) for the analysis of carbohydrates from biomass. We have purchased a DB-1701 GC Column and plan to use it to verify that the second large peak is fructose. If it is, then a different workup method will be used to determine whether the fructose is formed during the pretreatment process or during the analysis.

It is important to remember that all of the organic acid-CO<sub>2</sub> studies to date involved a binary mixture just below its critical point. Since scCO<sub>2</sub> has significantly better penetrating power than gaseous CO<sub>2</sub>, it is expected that pretreatments done in the

supercritical state will be even more effective than the current results. Having the mixture completely supercritical should also facilitate a more thorough removal of the organic acid from the biomass after pretreatment.

### **Sulfone**

The initial tests using BS suggest that it might be a very effective biomass pretreatment solvent. The separation difficulties, however, make it difficult to fully analyze the results. Using PS will improve the separation considerably, but a new workup and analysis will be needed in order to determine its effectiveness as a pretreatment method. The ASTM standard mentioned for the organic acid-enhanced scCO<sub>2</sub> analysis could be an appropriate analytical technique and should be examined to further understand the sulfone pretreatment effects.

PS does not, however, seem to be a suitable cellulose solvent. Neither NMR nor HPLC analysis confirmed that PS was able to dissolve an appreciable amount of cellulose at any conditions. Additionally, the CrI of cellulose only decreased slightly after treatment in PS, suggesting that little was actually dissolved in the solvent. These results indicate that further studies involving cellulose dissolution in PS should be discontinued.

## REFERENCES

1. A. J. Ragauskas, C. K. Williams, B. H. Davison, G. Britovsek, J. Cairney, C. A. Eckert, W. J. Frederick, J. P. Hallett, D. J. Leak, C. L. Liotta, J. R. Mielenz, R. Murphy, R. Templer and T. Tschaplinski, *Science*, 2006, **311**, 484-489.
2. A. J. Ragauskas, M. Nagy, D. H. Kim, C. A. Eckert, J. P. Hallett and C. L. Liotta, *Industrial Biotechnology*, 2006, **2**, 55-63.
3. R. F. Association, RFA - The Industry - Industry Statistics, <http://www.ethanolrfa.org/industry/statistics/>, 2008.
4. T. Gardner, Corn is not the future of U.S. ethanol: DOE, <http://www.reuters.com/article/scienceNews/idUSN2830990020070328>, 2008.
5. N. Mosier, C. Wyman, B. Dale, R. Elander, Y. Y. Lee, M. Holtzapple and M. Ladisch, *Bioresource Technology*, 2005, **96**, 673-686.
6. C. E. Wyman, B. E. Dale, R. T. Elander, M. Holtzapple, M. R. Ladisch and Y. Y. Lee, *Bioresource Technology*, 2005, **96**, 1959-1966.
7. G. C. Akerlof and H. I. Oshry, *J. Am. Chem. Soc.*, 1950, **72**, 2844-3101.
8. B. Kuhlmann, E. Arnett and M. Sissen, *J. Org. Chem.*, 1994, **59**, 3098-3101.
9. D. Bröll, C. Kaul, A. Kramer, P. Krammer, T. Richter, M. Jung, H. Vogel and P. Zehner, *Angew. Chem. Int. Ed.*, 1999, **38**, 2998-3014.
10. K. Chandler, F. Deng, A. K. Dillow, C. L. Liotta and C. A. Eckert, *Ind. Eng. Chem. Res.*, 1997, **36**, 5175-5179.
11. K. Chandler, C. L. Liotta, C. A. Eckert and D. Schiraldi, *AIChE J.*, 1998, **44**, 2080-2087.
12. H. P. Lesutis, *Chem. Commun.*, 1999, 2063-2064.
13. W. L. Marshall and E. U. Franck, *Journal of Physical and Chemical Reference Data*, 1981, **10**, 295-304.
14. C. Liu and C. E. Wyman, *Bioresource Technology*, 2005, **96**, 1978-1985.
15. S. E. Hunter and P. E. Savage, *Industrial & Engineering Chemistry Research*, 2003, **42**, 290-294.
16. S. E. Hunter, C. E. Ehrenberger and P. E. Savage, *Journal of Organic Chemistry* 2006, **71**, 6229-6239.

17. K. Khosravi-Darani and E. Vasheghani-Farahani, *Critical Reviews in Biotechnology*, 2005, **25**, 231-242.
18. A. Demirbas, *Energy Conversion and Management*, 2001, **42**, 279-294.
19. X. J. Pan and Y. Sano, *Bioresource Technology*, 2005, **96**, 1256-1263.
20. J. A. Briones, J. C. Mullins, M. C. Thies and B. U. Kim, *Fluid Phase Equilibria*, 1987, **36**, 235-246.
21. K. McHugh, *Clinical Radiology*, 2001, **56**, 866-866.
22. H. S. Byun, K. Kim and M. A. McHugh, *Industrial & Engineering Chemistry Research*, 2000, **39**, 4580-4587.
23. D. Vinci, M. Donaldson, J. P. Hallett, E. A. John, P. Pollet, C. A. Thomas, J. D. Grilly, P. G. Jessop, C. L. Liotta and C. A. Eckert, *Chemical Communications*, 2007, 1427-1429.
24. M. Donaldson, in *Chemical and Biomolecular Engineering*, Georgia Institute of Technology, Atlanta, 2008.
25. T. J. S. Baker, L. R.; Johnson, D.C., *IPC Technical Paper Series*, 1978, **58**, 1-6.
26. C. J. N. Johnson, M.D.; Haigh, F.C., *IPC Technical Paper Series*, 1975, **5**, 1-15.
27. T. D. Heinze, R.; Koschella, A; Kull, A.H.; Klohr, E-A.; Koch, W., *Macromolecular Chemistry and Physics*, 2000, **201**, 627-631.
28. T. Heinze, K. Schwikal and S. Barthel, *Macromolecular Bioscience*, 2005, **5**, 520-525.
29. E. Hill, in *School of Chemical and Biomolecular Engineering*, Georgia Institute of Technology, Atlanta, 2007.
30. E. Newton, in *School of Chemical and Biomolecular Engineering*, Georgia Institute of Technology, Atlanta, 2005.
31. T. Chamblee, in *School of Chemistry and Biochemistry*, Georgia Institute of Technology, Atlanta, 2004.
32. H. P. Lesutis, R. Glaser, C. L. Liotta and C. A. Eckert, *Chemical Communications*, 1999, 2063-2064.
33. S. A. Nolen, C. L. Liotta, C. A. Eckert and R. Glaser, *Green Chemistry*, 2003, **5**, 663-669.
34. L. Draucker, in *School of Chemical and Biomolecular Engineering*, Georgia Institute of Technology, Atlanta, 2007.

35. A. S. Bommarius, *Metabolic Engineering*, 2008.
36. S. D. Mansfield and R. Meder, *Cellulose*, 2003, **10**, 159-169.
37. A. Sluiter, B. Hames, R. Ruiz, C. Scarlata, J. Sluiter and D. Templeton, ed. D. o. Energy, 2005.
38. M. G. I. Safarov, U.B., *Zhurnal Organicheskoi Khimii*, 1976, **12**, 1660-1664.
39. ASTM International, 2007.

## **CHAPTER 4: EMPLOYING SUPERCRITICAL FLUID CHROMATOGRAPHY FOR GREEN METABOLOMICS**

### **INTRODUCTION**

Metabolites, the end products of cellular regulatory processes, can be considered the ultimate response of biological systems to genetic, pathophysiological or environmental stresses. Metabolomic analysis can reflect the pathological state of various organs and aid in the early detection of disease. While proteomic and genomic technologies are more mature, metabolome analysis tools, which rely heavily on chemical separations, are still evolving.

A substantial challenge is analyzing and identifying potential metabolic biomarkers accurately. Supercritical Fluid Chromatography (SFC) can separate a mixture of small molecules rapidly based on their specific volatility in supercritical fluids and affinity to the separation column. More importantly, however, are the advantages of higher efficiency and better resolution than HPLC and/or GC at ambient conditions. Many common metabolites, however, have limited solubility in the supercritical fluid phase (usually  $\text{scCO}_2$ ). This provides an opportunity for researchers to improve the entire SFC process and introduce it as a standard analytical tool for metabolomics research.

This project has two main aspects. The first focus is on enhancing metabolite solubility by chemical modification using a silylation reagent to derivatize amino acids (model metabolites). The ultimate goal is to target complete metabolomes in physiological samples. The second part of the project involves the SFC separation and subsequent analysis via UV of model metabolites.

## **BACKGROUND**

### **Metabolites**

Metabolites, the end products of cellular regulatory processes, represent the endpoint of many cell-signaling events.<sup>1</sup> The study of metabolites, called metabolomics (or metabonomics for quantitative studies), refers to the global profiling of metabolites in a cell, tissue, or organism, and is a quickly emerging field in biological research. Researchers use it to complement and enhance knowledge gained from genomics and proteomics.<sup>2</sup> Metabolites are influenced by genetics, epigenetic factors, and environmental stresses.<sup>1</sup> Since metabolites can reflect pathological states, they can aid in the early detection of disease. Metabolites have been used to detect silent mutations in yeast,<sup>2</sup> infections in mice,<sup>3</sup> and are currently being screened for cancer research.<sup>1</sup> Researchers narrow their overall focus by considering only a few specific compounds (metabolite target analysis), examining certain classes of compounds (metabolic profiling), or identifying patterns with no specific identification (metabolic fingerprinting).<sup>4</sup> Improving analytical techniques for metabolomics research, however, allows a more holistic approach to be taken.

### **SFC**

A number of analytical methods are currently used in metabolomics research. The most common are <sup>1</sup>H NMR, HPLC-MS, GC-MS, and capillary electrophoresis,<sup>3</sup> but each of these methods has its limitations. SFC can be coupled to a variety of detectors including UV-Vis and MS, and has the capability to outperform these other methods. SFC has a greater efficiency and improved resolution over LC-MS or GC-MS at ambient

conditions.<sup>5</sup> It is a “green” process because it uses significantly less solvent than LC,<sup>6</sup> and the solvent is intrinsically volatile, thus desolvation during electrospray ionization for MS analysis is more efficient.

The major drawback of using SFC for metabolomics research is the limited solubility of most target molecules, which is also true for GC analysis. In the past, SFC has been used mostly for separations involving nonpolar or relatively low polarity compounds. Although SFC has been used in the past for peptide separation, the analysis required significant use of co-solvents.<sup>6</sup>

### **Improving SFC for Metabolomics**

Two primary methods can be used to improve the performance of SFC for metabolomics research. The first involves enhancing the solubility of the analytes of interest (amino acids, peptides, small organic molecules, etc.) in the supercritical fluid phase. The second alternative is to change the SFC mobile phase to improve the solubility of the molecules. Details about both options are explained further in the following sections.

#### Enhance Analyte Solubility

There are several known functional groups used in research to increase the solubility of targetted molecules in scCO<sub>2</sub>. These functional groups, which are called CO<sub>2</sub>-philic groups, include fluoroether, fluoroalkyl, fluoroacrylate, and siloxane.<sup>7, 8</sup> In GC analysis, silyl groups are often added to amino acids in order to make them more volatile. For example, various hydroxyl and amino compounds that were nonvolatile and unstable at 200-300 °C were analyzed successfully via GC after being silylated.<sup>9</sup>



Molecules are more soluble in CO<sub>2</sub> after silylation because the silyl groups replace some of the hydrogens that form hydrogen bonds. The polarity of the compound is also reduced, making it more volatile.

Silyl groups have been studied in GC, MS, and the combinations of both. For GC/MS, t-butyldimethyl silyl is the most common choice for silylation. It is usually added to a hydroxide using chloro(dimethyl)t-butyl silane. This is often done in *N,N*-dimethyl formamide (DMF) in the presence of a base such as imidazole or pyridine. The t-butyldimethyl silyl ether is generally preferred to the trimethyl silyl because the former compound is more stable to alkaline conditions, to hydrogenolysis, and to solvolysis.<sup>9,10</sup>

#### Optimize SFC Mobile Phase

Several techniques can improve the solubility of polar compounds in the SFC mobile phase. One solution is to use a fairly polar mobile phase. Ammonia, sulfur dioxide, nitrous oxide, and Freon-23 have all been utilized to improve separation of polar compounds. Another approach is to add a co-solvent, usually a protic solvent such as methanol (MeOH), to modify the CO<sub>2</sub> and improve its solvation properties.<sup>11</sup> Finally, using additives such as a highly polar or ionic compound will improve the peak shape and solubility.<sup>12</sup> These additives are often acidic and play two roles. They can increase the solvation power of scCO<sub>2</sub>, and also interact with the stationary phase of the analytical column. A fairly recent example was the addition of trifluoroacetic acid (TFA) to a scCO<sub>2</sub> mobile phase modified with MeOH. This system was used to separate peptides up to 40-mers. The TFA was believed to be effective for two reasons: it suppresses the deprotonation of the peptide carboxylic acid and protonates the amino groups.<sup>6</sup>

## **Project Goals**

This study began as a collaboration between our research lab, Dr. Facundo Fernández (School of Chemistry and Biochemistry, Georgia Tech), and Dr. Andrei Fedorov (School of Mechanical Engineering, Georgia Tech). The research plans required our lab to silylate amino acids and optimize the SFC separation and UV-analysis. Once our analytical process was optimized, we planned to interface the SFC instrument with a MS in Dr. Fernández's lab. The identification and quantification of metabolites could be completed by standard nanoelectrospray ionization, or a new technology called *AMUSE* (Array of Micromachined UltraSonic ElectroSprays), invented by Dr. Fedorov and co-developed by Dr. Fernández. This technology can enhance the ability of mass spectrometry (MS) to accurately and efficiently analyze the samples in an array format.

This metabolomics project had two main aspects. The first project goal involved repairing an old SFC instrument that had been cannibalized for parts. Once the SFC was functional, polar amino acids were silylated by several techniques in order to improve their solubility in  $scCO_2$ . Additional studies for this project involved using organic co-solvents to improve the separation of amino acids in the SFC.

## EXPERIMENTAL

### Materials

#### SFC

The following materials were used as received: carbon dioxide gas (Air Gas, SFC grade, 99.99%), methanol (BDH, 99.8%), ethanol (Acros, 190 proof, 95.0% ACS spectrophotometric grade), and 2,2,2 trifluoroethanol (Alfa Aesar, 99%).

#### Amino Acids

*N*-Boc-L-phenylalanine (Alfa Aesar, 99%) was used as received. The following amino acid starting materials underwent chemical modification: L-cysteine (TCI America, 98%), L-lysine hydrate (Aldrich, 97%), L-serine methylester hydrochloride (Aldrich, 98%), L-tyrosine methylester hydrochloride, and L-tryptophan methylester hydrochloride. L-tryptophan methyl ester hydrochloride (Alrich, 98%) was neutralized prior to use.

#### Synthesis of Silylated Amino Acids

*Initial Silylation Reagent: Synthesis of 1-[2-(4-chloromethyl-phenyl)-ethyl]-1,1,3,3,3-pentamethyldisiloxane<sup>10</sup> (Figure 4.1)*

The 4-vinyl-benzyl chloride (5.0 g, 0.0337 mol) was added to heptane (20 mL) and put under nitrogen. The mixture was heated to 75 °C. The catalyst, platinum(0)-1,3-divinyl-1,1,3,3-tetramethyl disiloxane complex (3 wt% xylene) (DVDS-Pt) (1.7 g, 1 %wt), was added to the solution. The pentamethyl disiloxane (5.75 g, 0.0388 mol, 1.15

equiv) in 5 mL of heptane was added slowly dropwise. The solution changed from a light yellow to a dark brown upon addition and the addition was stopped whenever the reaction temperature increased by more than 2 °C. After the addition was complete, the temperature was reduced to 70 °C and the reaction was heated for 3 hours. After 3 hours, the reaction was allowed to cool to room temperature and was stirred overnight. To work up the reaction, the heptane was removed under reduced pressure. A column of silica gel in hexane was run and all the fractions combined. The hexane was removed under reduced pressure to give a clear liquid. Yield was 50%.

1-[2-(4-chloromethyl-phenyl)-ethyl]-1,1,3,3,3-pentamethyldisiloxane:  $^1\text{H}$  NMR ( $\text{CDCl}_3$ ) ppm: 0.1 (15, m), 0.9 (2, m), 1.3 (2, m), 2.3 (2, m), 2.7 (2, m), 4.6 (2, s), 7.2 (4, m).  $^{13}\text{C}$  NMR ( $\text{CDCl}_3$ ) ppm: 1.516-2.156, 20.39, 29.2533; 46.49, 129.42-127.44, 134.50, 145.56. GC-MS analysis was done on a HP GC 6890/ HP MS 5973. MS(m/z): 300 ( $\text{M}^+$ ). EA: calculated, C, 55.87%, H, 8.41%. Found, C, 55.82%, H, 8.41%.

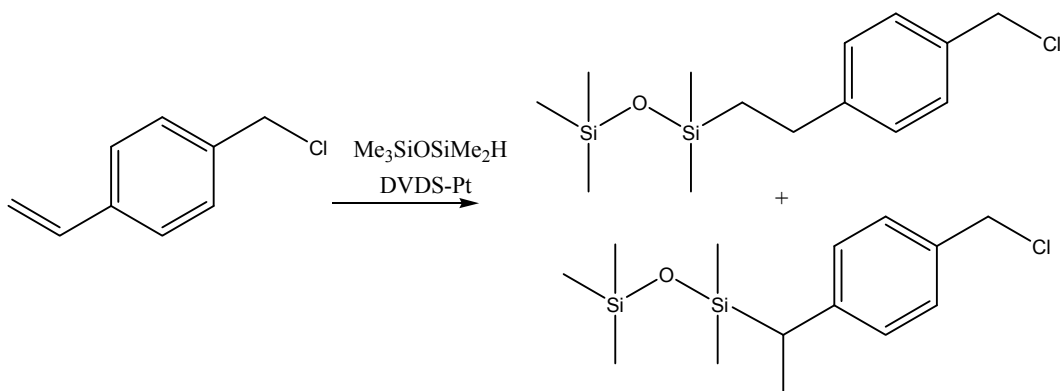


Figure 4.1: Synthesis of 1-[2-(4-chloromethyl-phenyl)-ethyl]-1,1,3,3,3-pentamethyldisiloxane with both isomers shown.

*Silylated Cysteine: Synthesis of 2-Amino-3-(4-chloromethylphenyl)propionic acid (Figure 4.2)*

Cysteine (0.33 g, 5x excess) and tetrabutylammonium chloride hydrate (0.014 g, 10 mol%) were added to ethylacetate (3 mL). The solution was put under nitrogen. 1-[2-(4-chloromethyl-phenyl)-ethyl]-1,1,3,3,3-pentamethyl disiloxane (0.3 mL) was added and the solution was heated to 70 °C for 48 hours. The reaction was tested by <sup>1</sup>H NMR and no reaction was observed. Triethylamine (0.1 mL) was added as an HCl scavenger, and the mixture ran five more days until reaction was observed to be complete by <sup>1</sup>H NMR. To work up the reaction, the excess cysteine was filtered off. The organic phase was washed with water three times and dried with magnesium sulfate. The solvent was removed under reduced pressure. The benzyl CH<sub>2</sub> peak appears to have shifted from 4.6 to 5.1 ppm in the <sup>1</sup>H NMR. Isolation of the product was not successful by a silica column using 50/50 EtOAc/Hexane, and flushing using 100% hexane, 100% ethyl acetate, and 100% methanol.

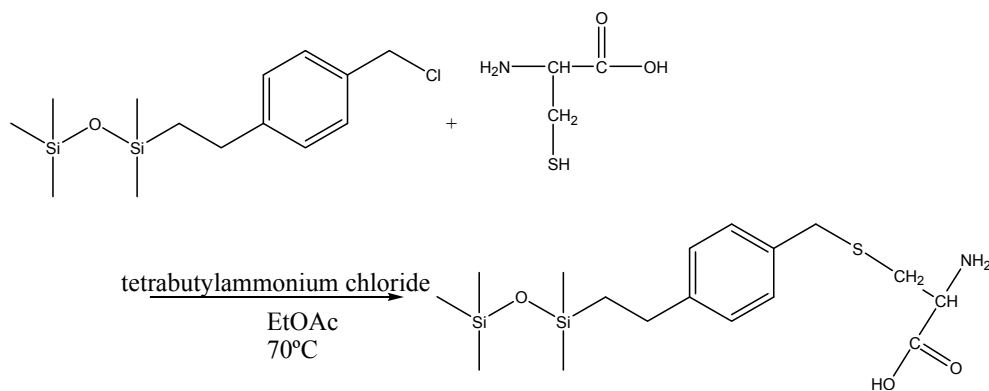


Figure 4.2: Reaction of cysteine with benzylchloride disiloxane.

*Silylated Lysine: Synthesis of 2-Amino-6-(4-[2-(1,1,3,3,3-pentamethyl-disiloxanyl)-ethyl]-benzylamino)-hexanoic acid (Figure 4.3)*

1-[2-(4-chloromethyl-phenyl)-ethyl]-1,1,3,3,3-pentamethyl disiloxane (1.2 mL) was added to ethylacetate (12mL) and put under nitrogen. Lysine hydrate (1.6 g, 5x excess) and tetrabutylammonium chloride (0.0494 g, 5 mol %) were added. The reaction was heated to 70 °C overnight. To workup the reaction, the lysine was removed by filtration. The organic phase was washed with water three times and dried by magnesium sulfate. The solvent was removed under reduced pressure. The benzyl CH<sub>2</sub> peak appears to have shifted from 4.6 to 5.1 ppm in the <sup>1</sup>H NMR. Isolation of the product was unsuccessful, however, by a silica column using a 25/75 hexane and ethyl acetate.

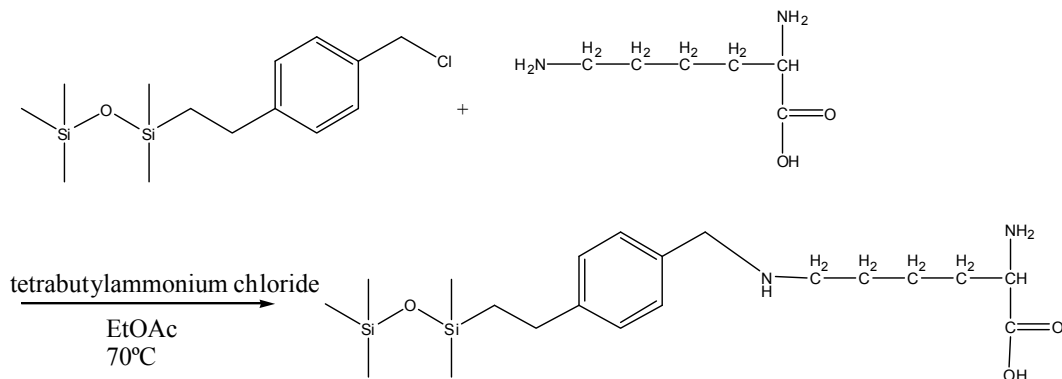


Figure 4.3: Reaction of lysine with benzylchloride disiloxane.

*Silylated Serine: Synthesis 2-amino-3-(methyl-diphenyl-silanyloxy)-propionic acid*

(Figure 4.4):

Serine methylester hydrochloride (0.5 g, 1 equiv) was dissolved in DMF (4 mL). Imidazole (0.4 g, 2 equiv) and chloro(methyl)diphenylsilane (0.8 g, 1.1 equiv) were added. The reaction was put under nitrogen and stirred overnight at room temperature. To work up the reaction, water (25 mL) was added to the reaction. The water was extracted with ether (3x50 mL). The ether layers were combined, washed with saturated aqueous NaCl, and dried with magnesium sulfate. The solvent was removed under reduced pressure. GC-MS showed 70% product, 2-amino-3-(methyl-diphenyl-silanyloxy)-propionic acid (retention time 13 min), and 30% starting material, chloro(methyl)diphenylsilane, which becomes methyl-diphenyl-silanol after a water wash (retention time 10 min). The mixture was distilled at 250 °C using vacuum, but trace amounts of starting material remained with the product.

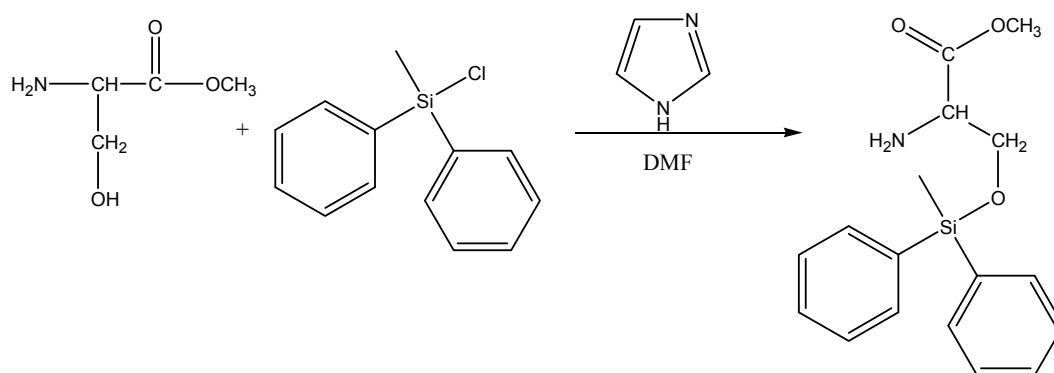


Figure 4.4: Synthesis of 2-amino-3-(methyl-diphenyl-silanyloxy)-propionic acid.

Different ratios of the starting materials were used to turn chloro(methyl)diphenylsilane into the limiting reagent since it was difficult to remove. The excess serine could be removed by a water wash. Serine methylester hydrochloride (0.4 g, 1.5 equiv) was dissolved in DMF (6 mL) and put under nitrogen. Imidazole (0.3 g, 2 equiv) and chloro(methyl)diphenylsilane (0.5 mL, 1 equiv) were added. The reaction was put under nitrogen and stirred overnight at room temperature. To work up the reaction, water (25 mL) was added to the reaction. The water was extracted with ether (3x50 mL). The ether layers were combined, washed with saturated aqueous NaCl, and dried with magnesium sulfate. The solvent was removed under reduced pressure. Analysis via GC-MS showed the hydrolyzed starting material, methyl-diphenyl-silanol.

*Initial Silyl-Tyrosine: Synthesis of 2-amino-3-(4-trimethylsilyloxy-phenyl)-propionic acid methyl ester (Figure 4.5)*

L-tyrosine methylester hydrochloride (1.4g, 1.5 equiv) was dissolved in DMF (6mL). Imidazole (0.5g, 2 equiv) and chlorotrimethyl silane (0.5mL, 1 equiv) were added. The reaction was put under nitrogen and stirred overnight at room temperature. To work up the reaction, water (25mL) was added to the reaction. The water was extracted with ether (3x50mL). The ether layers were combined, washed with saturated aqueous NaCl, and dried with magnesium sulfate. The solvent was removed under reduced pressure.



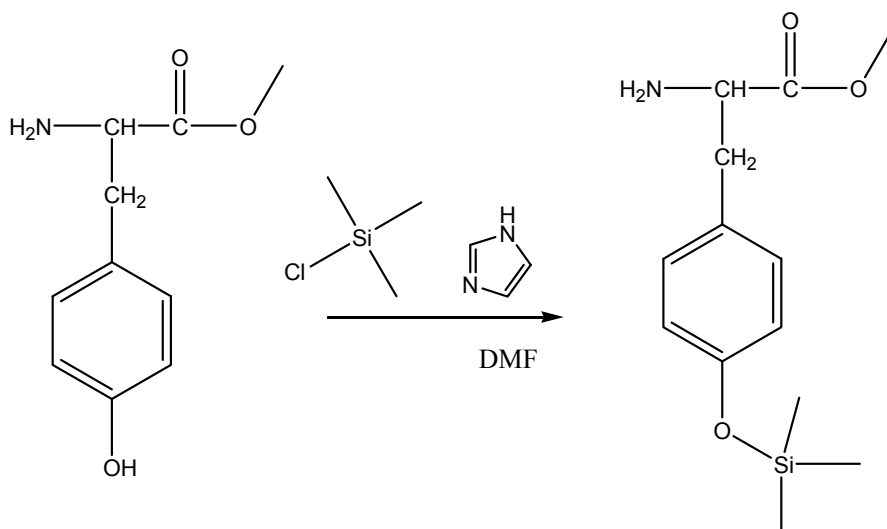


Figure 4.5: Synthesis of 2-amino-3-(4-trimethylsilyloxy-phenyl)-propionic acid methyl ester.

*Synthesis of Final Silylated Tyrosine: 3-[4-(tert-butyl-dimethyl-silanyloxy)-phenyl]-2-formylamino-propionic acid methyl ester (Figure 4.6)*

L-tyrosine methylester hydrochloride (0.5 g, 1 equiv) was dissolved in DMF (10 mL). Chlorodimethyl t-butyl silane (0.7 g, 2.2 equiv) and imidazole (0.5 g, 3.3 equiv) were added. The reaction was put under nitrogen and stirred at room temperature for five days. The reaction solution turns yellow. To work up the reaction, ether (40 mL) was added and was washed with water (5x50 mL). The organic phase was dried with magnesium sulfate and the solvent was removed under reduced pressure. A silica plug of 90/10 CH<sub>2</sub>Cl<sub>2</sub>/EtOAc was used to remove the silyl impurity. An ethyl acetate flush of the plug contained the pure product, a yellow oil (32% yield), without optimization.

3-[4-(tert-butyl-dimethyl-silyloxy)-phenyl]-2-formylamino-propionic acid methyl ester:

$^1\text{H}$  NMR ( $\text{CDCl}_3$ ) ppm: 0.18 (s, 6H), 0.97 (s, 9H), 3.1 (d, 2H), 3.73 (s, 3H), 4.9 (m, 1H), 6.05 (s, 1H), 6.7 (d, 2H), 6.9 (d, 2H), 8.1 (s, 1H).  $^{13}\text{C}$  NMR ( $\text{CDCl}_3$ ) ppm: -4.46, 18.16, 25.62, 36.99, 51.86, 52.41, 120.19, 127.93, 130.22, 154.88, 160.38, 171.57. MS(m/z): 338.0 EA: calculated C, 60.50%, H, 8.06%, N, 4.15%. Found C, 60.37%, H, 8.22%, N, 3.99%.

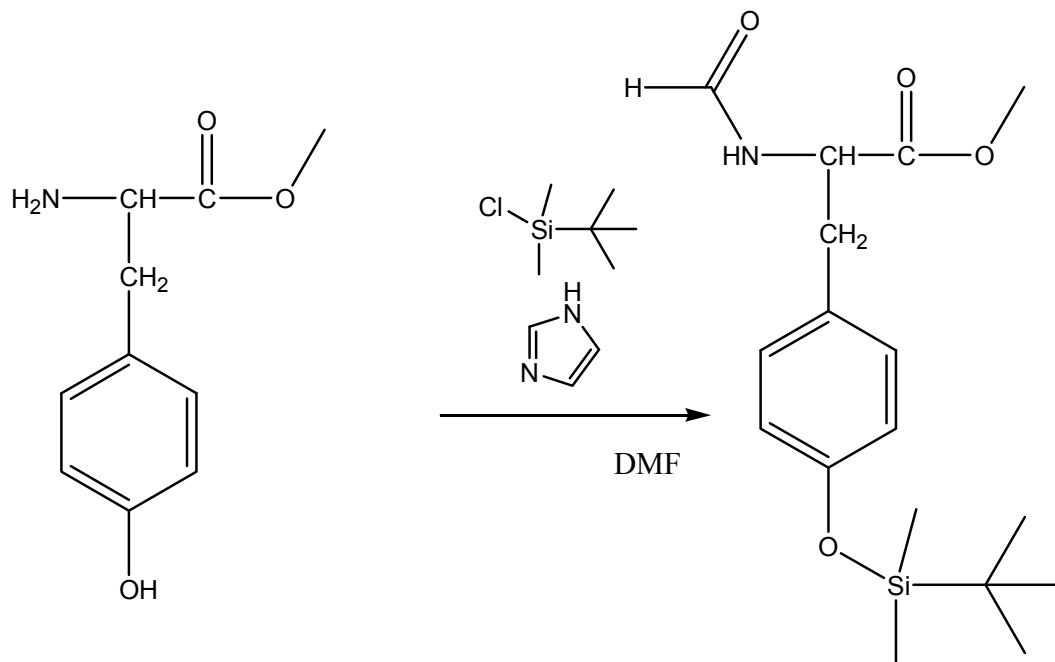


Figure 4.6: Synthesis of 3-[4-(tert-butyl-dimethyl-silyloxy)-phenyl]-2-formylamino-propionic acid methyl ester.

## **Analysis**

### Silylation of Amino Acids

$^1\text{H}$  and  $^{13}\text{C}$  NMR spectra were recorded using a Varian Mercury Vx 400 spectrometer using residual  $\text{CDCl}_3$  peak as an internal reference. Mass Spectrometry samples were submitted to the Mass Spectrometry Facility and used ESI-MS unless noted. GC-MS analysis was done on a Hewlett-Packard GC 6890 / Hewlett-Packard MS 5973 equipped with a HP-5MS (Agilent, 5% phenyl-methylpolysilane) column. Elemental analyses were submitted to Atlantic Microlabs, Inc.

### SFC

The SFC, consisting of a Fluid Control Module (FCM), Thermal Control Module (TCM), and autosampler, was purchased from Berger Instruments. It was also equipped with a UV-Vis detector (Hewlett Packard, Model 1050). The system was controlled by SFC 3D Chemstation (Version 3.4) software supplied by Berger Instruments. The separation column was a SFC 2-ethylpyridine column (150 mm length, 5  $\mu\text{m}$  particle size, 4.6 mm ID) purchased from Princeton Chromatography. The fiber optic detection was done via an Ocean Optics spectrometer (USB2000, 190-420 nm) controlled by OOIBase32 (Version 2.0.2.2) software supplied by Ocean Optics. The light source for the fiber optics detection was a Mikropack DH-2000-BAL UV-Vis-NIR Lightsource containing deuterium and halogen bulbs.

## RESULTS AND DISCUSSION

### Rebuilding the SFC

The Berger SFC was completely nonfunctional at the beginning of this project. Parts of it had been cannibalized for other projects and were missing completely. The initial portion of this project was therefore to determine which parts of the SFC were still usable, and replace any pieces needed in order to make the instrument serviceable.

#### Initial Assessment and Repairs

##### *Primary SFC Unit – Flow Control Module (FCM)*

All of the SFC parts were examined and tested to determine functionality. The components inside the SFC were identified by comparison with similar parts in a HPLC, by labels on some components, and by visual inspection. The FCM of the Berger SFC is comprised of the following components: primary pump for CO<sub>2</sub> (or other supercritical solvent), a secondary pump for a co-solvent, a solvent mixer, a pressure transducer, and a backpressure regulator. The additional modules mentioned earlier (the autosampler, a thermostated oven (TCM), and the UV-Vis detector) were controlled by the computer.

A cursory examination of the primary pump revealed that one of the two glass pistons had broken, and the pump chamber was no longer sealed. The secondary co-solvent pump was also nonfunctional. The pressure transducer seemed to work properly, but the backpressure regulator was not able to hold pressure because the mounting bolts had been sheared off during a previous modification. More importantly, there was no established flow path connecting all of the components in the SFC.

The primary pump was replaced by an Isco D500 syringe pump and the secondary pump was removed since co-solvents were not originally involved. A modification was made to the backpressure regulator so it would accept new mounting bolts. The flow path was then partially repaired by using HIP tubing ( $1/16$  inch OD, 0.030 inch ID) to connect the Isco pump sequentially to the solvent mixer, the backpressure regulator, the pressure transducer, and the injector. More HIP tubing was used to connect the injector to the analytical column (kept inside the oven), and from the column to the UV-Vis detector.

#### *Additional SFC Modules*

Initial testing determined that the oven was operating properly. Although the UV-Vis detector was also working, there was a communication problem between the computer and the detector. After the injection, the method would stop running immediately and the UV-Vis data was not recorded. The source of the communication error was never found, but the problem was solved by manually starting the detector, using the control panel located on it, during each sequence. The manual activation of the detector initiated data recording in real-time and also started the method.

The autosampler required repairs as well. It communicated with the computer, but the needle was misaligned properly and broke after only two runs. The needle was replaced multiple times with extra syringe needles, and a guidance system was built. The guidance system forced the injection needle to stay straight while puncturing the sample vial septum, and provided additional support to the needle to keep it from breaking. Once the guidance system was built, the autosampler functioned as expected. Figure 4.7 illustrates the entire SFC system after initial repairs and modifications.

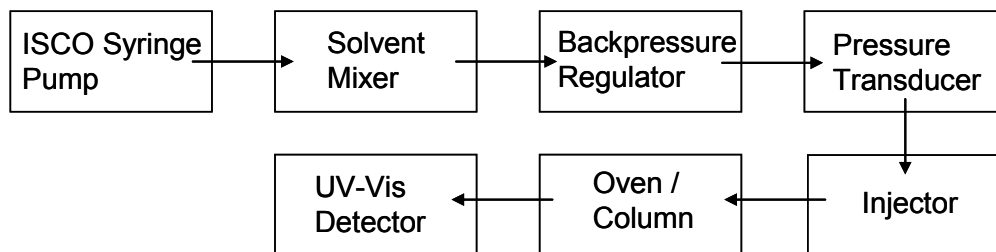


Figure 4.7: Initial reconstituted flow path of the SFC.

### Further System Modifications

#### *Testing the Rebuilt SFC*

An initial system test was attempted after the above modifications were made. The  $\text{scCO}_2$  was unable to pass completely through the system. By testing each module individually, it was determined that the source of the blockage was the modified backpressure regulator. Attempts to repair the backpressure regulator were not successful, so a decision was made to bypass both the backpressure regulator and the pressure transducer. Instead, an external pressure transducer was added to the SFC system, and an external flow control system was built. The external pressure transducer (Druck, PDCR 910), connected to an external indicator (Druck, DPI 260), was placed between the analytical column outlet and the UV-Vis detector to ensure the system was still supercritical before the analytes entered the detector. The external flow control system will be discussed in detail in the next section.

### *External Flow Control*

A simple external flow control system consisting of the Isco syringe pump and two HIP needle valves was implemented. The decision to use the Isco flow meter and needle valves was made because there was no simple way to use the computer to control the flow rate in the system. The Isco was run at constant pressure; the flow was varied between 2000 psi and 3000 psi, depending on the experiment. The first valve, placed between the Isco pump and the injection assembly, was used to choke down the Isco flow down to a rate between 0.5 mL/min and 1.5 mL/min. This flow range was chosen because it has previously been used in the literature.<sup>6</sup> The second needle valve was placed after the UV-Vis detector. It was kept mostly closed in order to constrict the outlet flow, allowing pressure to build inside the SFC. The valve was set to try to keep the internal pressure of the SFC around 2000 psi to ensure the CO<sub>2</sub> was supercritical.

Temperature control was a critical aspect of this control system. Gas expanding across a valve cools rapidly, and additional measures were taken to try to keep the temperature, and thus the flow, constant. Without temperature control across the valves, the CO<sub>2</sub> could cool enough to stop being in a supercritical phase. The temperature of the valves was controlled initially by using two water baths. The first valve was kept in a 40 °C water bath, and the second valve was placed in a room temperature water bath.

Even with the water baths used for temperature control, the flow rate of the system varied drastically. A heating jacket was added to the Isco syringe pump to provide temperature control at the CO<sub>2</sub> source also. The jacket was connected to a refrigerated constant temperature circulator (VWR 115) kept at 40 °C so that the CO<sub>2</sub> would be already supercritical when pumped into the SFC. This modification helped

stabilize the flow rate, although it still tended to decrease over time. Since the significant decrease in flow rate continued to occur only after the instrument had been used for some time, it is likely that the temperature baths for the valves were not sufficiently controlled.

One additional attempt made to steady the flow was to set the Isco controller to constant flow instead of constant temperature. The pressure of the SFC system, however, would vary by as much as 30% of the total pressure when using this control system. These fluctuations made it impossible to ensure that the CO<sub>2</sub> was supercritical at all times, and it was decided to continue using the Isco at constant pressure despite the flow rate variations.

## **Silylation of Amino Acids**

### Cysteine

With the initial SFC repairs made, the next major goal of the project was finding a suitable silylation method suitable for multiple amino acids. Since the SFC had only a UV-Vis detector, either the silyl group or the substrate must be UV-active. Our group had recently worked with a UV-active silyl group for a previous project, so we began with the same synthesis used for a siloxylated phase transfer catalysis project.<sup>13, 14</sup> Cysteine was chosen as the initial amino acid due to the presence of its thiol group, which can act as a nucleophile. First, 1-[2-(4-chloromethyl-phenyl)-ethyl]-1,1,3,3,3-pentamethyl disiloxane was synthesized from 4-vinylbenzylchloride and pentamethyl disiloxane using platinum(0)-1,3-divinyl-1,1,3,3-tetramethyl disiloxane complex (3 wt % xylene) catalyst, as shown in Figure 4.1.<sup>10</sup>



The 1-[2-(4-chloromethyl-phenyl)-ethyl]-1,1,3,3,3-pentamethyl disiloxane with reacted with cysteine (5x excess) in ethylacetate in the presence of a commercially available PTC, tetrabutylammonium chloride (10 mol %), at 70 °C for 48 hours. This reaction is illustrated in Figure 4.2. No reaction was observed, so triethylamine (0.1 mL) was added to act as an HCl scavenger and allowed to react for 5 days. A shift in the benzyl CH<sub>2</sub> peak from 4.6 to 5.1 ppm was observed in the <sup>1</sup>H NMR. Separation with a silica column using ethyl acetate and hexane was attempted but unsuccessful.

### Lysine

After the separation difficulties encountered with cysteine, the same reaction was attempted with lysine, which was the substrate used previously in the siloxylated phase transfer catalysis project.<sup>13, 14</sup> The 1-[2-(4-chloromethyl-phenyl)-ethyl]-1,1,3,3,3-pentamethyldisiloxane was reacted with lysine (5x excess) in ethylacetate in the presence of a commercially available PTC, tetrabutylammonium chloride (5 mol %), at 70 °C for 24 hours. This reaction is depicted in Figure 4.3. The same shift was observed in the <sup>1</sup>H NMR of the benzyl CH<sub>2</sub> peak, but separation with a silica column using ethyl acetate and hexane was still unsuccessful. It was hypothesized that the benzyl group and siloxane chain may hinder the volatility of the amino acid due to the large mass. Thus, the decision was made to shift the focus to a procedure in the literature that used distillation as a purification method. The reasoning was that if it was volatile enough to be distilled, it could be volatile enough to be soluble in a SCF.

### *Serine*

The next synthesis was a modification of a serine procedure found in the Journal of Organic Chemistry, which reacted chloro(methyl)diphenyl silane with cyclohexylmethanol.<sup>15</sup> This reaction is illustrated in Figure 4.4. Initially, chloro(methyl)diphenyl silane (1.1 equiv) was added to serine methylester hydrochloride (1 equiv), with imidazole (2 equiv) as an HCl scavenger, in DMF at room temperature. Analysis of the crude product via GC-MS showed 70% conversion. The original procedure used distillation to purify the product, but trace amounts of the starting material still remained even after distillation. The starting material observed in the GC-MS was methyl-diphenyl-silanol, which is formed during the workup when water displaces the chlorine in the chloro(methyl)diphenyl silane. An attempt was made to facilitate the separation by switching the limiting reagent to the chloro(methyl)diphenylsilane (1 equiv), and using an excess of the serine (1.5 equiv), which could be removed by a water wash. The GC-MS, however, still showed the presence of the starting material methyl-diphenyl-silanol, so this route was abandoned.

### *Tyrosine*

At this point, it was decided to a lighter silane was needed in order to purify the silylated amino acid from the starting material. Instead of continuing to pursue UV-active silanes, it was decided to change to a UV-active amino acid. There were two motivations for changing to a lighter silane group. The first reason was that a lighter silane would likely be more soluble in a SCF. Additionally, a lighter silane should be easier to remove, facilitating product purification from starting material.

L-tyrosine was chosen as the UV active amino acid because its hydroxyl group can be used for silane attachment. Initially, L-tyrosine methylester hydrochloride (1.5 equiv) and chloro trimethyl silane (1 equiv) were reacted with imidazole (2 equiv) in DMF at room temperature overnight. This reaction can be seen in Figure 4.5. The same general procedure for the chloro(methyl)diphenyl silane and serine was followed. This reaction was only tried once, however, due to the instability of the trimethyl siloxane bond in water.

L-tyrosine methylester hydrochloride (1 equiv), chloro(dimethyl)t-butylsilane (2.2 equiv), and imidazole (3.3 equiv) were reacted in DMF at room temperature for five days. The workup was modified from a procedure outlined in the Journal of Organic Chemistry (JOCS).<sup>16</sup> One addition was that a short silica plug was needed to purify the compound (90/10 CH<sub>2</sub>Cl<sub>2</sub>/EtOAc to remove the silyl impurity, then 100% ethylacetate flush to obtain product).

During analysis, the tyrosine was discovered to have reacted with the DMF to add an aldehyde to the amine, resulting in a new compound. The new compound can be seen in Figure 4.6. Although unexpected, the modification of the amine should not be a problem because it will likely increase the CO<sub>2</sub>-philicity and the volatility in the SFC by decreasing the hydrogen bond capability of the amine.

## Preliminary Results

### Small Aromatic Molecules

Before testing the amino acids of interest, the SFC system and detector were tested with small aromatic molecules. Since the SFC was only connected to the UV-Vis detector, just UV-active compounds could be tested. Toluene and benzyl alcohol were each dissolved in MeOH and injected into the SFC. Although both initial injections resulted in a peak in the UV-Vis chromatograph, a peak was still seen during the subsequent injections of MeOH that were run to clean the column between samples. The prolonged presence of the analyte peaks suggested that the molecules were strongly retained on the column. The retention was so strong that multiple MeOH injections were required in order to clean the column before another sample injection could occur.

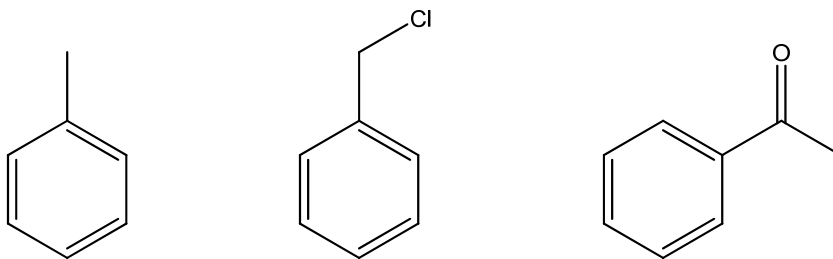


Figure 4.8: Structures of toluene (left), benzyl chloride (center), and acetophenone (right).

Samples comprised of multiple analytes were also tested. Toluene and acetophenone were dissolved in MeOH and injected in order to detect a separation of the compounds. No separation was observed, and both molecules were still strongly retained on the column. The Princeton ethylpyridine column is specifically designed for the separation of amino acids and peptides, however, so it was postulated that these molecules were too small to be successfully separated. From this point, all experiments involved amino acids, peptides, or larger organic molecules.

### Initial Amino Acid Analysis

The first trials involved injecting samples of silylated tyrosine and neutralized tryptophan dissolved in MeOH. Tryptophan was chosen because it is UV-active, can be easily neutralized via calcium carbonate in a common procedure, and is considered to be one of the hydrophobic amino acids. Silylated tyrosine and neutralized tryptophan were prepared both as individual samples and as a mixture. Peaks were detected by the UV-Vis spectrometer for both individual amino acids. A slight separation was also seen between the silylated tyrosine and the neutralized tryptophan when prepared as a mixture.

The absorbances of all peaks in the UV-vis spectrum however, were significantly lower than anticipated. The small peak magnitude suggested that both amino acids were less soluble than expected. While there are several possible explanations for this occurrence, the most simple is that the CO<sub>2</sub> was not supercritical at the time of analysis. The solubility of the amino acids should be at least an order of magnitude less in gaseous CO<sub>2</sub> than in scCO<sub>2</sub>. The flow path and system pressure were examined again in order to ensure that the entire system was supercritical.

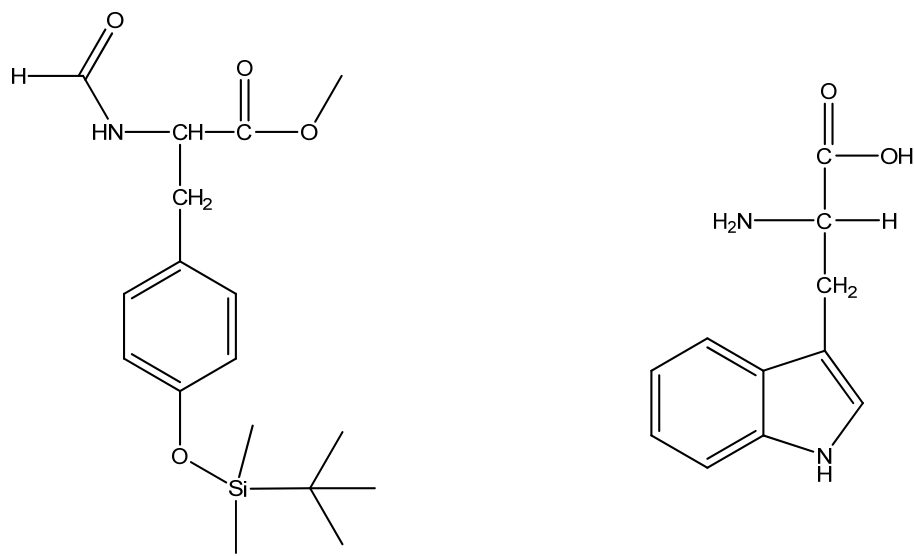


Figure 4.9: Structures of silylated tyrosine (left) and neutralized tryptophan (right).

#### Further Investigation of the SFC Flow Path

The pressure transducer placed immediately after the analytical column displayed a pressure above 2000 psi, but no other gauge was in the system to ensure the entire SFC flow path was kept at supercritical conditions. Another pressure transducer was placed directly after the UV-Vis detector to determine whether or not the amino acids were in scCO<sub>2</sub> during the analysis. The second pressure indicator read approximately 600 psi, signifying a pressure drop of nearly 1800 psi in the system. As can be seen in Figure 4.10, CO<sub>2</sub> does not become supercritical until approximately 1400 psi at 40 °C.<sup>17</sup> This meant that the system was nowhere near supercritical conditions during analysis, suggesting that precipitation occurred on the column, which could explain the significantly smaller peaks.

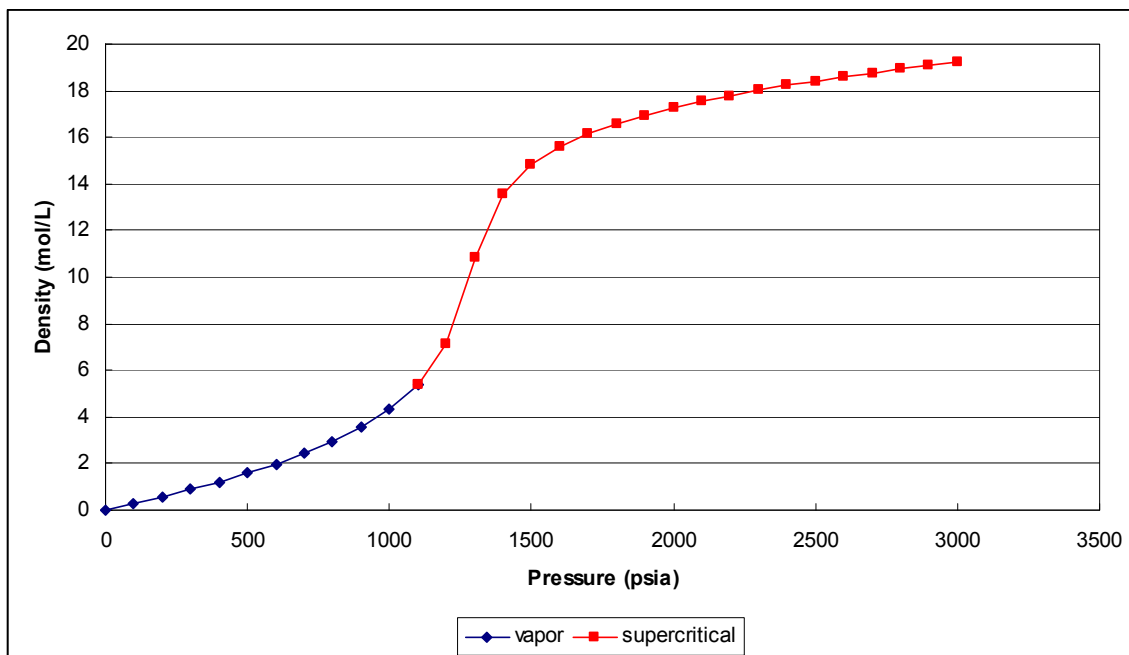


Figure 4.10: Density and phase behavior of carbon dioxide at 40 °C.<sup>17</sup>

The tubing in the system was streamlined and the first flow control valve was removed in an attempt to minimize the overall pressure drop in the system. After these modifications were made, a rough estimation of the expected pressure drop in the analytical column was calculated using Equation 3.<sup>18</sup> The pressure drop through the tubing was assumed to be negligible. This calculation suggested that the system should only experience a pressure drop of approximately 100 psi, but the previous drop of 1800 psi was still occurring. The overall pressure of the SFC was then increased by setting the Isco syringe pump to its maximum pressure of 3500 psi instead of 2000 psi. This increased the outlet pressure to approximately 1000 psi, which is still well below the supercritical threshold. Once the outlet pressure reached this higher pressure, however, a substantial leak in the UV-Vis flow cell became both visibly and audibly noticeable.

$$\frac{\Delta P}{L} = \frac{150 \bar{V}_o \mu (1 - \varepsilon)^2}{\Phi_s^2 D_p^2 \varepsilon^3} \quad (\text{Equation 3})^{18}$$

where  $\Delta P$  is the pressure drop

$L$  is the column length

$\bar{V}_o$  is the linear fluid velocity

$\mu$  is the viscosity of the SCF

$\Phi_s$  is the sphericity of the packing material

$D_p$  is the diameter of the packing particles

A close examination revealed that the leak in UV-Vis detector originated from a cracked window in the pressure cell. The damage was extensive enough to require a complete replacement of the high pressure flow cell. It was decided, however, to switch to a different analytical technique instead of replacing equipment in a detector that was over 10 years old.

#### Fiber Optic Flow Cell Fabrication

A new UV-Vis detector was assembled using fiber optic technology following the suggestion of Dr. Frank Bright at the State University of New York at Buffalo (SUNY-Buffalo). His research group has used this design before for high-pressure applications.<sup>19, 20</sup> Two optical fibers (24 in, Ocean Optics, 600  $\mu\text{m}$ , solarization-resistant coated with polyamide) were cut and polished according to the procedure. Each optical fiber was secured in HIP tubing with epoxy (Ocean Optics, standard epoxy). These HIP tubing sheaths were aligned along one axis of a HIP cross fitting. The flow path of the



SFC was placed perpendicular to the optical fibers, allowing the  $scCO_2$  and analytes to pass by the fibers for analysis. One optical fiber was connected to a light source, and the other was connected to the spectrometer.

This new UV-Vis flow cell was tested and found to be capable of holding pressure at 3000 psi. The schematic of the flow cell is depicted in Figure 4.11. The spectrometer was controlled, and the data was recorded, by OOIBase32 software. This software was installed on a separate computer so it would not interfere with the program controlling the rest of the SFC modules.

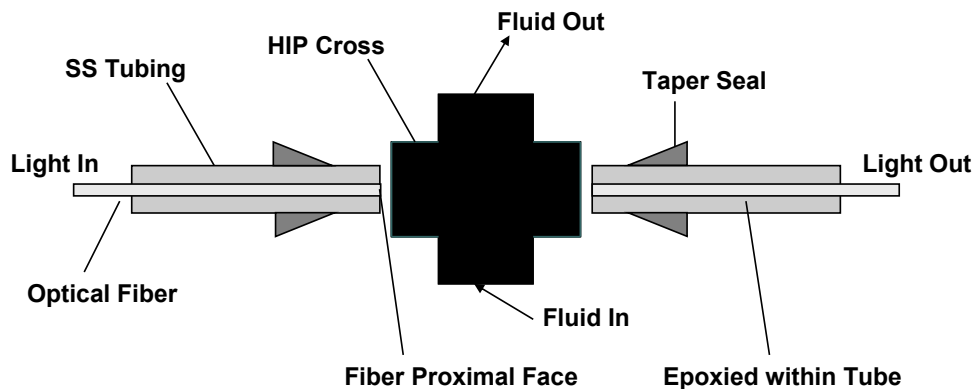


Figure 4.11: Schematic of the fiber optic UV-Vis flow cell. Design provided by Dr. Frank Bright (SUNY-Buffalo).

## Analysis of Amino Acids with Fiber Optic Detector

### *Initial Test*

The first test of the new UV-Vis fiber optic detector was a mixture of three amino acids. We had determined that at least three needed to be separated to demonstrate the proof of concept. In addition to the silylated tyrosine and neutralized tryptophan, boc-phenylalanine (Figure 4.12) was chosen because it is UV-active, commercially available as a neutral species, and is mostly hydrophobic. Silylated tyrosine, boc-phenylalanine, and neutralized tryptophan (all dissolved in MeOH) were injected into the SFC. Peaks were visible in the UV-Vis spectrum, as can be seen in Figure 4.13. The slight separation between two major peaks, as well as the presence of a small secondary peak around 450 seconds, suggested that the column was at least partially separating the three amino acids in the mixture. The significant rise in the baseline, however, was unexpected and not easily explained. This led to a closer investigation of each individual amino acid.

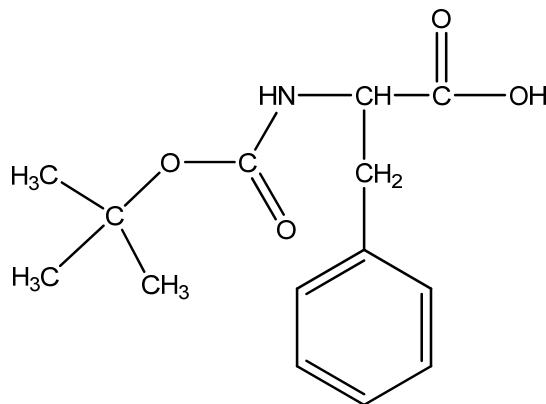


Figure 4.12: Structure of boc-phenylalanine.

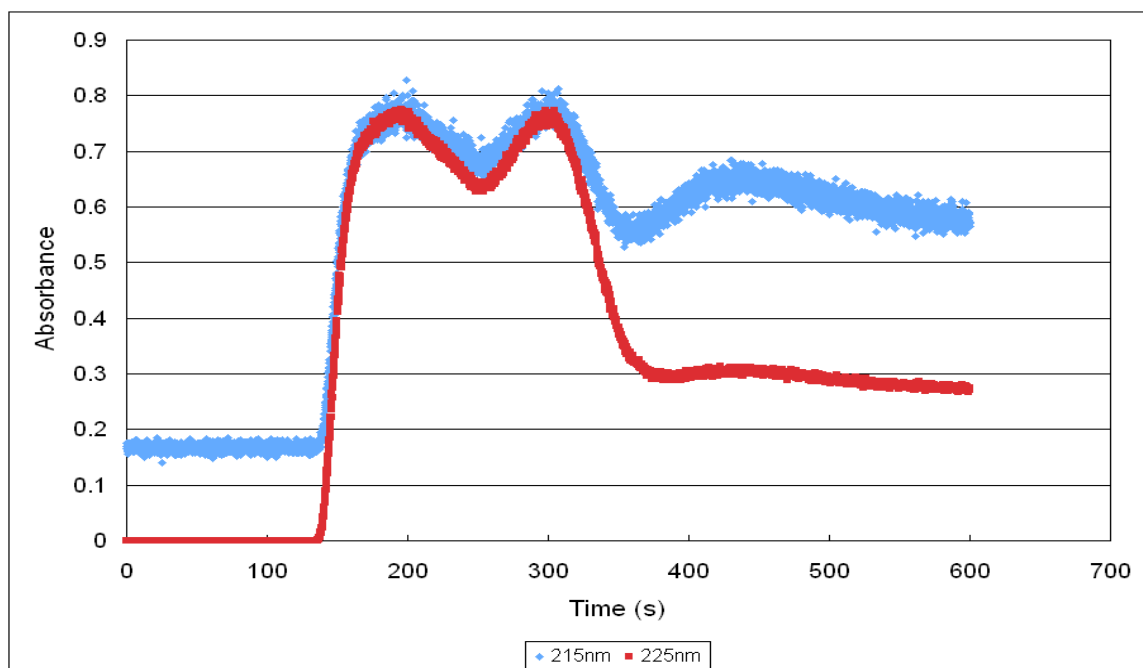


Figure 4.13: UV-Vis spectrum of silylated tyrosine, boc-phenylalanine, and tryptophan in  $scCO_2$  at 215 nm and 225 nm (2465 psi, 40 °C).

### *Individual Amino Acids*

Each amino acid was tested separately to determine if only one amino acid was the cause for the baseline drift. In order to ensure the spectra would be visible, highly concentrated samples of each amino acid were prepared in MeOH. The UV-Vis signatures of the individual amino acids are shown in Figure 4.14-4.16. As can be seen, the silylated tyrosine and the neutralized tryptophan peaks both have a steady baseline. The boc-phenylalanine peak, however, trails significantly and the baseline is raised for most of the 600 second analysis. The baseline drift in Figure 4.13 is thus attributed to irreversible retention of the boc-phenylalanine in the sample.

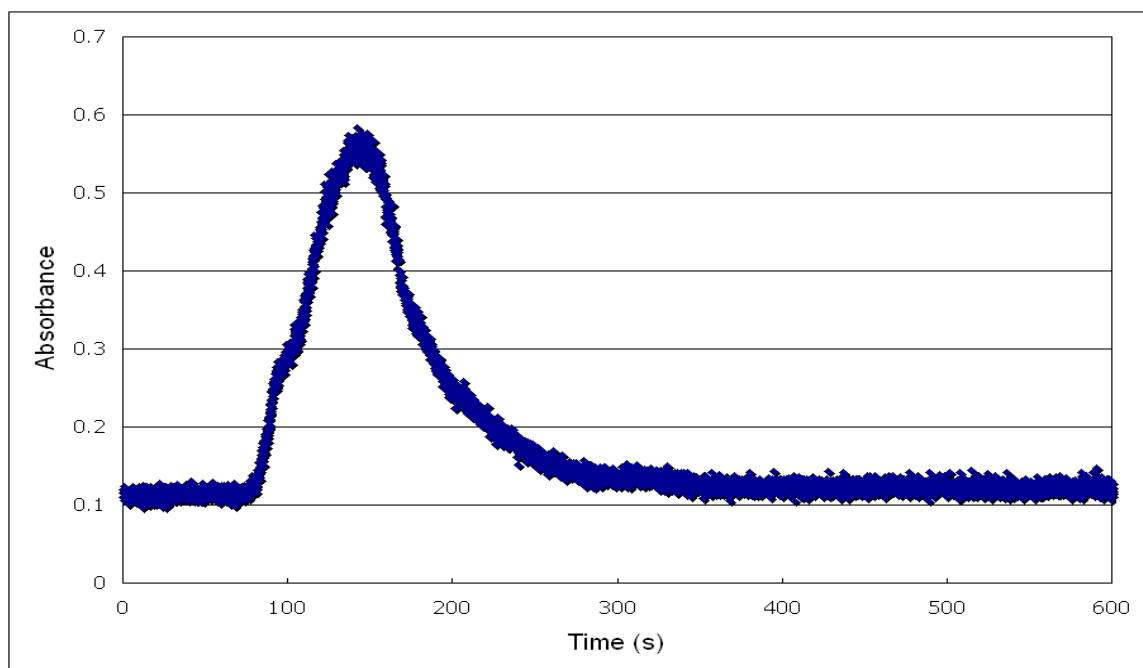


Figure 4.14: UV-Vis spectra of saturated silylated tyrosine in MeOH at 215 nm (2464 psi, 40 °C).

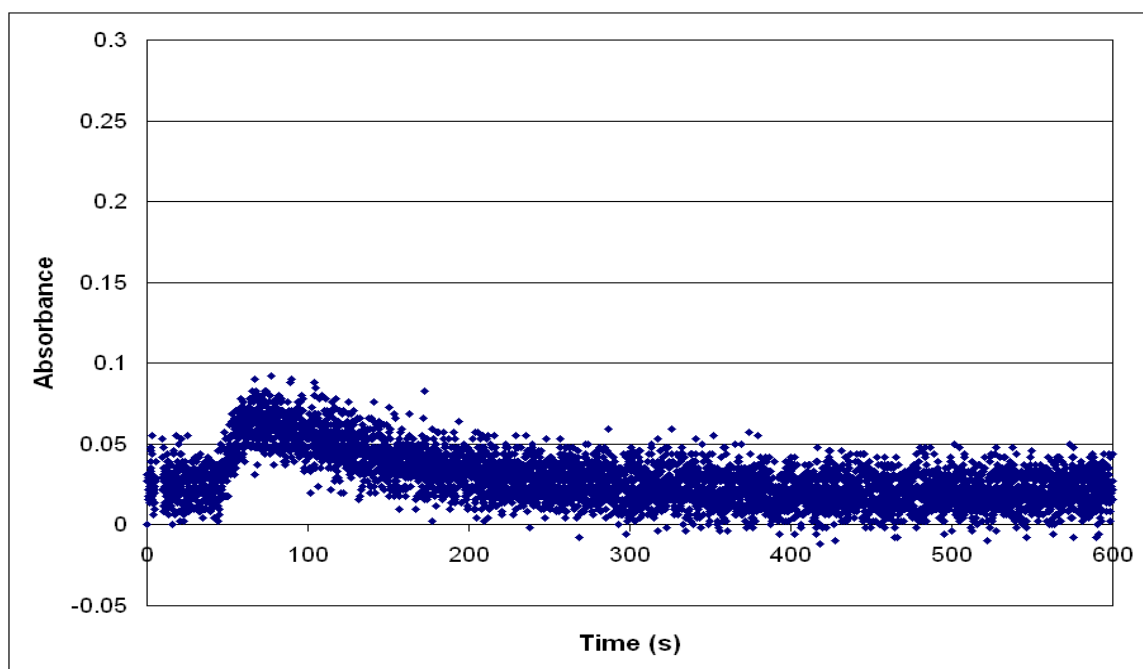


Figure 4.15: UV-Vis spectra of neutralized tryptophan (0.06 g/mL) in MeOH at 215 nm (2466 psi, 40 °C).

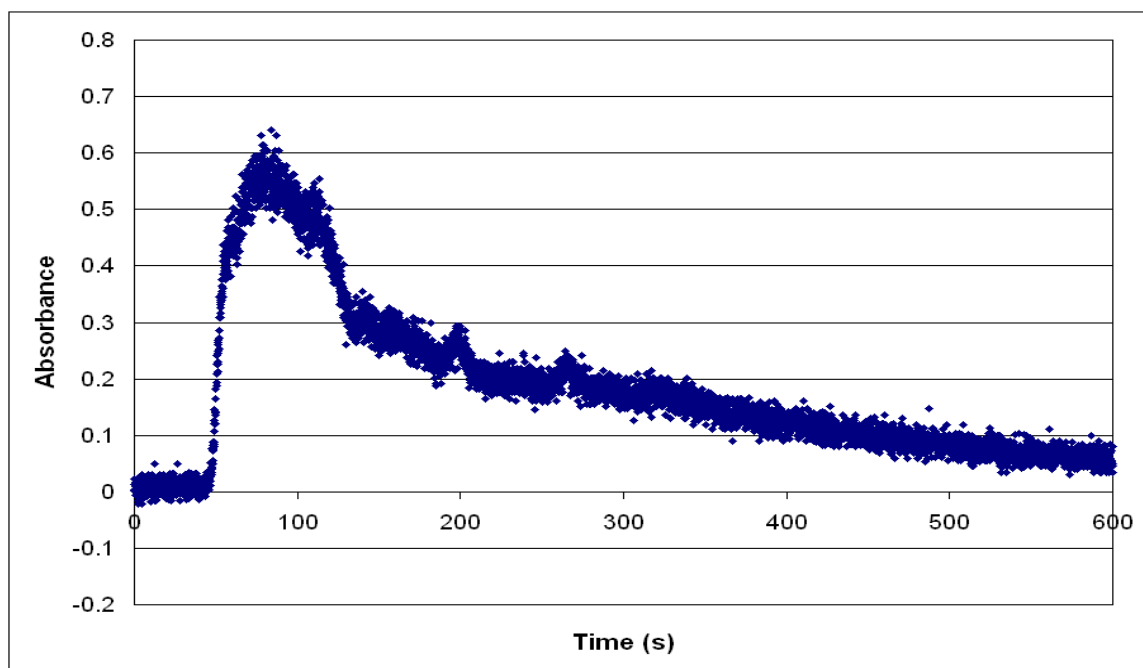


Figure 4.16: UV-Vis spectra of saturated boc-phenylalanine in MeOH at 215 nm (2468 psi, 40 °C).

After determining the cause of the rising baseline, focus turned to separating the three peaks seen in Figure 4.13. The column was rinsed with multiple injections of MeOH prior to injecting a sample of silylated tyrosine. Unexpectedly, the initial sample had no UV-Vis spectra. The MeOH rinse injected immediately afterwards, however, displayed a nice peak at the expected elution time of silylated tyrosine. The UV-Vis spectra of the original injection and the MeOH rinse can be seen in Figure 4.17.

It was hypothesized that the silylated tyrosine (0.07 g/mL) was too concentrated to be completely soluble in  $scCO_2$  and was thus sticking to the column. The theory was tested by diluting the sample and running the new sample. No peak was visible again,

and additional MeOH washes confirmed that enough silylated tyrosine was sticking to the column to necessitate multiple injections of MeOH before the column was completely cleaned. The spectra of these samples can be seen in Figure 4.18.

At this juncture, it was decided that the silylated tyrosine was not soluble enough in scCO<sub>2</sub> for this procedure to be effective. Although the silylation procedure did improve the overall solubility, it was not considered sufficiently effective to continue the silylation process with other amino acids. Instead, focus turned to enhancing the solubility of straight amino acids with the use of co-solvents.

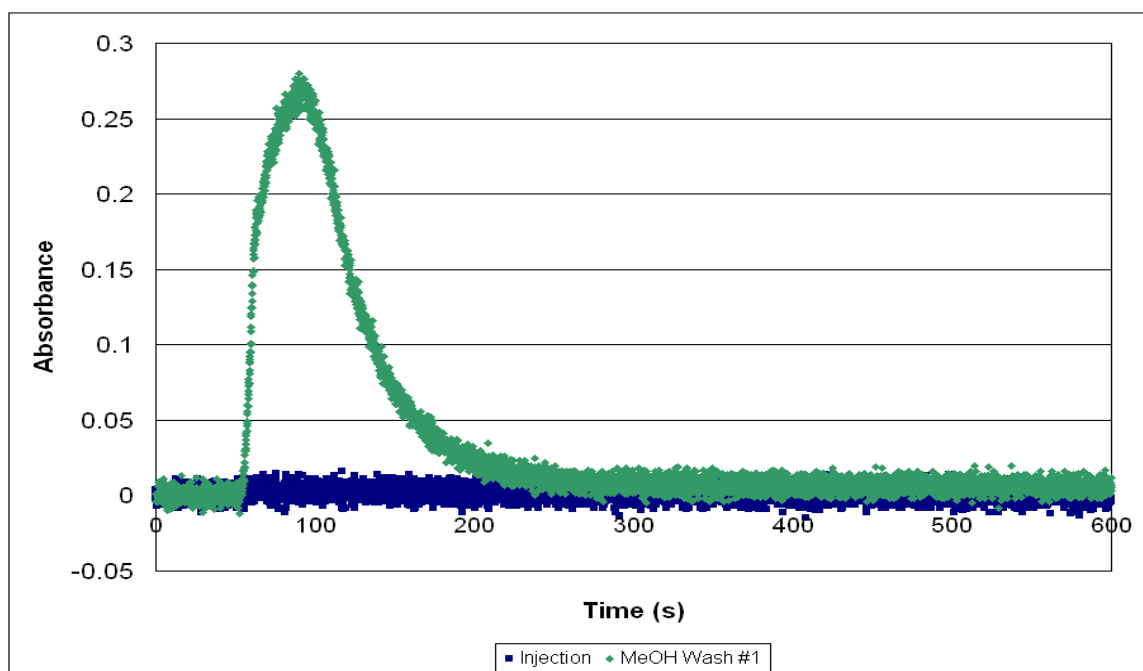


Figure 4.17: UV-Vis spectra of concentrated silylated tyrosine (0.07 g/mL) in MeOH, and the first MeOH wash, at 225 nm (2467 psi, 40 °C).

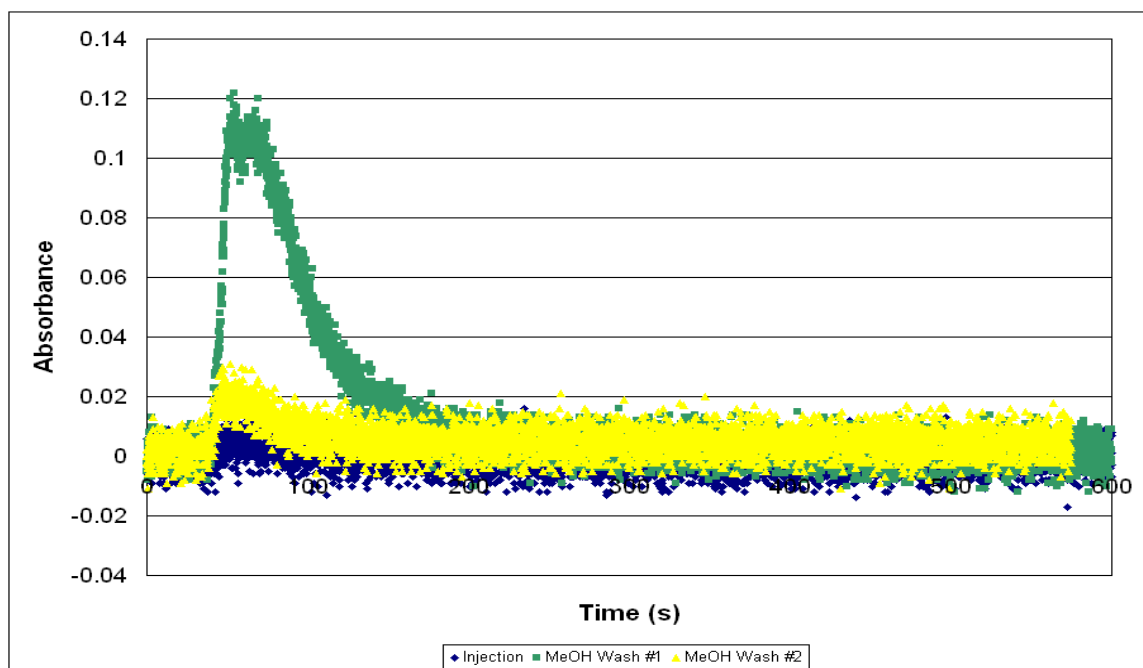


Figure 4.18: UV-Vis spectra of diluted silylated tyrosine (0.035 g/mL) in MeOH, and two MeOH washes, at 225 nm (2465 psi, 40 °C).

### Co-solvents in scCO<sub>2</sub>

The MeOH rinse injections most likely removed the silylated tyrosine stuck to the column for one of two reasons. One possibility is that the MeOH interacted with the ethylpyridine functionality of the column more strongly than the silylated tyrosine did, allowing the silylated tyrosine to pass once the MeOH began interacting with the column. The more likely option is that the MeOH acted as a co-solvent in the scCO<sub>2</sub> and significantly enhanced the solubility of the silylated tyrosine; thus the mobile phase was able to pass the silylated tyrosine through the column. Regardless of the reason, running MeOH through the system seemed to improve the process. It was decided to try several co-solvents with the scCO<sub>2</sub> to see if any co-solvent offered significantly better

performance than the others. The solvents chosen were MeOH, which has been used in with proteomic SFC analysis in the past,<sup>6</sup> EtOH, and trifluoroethanol, which our group has used before to enhance solubility in supercritical fluids.<sup>21</sup>

### Replacing the Co-solvent Pump

As mentioned earlier, the liquid co-solvent pump was nonfunctional at the beginning of this project. After the decision to test co-solvents was made, a new solvent pump first had to be incorporated into the SFC. Dr. Fernández had an old Isco micro flow pump available, and since the Isco 500D pump seemed to be effective in the system, it was decided to incorporate the micro flow pump for the co-solvent. An HIP tee fitting was used to combine the co-solvent from the Isco  $\mu$ LC-500 micro flow pump and the CO<sub>2</sub> from the Isco D500 pump. Check valves were added both pump lines so that solvent would not be pulled back into the pump.

### Testing the Co-Solvent Pump

The  $\mu$ LC-500 micro flow pump also has its own flow controller. It was uncertain, however, if the pump was strong enough to push that amount of co-solvent into the scCO<sub>2</sub> stream. A simple test using GC-FID was used to determine that the flow set point was the actual flow of co-solvent through the SFC. A flask filled with a known volume of MeOH was placed at the exit of the SFC. Both Isco pumps were turned on and the system was allowed to run for four minutes. A sample was taken from the flask and ran through the GC-FID. The resulting ratio of ethanol to methanol was 0.133, which corresponded to a ethanol flow rate of 53.1  $\mu$ L/min. The  $\mu$ LC-500 micro flow pump had been set for a flowrate of 50  $\mu$ /min, so this test suggested our control was fairly accurate.



## MeOH Co-solvent

Methanol was chosen as a co-solvent for two reasons. The MeOH washes were effective at removing amino acids stuck to the column, suggesting that the solvation properties are significant. It was also tested because Zheng et al. used MeOH in their SFC separation of polypeptides. Their system used between 5% to 50% of MeOH in a timed method.<sup>6</sup> Although we felt it unlikely that a 50/50 mixture of MeOH and scCO<sub>2</sub> would remain supercritical at those conditions, we ranged our co-solvent flowrate from 5 to 50% as well. Despite the polar co-solvent, however, the peaks behaved similarly to when only scCO<sub>2</sub> was used. The results are depicted in Figure 4.19. These spectra were taken for approximately 20% MeOH, but all results were similar in the 10-50% range.

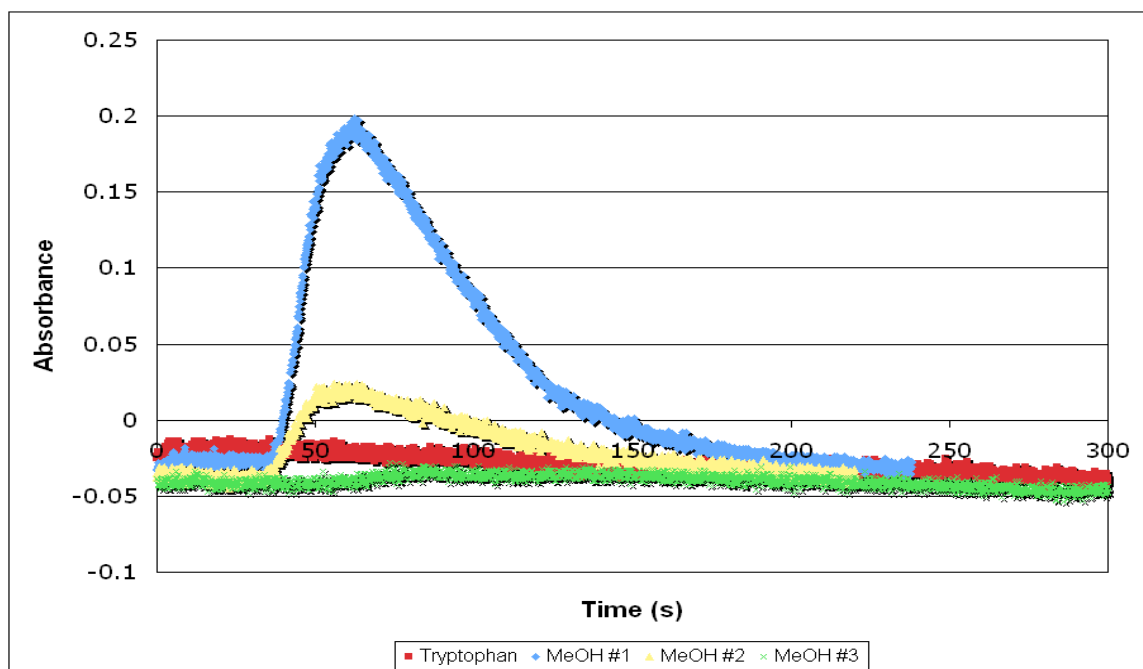


Figure 4.19: Initial tryptophan peak (neutralized) followed by MeOH washes in scCO<sub>2</sub> and 20% MeOH co-solvent.

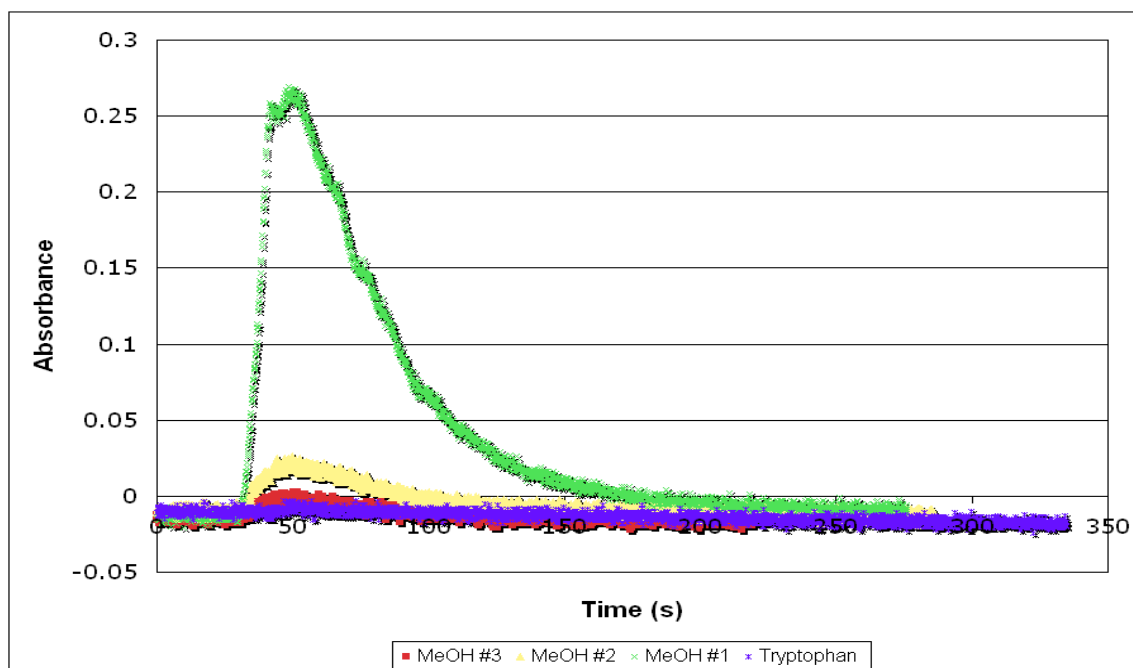


Figure 4.20: Initial tryptophan peak (neutralized) followed by MeOH washes in scCO<sub>2</sub> and 20% EtOH co-solvent.

### Ethanol Co-Solvent

Ethanol was tried as a co-solvent to provide a direct comparison to trifluoroethanol. As with the MeOH trials, the flow rate of the EtOH co-solvent varied from 10-50% of the total flow. Figure 4.20 shows the results of the initial sample injection followed by MeOH injections to rinse the column. The results are very similar to the MeOH results, suggesting that there is no significant difference between the solvents for this purpose.

## Trifluoroethanol Co-Solvent

Trifluoroethanol was tested under similar conditions. The trifluoroethanol flow rate was varied from 10-50% of the total flow. The results, which are depicted in Figure 4.21, were similar to both MeOH and EtOH. As can be seen, the major exception is that the peak from the first MeOH wash trailed significantly. Since no peak was seen upon the initial injection, however, using the more expensive trifluoroethanol co-solvent does not seem to offer any improvements over the simple alcohols.

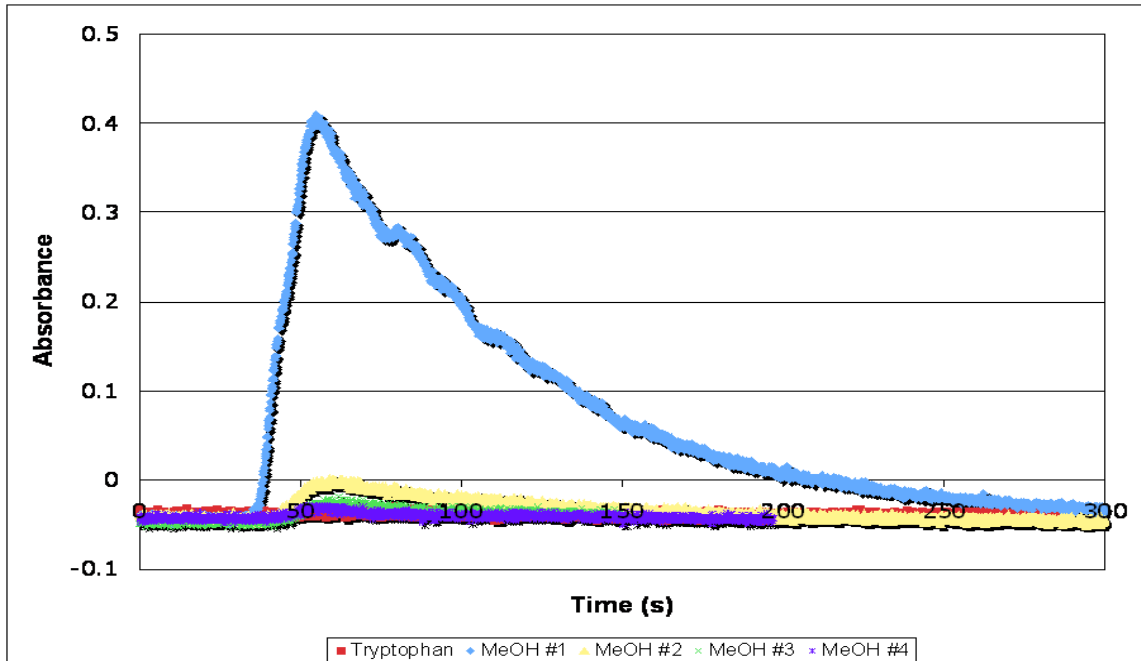


Figure 4.21: Initial tryptophan peak (neutralized) followed by MeOH washes in  $\text{scCO}_2$  and 20% trifluoroethanol co-solvent.

An issue with the trifluoroethanol co-solvent became apparent the following day. Even though several injections of MeOH had been immediately after the experiments to clean it, the first injection of MeOH the following morning yielded a peak in the UV-Vis spectrum. This hangover peak can be seen in Figure 4.22. Although we are not certain why the peak occurred, it is possible that the trifluoroethanol was retained strongly to the column even through the MeOH washes. It is possible that, while sitting overnight, the trifluoroethanol reacted with the ethylpyridine stationary phase of the column and that product eluted the following morning.

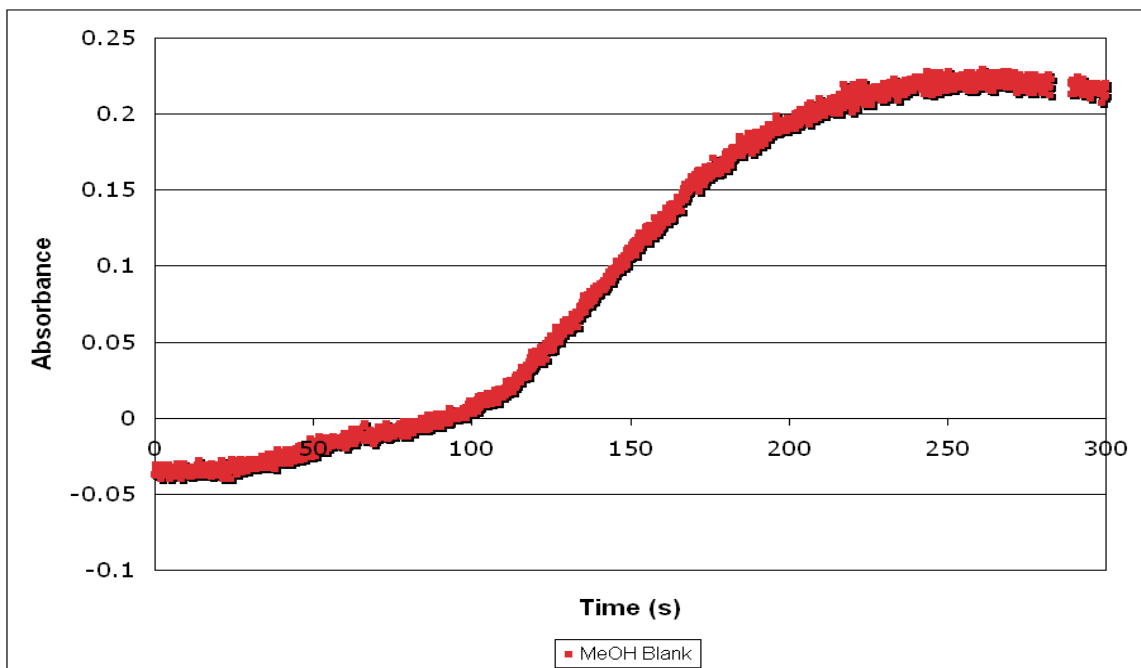


Figure 4.22: Hangover spectrum after trifluoroethanol co-solvent runs.

Regardless of the actual reasons for the hangover peak, it seems that trifluoroethanol is not an appropriate co-solvent when an ethylpyridine column is used for analyte separation. There are two possible paths forward if trifluoroethanol is going to be pursued as a co-solvent. One is to decrease the amount added to the system, making it more of an additive. Another possibility is to change the column from the Princeton ethylpyridine column to a Phenomenex Luna Cyano column, which has been used in the past for SFC separations with trifluoroethanol, methanol, and CO<sub>2</sub>.<sup>22</sup>

## **CONCLUSIONS AND RECOMMENDATIONS**

We have rebuilt a SFC instrument that is capable of utilizing both a primary mobile phase and a co-solvent. Although the flow control implemented with the Isco flow controllers is not perfected, rough control over the flow rates has been achieved with the current system. A fiber optic UV flow cell has been built and interfaced with the SFC, providing an inexpensive means for high-pressure detection of the desired analytes.

Several attempts at silylating amino acids were successful. The silylated tyrosine used most often in this project was a new molecule and was characterized fully. Although the t-butyl silane silylation approach was abandoned partway through the project, there might be reason to revisit it. The silylation method was abandoned because the silylated amino acid was sticking to the column. We originally hypothesized that this meant the silylation did not enhance the solubility enough to be useful. We have since demonstrated, however, that all amino acids tested are currently sticking to the column even though past research in the literature has shown this does not happen. This is most likely due to insufficient control of the instrumental parameters, including the flow rate

and temperature. If better flow and temperature control over the SFC can be achieved, it is possible the silylation will again prove to be a useful technique for enhancing the solubility of various metabolites.

Another issue may be that the current SFC analytical column is no longer functioning properly. The appearance of the hangover peak suggests that at least part of the column has degraded during the course of these studies. It is important to replace the column before beginning a more detailed analysis. Additionally, changing the ethylpyridine to another column has several benefits. The Phenomenex Luna Cyano column mentioned earlier has been shown to work with trifluoroethanol, so that removes the possible chemical incompatibility issue. It also may have more favorable interactions with the silyl groups we are adding to the amino acids in order to enhance the solubility.

The most important path forward for this project, however, is the implementation of a better flow control system. One possible way to achieve this control is to interface the SFC with LabVIEW software (National Instruments). Using LabVIEW provides us the opportunity to use a backpressure regulator with computer control, which should greatly stabilize the  $scCO_2$  flow. Once the flow rate of the mobile phase has stabilized, the system should operate significantly better. This option is less expensive than buying a new SFC, which has substantially more capability than that required for us to complete this project.

## REFERENCES

1. M. Bizzarri, A. Cucina, F. Conti and F. D'Anselmi, *Acta Biotheoretica*, 2008, 56, 173-196.
2. J. L. Griffin, *Philosophical Transactions of the Royal Society B-Biological Sciences*, 2006, 361, 147-161.
3. I. Garcia-Perez, P. Whitfield, A. Bartlett, S. Angulo, C. Legido-Quigley, M. Hanna-Brown and C. Barbas, *Electrophoresis*, 2008, 29, 3201-3206.
4. O. Fiehn, *Comparative and Functional Genomics*, 2001, 2, 155-168.
5. J. D. Pinkston, *European Journal of Mass Spectrometry*, 2005, 11, 189-197.
6. J. Zheng, J. G. Pinkston, P. H. Zoutendam and L. T. Taylor, *Analytical Chemistry*, 2006, 78, 1535-1545.
7. J. M. Desimone, Z. Guan and C. S. Elsbernd, *Science*, 1992, 257, 945-947.
8. A. V. Yazdi and E. J. Beckman, *Industrial & Engineering Chemistry Research*, 1996, 35, 3644-3652.
9. T. P. Mawhinney and M. A. Madson, ed. USPTO, US, 1984.
10. Arren, D. H. C., Coggio, W. D., Parker and D. S., United States, 1997.
11. T. A. Berger and J. F. Deye, *Analytical Chemistry*, 1990, 62, 1181-1185.
12. T. A. Berger and J. F. Deye, *Journal of Chromatography*, 1991, 547, 377-392.
13. R. Charney, in *School of Chemistry and Biochemistry*, Georgia Institute of Technology, Atlanta, 2008.
14. M. Donaldson, in *Chemical and Biomolecular Engineering*, Georgia Institute of Technology, Atlanta, 2008.
15. S. E. Denmark, R. P. Hammer, E. J. Weber and K. L. Habermas, *Journal of Organic Chemistry*, 1987, 52, 165-168.
16. D. W. Hansen and D. Pilipauskas, *Journal of Organic Chemistry*, 1985, 50, 945-950.

17. E. W. M. Lemmon, M.O.; Friend, D.G., in *NIST Chemistry WebBook, NIST Standard Reference Database Number 69*, ed. P. J. M. Linstrom, W.G., National Institute of Standards and Technology, Gaithersburg, MD, 2005.
18. W. L. McCabe, J. C. Smith and P. Harriott, *Unit Operations of Chemical Engineering*, McGraw Hill Higher Education, New York, NY, 2001.
19. J. K. Rice, R. A. Dunbar and F. V. Bright, *Applied Spectroscopy*, 1994, 48, 1030-1032.
20. J. Zagrobelny, M. Li, R. Wang, T. A. Betts and F. V. Bright, *Applied Spectroscopy*, 1992, 46, 1895-1897.
21. B. L. Knutson, S. R. Sherman, K. L. Bennett, C. L. Liotta and C. A. Eckert, *Industrial & Engineering Chemistry Research*, 1997, 36, 854-868.
22. B. Bolanos, M. Greig, M. Ventura, W. Farrell, C. M. Aurigemma, H. Li, T. L. Quenzer, K. Tivel, J. M. R. Bylund, P. Tran, C. Pham and D. Phillipson, *International Journal of Mass Spectrometry*, 2004, 238, 85-97.



## **CHAPTER 5: CONCLUSIONS AND RECOMMENDATIONS**

### **INTRODUCTION**

The development of new sustainable systems will improve current industrial processing techniques and make chemical process more environmentally benign. Most of the improvements in this thesis involved novel, sustainable solvent systems that could be incorporated into the development of new processes. Some projects were exploratory studies undertaken to determine whether or not an alternative solvent system was an effective strategy. In several cases, our novel system proved ineffective. For others, however, the results were promising and further examination should occur to ascertain if a novel solvent systems would be an appropriate process. This chapter will discuss possible paths forward for several of the more promising projects studied in this thesis.

### **CONTINUOUS FLOW REACTOR**

The continuous flow reactor project was considered a complete success. A continuous flow reactor was designed and built that obtained quantitative yields for the first two steps of the desired synthesis. There are two possible paths forward for this project. The first path forward entails incorporating the final step of the original synthesis into the continuous flow reactor system. The second possible path forward is to find another application for the continuous flow reactor system we designed.

## Hydrochloric Acid Hydrolysis

As mentioned in Chapter 2, the final step of the original synthesis was the hydrolysis of the diazoketone to yield the  $\alpha$ -chloroketone. Building the reactor itself should be straightforward; the same configuration used for the first two steps should work for this one also. There are several additional considerations that should be taken into account, however, when designing the reactor system.

The acid chloride used in the first two steps caused multiple compatibility issues. Over the course of the project, multiple pieces of HPLC tubing had to be replaced because the acid chloride had completely corroded the stainless steel. The extent of the corrosion was so severe as to break several pieces of tubing, and several stainless steel fittings, over the course of several months. It is likely that the hydrochloric acid will be more severe and the corrosion will occur at a faster rate.

In order to mitigate this safety concern, the entire continuous flow reactor should be replaced every 3-4 months if the reactor is going to be constructed of stainless steel. This is the most cost effective solution; otherwise, the reactor should be made from a more acid-resistant material, such as hastelloy or Inconel, or it should be coated before use (as mentioned in Chapter 2). The other significant material of construction concern is for the pump. The acid chloride began corroding the pump chamber of the Eldex Optos pump within 3 months. Another acid resistant pump, such as one constructed from CTFE, will need to be purchased if the hydrochloric acid step is added to the system.

The other opportunity for the continuous flow reactor system is to find other reactions that would benefit from its design. Possible reactions of interest include ones containing a significant exotherm, reactions involving hazardous materials, and reactions that require only a short residence time. Although the first two types of reactions are varied and have potential, the rest of this section will focus on applying the continuous flow reactor to reactions requiring only short residence times.

### **Carbohydrate Reactions in Continuous Flow Reactors**

Recent research has focused on the conversion of glucose and other carbohydrates to value-added products in continuous flow reactors. Glucose has been converted completely to gaseous products ( $\text{H}_2$ ,  $\text{CO}_2$ ,  $\text{CH}_4$ , and  $\text{CO}$ ) in supercritical water (650 °C to 750 °C) in a microchannel reactor with a residence time of 2 seconds.<sup>1</sup> Other recent promising research includes the catalytic conversion of fructose and glucose to HMF in five minutes with microwave heating,<sup>2</sup> and the use of subcritical water for production of hexose degradation products.<sup>3</sup>

It is widely recognized that hot water flow reactors are more effective at biomass pretreatment than batch ones. It is also likely that a flow reactor will prove to be a better process for the production of value-added chemicals. The fine temperature control allowed by small-scale continuous flow reactors allow the products to stay at the desired temperatures for only the desired amount of time. This means that once the kinetics have been determined for the reactions of interest, a continuous flow reactor could help maximize potential yields. Much of the value-added chemical research is still being conducted in batch reactions, leaving us with an opportunity.

Additionally, the various designs of our continuous flow reactors could be useful. Microchannel reactors, such as that used by Goodwin,<sup>1</sup> must be fabricated and tend to be expensive. If the HPLC tubing could be used as effectively, it represents a way to cut costs significantly while still forming the desired product.

## **BIOMASS PRETREATMENT**

The chapter on biomass pretreatment discussed three novel solvent approaches: CO<sub>2</sub>-enhanced near-critical water, organic acid-enhanced scCO<sub>2</sub>, and sulfones. At this juncture, the organic acid-enhanced scCO<sub>2</sub> suffers from downstream acid separation difficulties and is probably not worth pursuing. The other two methods do have some benefits, and possible conclusions and path forwards will be discussed for each.

### **CO<sub>2</sub>-Enhanced NCW**

There is currently a lot of research focusing on the supercritical and near-critical pretreatment of lignocellulosic biomass. Most of these methods, however, are energy intensive and thus not overly attractive processes. Our research has shown that adding CO<sub>2</sub> seems improve the acidity of the NCW, providing hydrolysis at lower temperatures. This could be quite beneficial, and studies should continue in this area.

It would also be useful to try this pretreatment method in a continuous flow reactor. The hot water flow through pretreatment methods tend to outperform their batch counterparts.<sup>4</sup> Although the solids handling would be difficult, designing a continuous flow process for this pretreatment method would likely yield the best results.

### **Piperylene Sulfone**

Although the acidity of the piperylene sulfone pretreatment has promise, this method will likely suffer from previously unexpected separation difficulties. The research outlined in Appendix C has shown that it is difficult to remove piperylene sulfone from the reaction mixture without significantly degrading both the carbohydrate feedstock and any useful products in the reaction mixture. If value-added compounds are not able to be recovered from the pretreatment process, it is unlikely that a method involving a specialty solvent, such as PS, will be economically-viable. Should a new separation method be developed, however, the PS pretreatment option would merit further examination. It would still be important to develop a new analytical technique in order to protect the BioRad Aminex HPX-87P and BioRad Aminex HPX-87H HPLC columns. The 87P column has a known sensitivity to PS, so precautions should be taken with the 87H as well.

## **SUPERCRITICAL FLUID CHROMATOGRAPHY FOR METABOLOMICS**

Although this project has not yet worked as anticipated, the results are promising to date. Literature has shown that SFC is a viable method to separate peptides,<sup>5</sup> which theoretically should be harder to analyze than metabolomes because the molecules are bulkier and thus less soluble in scCO<sub>2</sub>. The SFC system we have rebuilt is an inexpensive analytical option when compared to the commercially-available SFCs. It is possible that the overall economics of SFC metabolomic separation could be improved by using more straightforward equipment.

Additionally, the potential success of the *AMUSE* platform for the MS analysis of proteomes and metabolomes is a high enough benefit to continue work on this project. Incorporating better flow control should greatly improve the performance of our SFC equipment, allowing the *AMUSE* technology to be properly tested. Different analytical columns should also be thoroughly examined, and an appropriate one purchased, in the effort to improve our current system. If our rebuilt SFC cannot function well even with a new column and flow control system, additional considerations into the purchase of a new SFC will need to be made.

## **ALTERNATIVE SOLVENTS FOR CELLULOSE DISSOLUTION**

Although not discussed in a chapter, this project is detailed in Appendix A. Cellulose dissolution is becoming more important as sustainable feedstocks are required for biomaterials and biofuels. Cellulose is the most abundant sustainable carbon source,

and it will be important to hydrolyze it efficiently in industrial bioprocesses. There are many aspects to improving cellulose hydrolysis. The two discussed in this section are designing new solvents and improving enzymatic hydrolysis in alternative solvents. Both aspects are important areas where our lab can help make contributions.

### **Designing New Cellulose Solvents**

Several suggestions for improving glycol-based ILs are discussed in Appendix A. There are other possible solvents, however, that should be considered. As our lab continues to develop reversible ILs, we should always test the solubility of not only cellulose, but also lignin, mono-, and disaccharides. There are many beneficial reactions (acetylations, carbanilations, etc.) that require cellulose to be completely, or at least nearly, dissolved.<sup>6</sup> By improving separation schemes, reversible ILs represent one way our group can contribute to the field of biomaterials.

### **Enhancing Enzymatic Stability in Alternative Solvents**

Protein engineering is an established approach for improving the stability of enzymes in specific environmental conditions. The improved stability occurs through rational or combinatorial design.<sup>7,8</sup> Directed evolution of enzymes is a specialized field, and collaborating with the Bommarius group on this project allows us to work on cellulose dissolution and hydrolysis from both major aspects. The promising results already obtained, as well as the high ceiling of future potential (new cellulose solvents, new biopolymeric building blocks, and improved cellulases) strongly suggest that work on this project should be continued.

## COFACTOR STABILITY IN ORGANIC-AQUEOUS SOLVENTS

Another project not discussed in the chapters, but studied extensively and discussed in Appendix B, is the determination of cofactor stability in mixed organic-aqueous systems. Although the OATS system has been previously been successful in bioprocessing applications,<sup>9</sup> it has been limited to simple enzymatic reactions. One way to extend its usefulness would be to demonstrate the ability to run more complicated enzymatic reactions, such as ones requiring cofactor generation. Cofactors, especially the nicotinamide ones, are expensive and represent a substantial portion of the processing cost for enzymatic reactions.<sup>10</sup>

Previous efforts involved running a reaction requiring cofactors in the OATS system, but the results were subpar. One possible explanation is that the cofactors were degrading substantially in the mixed organic-aqueous solvent. In order to test this hypothesis, UV studies were completed over time. While rough half-life data was obtained for the degradation of reduced nicotinamide cofactors, it was not possible to ascertain the stability of the acetonitrile or isopropanol mixed solvent systems (unpublished results).

Capillary electrophoresis was examined as a possible analytical technique to determine cofactor stability in the mixed solvent systems consisting of acetonitrile and isopropanol. Unexpected difficulties were encountered when attempting to run the mixed solvent samples through the CE, however, and these problems are not yet fully understood. If the CE cofactor studies are to continue, it would be beneficial to collaborate with an expert in the field of CE analysis.



HPLC is another analytical method that could possibly be used to ascertain cofactor stability. CE has gained popularity because its separation efficiency is higher, but HPLC has been used in the past to separate and study nicotinamide cofactors.<sup>11, 12</sup> Although the separation is inferior, the interactions of organic solvent samples with HPLC is well understood, and our lab already has this analytical capability.

It is important to understand the stability of cofactors under varying conditions including temperature, pH, buffer choice, and organic solvent choice. These studies should be fairly straightforward once the proper methodology is developed on the HPLC. At this juncture, considering the issues faced when using the CE, I suggest switching the analytical technique and continuing this project. It will be imperative to understand cofactor stability if further OATS enzymatic systems are going to be developed.

## REFERENCES

1. A. K. Goodwin and G. L. Rorrer, *Industrial & Engineering Chemistry Research*, 2008, **47**, 4106-4114.
2. X. Qi, M. Watanabe, T. M. Aida and R. L. Smith Jr, *Catalysis Communications*, 2008, **9**, 2244-2249.
3. J. Ohshima, S. H. Khajavi, Y. Kimura and S. Adachi, *European Food Research and Technology*, 2008, **227**, 799-803.
4. N. Mosier, C. Wyman, B. Dale, R. Elander, Y. Y. Lee, M. Holtzapple and M. Ladisch, *Bioresource Technology*, 2005, **96**, 673-686.
5. J. Zheng, J. G. Pinkston, P. H. Zoutendam and L. T. Taylor, *Analytical Chemistry*, 2006, **78**, 1535-1545.
6. H. Xie, A. King, I. Kilpelainen, M. Granstrom and D. S. Argyropoulos, *Biomacromolecules*, 2007, **8**, 3740-3748.

7. G. R. Castro and T. Knubovets, *Critical Reviews in Biotechnology*, 2003, **23**, 195-231.
8. K. M. Polizzi, A. S. Bommarius, J. M. Broering and J. F. Chaparro-Riggers, *Current Opinion in Chemical Biology*, 2007, **11**, 220-225.
9. E. Hill, in *School of Chemical and Biomolecular Engineering*, Georgia Institute of Technology, Atlanta, 2007.
10. H. K. Chenault and G. M. Whitesides, *Applied Biochemistry and Biotechnology*, 1987, **14**, 147-197.
11. S. A. Margolis, B. F. Howell and R. Shaffer, *Clinical Chemistry*, 1976, **22**.
12. M. Pace, P. L. Mauri, C. Gardana and P. G. Pietta, *Journal of Chromatography*, 1989, **476**, 487-490.

# **APPENDIX A: CELLULOSE SOLUBILITY AND IMPACT ON CRYSTALLINITY IN ALTERNATIVE SOLVENTS**

## **INTRODUCTION**

As mentioned in Chapter 3, ethanol is an attractive sustainable alternative to fossil fuels, but the large-scale manufacturing process of ethanol must be improved drastically. While the pretreatment of lignocellulosic biomass is one significant challenge facing ethanol production, another important challenge is improving the efficacy of cellulose hydrolysis for glucose production. There are two main pathways for cellulose hydrolysis: chemical processes (acid and base-catalyzed hydrolysis) and enzymatic pathways (typically involving cellulases). Enzymes generally provide higher selectivity and do not promote the formation of glucose degradation products, which are commonly seen with traditional chemical processes, but are also more expensive. In order for cellulases to break down cellulose effectively in processes, it is essential to reduce the overall crystallinity of the biopolymer.

Dissolving cellulose is one way to reduce the crystallinity. Some alternative solvents, including ionic liquids (ILs) and deep eutectic solvents (DESs), are possible options for cellulose dissolution. Additionally, as “tunable” solvents, they could be designed specifically to enhance enzymatic activity, which allows the development of a one-pot process where both dissolution and hydrolysis occur.

## **BACKGROUND**

### **Enzymatic Hydrolysis of Cellulose to Glucose**

The enzymatic hydrolysis of cellulose to glucose is one of the more challenging steps in the production of ethanol. The difficulties arise both from the physical characteristics of cellulose, and the actual enzymatic process required. As for the physical characteristics, cellulose is comprised of both highly crystalline and amorphous regions. Crystalline cellulose restricts enzymatic access, making the hydrolysis difficult.<sup>1</sup> The processing differences between amorphous and crystalline cellulose will be discussed later.

Hydrolyzing cellulose into glucose requires the cooperative effort of multiple enzymes. The hydrolysis of crystalline cellulose involves synergism between two main types of cellulases. Endoglucanases hydrolyze glycosidic bonds at random in the middle of cellulosic chains, which produces new chain ends. Cellobiohydrolases are exoglucanases that cleave glycosidic bonds from cellulose chain ends in a processive manner, producing cellobiose, which is a dimer of glucose. Thus cellobiohydrolases require the action of endoglucanases to function efficiently.<sup>2</sup> Cellobiose is ultimately hydrolyzed into glucose by  $\beta$ -glucosidase, an enzyme that is usually added in excess into the system. Excess is used not only to reach full conversion, but also minimize product inhibition of cellobiohydrolases.<sup>2,3</sup>

## **Importance of Cellulose Dissolution**

. The enzymatic hydrolysis of cellulose to glucose is a difficult industrial process. The main problem is that cellulose is not soluble in the aqueous environment where enzymes operate most efficiently. This means the enzymatic hydrolysis occurs heterogeneously, and the inherent transport limitation slows hydrolysis.<sup>4</sup> To overcome this difficulty, many solvents, and their effects on cellulose, have been studied.

In certain solvents, cellulose “swells” and the degree of crystallinity is reduced because the hydrogen bonds connecting the cellulose chains are disrupted. While it is believed that hydrolysis kinetics will improve with “solvent-swollen” cellulose, it is known that the kinetics improve much more significantly when the cellulose starting material is mostly amorphous and significantly less crystalline.<sup>4</sup> Thus a solvent that dissolves cellulose is preferred over a solvent that just causes swelling.

Pretreatment methods used for lignocellulosic materials tend to disrupt cellulose crystallinity, but this is not the primary goal of pretreatment.<sup>5</sup> Even if the lignocellulosic biomass undergoes one of the common pretreatment methods, such as acid or base pretreatment, additional processing would be required to render the cellulose amorphous.<sup>6</sup> Thus a different approach is needed in order to improve the overall hydrolysis kinetics of cellulose to glucose. This new process would ideally utilize one solvent that can both dissolve cellulose and promote reasonable enzymatic activity.

There are several nontraditional solvent classes known either to dissolve cellulose or to maintain reasonable enzymatic activity. The properties of these solvents, and their possible applications toward cellulose dissolution and hydrolysis, will be discussed in the following sections.

## Ionic Liquids

Ionic liquids (ILs) are a class of solvents that have been examined extensively for cellulose dissolution. Several ILs, including the imidazole-based and pyridine-based ones shown in Figure A.1, have demonstrated the ability to dissolve cellulose.<sup>7-10</sup> In some cases, cellulose was soluble enough for acetylation and carboxymethylation reactions to occur.<sup>11</sup> More importantly, studies have shown by NMR that cellulose becomes amorphous upon dissolution in these ILs, and the amorphous characteristic is retained after precipitation of the cellulose from the IL. Additionally, the cellulase hydrolysis kinetics of this recovered cellulose was up to 90 times faster than the rate of untreated cellulose.<sup>4</sup> Such results illustrate the potential promise of ILs in the field of cellulose dissolution.

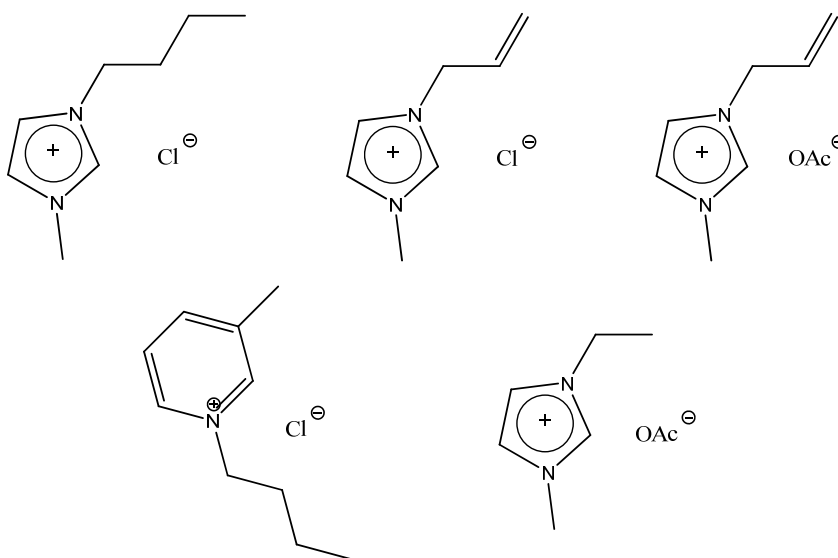


Figure A.1: Ionic liquid structures of [Bmim]Cl (top left), [Amim]Cl (top center), [Amim][OAc] (top right), [Bmpy]Cl (bottom left), and [Emim][OAc] (bottom right).

From a processing standpoint, ideally the enzymatic hydrolysis of cellulose would occur in the dissolution media. Combining the dissolution and hydrolysis processes removes the need for a separation step, which would significantly lower processing costs. Imidazole-based ILs are not ideal solvents for enzymatic transformations,<sup>12</sup> although some enzymes have been shown to retain at least nominal activity when ILs are used as the reaction media. For example, Novozyme 435, a lipase B from *Candida Antarctica* (CALB), and  $\alpha$ -chymotrypsin have both been used as biocatalysts in several ILs. Although they have been utilized, the above enzymes were either immobilized or suffered from reduced enzymatic activity.<sup>13</sup>

Additionally, imidazole-based ILs are not desirable for sustainable technology. Even though ILs have low vapor pressures and are generally nonflammable, allowing them to be characterized as “green” or “environmentally-benign” solvents, the imidazole-based ILS are toxic to fish and rats. At this time, their effect on humans is unknown.<sup>14, 15</sup> ILs are very stable and thus not biodegradable; even ones that are considered biodegradable only partially break down.<sup>16</sup> As renewable alternative fuels are developed, it is imperative that the processes to produce them are also sustainable. In addition to health and environmental effects, ILs are expensive solvents, making it difficult to economically justify their use in either biofuels or biomaterials.<sup>5</sup>

### **Deep Eutectic Solvents**

The limited enzymatic activity, general toxicity, and overall expense of imidazole- or pyridine-based ILs validate the need to examine additional solvents for cellulose dissolution and hydrolysis. Deep eutectic solvents (DESs) are plausible alternatives to ILS for cellulose dissolution. DESs, which are made from combining two

or more components in specific molar ratios to form a eutectic, are an alternative solvent class with similar properties to ILs. The most significant difference between these two types of ionic solvents is that DESs are a mixture to at least two compounds, while ILs are composed of only one salt species. The most common combination of compounds involves a quaternary ammonium salt, such as choline chloride or ethylammonium chloride, and a hydrogen-bond donor.<sup>17</sup> The structures of choline chloride and ethylammonium chloride are shown in Figure A.2.

DESs can be considered green solvents as well. Like ILs, their vapor pressures are minimal. More importantly, they are often made from nontoxic, low cost bulk compounds that are widely available.<sup>18</sup> As DESs are formed simply by combining compounds, the preparation is facile and involves no waste. Another advantage is that they do not react with water.<sup>17</sup> Thus these solvents are both inexpensive and environmentally-friendly.

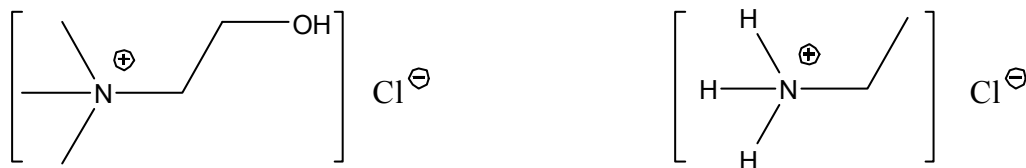


Figure A.2: Structures of choline chloride (left) and ethylammonium chloride (right).



Researchers have tested the viability of using DESs for enzymatic reactions by examining the lipase-catalyzed transesterification of ethyl valerate with 1-butanol in DESs made from combining either choline chloride or ethylammonium chloride with one of the five compounds shown in Figure A.3. CALB and immobilized CALB (*i*CALB) provided similar conversions in those 10 DESs and in toluene. Additionally, lipase A from *Candida antarctica* (CALA) showed activity in all of the those DESs.<sup>19</sup> These satisfactory enzymatic activities suggest that cellulase might also function adequately in certain DESs. These 10 DESs known to maintain nominal activity were the first DESs tested for effective cellulose dissolution.

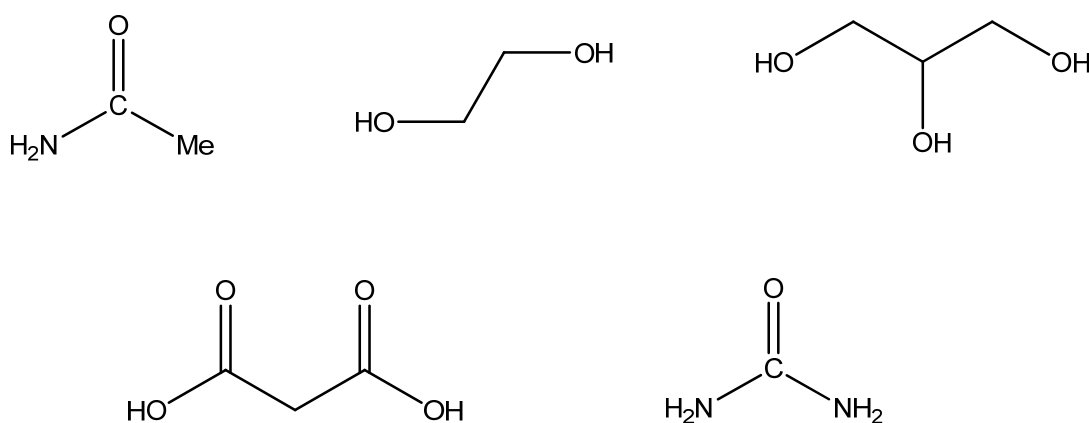


Figure A.3: Structures of acetamide (top left), ethylene glycol (top middle), glycerol (top right), malonic acid (bottom left), and urea (bottom right).

Other DESs in the literature include low-temperature melts made from carbohydrates and urea derivatives.<sup>18, 20, 21</sup> Since cellulose is a polymer of glucose, the possibility of using mixtures of urea and monosaccharides was also examined. Solvents involving both fructose and glucose were tested, although a salt needed to be added to the glucose system because it does not form a DES at low temperatures with urea.<sup>18</sup>

### **Tetra-Alkyl Ammonium Ionic Liquids**

Zhao and coworkers recently published some studies comparing the ability of several ionic liquids to dissolve cellulose. Their research revealed that there are three important factors for cellulose dissolution. The first necessary feature is the ability of the anion to hydrogen bond with the cellulose. The second requirement is that the cation must contain oxygen. The final factor is that the cation should not be too bulky.<sup>22</sup>

Most imidazole- and pyridine-based ILs use a halogen anion as the negatively charged species in the salt. These ILs work well for cellulose dissolution because, due to their high thermal stability, dissolution reactions can be run at higher temperatures with no solvent degradation occurring. Additionally, it has been shown that the chlorine anion hydrogen bonds with the hydroxy groups on the cellulose, which enhances the dissolution.<sup>23-25</sup> These properties, however, also have drawbacks. Several ILs containing chlorine anions have high melting points that exceed the optimal temperature range for most enzymes. More importantly, these ILs are hygroscopic and thus destabilize most enzymes.<sup>22</sup>

Other options for the anion include dicyanamide (dca), formate, and acetate ions. The results from Zhao et al. indicate that dca ILs were not able to dissolve cellulose, which they attribute to the inability to hydrogen bond. Dissolution also did not occur in ILs containing formate as the anion, which they hypothesized are too basic. ILs containing acetate ions were thus the most suitable for both cellulose dissolution and for retaining enzymatic activity in some solvent systems.<sup>22</sup>

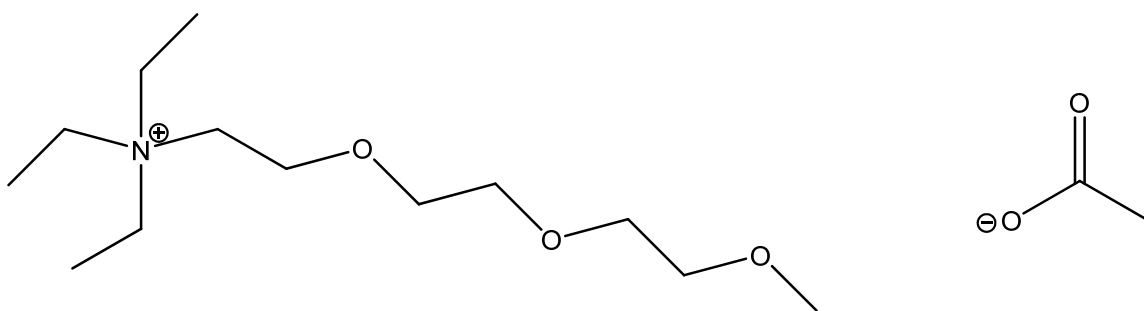


Figure A.4: Structure of [Et<sub>3</sub>N-Glycol][acetate].

The most promising IL synthesized by Zhao et al. was the glycol-based IL [Et<sub>3</sub>N-Glycol][acetate]. The structure of this IL is depicted in Figure A.4. Their results show that this IL is capable of dissolving up to 10% cellulose, and that Novazyme 435 had an initial rate of 0.83  $\mu\text{mol}/\text{min}\cdot\text{g}$  in it at 60 °C for the enzymatic transesterification of the crown ether N-acetyl-L-phenylalanine ethyl ester (Ac-L-Phe-OEt) with 1-propanol. This is greater than four times its activity in *tert*-butanol. Based upon their results, further modifications to this IL could enhance cellulose solubility even more. Some possible modifications include changing the length of the glycol chain, adjusting the length of the hydrocarbon chains on the nitrogen, and replacing the nitrogen with phosphorus.

This appendix examines the cellulose dissolution capability of several DESs and ILs, and the subsequent impact on cellulose crystallinity. The solvents examined include DESs, commercially-available ILs, and glycol-based ILs, both from the literature and modified by our lab. The initial hydrolysis kinetics of cellulase in aqueous buffer on the cellulose recovered from some dissolution media are also determined.

## **EXPERIMENTAL**

### **Materials**

#### DESs

The following materials were all used as received from the suppliers: choline chloride (Acros Organics, 99%), ethylamine hydrochloride (Aldrich, 98%), acetamide (99%, Alfa Aesar), ethylene glycol (Sigma-Aldrich, Reagent Plus >99%), glycerol (Aldrich, ACS Reagent 99.5%), malonic acid (Alfa Aesar, 99%), urea (Fluka, puriss ACS >99.5%), glucose (D-(+)-glucose Sigma, 99.5%), fructose (Sigma, min 99%) calcium chloride dehydrate (EMD, ACS grade crystals), and cellulose (Fluka, Avicel PH-101, 60% crystallinity).

#### ILs

The following materials were used as received: [Bmim][Cl] (Sigma, 98% purity) and cellulose (Fluka, Avicel PH-101, 60% crystallinity).

Synthesis of Triethyl (2-(2-methoxyethoxy)ethoxy) ethylammonium acetate

*2-(2-(2-methoxyethoxy)ethoxy)ethyl benzenesulfonate (MMGBS)*

Sodium hydroxide (30.5 g, 0.763 mol) was dissolved in 150 mL of distilled water and was then added into the 1 L round bottom flask containing a mixture of tri(ethylene glycol) monomethyl ether (TEGMME, 48.7 mL, 0.305 mol), toluene (100 mL), a catalytic amount of hexadecyltrimethylammonium hydroxide (1 mL, 0.0207 mol), and a stir bar. The solution was cooled to 0 °C using an ice bath. Benzenesulfonyl chloride (42.8 mL, 0.336 mol) was added slowly to the solution. The temperature of the solution was monitored during the addition, making sure to keep the temperature below 70 °C.

Once the addition was complete, the reaction flask was removed from the ice bath, placed into a heating mantle, and equipped with a condenser. The reaction mixture was maintained at 70 °C with a constant stirring for 5 h. The solvent was removed through rotary evaporation. The solid residue was dissolved in dichloromethane and washed once with distilled water. After drying the organic layer over sodium sulfate, dichloromethane was evaporated with a rotary evaporator. The pale yellow liquid (63.4 g, 0.208 mol, 68.2 %) was used without further purification.

$^1\text{H}$  NMR (400 MHz, DMSO- $d_6$ )  $\delta$  7.89 (d, 2H), 7.78 (t, 1H), 7.67 (t, 2H), 4.23 (t, 2H), 3.58 (t, 2H), 3.44 (m, 8H), 3.22 (s, 3H).  $^{13}\text{C}$  NMR (400 MHz, DMSO- $d_6$ )  $\delta$  134.2, 129.7, 127.5, 71.3, 71.2, 70.2, 69.9, 67.8, 58.0, 54.8.

N,N-2-(2-(2-methoxyethoxy)ethoxy)ethanamine (Et<sub>2</sub>NGlycol)

In a 500 mL round bottom flask equipped with a stir bar, diethylamine (9.27 mL, 0.0896 mol), toluene (50 mL), and a catalytic amount of hexadecyltrimethylammonium hydroxide (1 mL, 0.0207 mol) were combined. Sodium hydroxide (10.8 g, 0.269 mol) was dissolved in distilled water (70 mL) and added to the reaction mixture. MMGBS (30.0 g, 0.0986 mol) was added slowly into the solution. The viscous mixture was stirred for 4 h at 70 °C. After removal of the solvent using rotary evaporation, water was added into the mixture to dissolve most of the precipitate. The aqueous solution was extracted at least three times with dichloromethane. After drying the organic layer with sodium sulfate, the solvent was evaporated yielding a pale yellow, viscous liquid (18.7 g, 0.0851 mol, 95.1 %).

<sup>1</sup>H NMR (400 MHz, DMSO-*d*<sub>6</sub>) δ 4.18 (t, 2H), 3.63 (t, 2H), 3.51 (m, 8H), 3.26 (s, 3H), 2.44 (q, 4H), 0.98 (t, 6H). <sup>13</sup>C NMR (400 MHz, DMSO-*d*<sub>6</sub>) δ 71.6, 70.1, 69.8, 59.5, 51.1, 48.9, 14.3.

N, N, N-Triethyl-2(2-(2-methoxyethoxy)ethoxy)ethanaminium bromide (Et<sub>3</sub>NGlycol-Br)

Glycol-substituted diethylamine (Et<sub>2</sub>NGlycol, 20.0 g, 0.0912 mol) was dissolved in dry acetonitrile (200 mL) in a 500 mL round bottom flask equipped with a stir bar. An excess amount of bromoethane (13.6 mL, 0.182 mol) was added to the flask. The mixture was refluxed at 80 °C under argon for 2 days. An orange liquid (27.5 g, 0.0839 mol, 92%) was isolated after the acetonitrile was removed using rotary evaporation. The crude product was purified by washing it with anhydrous diethyl ether (50 mL).

$^1\text{H}$  NMR (400 MHz,  $\text{DMSO-}d_6$ )  $\delta$  3.78 (t, 2H), 3.57 (t, 2H), 3.49 (m, 6H), 3.33 (q, 8H), 3.17 (s, 3H), 1.16 (t, 9H).  $^{13}\text{C}$  NMR (400 MHz,  $\text{DMSO-}d_6$ )  $\delta$  71.3, 69.8, 69.6, 69.5, 60.3, 58.0, 57.9, 7.3.

N, N, N-Triethyl—2(2-(2-methoxyethoxy)ethoxy)ethanaminium acetate  
( $\text{Et}_3\text{N}$ Glycol-OAc)

The bromide anions in  $\text{Et}_3\text{N}$ Glycol-Br were replaced with acetate using an anion exchange resin, Amberlite<sup>®</sup> IRA-400 chloride form. About 100 mL of the resin (Amberlite<sup>®</sup> IRA-400 Cl, 1.40 meq/mL by wetted bed volume, 16-50 mesh) was packed in a glass chromatography column and washed thoroughly with 1:1 distilled water/methanol until no yellow color was observed in the eluent. The chlorine anions on the resin were exchanged with acetate anions ( $\text{CH}_3\text{COO}^-$ ) by slowly washing the column with an excess amount of sodium acetate (>15 g) solution. The column was then washed with distilled water to remove the salt residues on the column. The ionic liquid [Glycol- $\text{Et}_3\text{-N}$ ]Br was diluted with 200 mL deionized water and slowly dripped through the column. The eluting solution was collected and decolorized with activated charcoal. Water was removed from the clear solution through a rotary evaporator under vacuum at 60 °C. The product was further dried in an oven at 50 °C over 24 h which yielded a viscous, orange liquid. This liquid was diluted with methanol and decolorized with activated charcoal. Methanol was removed from the pale yellow liquid, yielding a colorless liquid (27.5 g, 0.839 mol, 100%).

IR (neet)  $\text{cm}^{-1}$ : 2875, 1582, 1453, 1098.  $^1\text{H}$  NMR (400 MHz,  $\text{DMSO-}d_6$ )  $\delta$  3.78 (t, 2H), 3.57 (t, 2H), 3.49 (m, 6H), 3.33 (q, 8H), 3.17 (s, 3H), 1.54 (s, 3H), 1.16 (t, 9H).  $^{13}\text{C}$  NMR (400 MHz,  $\text{DMSO-}d_6$ )  $\delta$  174.7, 71.5, 69.7, 63.8, 58.2, 56.0, 53.1, 25.2, 7.4. HRMS  $\text{C}_{13}\text{H}_{30}\text{NO}_3$  calculated 248.2226, found 248.2216.

This synthesis was carried out as described in the Electronic Supplementary Information (ESI) from Zhao et al.<sup>22</sup> In order to optimize yields, the reaction times for steps one and two were increased to 5 and 4 hours, respectively. Additionally, the  $\text{Et}_3\text{NGlycol-OAc}$  was decolorized with charcoal a second time using methanol to improve the purity of the final product. Degradation was observed during removal of the water; the lower boiling methanol is easily removed at lower temperatures, however, preventing the IL from degrading. The total synthetic process is depicted in Figure A.5.

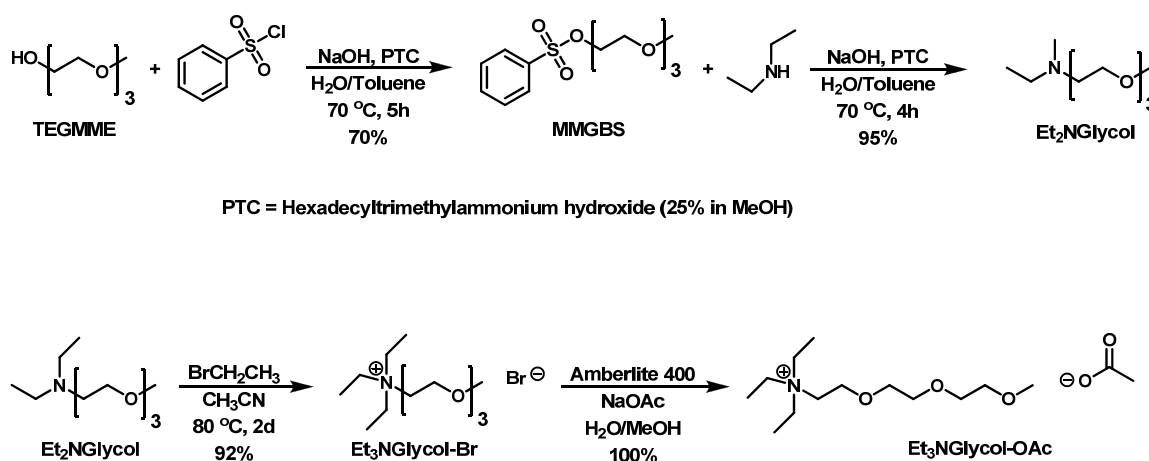


Figure A.5: Total synthesis of triethyl (2-(2-methoxyethoxy)ethoxy) ethylammonium acetate).



## **Methods**

### Phosphoric Acid Swollen Cellulose

Phosphoric acid swollen cellulose (PASC) stock solution was prepared based by the procedure used by Schülein.<sup>26</sup> Avicel cellulose was wetted with water and cold 85% ortho-phosphoric-acid was added. The suspended mixture was gently stirred in an ice bath for 1 h. Cold acetone was added while stirring continued. The resulting slurry was put in a Buchner filter and washed multiple times with cold acetone. The solid was dried as much as possible between washes. After acetone, the solid was washed twice with water, again dried as much as possible between washes. The obtained swollen cellulose was kept in a closed container and used without further modification, after the water content was determined.

### Deep Eutectic Solvents

The first set of DES solvents analyzed contained either choline chloride (ChCl) or ethylammonium chloride (EAC) as the ammonium salt. The five hydrogen bond donors examined were acetamide, ethylene glycol, glycerol, malonic acid, and urea. Initial cellulose dissolution studies occurred at 125 °C for choline chloride DESs and 80 °C for the ethylammonium chloride ones. The lower temperature was chosen for the EAC DESs because they were less thermally stable than the ChCl counterparts. For the step-wise studies, only 80 °C was used in order to have all DES at identical conditions.

Table A.1: Molar ratios of DES mixtures.

<b>ChCl DES</b>		<b>EAC DES</b>	
Component	Molar Amounts	Component	Molar Amounts
ChCl	0.05 M	EAC	0.05 M
H Donors	0.1 M	H Donors	0.075 M

The appropriate molar ratio for each component of the DES was weighed and placed in a round bottom flask with a stir bar. These molar ratios, determined from the literature, can be found in Table A.1. The flask was placed in a mineral oil bath heated to 60 °C or 80 °C and stirred at 400 rpm. This allowed the components to melt and become the liquid DES. After the solution was stirred for one hour, the temperature of the oil bath was increased to the cellulose dissolution temperature. The DES was kept at that temperature to equilibrate for one hour before adding cellulose. For the initial experiments, 10 wt% cellulose was measured out and placed in the flask. The mixture was allowed to equilibrate for 3 hours. For the step-wise addition experiments, small amounts of cellulose (~50 mg) were measured out and added to the flask each hour.

Once the experiment was over, the DES/cellulose mixture was dumped into 100 mL rinse MeOH to dissociate the DES. The cellulose crashed out immediately after addition to MeOH. The entire solution was filtered using Whatman medium porosity cellulose paper and allowed to dry overnight on the filter. The cellulose was scraped into vials and given to the Bommarius lab, where it was dried in an oven overnight at 60 °C before the crystallinity analysis was completed via solid-state NMR.

### Ionic Liquids

A similar study was done with the ILs. The oil bath was heated to 110 °C and was stirred at 400 rpm. Once the oil reached temperature, 5 g of the IL was placed in a test tube. The test tube was kept at temperature for an hour to allow thermal dquilibrium. Cellulose (20 – 70 mg) was added to the flask, and more was added upon dissolution of the previous sample (5-15 min). The cellulose dissolution was determined when the cellulose stopped going into solution.

Once the experiment was over, the cellulose was precipitated out of the IL by adding MeOH. The entire solution was filtered using Whatman medium porosity cellulose paper and dried overnight on the filter. The cellulose samples were given to the Bommarius lab, where they were dried in an oven overnight at 60 °C before the crystallinity analysis was completed via solid-state NMR.

### Solid-State NMR

All cellulose samples precipitated from the alternative solvents were analyzed via solid-state NMR by the Bommarius research group to determine the crystallinity index.<sup>6, 27</sup> Solid-state  $^{13}\text{C}$  NMR was performed on a Bruker Avance/DSX-400 spectrometer using a Bruker 4-mm MAS probe to measure temperature. The solid-state cross polarization/magic angle spinning (CP/MAS)  $^{13}\text{C}$  NMR experiments were operated at frequencies of 100.55 MHz for  $^{13}\text{C}$ . All experiments were carried out at ambient temperature. The samples (~ 35% moisture content) were packed in 4 mm zirconium dioxide rotors and spun at 10 kHz. Acquisition was carried out with a CP pulse sequence using 5  $\mu\text{s}$  pulse and 2.0 ms contact pulse.

## RESULTS AND DISCUSSION

### Improved Hydrolysis of Amorphous Cellulose

Before focusing on the dissolution properties of alternative solvents, tests were run to determine any improvement on the enzymatic production of glucose when the cellulose starting material was amorphous cellulose instead of crystalline. A commercially-available mix of cellulases comprised of endoglucanase (I, II), cellobiohydrolase (I-reducing end, II-non reducing end), and  $\beta$ -glucosidase were used to hydrolyze various cellulose samples into glucose. These enzymes have been used before by the Bommarius research group to test glucose production from pretreated lignocellulosic biomass.<sup>6</sup> Cellulose was rendered amorphous by treating it in phosphoric acid, a well-known literature procedure.<sup>26</sup> The hydrolysis was run at 50 °C and 900 rpm on a 1 mL scale. 20 mg cellulose samples were placed in sodium acetate buffer (50 mM, pH 5). The glucose concentration was analyzed with a spectrometer using the dinitrosalicylic acid (DNS) assay.<sup>28</sup>

As can be seen in Figure A.6, enzymes were able to produce nearly 4x more glucose from amorphous cellulose than from untreated Avicel over a 3 hour time period. It takes approximately 2-2.5 hours to fully convert the phosphoric acid pretreated sample. An even more drastic result is depicted in Figure A.7. Achieving the full conversion of untreated Avicel takes 25x times longer when the cellulose is untreated. Such drastic results illustrate the importance of decreasing cellulose crystallinity before initiating enzymatic hydrolysis.

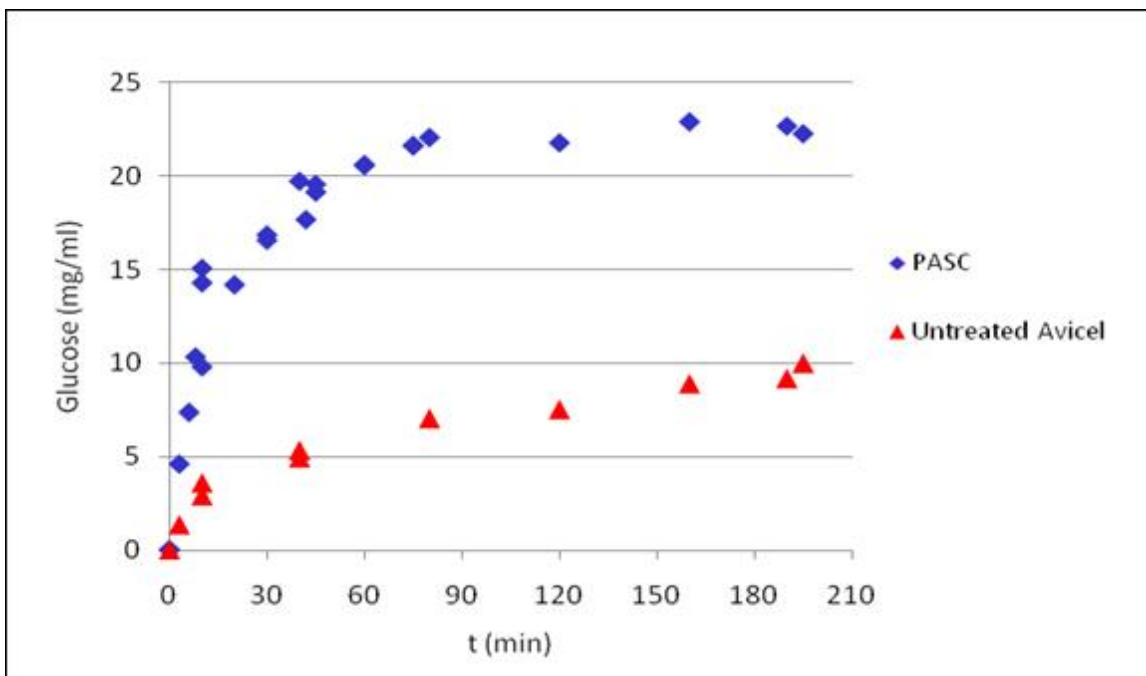


Figure A.6: Enzymatic hydrolysis of untreated and amorphous cellulose to glucose over 3.5 hours.

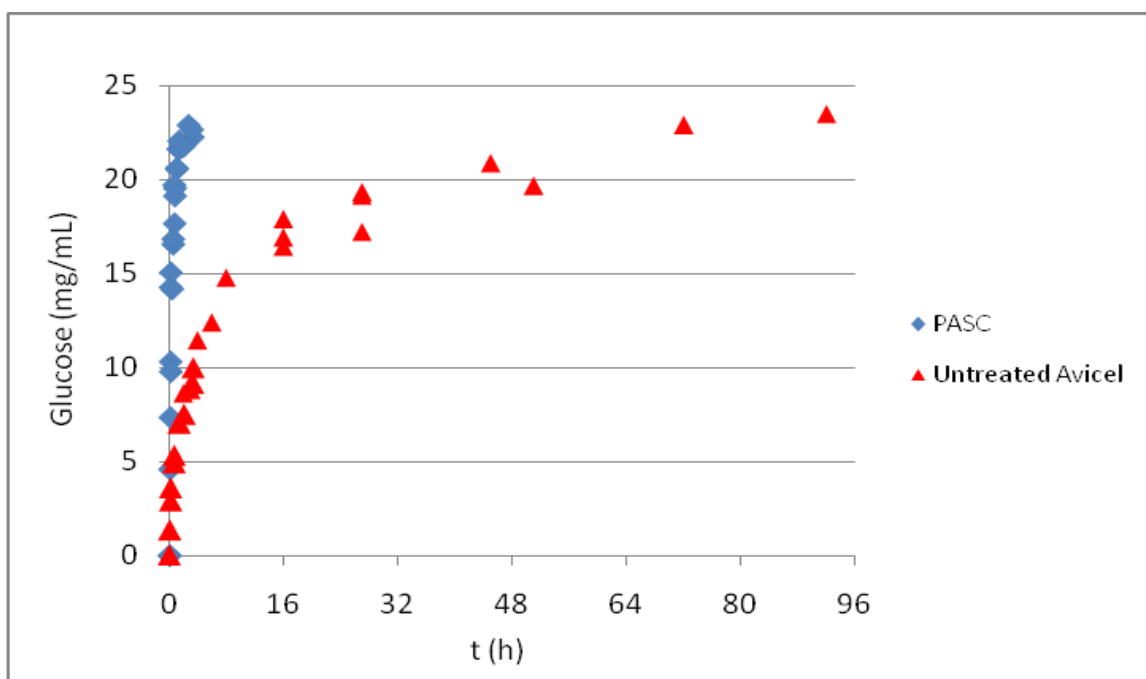


Figure A.7: Enzymatic hydrolysis of untreated and amorphous cellulose to glucose over 4 days.

## **DES Studies**

A total of 12 DESs were made and the capability of each for cellulose dissolution was tested. There were three types of DES tested: those made from choline chloride (ChCl), those made from ethylammonium chloride (EAC), and those made from urea and a carbohydrate. The hydrogen donors for the first two classes were as follows: ethylene glycol (EG), glycerol (G), malonic acid (MA), urea (U), and acetamide (A).

### Choline Chloride DESs

The DESs made from choline chloride were the most stable. All were able to withstand the high cellulose dissolution temperature of 125 °C, although a few discolored slightly after several hours in the oil bath. The dissolution was also attempted at 80 °C, both by adding the cellulose all at once, and by adding the cellulose in 50 mg increments. Cellulose did not visibly dissolve under any conditions tested in any of these 5 DESs. Although some of the mixtures seemed to swell the cellulose, no significant difference was observed

Despite no visible cellulose dissolution, the DES mixtures were added to MeOH to precipitate out any cellulose that might have gone into solution. The cellulose was rinsed thoroughly to remove any residual ions, and the crystallinity index was tested via solid-state NMR. The results are shown in Figure A.8. As can be seen, the crystallinity index of cellulose treated in the DESs varied only slightly, and most variations are within error of the determination method. The bar in Figure A.8 represents the average crystallinity of untreated cellulose (61-62%).

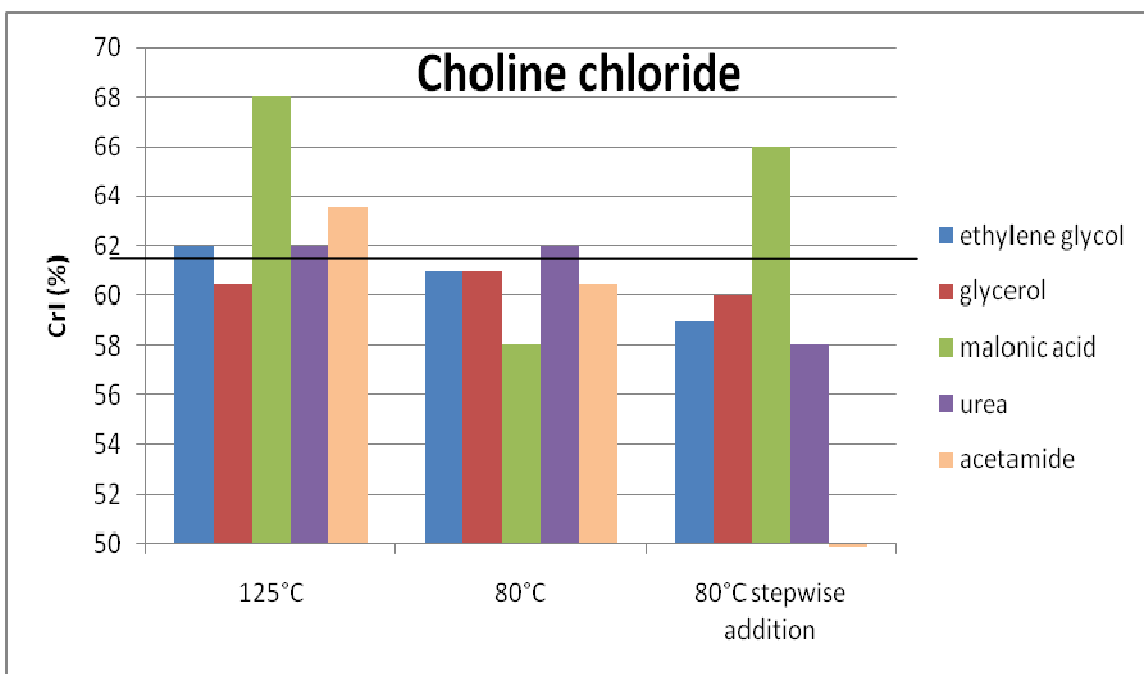


Figure A.8: Crystallinity index of cellulose pretreated in choline chloride DESs.

One significant difference is the increase in the cellulose crystallinity from the ChCl: MA mixture. Although no further studies were completed, it is believed that the increase occurred because the malonic acid caused amorphous regions of the cellulose sample to undergo acid-catalyzed hydrolysis. The amount of amorphous cellulose would have decreased, thus increasing the overall crystallinity index of the cellulose sample. There is no data for the step-wise addition of cellulose to the ChCl:A DES because the crystallinity index could not be determined. This is probably due to the presence of residual ions on the cellulose interfering with the method. The experiment was not repeated because this type of dissolution media did not seem promising.

## Ethylammonium Chloride DESs

Similar experiments were conducted with the ethylammonium chloride DESs. The high dissolution temperature of 120 °C, however, was not viable for most of these mixtures. Except for the ethylammonium chloride:urea mixture, the DESs either darkened immediately, or one of the components visibly boiled off. A lower dissolution temperature of 80 °C was used for subsequent experiments.

Although this temperature worked better, the ethylammonium chloride DESs were still not completely stable. The most notable instability was for the EAC:A mixture. Crystals formed at the top of the reaction flask within an hour of being heated at 80 °C. <sup>1</sup>H NMR analysis confirmed that the crystals were pure acetamide. It is likely that a few other EAC DESs were also not completely stable because small amounts of vapor rising from the reaction flasks were visible.

The crystallinity index of the cellulose treated in each DES mixture is shown in Figure A.9. As before, no drastic difference was seen in the crystallinity index for any of the samples. The 80 °C EAC:U sample also could not be determined, again probably due to residual ions. The crystallinity of the MA samples again increased, although a slight decrease could be seen for the 120 °C EAC:U and the 80 °C EAC:EG and EAC:G samples. The increase was again attributed to acid-catalyzed hydrolysis of the initial amorphous regions, but the slight decrease in crystallinity index for the 120 °C EAC:U and 80 °C EAC:EG was examined further.



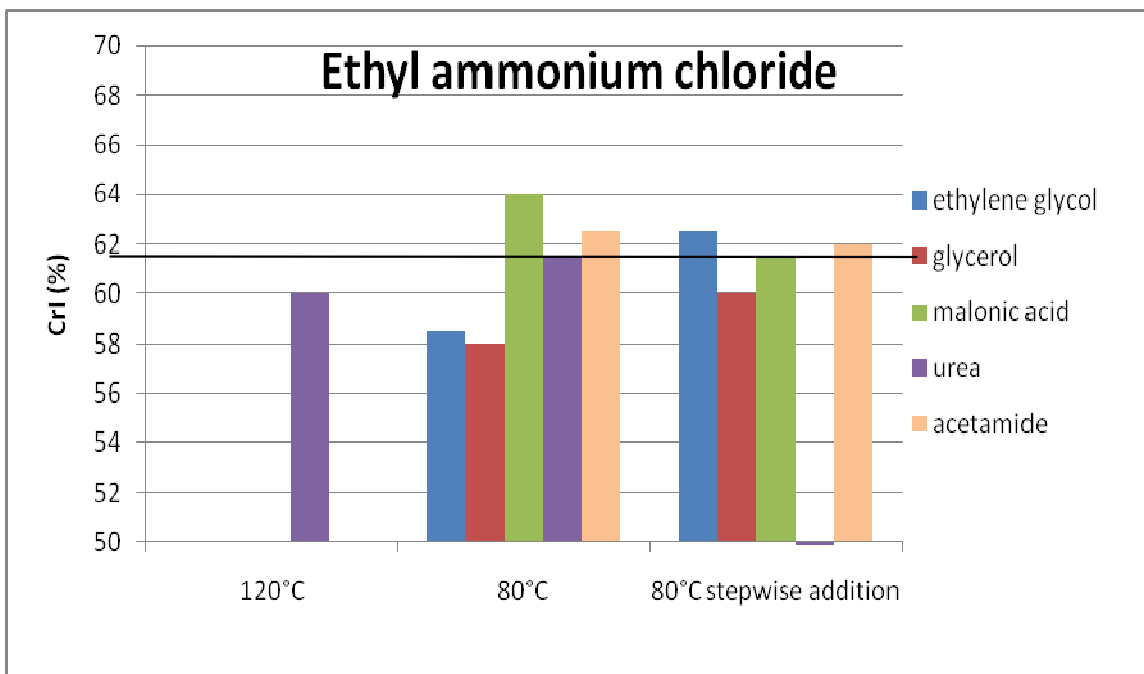


Figure A.9: Crystallinity index of cellulose pretreated in ethylammonium chloride DESs.

Cellulose hydrolysis studies similar to those done for the untreated Avicel cellulose vs. phosphoric acid-treated cellulose were completed on both of these treated samples. The results for the EAC:U cellulose sample are depicted in Figure A.10. As can be seen, the hydrolysis rate of the treated cellulose actually decreased significantly and corresponds to a 30% decrease in glucose concentration after 20 hours. It is possible, however, that this decrease is due to the presence of either residual ions left on the cellulose, or from residual MeOH left on the cellulose after washing it thoroughly, as no change in CrI was observed. Both are known to inhibit enzymatic activity.

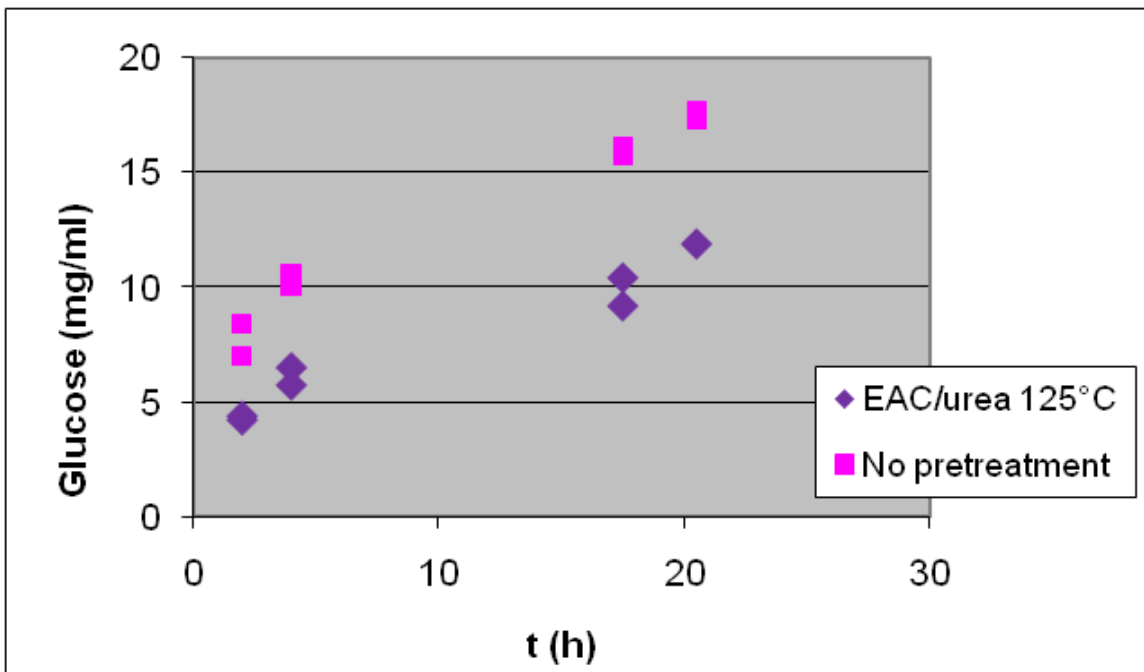


Figure A.10: Enzymatic hydrolysis of untreated and EAC:U treated (120 °C) cellulose to glucose over 20 hours.

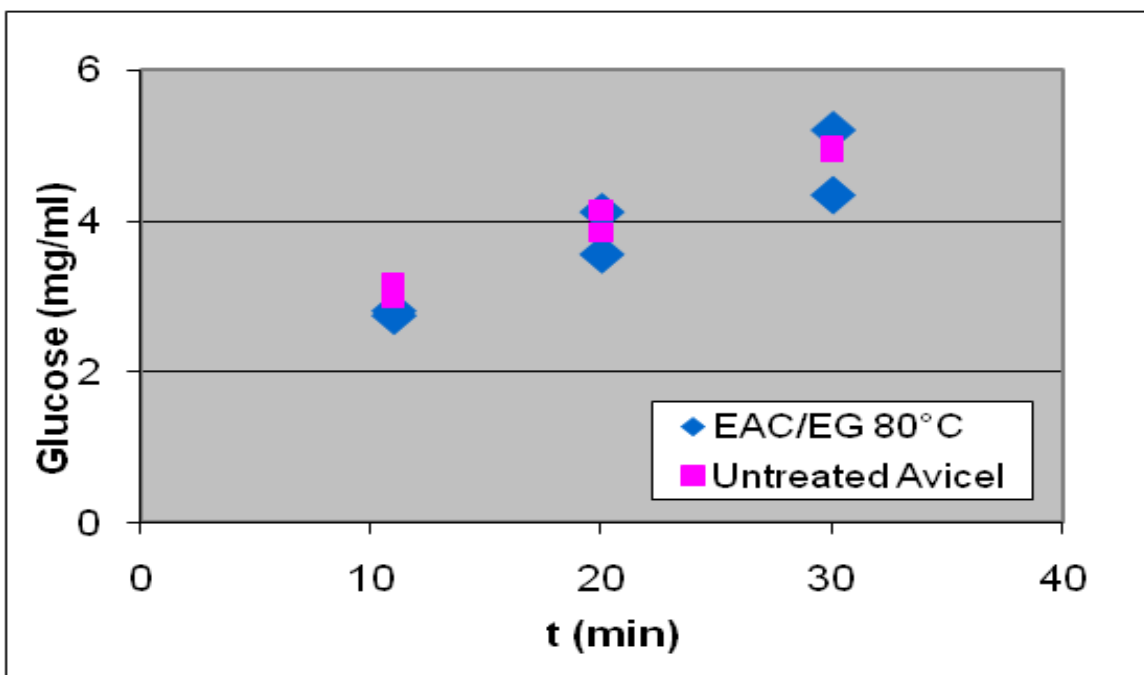


Figure A.11: Enzymatic hydrolysis of untreated and EAC:EG (80 °C) treated cellulose to glucose over 30 minutes.

Similarly, the results for the EAC:EG sample are shown in Figure A.11. These results imply that there is no difference in the hydrolysis rates between the untreated Avicel and the cellulose treated in EAC:EG, which is important because it indicates that a small decrease in the crystallinity index is not sufficient to improve hydrolysis rates. The results also indicate that there might be some critical threshold that must be met before a noticeable difference in hydrolysis rates occurs. The results showed that none of the EAC DESs tested were able to significantly decrease the CrI, so it was decided these solvents were not the best path forward and this route was abandoned.

#### Urea:Carbohydrate DESs

Several DESs made from combining urea and a carbohydrate were also examined. Urea and fructose were combined in a 2:1 molar ratio and dissolved at 80 °C. Similarly, urea, glucose, and fructose were combined in a 2:1:1 molar ratio and dissolved at 80 °C. Both combinations formed a melt at 80 °C. After adding cellulose, however, both DESs also solidified within an hour. It is possible that adding cellulose, which is structurally similar to glucose or fructose, caused the eutectic point to shift. This DES system was not pursued further.

#### **IL Studies**

The first IL tested for cellulose dissolution was triethyl (2-(2-methoxyethoxy)ethoxy) ethylammonium acetate, the glycol-substituted IL that worked best for Zhao et al.<sup>22</sup> It was synthesized in our lab and characterized by both <sup>1</sup>H NMR and <sup>13</sup>C NMR before use.

The IL was put in a test tube and placed in a 120 °C oil bath for an hour to allow it to equilibrate. After an hour, the solution has darkened slightly from its original pale yellow coloring. Cellulose was added in small increments (approximately 25-50 mg) and allowed to dissolve. Initially it took only 5 minutes to dissolve. As more was added, the dissolution time increased to approximately 15 minutes. The IL started to get increasingly darker as time progressed. The last amount of cellulose had just been added, bringing the total to 10% wt cellulose, when the solution began to solidify.

This solid originally appeared to be dark brown in color. On closer inspection, however, it became apparent that the solid itself was transparent and the color came from a residual dark brown liquid covering its surface. Adding MeOH to the liquid immediately precipitated out more solid. The solid was rinsed copiously with MeOH.

The solid appeared to be a polymer. Attempts to dissolve it in MeOH, H<sub>2</sub>O, THF, and DMSO were unsuccessful, so we were unable to characterize it by gel permeation chromatography (GPC). A solid-state IR was run to determine the functional groups present in the solid. The IR spectrum is shown in Figure A.12. The –OH peak is readily apparent in this spectrum, and was not visible in the IR of the final IL. There are also a N-C peak and a sharp CH<sub>2</sub>-O peak, however, suggesting the presence of the IL. It is likely the solid has been formed from both IL, or possibly degraded IL, and cellulose.

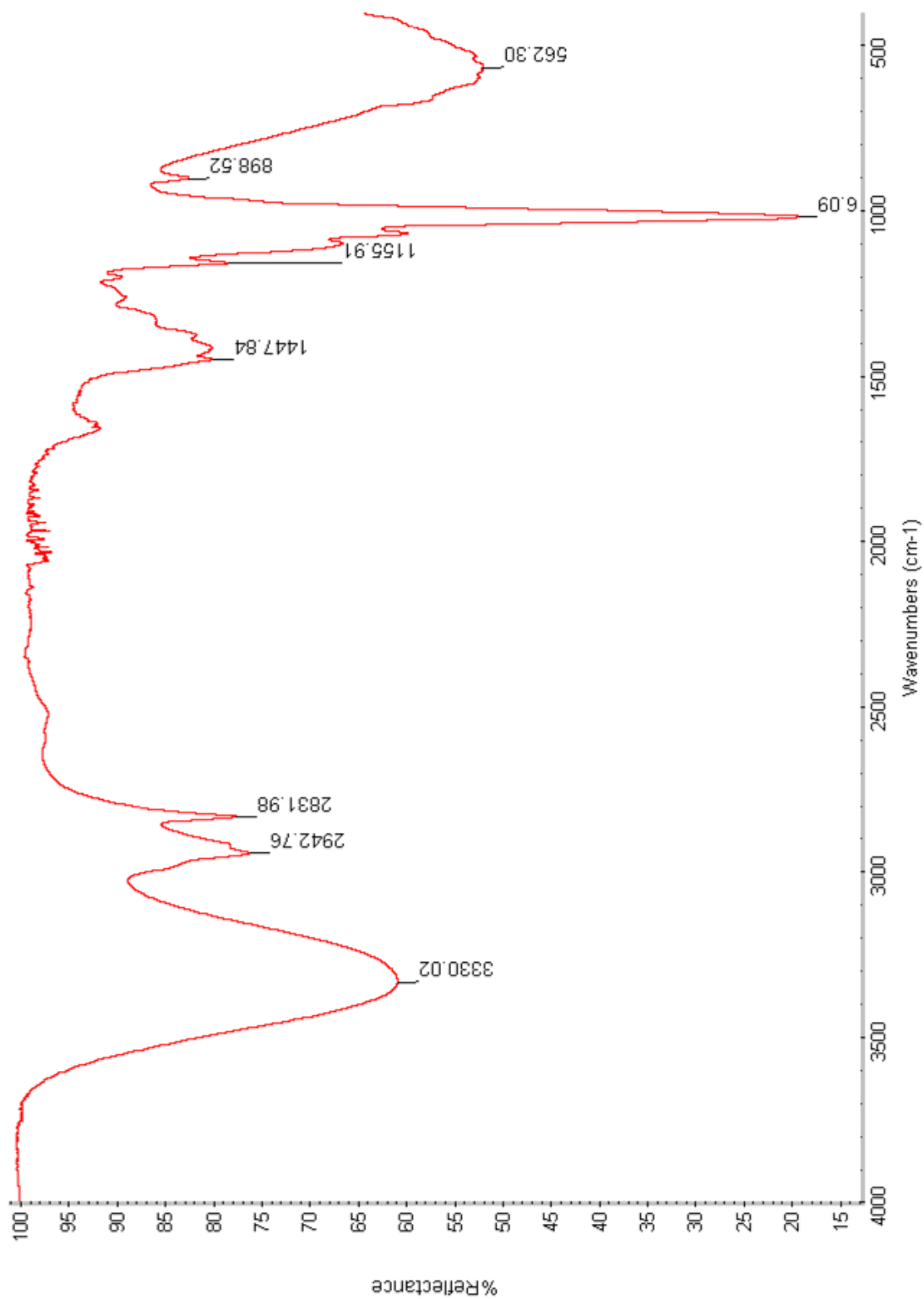


Figure A.12: IR spectrum of solid formed from IL-cellulose mixture.

Although further characterization has not been done to date, more studies are planned to characterize the polymer as much as possible. A DSC-TGA will be run to determine the melting point. It has also been submitted to the MS lab, although the original method used provided little useful information.

### **Path Forward**

This project is still ongoing. The next planned experiment is to dissolve cellulose in [Bmim][Cl] and have the Bommarius lab run its hydrolysis study on the resulting cellulose. Triethyl (2-(2-methoxyethoxy)ethoxy) ethylammonium acetate is being synthesized again in the lab. Once it is purified, it will be further characterized by Karl-Fischer and a DSC-TGA will be run to determine its temperature stability. The dissolution experiment will be repeated at a lower temperature, and the hydrolysis study completed by the Bommarius lab. The synthesis of another glycol-substituted IL, tripropyl (2-(2-methoxyethoxy)ethoxy) ethylammonium acetate, is also currently being done. The same characterization and dissolution studies will be completed for this IL.

### **CONCLUSIONS AND RECOMMENDATIONS**

This project has examined several classes of alternative solvents and determined the capability of multiple solvents for cellulose dissolution. At this point in time, alternative ionic liquids, especially glycol-substituted ones, seem the most promising path for a sustainable cellulose solvent. None of the tested DES solvents were effective cellulose solvents, although it is possible another class of them could be.

The glycol-substituted IL triethyl (2-(2-methoxyethoxy)ethoxy) ethylammonium acetate was successfully able to dissolve nearly 10% cellulose. The solution did turn to a solid over time, but this is more likely due to decomposition of the IL rather than an inability of the solvent to dissolve cellulose. Further studies with the IL will be completed at both shorter temperatures and shorter times.

ILs are tunable solvents; the functional groups on both the anions and cations can be changed to optimize solvent properties. To date, only one glycol-substituted IL has been fully synthesized in our lab, but another synthesis has already begun. These ILs will form the basis for further modification and optimization. Future choices for modification include changing the length of the glycol chain, changing the spacing of the oxygen in the chain, changing the alkyl chains on the quaternary ammonium, and changing the ammonium to phosphonium. All of these options provide possible ways to improve cellulose solubility in an IL.

Possibly enzymatic activity will also be examined in some of the best cellulose dissolution ILs. While it is not absolutely necessary to have the hydrolysis enzymes active in the same solvent, it would simplify processing and make the process more economically-viable. The current process involves precipitating out the dissolved cellulose by adding MeOH. In order to recycle the IL, the MeOH would have to be removed. An economic study should be done to determine the feasibility of this process.

The polymer formation will also be further studied because there is high interest in polymers that can be derived from renewable resources. Even if this cellulose-IL polymer is not valuable, it is possible that other polymers with useful properties can be formed in a similar fashion.

Although still in the early stages, this project has significant importance in the fields of biocatalysis, renewable energy, and biomaterials. Solvents that can dissolve cellulose have been sought for decades. Creating sustainable solvents that are also able to support enzymatic activity will be even more important in future years as biomaterials and biofuels continue to play a more important role in today's chemical processes

## REFERENCES

1. X. J. Pan, C. Arato, N. Gilkes, D. Gregg, W. Mabee, K. Pye, Z. Z. Xiao, X. Zhang and J. Saddler, *Biotechnology and Bioengineering*, 2005, **90**, 473-481.
2. T. T. Teeri, *Trends in Biotechnology*, 1997, **15**, 160-167.
3. D. Cullen and P. Kersten, in *Applied Molecular Genetics of Filamentous Fungi*, eds. J. R. Kinghorn and G. Turner, Chapman & Hall, New York, 1992.
4. A. P. Dadi, C. A. Schall and S. Varanasi, *Applied Biochemistry and Biotechnology*, 2007, **137**, 407-421.
5. N. Mosier, C. Wyman, B. Dale, R. Elander, Y. Y. Lee, M. Holtzapple and M. Ladisch, *Bioresource Technology*, 2005, **96**, 673-686.
6. A. S. Bommarius, A. Katona, S. E. Cheben, A. S. Patel, A. J. Ragauskas, K. Knudson and Y. Pu, *Metabolic Engineering*, In Press.
7. D. A. Fort, R. C. Remsing, R. P. Swatloski, P. Moyna, G. Moyna and R. D. Rogers, *Green Chemistry*, 2007, **9**, 63-69.
8. D. B. Zhao, Y. C. Liao and Z. D. Zhang, *Clean-Soil Air Water*, 2007, **35**, 42-48.
9. T. Heinze, K. Schwikal and S. Barthel, *Macromolecular Bioscience*, 2005, **5**, 520-525.
10. R. P. Swatloski, S. K. Spear, J. D. Holbrey and R. D. Rogers, *Journal of the American Chemical Society*, 2002, **124**, 4974-4975.
11. S. Barthel and T. Heinze, *Green Chemistry*, 2006, **8**, 301-306.



12. M. B. Turner, S. K. Spear, J. G. Huddleston, J. D. Holbrey and R. D. Rogers, *Green Chemistry*, 2003, **5**, 443-447.
13. Y. H. Moon, S. M. Lee, S. H. Ha and Y. M. Koo, *Korean Journal of Chemical Engineering*, 2006, **23**, 247-263.
14. C. Pretti, C. Chiappe, D. Pieraccini, M. Gregori, F. Abramo, G. Monni and L. Intorre, *Green Chemistry*, 2006, **8**, 238-240.
15. T. S. Jin, Y. Yin, L. B. Liu, Y. Zhao and T. S. Li, *Chinese Journal of Organic Chemistry*, 2007, **27**, 261-265.
16. N. Gathergood, P. J. Scammells and M. T. Garcia, *Green Chemistry*, 2006, **8**, 156-160.
17. A. P. Abbott, D. Boothby, G. Capper, D. L. Davies and R. K. Rasheed, *Journal of the American Chemical Society*, 2004, **126**, 9142-9147.
18. G. Imperato, E. Eibler, J. Niedermaier and B. Konig, *Chemical Communications*, 2005, 1170-1172.
19. J. T. Gorke, F. Srienc and R. J. Kazlauskas, *Chemical Communications*, 2008, 1235-1237.
20. G. Imperato, S. Hoger, D. Lenoir and B. Konig, *Green Chemistry*, 2006, **8**, 1051-1055.
21. G. Imperato, R. Vasold and B. Konig, *Advanced Synthesis & Catalysis*, 2006, **348**, 2243-2247.
22. H. Zhao, G. A. Baker, Z. Y. Song, O. Olubajo, T. Crittle and D. Peters, *Green Chemistry*, 2008, **10**, 696-705.
23. R. C. Remsing, R. P. Swatloski, R. D. Rogers and G. Moyna, *Chemical Communications*, 2006, 1271-1273.
24. T. G. A. Youngs, C. Hardacre and J. D. Holbrey, *Journal of Physical Chemistry B*, 2007, **111**, 13765-13774.
25. T. G. A. Youngs, J. D. Holbrey, M. Deetlefs, M. Nieuwenhuyzen, M. F. C. Gomes and C. Hardacre, *Chemphyschem*, 2006, **7**, 2279-2281.
26. M. Schulein, *Journal of Biotechnology*, 1997, **57**, 71-81.
27. S. D. Mansfield and R. Meder, *Cellulose*, 2003, **10**, 159-169.
28. P. Bernfeld, *Methods in Enzymology*, 1955, **1**, 149-158.

## **APPENDIX B: COFACTOR STABILITY IN ORGANIC-AQUEOUS SOLVENTS**

### **INTRODUCTION**

Enzymatic catalysis is gaining popularity as an everyday processing option in a variety of industries. OATS is a facile process that allows enzymes to be used with hydrophobic substrates in an industrially-feasible system. While our group has already demonstrated its effectiveness for simple lipase reactions, we recognize that industry will need a more robust system for many desired reactions. One of the most challenging aspects for OATS is to incorporate reactions requiring cofactors. The stability of cofactors in organic solvents, however, is not well understood. Before the OATS system can be designed to optimize cofactor regeneration, a further study of cofactor behavior in organic solvents is needed. This appendix examines the stability of nicotinamide cofactors in several organic solvents compatible with OATS.

### **BACKGROUND**

#### **Benefits of Biocatalysis**

Biocatalysis has significant advantages over traditional chemical pathways including high substrate specificity, ambient reaction conditions, and process sustainability. Since enzymes are capable of catalyzing many reactions in a single step, some of which are achievable only through multiple steps in traditional chemical synthesis, biocatalysis can also provide a more efficient manufacturing process.<sup>1</sup> Enzymatic catalysis offers other tangible benefits including decreasing waste, minimizing

energy use, and diminishing the need for toxic compounds. Despite these advantages, enzymes also have several drawbacks. The operating conditions must be mild, the process solvent must include a substantial amount of water for enzymatic activity, and many target substrates and/or products are insoluble in aqueous reaction media.<sup>2</sup>

The latter issue has been addressed in several ways. Enzymes can be immobilized to improve their stability, but the resulting biphasic system has intrinsic inter-phase mass-transfer limitations.<sup>3</sup> The immobilization process also tends to reduce the activity by restricting enzyme access to the substrate and by enzyme leaching from the solid support. Some alternative solvents have been examined, including supercritical fluids and ionic liquids.<sup>4</sup> These monophasic systems, however, are often impractical due to insufficient enzyme recovery and recycle and/or complicated product purification.

### **Organic-Aqueous Tunable Solvents (OATS)**

With these inherent system limitations, there is an apparent need for novel, sustainable technologies capable of promoting biocatalysis. New processes being developed need to meet two important goals: potential loss in enzymatic activity must be minimized and a wider variety of substrates must be compatible. One system capable of achieving these goals is Organic-Aqueous Tunable Solvents (OATS). This alternative, sustainable process system suitable for biocatalysis has been examined by collaboration between our research group and the research group of Andreas Bommarius. OATS uses CO<sub>2</sub> as a switch to split a monophasic organic-aqueous mixture into separate phases. Since the homogeneous reaction phase contains both organic solvent and water, hydrophobic substrates have enhanced solubility. Hydrophobic substrates can thus be accessed by enzymes easily, significantly improving the reaction rate in pure water.

Several organic solvents have been used in the OATS process including (1,4)-dioxane, acetonitrile, THF, acetone, and ethyl acetate.<sup>5</sup> This versatility allows the chemical properties of the system to be tuned depending on the desired enzymatic reaction.

The initial monophasic mixture is optimized for enzymatic activity and substrate solubility, providing homogeneous catalysis. The organic solvent, buffer salt, and buffer concentration can all be tuned to optimize the reaction. When the reaction is complete, the addition of CO<sub>2</sub> partitions the enzyme into the aqueous phase and the product into the organic phase. This heterogeneous separation is a facile way to recover and recycle the enzyme, significantly lowering processing costs. After the product is isolated from the organic phase, the organic solvent can also be recycled to reduce waste. Figure B.1 illustrates the process schematic.

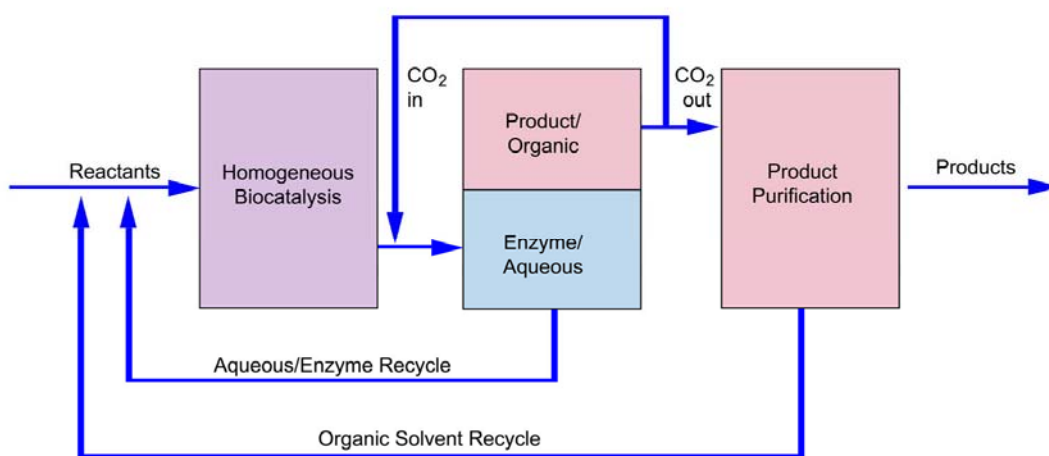


Figure B.1: OATS process schematic as depicted by E. Hill.<sup>6</sup>

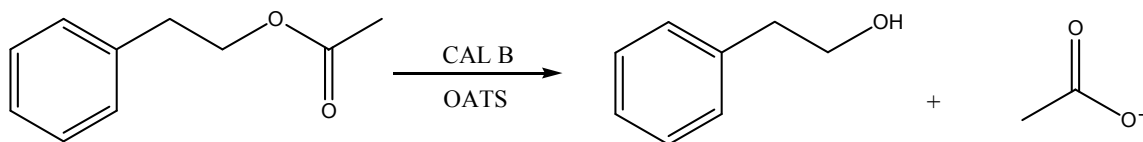


Figure B.2: Model reaction for CAL B ester hydrolysis.

Previous research demonstrated that OATS is a successful system for lipase-catalyzed ester hydrolysis. Our collaboration has shown that *Candida antarctica* lipase B (CAL B) can hydrolyze 2-phenylethyl acetate to 2-phenylethanol and acetate in the OATS system. This reaction is illustrated in Figure B.2. By adding a sodium phosphate buffer to the initial (1,4)-dioxane/water (40/60%) solvent, the OATS process was able to provide nearly five-times the yield of the traditional dioxane biphasic system used for this reaction. The salt buffer is needed to maintain pH in the optimal range, which otherwise would lower significantly by the carbonic acid formed as CO<sub>2</sub> dissolves into the water. Additionally, the enzyme was able to be recycled six times without significant loss in enzymatic activity.<sup>1</sup>

The OATS system has also been effectively demonstrated for chiral reactions. Both the pharmaceutical and agricultural industries are interested in the production of single enantiomers to use as intermediates or precursors. In order to establish the OATS system as a viable process for chiral resolution, the selective CAL B ester hydrolysis of *rac*-1-phenylethyl acetate to (*R*)-1-phenylethanol and (*S*)-1-phenylethyl acetate was chosen as a model reaction. The reaction is shown in Figure B.3. For this hydrolysis, the reaction medium consisted of 30% dioxane and 70% water. The enantiomeric excess (ee) of the reaction was greater than 99% both before and after the CO<sub>2</sub>-induced separation.

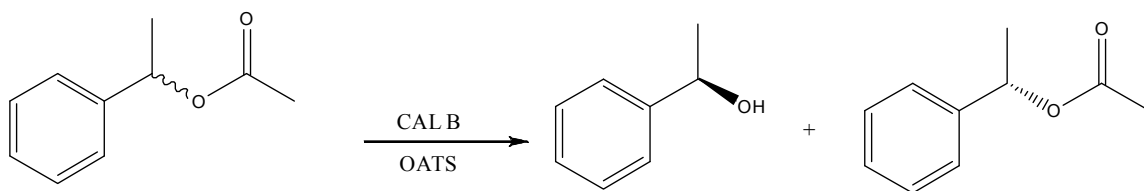


Figure B.3: Model chiral reaction for CAL B ester hydrolysis.

There are two major goals to achieve with the OATS system in order to enhance its versatility. The first goal is to successfully run pertinent reactions not catalyzed by lipases. Currently, both confirmed enzymatic OATS reactions have used lipase, which is among the most robust class of enzymes. An important step would be demonstrating that OATS can support a more pharmaceutically-relevant enzyme. The second goal is to run more complex enzymatic reactions, most notably reactions involving cofactors.

### Enzymatic Cofactors

Cofactors, sometimes called coenzymes, are nonprotein components such as metal ions and organic molecules that are needed for proper enzyme function. Generally, enzymes are bound to their natural cofactors; synthetic substitutes, which can be manufactured much cheaper, will not work properly.<sup>2</sup> When designing an enzyme-catalyzed process requiring cofactors, they must either be regenerated or continually added stoichiometrically to the system.

There are several advantages to regenerating cofactors rather than adding them stoichiometrically. Most importantly, the majority of cofactors are expensive, and continuously adding another expensive reagent is prohibitive to industrial-scale enzymatic reactions.<sup>7</sup> Additionally, the equilibrium position of the reaction can be

positively influenced by the cofactor, shifting the equilibrium to favor the product. From a downstream processing viewpoint, regenerating cofactors removes the accumulation of side-products, which facilitates the final separation of product from process stream.<sup>8</sup>

The nicotinamide cofactors NAD<sup>+</sup> (nicotinamide adenine dinucleotide) and NADP<sup>+</sup> (nicotinamide adenine dinucleotide phosphate), with the reduced forms NADH and NADPH, are some of the most widely needed cofactors. The structures of NAD<sup>+</sup> and NADH are depicted in Figure B.4. They are essential for enzymatic reactions requiring the removal or addition of hydrogen, such as reactions catalyzed by oxidoreductases.<sup>2</sup> One of the most established way to regenerate NAD(P)H is by combining the desired enzymatic reaction with a second one: the dehydration of glucose-6-phosphate by glucose-6-phosphate dehydrogenase.<sup>7</sup>

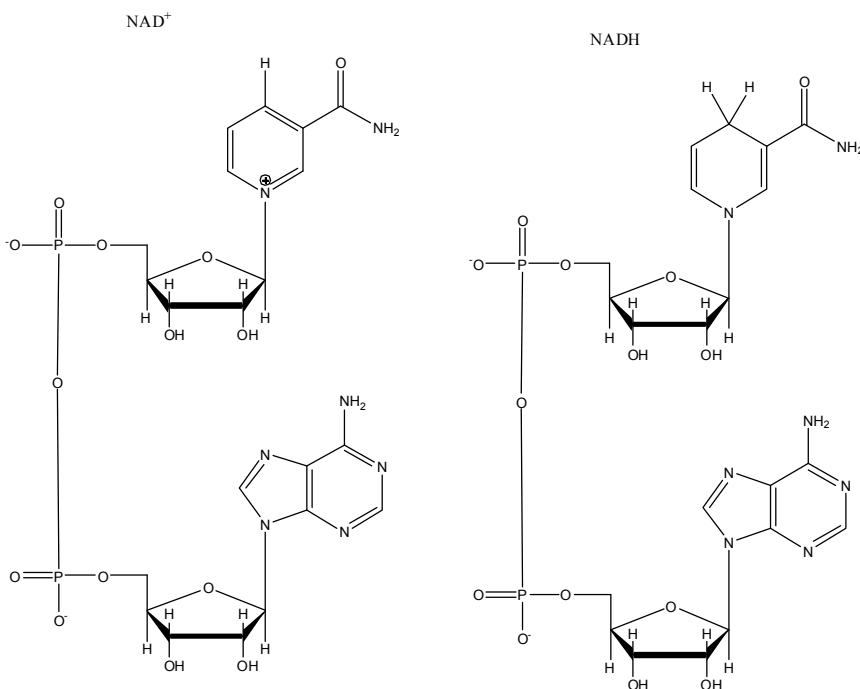


Figure B.4: Structures of the nicotinamide cofactors NAD<sup>+</sup> (left) and NADH (right).

## OATS with Cofactors

One previous attempt was made to demonstrate that the OATS system is compatible with enzymatic reactions requiring cofactors. Merck and Co., Inc. asked our research groups to use OATS for the ketoreductase reaction and cofactor regeneration scheme shown in Figure B.5. Merck had been running the reaction in 10% THF, but thought our system might provide more satisfactory results. Research began by investigating the effects of salt concentrations, organic concentrations, and CO<sub>2</sub> pressure on the system. A closer look at the reaction revealed that the system was not homogeneous, but rather formed a slurry under the aforementioned conditions. Initial experiments indicated that (1,4)-dioxane was a better organic solvent for this reaction, so the solvent was switched. Even under the improved processes conditions, however, the activity of KRED 101 and GDH 103 was greatly reduced after prolonged exposure to the (1,4)-dioxane buffered solution.

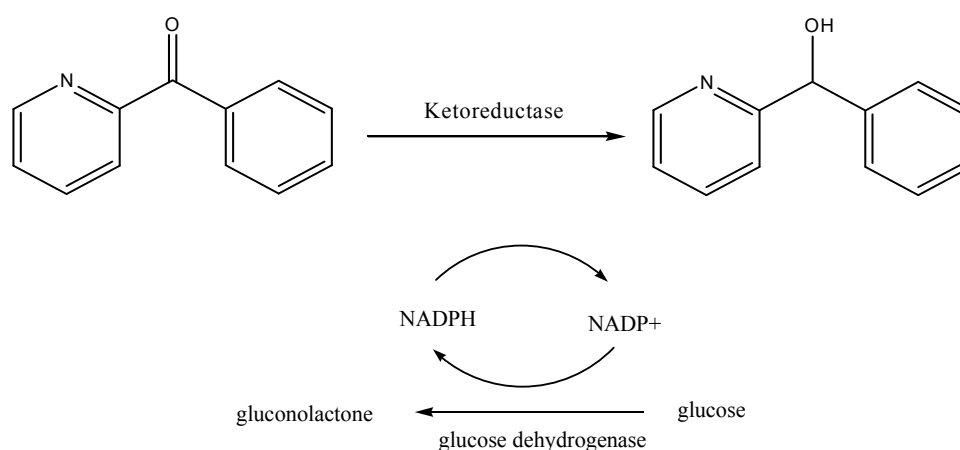


Figure B.5: Ketoreductase reaction of 2-benzoylpyridine (2BP) to phenyl-pyridin-2-yl methanol (PPM) using KRED 101, coupled with GDH 103 to regenerate the cofactors.



The conversion was so low, it was apparent that the system was facing several challenges. Since the dioxane system was homogeneous, it was unlikely that transport was the limiting factor. The next most probable complication involved the stability of the cofactors NADPH and NADP<sup>+</sup> in the mixed organic-aqueous solvents.

### **Cofactor Stability**

The stability of cofactors in aqueous solvents has been studied for decades since an enzymatic system should be designed to optimize performance of both enzymes and cofactors. Generally, NAD(P)<sup>+</sup> is stable under acidic conditions while NADP(H) is stable under basic conditions.<sup>8</sup> NADH is known to undergo acid-catalyzed hydration, which eventually transforms it into a cyclic ether. Conversely, NAD<sup>+</sup> not only reacts with hydroxide ions, but is also susceptible to the enzymatic addition of nucleophiles.<sup>7</sup> Additionally, some studies have shown that NADH is significantly more stable than NADPH under similar conditions. At 30 °C and pH 2 - 4.5, NADPH was found to degrade nearly 80% faster than NADH.<sup>9</sup> In order to optimize an enzymatic system requiring cofactors, it is necessary to understand the degradation kinetics of both the reduced and oxidized forms of the cofactor. Otherwise, one cofactor form might be completely degraded and the system would subsequently fail.

Previous research was undertaken in our lab to determine the stability of the nicotinamide cofactors NADH and NADPH in three mixed organic-aqueous solvents: acetonitrile, dioxane, and isopropanol (IPA). The aqueous buffer used in this experiment was 4-(2-hydroxyethyl)-1-piperazineethanesulfonic acid (HEPES, 100 mM). The cofactors were placed in the various mixed solvents and the change in concentration was detected via UV for several hours. The results are summarized in Table B.1.

Table B.1: Results of cofactor stability studies completed by Liz Hill using UV spectrometry (results not published).

<b>Organic Solvent</b>	<b>Cofactor</b>	<b>K</b>	<b>t<sub>1/2</sub> (hr)</b>
100 mM HEPES	NADPH	3.33E-04	34.7
40% Dioxane	NADPH	5.00E-03	2.3
50% ACN	NADPH	2.00E-04	57.8
50% IPA	NADPH	1.27E-04	91.2
100 mM HEPES	NADH	1.00E-04	115.52
40% Dioxane	NADH	3.33E-03	3.47

Several important conclusions were drawn from these studies. First, it became readily apparent that the UV spectrometric method was not sufficient for these experiments. It was obvious for several reasons. First, the rate and half-life could not be determined for NADH in either acetonitrile or isopropanol because the concentration appeared to be increasing with time. This suggests some sort of solvent interference is occurring with the analytical technique. Additionally, these results imply that NADPH is more stable in 50% mixtures of ACN/HEPES and IPA/HEPES than in HEPES alone. Although not impossible, these results would be unexpected if true.

In order to understand better solvent effects and cofactor stability, Liz recommended that future cofactor stability studies be analyzed via another method. Cofactor stability has been studied by a variety of methods over the past several decades. Although UV spectrometry and HPLC are popular analytical methods in cofactor research,<sup>7, 9-11</sup> many recent studies have utilized capillary electrophoresis (CE) for cofactor analysis.<sup>12, 13</sup> Since CE has been effective for this type of study before, it was decided to use CE for the analysis.

## Capillary Electrophoresis

Capillary electrophoresis is an analytical technique used most often for the separation of biomolecules or chiral molecules. It separates molecules based on their mass-to-charge ratio, typically in a silica capillary with an inner diameter between 20 and 200  $\mu\text{m}$ .<sup>14</sup> The capillary is filled with an electrolyte, often a buffered aqueous solution, and an electric field is applied across the capillary to induce migration of the charged species. The buffer chosen to induce the separation is referred to as the background electrolyte. The outside of the silica capillaries is usually coated with some type of polymer, significantly enhancing the overall stability of the capillary, which can break easily due to its small diameter. The inside of the silica capillaries are often kept uncoated, but can also be chemically treated, or capped, to enhance the separation.

The uncoated silica capillaries are the most common to work with since they are cheaper and easier to prepare. The inner walls of uncoated capillaries are negatively charged due to the presence of silanol groups, a chemical state that is usually enhanced by treating the capillary with a basic solution (often NaOH) before beginning the desired analysis. The reproducibility of experimental results is strongly influenced by the consistency of the charge on the capillary walls.<sup>15</sup> Many capillary electrophoresis methods involve rinsing the capillary with a dilute NaOH solution between experimental runs in order to maintain this charge, although this is not always necessary.

The electrolytes in the buffer separation solution are attracted to the negatively charged capillary wall, forming an additional electrical layer. Once the electric field is applied across the capillary, the cations in this layer flow towards the cathode, producing a bulk flow of buffer in that direction called the electroosmotic flow.<sup>14</sup> The

electroosmotic flow thus forces all chemical species in the capillary to flow towards the cathode regardless of their specific charge. These species will move at different rates based on their mass and charge, providing a separation technique and giving each molecule a specific migration time dependent on the exact system parameters including background electrolyte, pH, and voltage applied.

UV-Vis is the most common detection method used in conjunction with capillary electrophoresis. A window is usually burned, by laser or flame, into the polymeric coating of the silica capillary, providing an optically transparent surface. As the chemical species migrate past the window, the UV absorbance is obtained. It is important to note that since the capillary itself is the detection cell, the path length (50-100)  $\mu\text{m}$  is significantly less than traditional UV detection.

Capillary electrophoresis has been used for decades to study cofactors. Nicotinamide cofactors have been studied in CE in a variety of buffer systems including sodium phosphate, 3-morpholinopropane-1-sulfonic acid (MOPS), and tris (hydroxymethyl) aminomethane (Tris) have been studied.<sup>13, 16</sup> To our knowledge, however, no literature exists that examines the stability of cofactors in mixed organic-aqueous solvents such as those used in the OATS system. This appendix describes the progress achieved in the investigation of cofactor stability in organic-aqueous solvent mixtures by CE.

## **EXPERIMENTAL**

### **Materials**

#### Buffers

All buffers for this experiment were used as received from the supplier. They include 3-morpholinopropane-1-sulfonic acid (MOPS, Sigma, minimum 99.5% titration), sodium phosphate (BDH, monobasic, monohydrate crystals, ACS grade), sodium citrate (Sigma, tribasic dihydrate, ACS grade, 99.9%) and tris (hydroxymethyl) aminomethane (Tris, BDH, ACS grade). The buffers were titrated to the desired pH by hydrochloric acid (VWR,  $6.000 \pm 0.030$  N or Alfa Aesar, 1.0 N) and sodium hydroxide (VWR,  $10.00 \pm 0.05$  N or Ricca Chemical Company, 0.100N). Deionized water ( $\text{diH}_2\text{O}$ ) was obtained from the filter in the Bommarius lab. Acetonitrile (Sigma-Aldrich, CHROMASOLV Plus, for HPLC, >99.9%) was degassed under  $\text{N}_2$  or argon before use, as were all buffers for the organic-aqueous studies.

#### Cofactors

NADH (Calbiochem, disodium salt) and  $\text{NAD}^+$  (Sigma,  $\beta$ -nicotinamide adenine dinucleotide) were used as received.

#### Internal Standards

All internal standards for this experiment were used as received from the supplier. They include nicotinamide (Sigma), thiourea (Sigma-Aldrich, ACS grade reagent), 4-picoline (Aldrich, 99%), vanillin (Aldrich, 99%), and anisole (Aldrich, 99%).

## Capillary Electrophoresis

All experiments were run on a Beckman-Coulter PA 800 capillary electrophoresis instrument. The capillaries were standard synthetic unfused capillaries coated with a polyamide (Polymicro Technologies, 75  $\mu\text{m}$  ID, 365  $\mu\text{m}$  OD). The capillaries were cut from a spool and windows were burned in the lab. Each capillary was conditioned using 1 M NaOH (J.T. Baker, made from pellets, 98%),  $\text{diH}_2\text{O}$ , and running buffer. The capillary was kept cool by recirculating capillary cartridge coolant (Beckman-Coulter, perfluorinated fluid).

## **Method**

### Capillary Conditioning

Before use, a conditioning method was run 3-4 times through a new capillary. The method involved initially rinsing with  $\text{diH}_2\text{O}$  for 1 min at 20 psi, followed by 1 mM NaOH for 5 min at 20 psi, and then finished with running buffer for 10 min at 20 psi. Once the conditioning was complete, the standard analytical method was run 5-20 times until the elution of the analyte peaks had stabilized. The standard method involved rinsing the capillary with  $\text{diH}_2\text{O}$  for 2 min at 20 psi, followed by injecting the sample at 0.5 psi for 5 seconds, and finally applying voltage (15-28 kV) for 10 minutes while recording the data.

### Cofactor Preparation

Stock solutions of the cofactors, in the appropriate aqueous buffers, were prepared before the start of every experiment. Any stock solution not used was kept in the 4  $^{\circ}\text{C}$  freezer, and occasionally used various tests to optimize the CE conditions and methods.

The stock solutions were typically 8-10 mM solutions. The appropriate dilutions were made in order to have the cofactor samples at the proper concentration. For most studies, the initial cofactor concentration was 1 mM.

Internal standards were used during most experiments to help reduce the CE error from the injection sample size. A stock solution of internal standard in the appropriate aqueous buffer was made once. In order to have a useful peak size, the cofactor concentration was kept at 400  $\mu$ M.

For the final set of studies, each cofactor sample of interest was made 5 times. The extra samples were sealed with regular GC vial caps and kept in the CE for temperature control. The samples were then switched every 12-18 hours in order to keep the sample volumes as constant as possible.

### Stability Studies

Samples were prepared in GC vials in 1 mM concentration, usually with an internal standard also included. For the aqueous buffer studies, the samples were placed in the CE and left throughout the course of the experiments. For the organic-aqueous mixture, samples were switched out with identical sealed samples (made at the same time) every 12-18 hours.

## RESULTS AND DISCUSSION

### Cofactor Stability in MOPS pH 7.0

The first buffer tested, 3-morpholinopropane-1-sulfonic acid (MOPS), was chosen for several reasons. Although 4-(2-hydroxyethyl)-1-piperazineethanesulfonic acid (HEPES) was the buffer most effective in the OATS system, it was not suitable for this cofactor stability study because it co-eluted with the analytes, distorting the peak signal. MOPS had been used previously in literature cofactor stability studies and can buffer in the appropriate pH range, so it was used instead.

Before the first stability studies were run, a calibration curve was developed in order to ensure the experimental concentrations were in the linear range. As can be seen in Figure B.6, the absorbance of NAD<sup>+</sup> is completely linear between 125  $\mu$ M and 1 mM. These results confirmed that 1 mM was an appropriate initial cofactor concentration. Additionally, the linear results established that the Beckman-Coulter instrument was again working properly after some repairs had been made. For separation of the NAD<sup>+</sup> calibration curve, and for subsequent MOPS experiments, a separation voltage of 28 kV was used. The cofactor peaks were analyzed at 254 nm.

After the calibration curve was constructed, the next step was to determine the stability of NAD<sup>+</sup> in 100 mM MOPS pH 7.0. A 1 mM solution of NAD<sup>+</sup> was sampled every 20 minutes for several hours. Although the average NAD<sup>+</sup> concentration did not change during this time, the individual measured concentrations varied by as much as 10%. This variation is depicted in Figure B.7. Since the most likely cause of the variation was an inconsistent injection volume, at this point we decided to use an internal standard for all subsequent experiments.



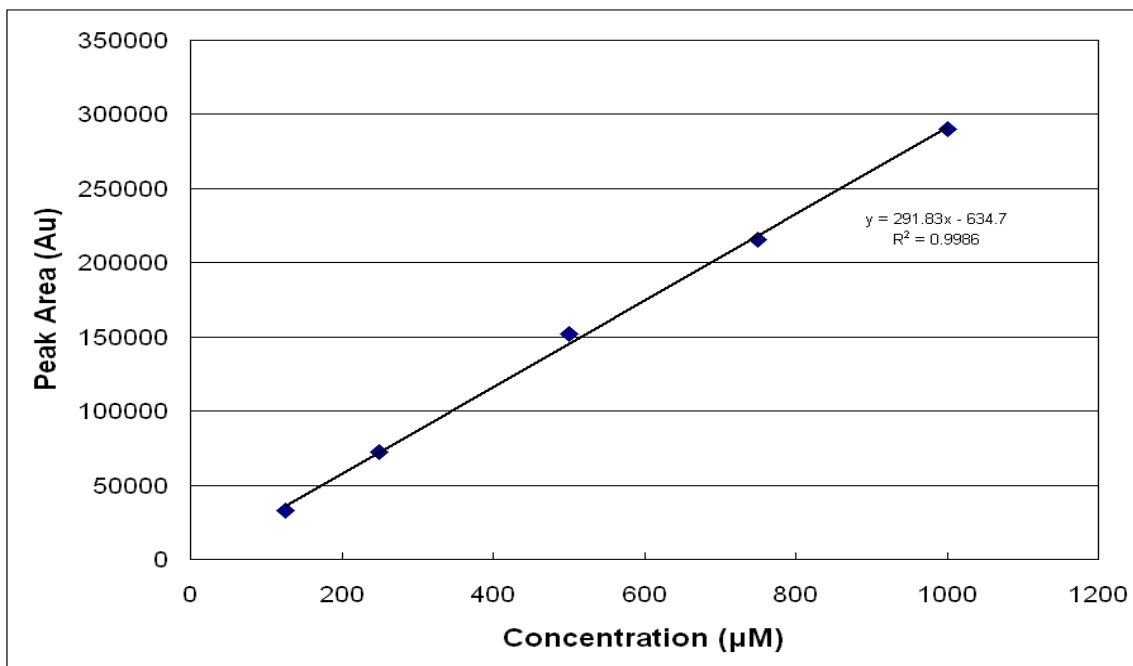


Figure B.6: Calibration curve of NAD<sup>+</sup> in 100 mM MOPS pH 7.0 (254 nm). Concentrations range from 125 µM to 1 mM.

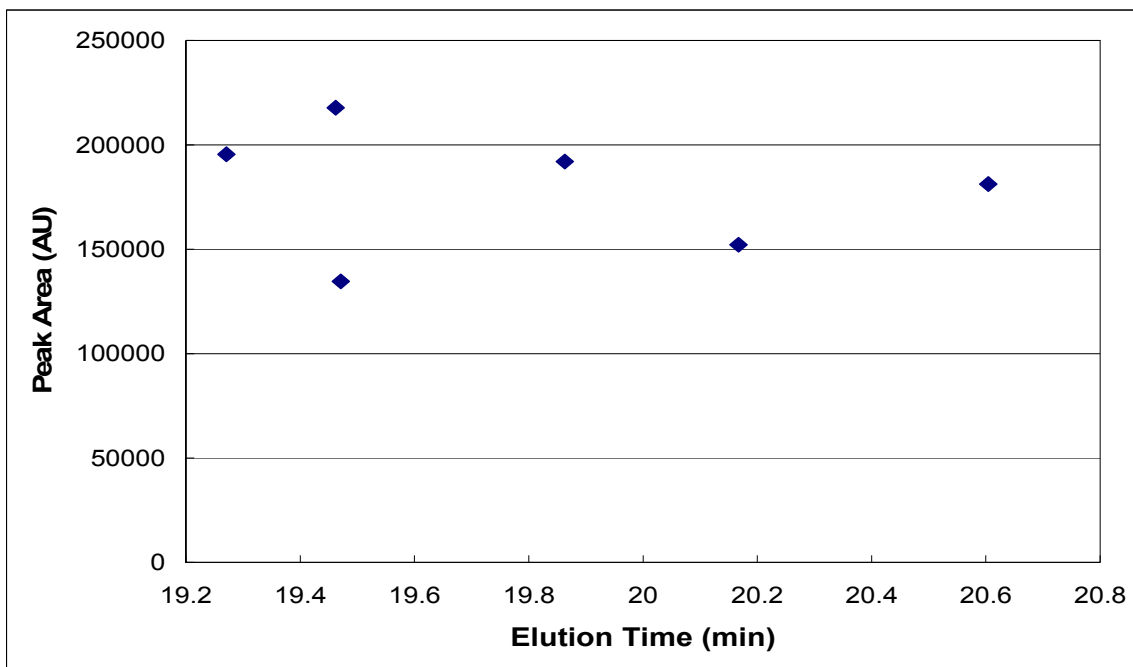


Figure B.7: Variation in peak area observed for NAD<sup>+</sup> in 100 mM MOPS pH 7.0 (254 nm). The data shows six subsequent samples taken within a 2 hour time span.

We recognized that the presence of an internal standard could affect the cofactors' stability, so an effort was made to use compounds similar in structure. The first internal standard studied was nicotinamide. Internal standards need to have two important properties: they must be completely stable in the aqueous buffer, and they cannot elute at the same time as the analytes of interest. In order to examine the stability of nicotinamide in 100 mM MOPS pH 7.0, a sample of 1 mM NAD<sup>+</sup>/400 μM nicotinamide was placed in the CE and analyzed. Three days later, the sample was analyzed again. The elution time of the nicotinamide peak shifted by nearly 8 minutes, suggesting that nicotinamide was not an appropriate internal standard.

The next internal standard examined was 4-picoline. A clear stock solution was made in 100 mM MOPS pH 7.0 buffer. Three days later, the solution had turned green, so the internal standard was never thoroughly tested on the CE. Thiourea was then examined as a possible internal standard after a suggestion made by Wai Keen Chung, a graduate student at Rensselaer Polytechnic Institute (RPI) who regularly uses CE in his research. Although we realized that thiourea would probably affect cofactor stability more than nicotinamide, the stability in MOPS was the more important issue at this point.

Samples were taken over a week period of time, and the thiourea concentration and elution time remained constant. Further studies concluded that having the internal standard significantly improved the consistency of the analysis. Without the internal standard, the relative standard deviation (RSD) of the peak areas varied between 6-8% for each experiment. When the internal standard was used to correct the areas, however, the RSD lowered to 2-4% for most experiments.

A sample of 1 mM NAD<sup>+</sup>/400  $\mu$ M thiourea was prepared and analyzed every few hours for a three day period of time. After the correction from the internal standard, it became obvious that NAD<sup>+</sup> was completely stable over a 3 day period of time. We continued to analyze the sample every day for 3 more days without any concentration change. Thus we concluded that NAD<sup>+</sup> is stable in 100 mM MOPS pH 7.0.

Studies were next done to determine the stability of NADH in 100 mM MOPS pH 7.0. A 1 mM NADH/400  $\mu$ M thiourea sample was analyzed every 20 minutes over 12 hours. The stability was determined by taking the ratio of the peak areas of NADH and thiourea, and analyzing it over time. The results are shown in Figure B.8. The experiment was not carried out long enough to determine order, as this data roughly fits zero, first, and second order plots. It did suggest, however, that our methods were effective enough to move forward with the project. Some experiments were also run in 50 mM MOPS pH 7.0, with little difference noticed in the preliminary studies.

At this point, another important decision was made. The MOPS separation buffer had been discoloring significantly if used for more than two samples, requiring the buffer to be changed constantly. The discoloration was most likely due to an oxidation/reduction reaction occurring when the voltage was applied to the buffer. In order to mitigate this issue, it was decided to switch the running buffer to phosphate buffer (pH 7.8). This buffer had been used in previous attempts to study cofactor stability in organic-aqueous mixtures by Liz Hill.

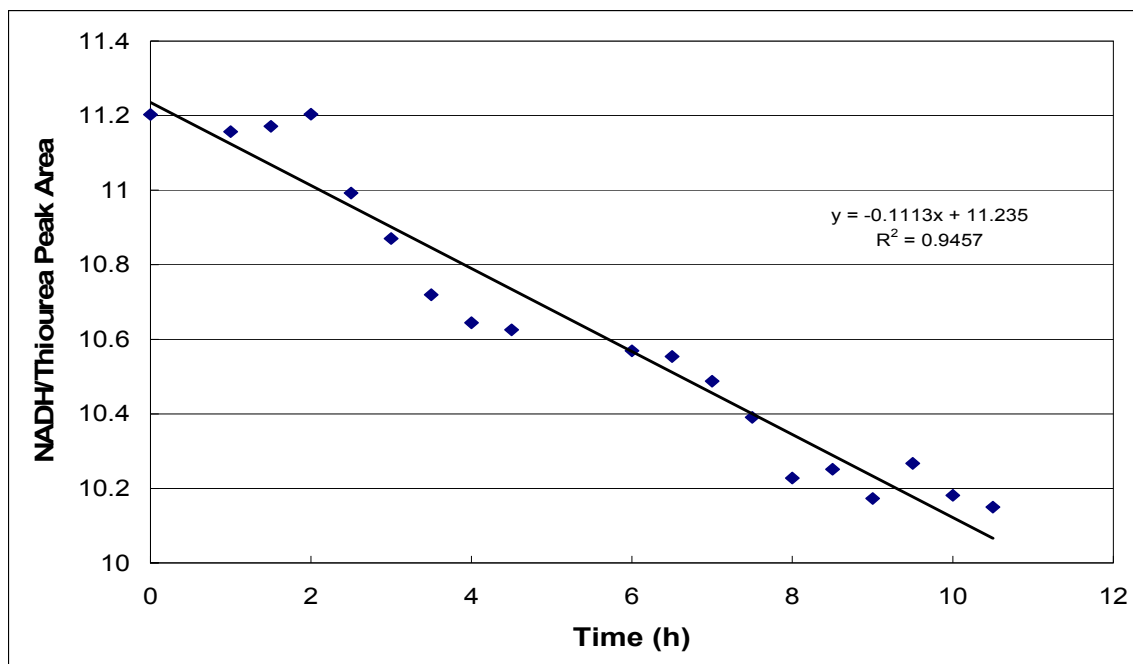


Figure B.8: Change in the ratio of NADH to thiourea over time.

### Cofactor Stability in Phosphate Buffer pH 7.8

After switching buffers, it was important to determine first that the method would efficiently separate NADH and NAD<sup>+</sup>. A sample of 1 mM NAD<sup>+</sup>/1 mM NADH/400 μM nicotinamide, in 100 mM phosphate pH 7.8, was run through the CE using the same method as before. The current maxed out almost immediately though, suggesting that the applied voltage (28 kV) was too high for this separation buffer. The phosphate buffer concentration was halved to 50 mM, and the separation voltage was thus lowered to 20 kV for most experiments. The sample was run again, with a substantial separation between the NAD<sup>+</sup> and NADH peaks. The results are shown in Figure B.9.

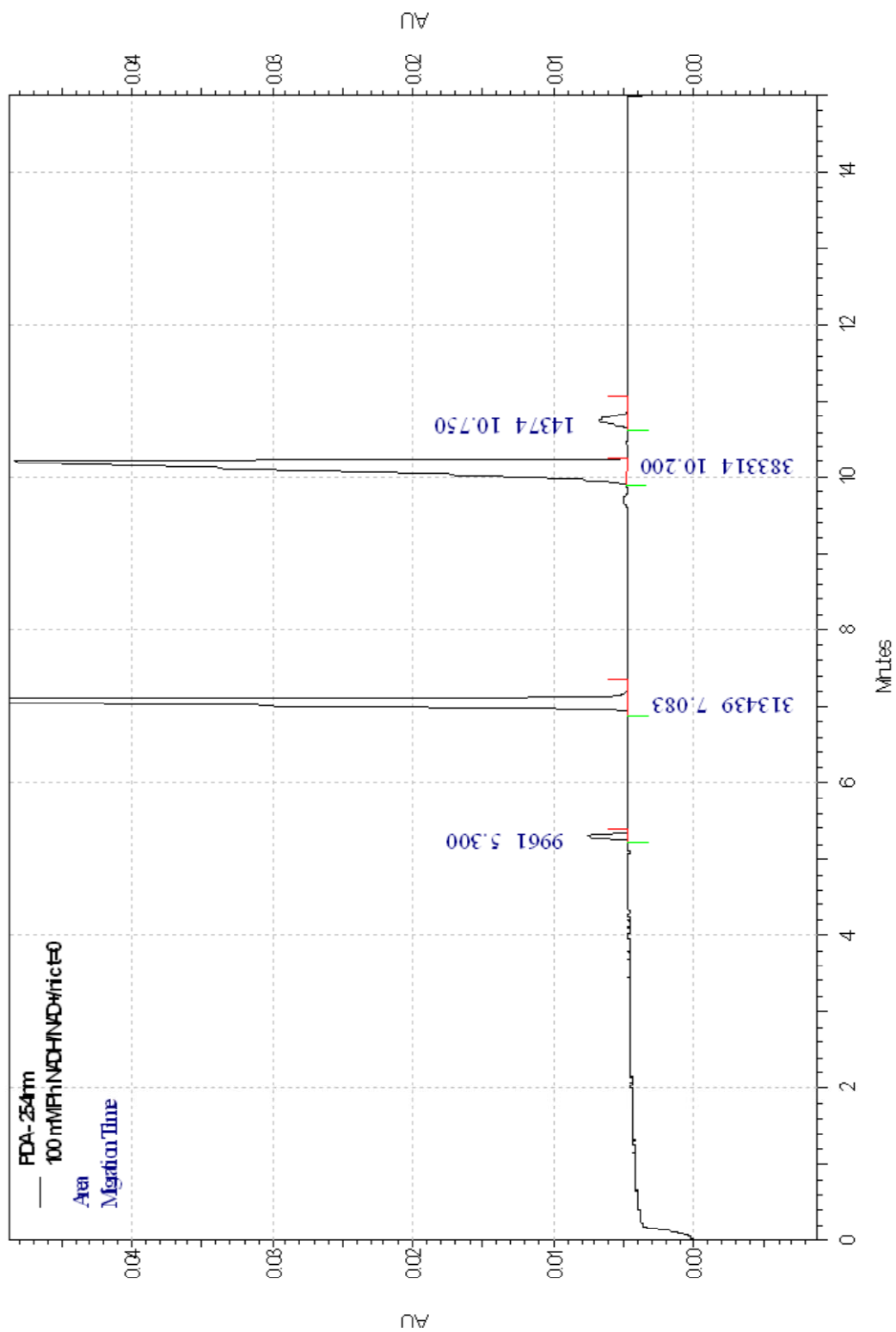


Figure B.9: Separation of nicotinamide, NAD<sup>+</sup>, and NADH in 50 mM phosphate pH 7.8 (254 nm) using 20 kV applied voltage.

These results were promising, so another stability study of NADH and NAD<sup>+</sup> was conducted in 50 mM phosphate pH 7.8. Nicotinamide (200 μM) was added as an internal standard, although having a higher concentration would have made it more accurate. Additionally, it was determined that nicotinamide is not stable in 50 mM phosphate pH 7.8 at room temperature. Thus the following stability results did not consider the internal standard concentration, making the results less accurate than those reported earlier.

The experimental results for the decomposition of NAD<sup>+</sup> over time are shown in Figure B.10. Similarly, the decomposition of NADH over time is shown in Figure B.11. The data is not accurate enough to determine the degradation order for either cofactor, but the results do clearly indicate that NAD<sup>+</sup> is significantly more stable than NADH under these experimental conditions.

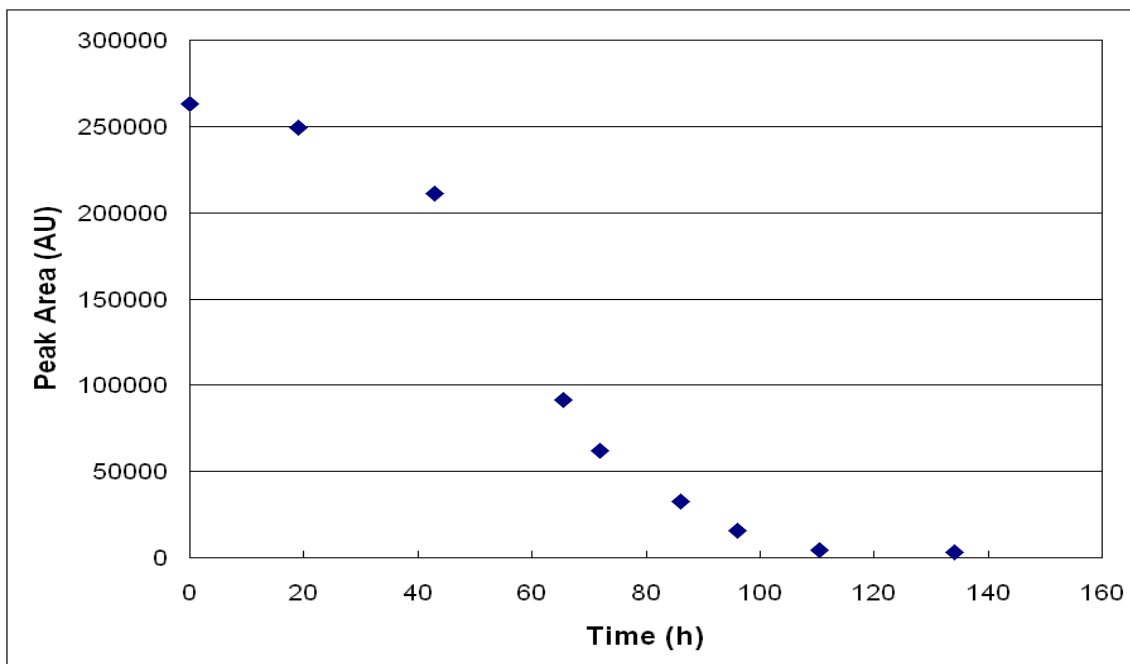


Figure B.10: Decomposition of NAD<sup>+</sup> over time (50 mM phosphate pH 7.8, 25 °C).

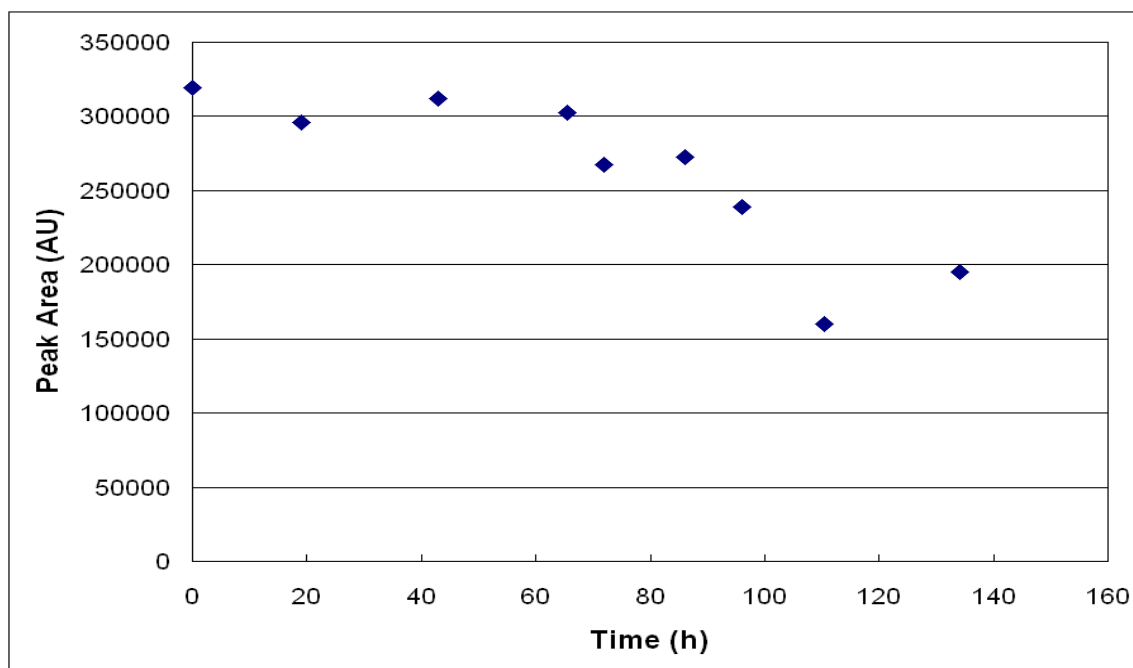


Figure B.11: Decomposition of NADH over time (50 mM phosphate pH 7.8, 25 °C).

The experiments were never repeated to provide more accurate results because the primary goal had been to determine whether or not phosphate would be an appropriate buffer for experiments using organic-aqueous mixtures. The above results, however, did suggest that the methodology and experimental conditions were sufficient enough to study the mixed organic-aqueous solvents of interest to the OATS system. One other important piece of information was learned during these experiments. The NADH degradation products began to overlap with the NADH product over time, making it difficult to accurately identify the peaks. Thus, for all subsequent experiments, it was decided to monitor NADH at 340 nm and NAD<sup>+</sup> at 254 nm.

### **Cofactor Stability in a Acetonitrile / Phosphate Buffer pH 7.8 Mixture**

With the promising results from the phosphate only study, an experiment was run to study the stability of NAD<sup>+</sup> in a 50/50 vol mixture of acetonitrile (ACN) and 100 mM phosphate pH 7.8. Combining these two solutions provide an overall 50 mM buffered solvent. For the first experiment, the final apparent pH (9.3) of the sample obtained by mixing the solvents was not adjusted.

Difficulties with this study became apparent during the first experiment. The applied voltage (20 kV) initially created a 70  $\mu$ A current in the system. Once the sample was injected, however, the current immediately dropped to 0  $\mu$ A. The experiment was repeated 3 times with the same result, suggesting that the phosphate separation buffer could not maintain a current when the sample in ACN/phosphate was injected. A dioxane/phosphate mixture was also tested to see if the problem was solely due to acetonitrile. The current also dropped with dioxane, suggesting it was the presence of the organic solvent causing current issues. A series of tests were thus run to improve the analytical method.

The factors examined during the course of these tests were separation buffer salt, separation buffer pH, and applied voltage. In all previous experiments, the separation buffer (either MOPS or phosphate) was the same buffer used in the cofactors samples. At this point, however, it was decided to try other salts commonly used as separation buffers. Since these salts were not of interest to the OATS system, the cofactor samples continued to be prepared in a 50/50 mixture of ACN and 100 mM phosphate buffer pH 7.8. Only the separation buffer was changed.



The separation buffer salt proved to be the most important factor. A variety of buffers were tried, including MOPS, phosphate, citrate, Tris-HCl, a mixture of ACN/phosphate, and a mixture of ACN/tris. The first three buffers had either been used previously or were suggested by Dr. Bommarius. Tris-HCl and higher pHs were tried after a review of the literature that also used ACN in the CE.<sup>17</sup> The pH of the separation buffer was varied between 7.0 and 10.0 depending on the buffer. Despite all of the options tried, the only separation buffer that maintained the current and allowed for observation of the cofactor peak was Tris-HCl. Both pH 8.5 and pH 9 were attempted, with pH 8.5 proving to be the better separation buffer.

The electropherogram depicted in Figure B.12 is the result using Tris-HCl pH 8.5 as the separation buffer. As can be seen, the peaks are significantly broader than those observed for samples not containing ACN. The nonideal peak shape made using an internal standard even more important.

Finding an appropriate internal standard, however, proved to be another challenge. Thiourea does not elute under the new analytical conditions, so a different internal standard needed to be found. Nicotinamide was retested, but proved unstable in the ACN/phosphate mixture. Vanillin was also tried, but it co-eluted with NAD<sup>+</sup>, making it an unsuitable choice. At this point, we have yet to identify an internal standard that is stable under the experimental conditions and suitable for analysis in samples containing ACN.

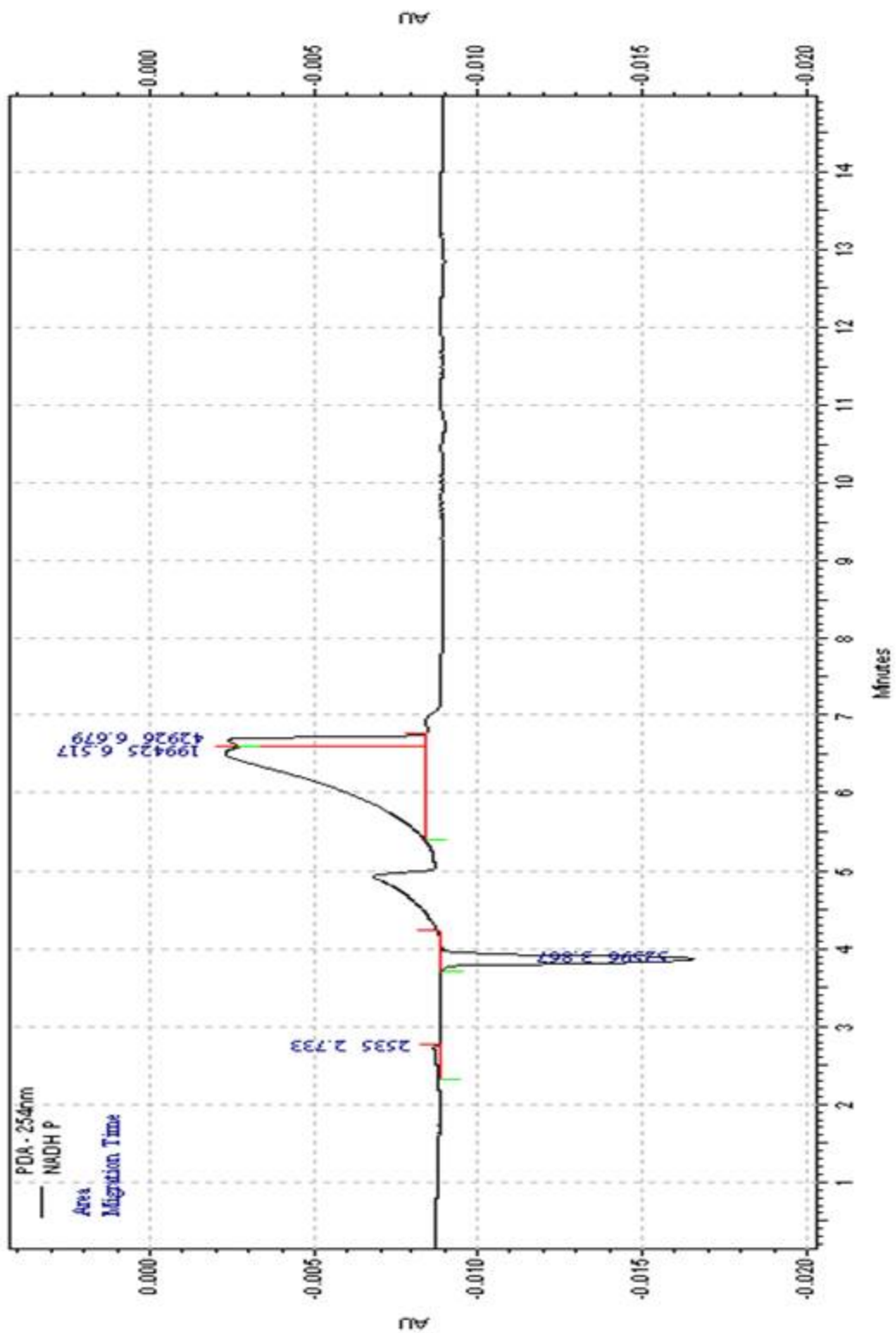


Figure B.12: Electropherogram of NAD<sup>+</sup> in a 50/50 vol mixture of acetonitrile (ACN) and 100 mM phosphate pH 7.8.

Since a suitable internal standard could not be found, one final set of experiments was run to determine if the accuracy could be improved by modifying the CE method. The Beckman-Coulter CE is capable of injecting the sample by three paths: pressure injection, electrokinetic injection, and a vacuum injection. Three identical samples were prepared and each was tested using one of the injection methods over the course of several hours. None of the three injection methods provided completely accurate data. Of the three injection methods, however, it was apparent that electrokinetic injection is the least reliable one. Both pressure and vacuum injection gave similar results, suggesting that the pressure injection used for all of the reported studies was sufficient.

## **CONCLUSIONS**

The overall goal of this project was to determine the best experimental conditions for cofactor stability. Eventually, it was hoped to incorporate these conditions into the OATS process. Several difficulties arose during the course of the studies, however, and the final goal was never accomplished.

The Beckman-Coulter CE instrument had multiple mechanical issues that needed to be fixed during the course of the project. Although it now seems to be functioning properly, the analysis from multiple subsequent injections is not very consistent. This suggests that perhaps there is variation between the injection volumes of the samples. It is possible that a standard Beckman-Coulter kit would need to be purchased and used to determine if the injector was functioning properly.

Regardless of the injection variations, the current CE method is not appropriate for the studies of interest. The cofactor peaks are broad and difficult to separate, making proper identification and analysis complicated. Additionally, an internal standard has not been found that is suitable for both the experimental conditions and the analytical parameters. Without an internal standard, it is difficult to minimize the inherent error of the CE system.

Due to the above challenges, I would not recommend continuing this project in its current state. If a faculty member or graduate student at Georgia Tech, who is knowledgeable about CE, was able to contribute knowledge, then it would probably be worth reexamining the project. At this point, however, we do not have a thorough enough understanding of CE to optimize the method and gather the data needed to make useful conclusions for the OATS system.

## REFERENCES

1. J. M. Broering, E. M. Hill, J. P. Hallett, C. L. Liotta, C. A. Eckert and A. S. Bommarius, *Angewandte Chemie-International Edition*, 2006, **45**, 4670-4673.
2. K. Faber, *Biotransformations in Organic Chemistry*, Springer, London, 2004.
3. F. Franks, C. N. Pace, K. Wilson, R. M. Daniel, P. J. Halling, D. S. Clark and A. Purkiss, *Philosophical Transactions of the Royal Society of London Series B-Biological Sciences*, 2004, **359**, 1234-1235.
4. R. A. Sheldon, *Green Chemistry*, 2005, **7**, 267-278.
5. E. M. Hill, J. M. Broering, J. P. Hallett, A. S. Bommarius, C. L. Liotta and C. A. Eckert, *Green Chemistry*, 2007, **9**, 888-893.
6. E. Hill, in *School of Chemical and Biomolecular Engineering*, Georgia Institute of Technology, Atlanta, 2007.

7. C. H. Wong and G. M. Whitesides, *Journal of the American Chemical Society*, 1981, **103**, 4890-4899.
8. H. K. Chenault and G. M. Whitesides, *Applied Biochemistry and Biotechnology*, 1987, **14**, 147-197.
9. J. T. Wu, L. H. Wu and J. A. Knight, *Clinical Chemistry*, 1986, **32**, 314-319.
10. L. Rover, J. C. B. Fernandes, G. d. O. Neto, L. T. Kubota, E. Katekawa and S. H. P. Serrano, *Analytical Biochemistry*, 1998, **260**, 50-55.
11. K. A. Markham, R. S. Sikorski and A. Kohen, *Analytical Biochemistry*, 2003, **322**, 26-32.
12. R. Mertens, L. Greiner, E. C. D. van den Ban, H. B. C. M. Haaker and A. Liese, *Journal of Molecular Catalysis B: Enzymatic*, 2003, **24-25**, 39-52.
13. J. Zhang, Y. J. Lou, J. Hoogmartens and A. Van Schepdael, *Electrophoresis*, 2006, **27**, 4827-4835.
14. P. A. Mabrouk, Marzilli, L.A., and Bedard, P., *The Chemical Educator*, 1996, **1**, 12.
15. I. Beckman-Coulter, Capillary Electrophoresis: A Simple Technique, <http://www.beckmancoulter.com/resourcecenter/labresources/ce/cedefinitionmode.s.asp>.
16. M. Nesi, M. Chiari, G. Carrea, G. Ottolina and P. G. Righetti, *Journal of Chromatography A*, 1994, **670**, 215-221.
17. H. Yang, R. J. Zhang, Y. Y. Lu, B. X. Ye, Y. J. Wu and S. S. Zhang, *Chromatographia*, 2008, **68**, 122-127.

# **APPENDIX C: PRODUCTION OF HIGH VALUE-ADDED CHEMICALS FROM CARBOHYDRATES USING PIPERYLENE SUFLONE**

## **INTRODUCTION**

Carbohydrates are currently being studied not only as a feedstock for alternative fuels, but also for biomaterials and chemical intermediates. Although a wide variety of molecules have been targeted as useful, the processing of the carbohydrates is a significant challenge facing industry in the 21<sup>st</sup> century. Recent research has focused on the production of 5-hydroxymethylfurfural (HMF), a furan derivate that can be obtained via the acid-catalyzed dehydration of carbohydrates. HMF can then be used to manufacture many potentially useful compounds.

The high processing costs for the current production of HMF are mostly due to the difficult separation. Since the reaction is acid-catalyzed, using piperylene sulfone (PS) in this process can offer multiple advantages. As discussed in Chapter 3, adding water to PS creates the in-situ acid sulfurous acid. Additionally, the PS can be easily converted to its volatile components, facilitating the separation of the product from the process solvent. This appendix examines ongoing efforts in the group in studying the production of HMF and HMF-derived compounds in our tunable, switchable solvent PS.

## BACKGROUND

As mentioned, 5-hydroxymethylfurfural (HMF) is a furan derivative that can be obtained via the acid-catalyzed dehydration of carbohydrates. The reaction of fructose to HMF is illustrated in Figure C.1. It is an important target molecule for several reasons. HMF can be converted to 2,5-furandicarboxylic acid (FDCA), a possible replacement for terephthalic acid in polymer processes, by selective oxidation.<sup>1</sup> This reaction is depicted in Figure C.2. Additionally, disubstituted furan derivatives from HMF are used by the pharmaceutical industry. Finally, HMF can be a precursor for a variety of liquid alkanes (C<sub>7</sub>-C<sub>15</sub>), which can be considered as replacement fuels.<sup>2</sup> A chart of potential products derived from HMF is depicted in Figure C.3.

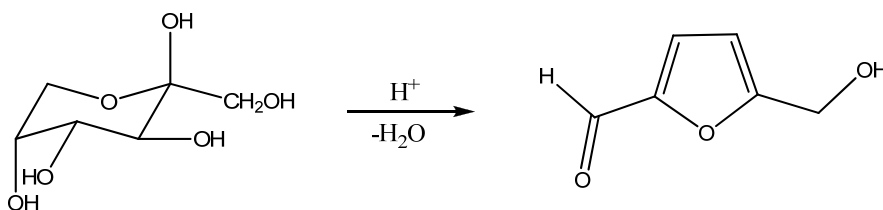


Figure C.1: HMF production from fructose.

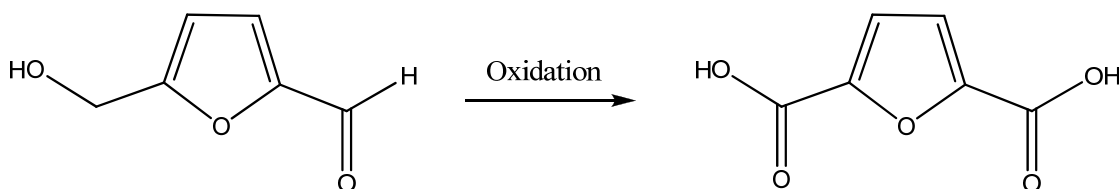


Figure C.2: Oxidation reaction of HMF to form to 2,5-furandicarboxylic acid.

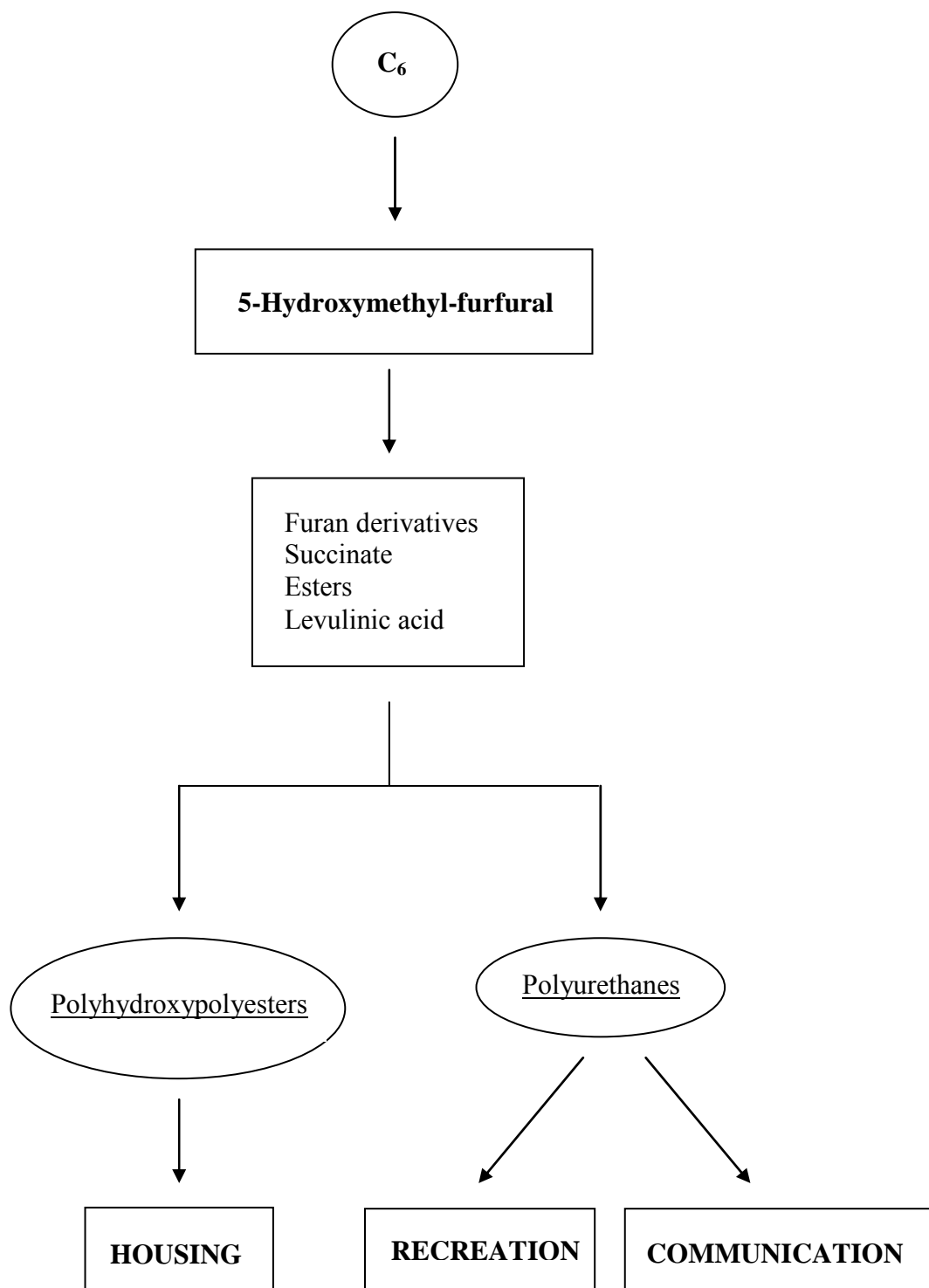


Figure C.3: Production of HMF derivatives from carbohydrate feedstock.



HMF is known to be produced from fructose, glucose, and the five-carbon sugar xylose. Traditionally, the highest yields for the conversion of HMF (>90%) can be achieved from fructose using high-boiling point organic solvents such as DMSO. DMSO prevents side reactions that lead to the production of levulinic acid and humans, increasing the yield of HMF.<sup>3</sup> This process, however, suffers from the energy intensive downstream separation.<sup>4, 5</sup> Although theoretically distillation could be used to separate HMF from the DMSO after production, the high reactivity of pure HMF leads to significant carbonization during distillation.<sup>6</sup> Distillation under reduced pressure has also been attempted in order to minimize the reactivity of HMF. The dehydration process, however, produces water which negatively impacts the vacuum capacity of the system. This makes vacuum distillation an even more expensive separation technique.<sup>7</sup>

The facile separation of the product from piperylene sulfone makes it an attractive solvent for this reaction. Since it is also a diprotic, apolar solvent, it was hypothesized that PS might also limit the side reactions of HMF during the reaction. Most current processes for the production of HMF use fructose as a feedstock, which has higher reaction rates and better selectivities than glucose.<sup>8</sup> Glucose is more readily available and thus would be a preferable feedstock from a cost perspective, so both carbohydrates were used as feedstock during the project.

## **EXPERIMENTAL**

### **Materials**

The following materials were used as received: fructose (Sigma, min 99%), glucose (D-(+)-glucose Sigma, 99.5%), and xylose (Sigma-Aldrich, Sigma ultra >99%). Piperylene sulfone was synthesized in our lab by the procedure explained in Vinci et al.<sup>9</sup> Argon gas (Air Gas, 99%) was used to decompose the PS after the reaction completed. Dichloromethane (BDH, ACS grade), ethyl ether (BDH, ACS grade), and chloroform (BDH, ACS grade) were used to extract product from the PS.

### **Methods**

Piperylene sulfone (1 mL), 0.1 mL H<sub>2</sub>O (10%), and carbohydrate feedstock (1 g) were placed in an oil bath heated at 80 °C under reflux for various time intervals. The reaction was stirred the entire time at 400 rpm. After the allotted time interval, the flask was removed from the oil bath. PS was removed overnight by both gentle heat and argon gas, or just heat, depending on the experiment. The samples for <sup>1</sup>H NMR and MS analysis were taken before removing any PS from the flask.

## **RESULTS AND DISCUSSION**

Fructose, glucose, and xylose were all used as feedstock for this reaction under various experimental conditions. Neither glucose nor xylose had any noticeable conversions under the conditions used. Fructose, however, did react to form a dark brown liquid.

## Fructose

### Initial Studies

The reaction mixture was analyzed via  $^1\text{H}$  NMR. Although the aldehyde functional group was observed as expected, the proton integration did not correlate with HMF. It was hypothesized that, under our experimental conditions, HMF was undergoing a condensation reaction with itself to form an ether. This reaction, which forms oxo-bis(5-methylfurfuraldehyde), is shown in Figure C.4.<sup>10, 11</sup> The condensation reaction is known in the literature, and the ether is often formed as a byproduct during HMF production. Since the ether is a more stable molecule under many reaction conditions. In order to corroborate the hypothesis, a sample was also sent to the MS lab. The MS (completed by ESI) results were consistent the the formation of oxo-bis(5-methylfurfuraldehyde).

### Product Analysis

Oxo-bis(5-methylfurfuraldehyde):  $^1\text{H}$  NMR ( $\text{CDCl}_3$ ) ppm: 9.42 (s, 2H, 2CH=O); 7.11 (d, 2H); 6.40 (d, 2H); 4.53(s, 4H,  $-\text{CH}_2\text{OCH}_2-$ )

MS (ESI): 235  $[\text{M}+1]^+$

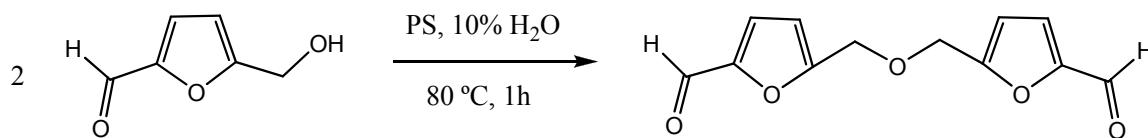


Figure C.4: Condensation reaction of HMF to form oxo-bis(5-methylfurfuraldehyde).

## Isolation Attempts

This product has not yet been isolated, so further analysis is not complete. Removing the PS by heat may have caused the oxo-bis(5-methylfurfuraldehyde) to decompose. Recent attempts were made to extract the product from PS using dichloromethane (DCM), ethyl ether, and chloroform, but the partition coefficients have not been high enough for a successful extraction. We are still investigating isolating the compound by decomposing the solvent under milder conditions.

## **CONCLUSIONS AND RECOMMENDATIONS**

The production of HMF from fructose was attempted in PS, a solvent similar to DMSO, but easier to remove. Although the formation of HMF in a pure form has not been observed, the condensation product of HMF, oxo-bis(5-methylfurfuraldehyde), has been identified in the reaction mixture. This product has not yet been isolated, but we are in the process of creating a separation scheme. Different isolation procedures are being tested and analyzed during this process.

Oxo-bis(5-methylfurfuraldehyde) is an interesting product in itself. It is a bifunctional bio-polymeric building block that could possibly be used to create a variety of bio-derived polymers.<sup>12</sup> Once the product has been isolated, some studies could be run to determine which polymers can be made, and what the properties of the polymers are. If any leads seem promising, we will consult with Dr. Charlotte Williams, a collaborator at Imperial College in London, England.

It is possible that further experimental condition modification will allow the formation of pure HMF. The primary goal of this project, however, was not to make HMF itself, but rather to make bio-derived building blocks. At this point, it seems this goal has been partially achieved. More work needs to be done to isolate and characterize before the project success can be fully determined.

## REFERENCES

1. T. Werpy and G. Peterson, 2004.
2. J. N. Chheda, G. W. Huber and J. A. Dumesic, *Angewandte Chemie-International Edition*, 2007, **46**, 7164-7183.
3. K. Nakamura and S. Morikawa, *Bulletin of Chemical Society of Japan*, 1980, **53**, 3705.
4. R. M. Musau and R. M. Munavu, *Biomass*, 1987, **13**, 67-74.
5. H. E. Vandam, A. P. G. Kieboom and H. Vanbekkum, *Starch-Starke*, 1986, **38**, 95-101.
6. J. N. Chheda and J. A. Dumesic, *Catalysis Today*, 2007, **123**, 59-70.
7. Y. Roman-Leshkov, J. N. Chheda and J. A. Dumesic, *Science*, 2006, **312**, 1933-1937.
8. B. F. M. Kuster, *Starch-Starke*, 1990, **42**, 314-321.
9. D. Vinci, M. Donaldson, J. P. Hallett, E. A. John, P. Pollet, C. A. Thomas, J. D. Grilly, P. G. Jessop, C. L. Liotta and C. A. Eckert, *Chemical Communications*, 2007, 1427-1429.
10. L. Cottier, G. Descotes, L. Eymard and K. Rapp, *Synthesis-Stuttgart*, 1995, 303-306.
11. C. Larousse, L. Rigal and A. Gaset, *Journal of Chemical Technology and Biotechnology*, 1992, **53**, 111-116.
12. D. Chundury and H. H. Szmant, *Industrial & Engineering Chemistry Product Research and Development*, 1981, **20**, 158-163.

# **APPENDIX D: OXIDATION OF CARBOHYDRATE STARTING MATERIALS TO GLUCARIC ACID AND OTHER TARGET OXIDATION PRODUCTS**

## **INTRODUCTION**

Petroleum supplies the world not only with transportation fuel, but also with a wide variety of commonly used materials. Biofuels made from lignocellulosic feed stock are gaining popularity as alternative fuel sources. It is also important to determine, develop, and optimize processes capable of making sustainable building blocks for biomaterials. Glucaric acid, created by the oxidation of glucose, is one of the renewable building blocks already identified as important in the field of biomaterials. Currently, however, there is no industrially-viable method for the production of glucaric acid from glucose. This chapter investigates the possibility of oxidizing carbohydrate starting materials with peroxycarbonic acid, which is formed from hydrogen peroxide and CO<sub>2</sub>.

## **BACKGROUND**

The United States depends on petroleum for more than just transportation fuel. Crude oil provides not only gasoline, but also is the base for lubricants, jet fuel, light carbon gas, plastics, dyes, solvents, and synthetic fibers.<sup>1</sup> In fact, it is the refining process, and the manufacturing of these byproducts into useful chemicals, that makes the production of gasoline so profitable. If biofuels are going to displace petroleum as a leading energy source, then it is imperative to develop economical means to create these additional products.

In 2004, the US Department of Energy released a list of the Top 12 Building Block Chemicals that can be derived from carbohydrates via chemical or biological conversion.<sup>2</sup> This list, which can be seen in Table D.1, identifies glucaric acid, also known as saccharic acid, as a target molecule required as a building block for new sustainable processes. It is most commonly produced from glucose by either direct oxidation using nitric acid<sup>3</sup>, or by catalytic oxidation using bleach.<sup>4</sup> The DOE is interested in glucaric acid for several reasons. There is a definite need in the polymer industry for nylons (polyhydroxypolyamides) created from sustainable resources, and glucaric acid has been identified as a possible starting material. It is also possible that glucaric acid can serve as a building block for a variety of branched polyesters. Finally, it is expected that glucaric acid will have interesting chelating properties for cations, making it a candidate for detergents and surfactants.<sup>2</sup>

Table D.1: Top 12 building blocks identified by the US DOE.<sup>2</sup>

<b>Building Blocks</b>
1,4 diacids (succinic, fumaric, and malic)
2,5 furan dicarboxylic acid
3 hydroxy propionic acid
aspartic acid
glucaric acid
glutamic acid
itaconic acid
levulinic acid
3-hydroxybutyrolactone
glycerol
sorbitol
xyolitol/arabinitol

The derivatives of glucaric acid, shown in Figure D.1, are also useful. For example,  $\alpha$ -ketoglucarates can also be building blocks for polymeric materials. While all of these uses are important, the actual technology developed to create glucaric acid efficiently and economically will have other applications. The US DOE has also identified that the oxidation of the 5-carbon sugars xylose and arabinose is an important future goal.<sup>2</sup>

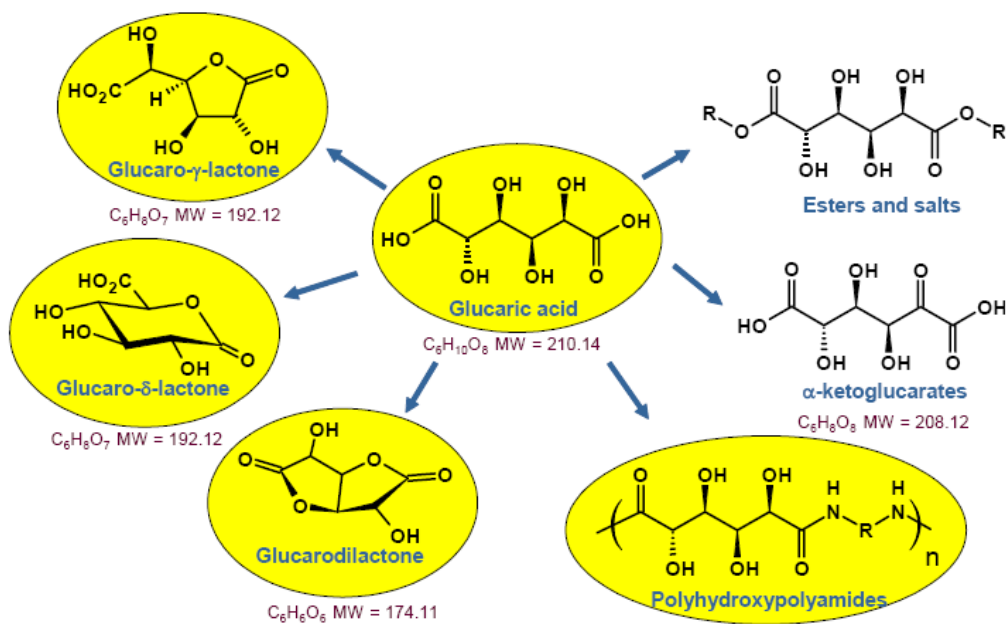


Figure D.1: Derivatives of Glucaric Acid.<sup>2</sup>



Although nitric acid oxidation is a possible pathway to glucaric acid, the subsequent neutralization and waste removal significantly adds to the overall cost of the process. Hydrogen peroxide, however, is cheap and readily available. More importantly, it decomposes to the benign products water and oxygen. Despite these advantages, the application of hydrogen peroxide to organic synthesis must overcome severe limitations. Usually additional catalysts must be added for activation of the hydrogen peroxide, or it must be converted to a more reactive peroxy acid.<sup>5</sup> The metal catalysts added to hydrogen peroxide are expensive, fairly unstable, and pose additional separation and recycling problems. Activation is usually achieved by forming peroxy acids in situ through the acid-catalyzed reaction of hydrogen peroxide and a carboxylic acid, which is typically reformed during the process and must be recycled or disposed.<sup>6</sup>

Our lab has had experience with the oxidation of various starting materials. We developed an epoxidation process several years ago that uses peroxycarbonic acid, the most simple activated hydrogen peroxide compound. The peroxycarbonic acid is generated by the addition of CO<sub>2</sub> in a reaction analogous to the formation of carbonic acid by combining water and CO<sub>2</sub>.<sup>5, 7</sup> The formation of peroxycarbonic acid can be seen in Figure D.2.

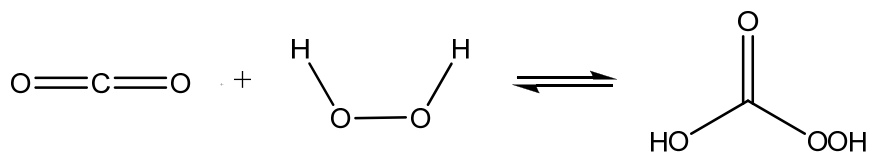


Figure D.2: Reactions of CO<sub>2</sub> and hydrogen peroxide.

Peroxycarbonic acid is unstable and has never been isolated in its pure form. Its presence, however, has been detected by several researchers via X-ray crystallography<sup>8</sup> and vibrational spectroscopy.<sup>9</sup> Our experimental results showed, however, that epoxidation of cyclohexene occurred only when CO<sub>2</sub> was added to activate the hydrogen peroxide; no product was formed without CO<sub>2</sub>. Improved product yield occurred upon the addition of NaHCO<sub>3</sub>, which likely ionizes the peroxycarbonic acid and shifts the equilibrium to favor the formation of more ionized oxidant.<sup>5</sup> This equilibrium can be seen in Figure D.3. It was determined that only a small amount was needed; more NaHCO<sub>3</sub> provided no substantial additional product yield. The final optimized reactant molar ratios of [cyclohexene:H<sub>2</sub>O<sub>2</sub>:H<sub>2</sub>O:NaHCO<sub>3</sub>:CO<sub>2</sub>] for the epoxidation of cyclohexene were [1:2.6:11.3:0.04:23.6] at 40 °C and 120 bar.<sup>5</sup> We expect the oxidation of glucose can also occur via peroxycarbonic acid. In order to test this theory, the optimized conditions above were used as a starting point with glucose replacing cyclohexene as the starting material.

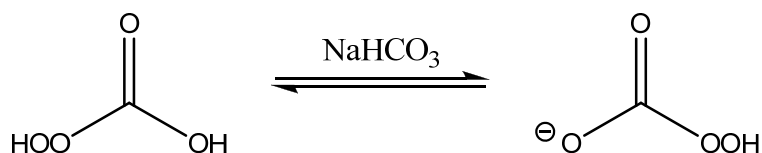


Figure D.3: Ionization Equilibrium of Peroxycarbonic Acid.

## **EXPERIMENTAL**

### **Materials**

All materials for this experiment were used as received from the suppliers. They include D-(+)-Glucose (Sigma, 99.5%), hydrogen peroxide (Sigma-Aldrich, 30% w/w with H<sub>2</sub>O), sodium bicarbonate (BDH, ACS grade), and carbon dioxide gas (Air Gas, SFE grade, 99.99%). For analytical purposes, deuterated water as purchased from Sigma-Aldrich.

### **Method**

A monosaccharide was weighed and placed in a saturator reactor. The appropriate molar ratios of hydrogen peroxide (30% w/w) and sodium bicarbonate were added along with a stir bar. The saturator was sealed with a nitrile rubber o-ring and placed on a stir plate set at 4000 rpm. A heating jacket run by a temperature controller was used to bring the saturator up to reaction temperature, and then control it for the duration of the experiment. The CO<sub>2</sub> gas was added by an Isco pump (set at constant pressure) after the saturator had reached the appropriate experimental temperature. Once the saturator reached temperature, experimental time began. After leaving the reactor running for the appropriate amount of the time, the heating jacket was turned off, the saturator removed from the jacket, and left to cool for 20 minutes. The reactor contents were then transferred to a vial for storage. All experiments were analyzed via <sup>1</sup>H-NMR.

## **RESULTS AND DISCUSSION**

### **Glucose Oxidation**

When removed from the saturator, the original glucose solution remained clear and was visibly unchanged. The  $^1\text{H}$  NMR confirmed that glucose did not react at 40 °C and 120 bars, even when allowed to react for over 24 hours. Thinking that perhaps the solution was too dilute, the first adjustment made was to double the concentration of glucose. This had no effect on the reaction. The reaction was next run at shorter times (between 2-6 hours) and analyzed. Again only glucose starting material could be seen in the  $^1\text{H}$  NMR. Increasing and decreasing the  $\text{CO}_2$  pressure also provided no change.

The temperature was increased in an attempt to facilitate the reaction. At 80 °C, the reaction had visibly darkened. The  $^1\text{H}$  NMR confirmed that glucose had reacted, but there were no peaks corresponding to glucaric acid. It is more likely that the glucose merely decomposed into a variety of decomposition products.

### **Additional Monosaccharide Oxidation**

The same experiment was repeated with three other monosaccharides: xylose, arabinose, and fructose. These monosaccharides were attempted in case any of them proved to be more susceptible to oxidation. Temperature, time, and pressure were all varied though the course of several experiments. Most experiments showed no change to the starting material when analyzed via  $^1\text{H}$  NMR.

The starting material always underwent physical change when heated to high temperatures. The  $^1\text{H}$  NMR analysis of these experiments, however, showed a mixture of products that could not be fully identified. It is unlikely, however, that the oxidation product was present.

## **CONCLUSIONS AND RECOMMENDATIONS**

This exploratory project briefly examined the possibility of using a sustainable in-situ oxidizing agent, peroxy-carbonic acid, to catalyze the oxidation of monosaccharides. The initial conditions tested were those optimized by a former member of the Eckert-Liotta research group. Several process parameters (temperature, time, and  $\text{CO}_2$  pressure) were also varied in an attempt to induce the oxidation reaction, with no success.

At the time of this project, the lab had no thorough analytical process other than  $^1\text{H}$  NMR to study the reactions. The lab now owns a Bio-Rad AMINEX-87H HPLC column that is capable of separating sugar degradation products. These experiments could be repeated and the resulting process sample could be analyzed more thoroughly to definitively ascertain whether or not any useful products were created by this process.

The general messiness of the  $^1\text{H}$  NMR spectra, however, suggests that even if a useful product were made, it would be difficult to separate from the rest of the process sample. At this point, the project was ended.

## REFERENCES

1. A. J. Ragauskas, C. K. Williams, B. H. Davison, G. Britovsek, J. Cairney, C. A. Eckert, W. J. Frederick, J. P. Hallett, D. J. Leak, C. L. Liotta, J. R. Mielenz, R. Murphy, R. Templer and T. Tschaplinski, *Science*, 2006, **311**, 484-489.
2. T. Werpy and G. Peterson, 2004.
3. C. L. Mehlretter and C. E. Rist, *Journal of Agricultural and Food Chemistry*, 1953, **1**, 779-783.
4. M. Ibert, F. Marsais, N. Merbouh and C. Bruckner, *Carbohydrate Research*, 2002, **337**, 1059-1063.
5. S. A. Nolen, J. Lu, J. S. Brown, P. Pollet, B. C. Eason, K. N. Griffith, R. Glaser, D. Bush, D. R. Lamb, C. L. Liotta, C. A. Eckert, G. F. Thiele and K. A. Bartels, *Industrial & Engineering Chemistry Research*, 2002, **41**, 316-323.
6. F. Ullmann, W. Gerhartz, Y. S. Yamamoto, F. T. Campbell, R. Pfefferkorn and J. F. Rounsaville, *Ullmann's encyclopedia of industrial chemistry*, VCH, Weinheim, Federal Republic of Germany ; Deerfield Beach, FL, USA, 1985.
7. R. E. Kirk, D. F. Othmer, J. I. Kroschwitz and M. Howe-Grant, *Encyclopedia of chemical technology*, Wiley, New York, 1991.
8. A. Adam and M. Mehta, *Angewandte Chemie-International Edition*, 1998, **37**, 1387-1388.
9. D. P. Jones and W. P. Griffith, *Journal of the Chemical Society-Dalton Transactions*, 1980, 2526-2532.

## **APPENDIX E: EXAMINING GAS-EXPANDED LIQUIDS AS A POSSIBLE LIGNOCELLUSIC PRETREATMENT**

### **INTRODUCTION**

The need for novel, sustainable lignocellulosic pretreatment methods was discussed in Chapter 2. Due to the substantial cost of downstream acid or base neutralization, designing an effective pretreatment method that uses a suitable in-situ catalyst could drastically improve the economics. Gas-expanded alcohols form alkylcarbonic acids upon the addition of CO<sub>2</sub>, a weak acid that could possibly promote hydrolysis of the lignocellulosic biomass.

Gas-expanded liquids also have good penetrating power, so this solvent has the potential to penetrate the rigid biomass matrix. Pure biomass contains a variety of extractive compounds such as phenols, fatty acids, and resins. These extractives can interfere with downstream processing, so there are advantages to finding a cost-effective pretreatment method that is also able to remove extractives.

This appendix discusses studies done to determine whether or not gas-expanded methanol has the capability to remove extractives and be an effective pretreatment method. Three types of biomass were studied: wood chips, corn stover, and switchgrass. Mass loss, identification of extracted compounds, and a chemical analysis of the remaining solid biomass were the indicators tested.

## BACKGROUND

### Gas-Expanded Liquids

Gas-expanded liquids (GXLs) are tunable solvents formed by dissolving a gas into an organic solvent under pressure. The result is a homogeneous mixture that can behave more like a liquid or a gas depending on the amount of gas dissolved in the solvent. GXLs are useful because they have better solvation properties than pure gases and better penetrating power than pure liquids. A qualitative comparison of GXLs to other solvents is illustrated in Figure A.1. By varying the amount of gas dissolved into the liquid, certain physiochemical properties, including density, dielectric constant, and polarity, can be tuned. Changes in both temperature and pressure can tune a GXL to obtain the desired solvent characteristics.<sup>1-3</sup>

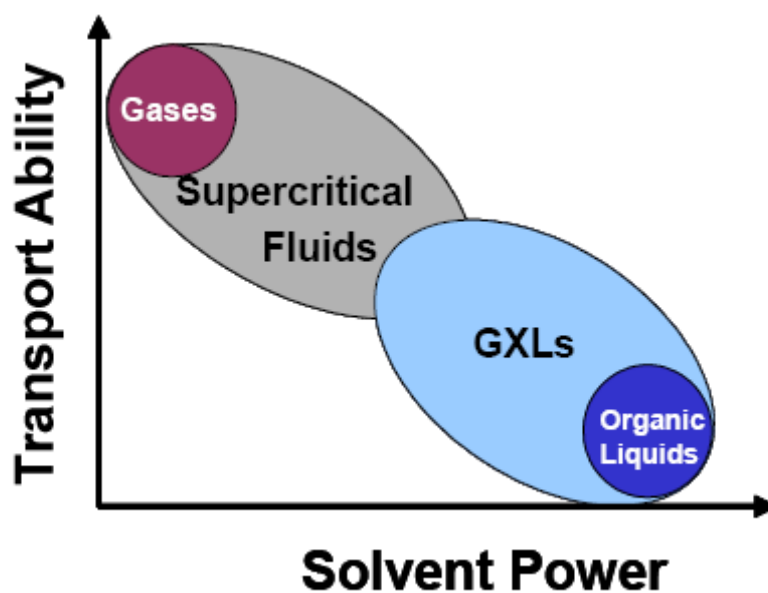


Figure E.1: Qualitative comparison of GXLs to other solvent classes.



CO<sub>2</sub> is often the gas used in GXLs because it is environmentally benign, relatively inert, and has a low critical temperature. It also has a substantial solubility in a variety of organic solvents (acetates, ethers, alcohols, and ketones) at only moderate pressures. Common organic solvents used previously in our lab for GXLs include tetrahydrofuran (THF), 1,4-dioxane, acetonitrile, and methanol.<sup>4-6</sup>

Methanol was the organic solvent chosen for several reasons. Most importantly, methylcarbonic acid is the strongest alkyl acid that can be formed by the addition of CO<sub>2</sub>, making it the most likely successful candidate for a strong acid-catalyzed process.<sup>7</sup> A schematic of the formation of alkylcarbonic acids can be seen in Figure A.2. Additionally, MeOH is inexpensive and lignin is reasonably soluble in it.<sup>8, 9</sup> As mentioned in Chapter II, an in-situ acid can catalyze the hydrolysis of lignocellulose and help fractionate the biopolymers. Additionally, the cellulose and hemicellulose can be converted into monosaccharides by acid-catalyzed hydrolysis.

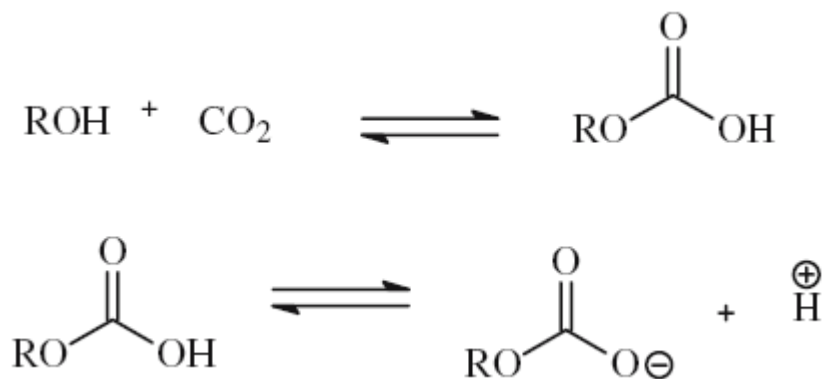


Figure E.2: Two equilibria reactions of alkylcarbonic acids.

Gas-expanded liquids represent a sustainable solvent class. Up to 80% of organic solvent can be replaced by dense-phase CO<sub>2</sub>, reducing waste.<sup>10</sup> CO<sub>2</sub> is environmentally benign, so the replacement also makes the process more environmentally favorable. Since the alkylcarbonic acids are in-situ acids, they are reversible by simple depressurization of CO<sub>2</sub>; no downstream neutralization and subsequent waste disposal is required.

### **Biomass Extractives**

Many small molecules are present in pure lignocellulosic biomass. Alditols, organic acids (aliphatic acids and aromatic acids), inorganic ions, and water insoluble materials are all included in the extractive material.<sup>11</sup> During traditional compositional analysis of lignocellulosic materials, the extractives are removed prior to processing by refluxing with hot water, ethanol, acetonitrile, or other organic solvents (NREL, TAPPI). Studies have shown that the presence of extractives in the pure biomass samples changes the amount of lignin and recoverable sugars detected, so a more accurate estimation of the lignin and carbohydrate concentration of pretreated samples can be obtained by first removing the extractives.<sup>12</sup>

Since ethanol is an appropriate solvent for removing extractives from biomass samples, it is reasonable that MeOH is also effective. GX-MeOH has the capability of removing even more extractives because it is a better penetrating solvent than pure MeOH. In addition to determining the effectiveness of GX-MeOH as a pretreatment method, this chapter will also evaluate the types of extractives that can be removed by GX-MeOH.

## **EXPERIMENTAL**

### **Materials**

All real biomass samples (pine chips, corn stover, and switchgrass) were obtained from the research group of Dr. Art Ragauskas (School of Chemistry and Biochemistry, Georgia Tech). To reduce the biomass size for experimentation, the biomass samples were ground with a Wiley mill and then sifted through a #4 sieve. Methanol (Sigma-Aldrich, HPLC grade), sulfuric acid (VWR, 98%, ACS grade), barium chloride titrate (VWR, 10%), acetone (VWR, ASC grade), sodium hydroxide (Fisher Scientific, pellets) were all used as received. Carbon dioxide gas (Airgas, SFC/SFE grade) was filtered prior to use.

### **Methods**

#### Parr Reactor

As in Chapter 3, the pressurized pretreatment experiments were completed in a 300 mL high-pressure Parr reactor (Parr Instrument Co.). The temperature and agitation were kept constant by a heating jacket and tachometer controlled by a Parr Model 4842 controller. CO<sub>2</sub> was added to the reactor with an Isco 500D syringe pump (set at constant pressure). The reactor pressure was also displayed on the Parr controller via a pressure transducer hooked into the reactor. The experimental setup of the Parr reactor can be seen in Figure 3.15.

### Analysis of Extractives from Wood Chips

Initial experiments involved treating woodchips, as received from the Ragauskas lab, with GX-MeOH to identify the extractives removed. 15 g of wood chips and 100 mL MeOH were added to the Parr reactor. The reactor was heated to 40 °C and pressurized with 17.4 bar CO<sub>2</sub>. The same amount of wood chips was treated with only MeOH in a different reactor. Both reactions were allowed to sit for three days. After the treatments were complete, the biomass was filtered and rinsed with MeOH until the filtrate ran clear. Samples were taken from the filtrate and analyzed with a Hewlett Packard 6890 Gas Chromatograph equipped with a Mass Selective Detector 5973 (GC-MS).

A third woodchip pretreatment was completed over three days at 40 °C and pressurized with 26.6 bar CO<sub>2</sub>. Samples were taken periodically throughout the experiment to determine how the extractive composition varied with time.

### Determination of Mass Loss

Biomass samples (wood chips, corn stover, and switchgrass) were weighed and placed in the Parr reactor. MeOH was measured and added to the reactor, and then the Parr was sealed shut by closing the bolts in a star pattern. The reactor was allowed to heat to the desired temperature, then the CO<sub>2</sub> was added.

After the desired reaction time, the heat was turned off and the CO<sub>2</sub> vented into a flask filled with MeOH. As before, the MeOH flask for this experiment was also designed to trap any possible volatile chemicals in the reaction mixture. The reactor was rinsed with MeOH and the slurry filtered via vacuum filtration. The biomass was rinsed with MeOH until the filtrate came off the biomass clear.

The biomass and filter were placed on a pre-weighed dish and allowed to dry for 2-3 days until the mass no longer dropped. The % mass loss was calculated by using the initial biomass weight and this final weight. The composition of the remaining solid was analyzed by a chemical method. The filtrate from the biomass was placed a crystallization dish and kept under the fumehood until all of the MeOH had evaporated, leaving dried extractives. <sup>1</sup>H NMR samples were made from the dried samples and analyzed by the research group of Art Ragauskas (Georgia Tech).

#### Biomass Composition Determination

The composition of the GX-MeOH pretreated biomass was analyzed using the procedure reported by Yang et al.<sup>13</sup> Untreated biomass was also analyzed by the same method for a comparison.

#### *Extractives*

The extractives were removed by Soxhlet extraction. The biomass sample was weighed and added to a Whatman 25mm x 88 mm cellulose thimble filter, and 60 mL of acetone (per gram of biomass) was added to the extraction chamber. The system was heated to 90 °C and allowed to reflux for 3 hours. The biomass sample was removed and dried until the weight remained constant. The acetone and extractives were transferred to a crystallization dish and the acetone was evaporated. The extractives were dried until a constant weight was obtained, and the mass balance closed within +/- 1%.

### *Hemicellulose*

150 mL of 0.5 mol/L NaOH solution was added for each g of the extractive-free biomass sample. The sample was then placed in 80 °C oil bath for 3.5 hours. The biomass sample was filtered and washed with distilled water until the approximate pH was 7.0. The sample was dried to a constant weight, and the difference between it and the initial weight was reported as the hemicellulose content.

### *Lignin and Cellulose*

30 mL of 98% sulfuric acid was added for each gram of the extractive-free, hemicellulose-free biomass sample. The solution was kept at ambient temperature for 24 hours, then placed in a 100 °C oil bath for 1 hour. The biomass was filtered and washed with distilled water until the sulfate ion in the filtrate was not detectable by a 10% barium chloride solution. The sample was dried to constant weight, and the recorded weight difference between it and the initial weight was recorded as the lignin content. The remainder was assumed to be the cellulose content.



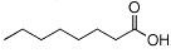


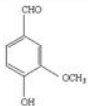

## **RESULTS AND DISCUSSION**

### **Woodchip Extractives**

Over 50 peaks were identified by the GC-MS from the wood chips pretreated by MeOH and GX-MeOH. A table of the peaks identified by the HP MS software library (with at least a 97% qualitative match) is depicted in Table E.1. Other peaks could possibly be identified, but pure components would have to be run for a comparison. The major classes of components were recovered: cyclic extractives, fatty acids, and resin acids. The peak areas in Table E.1 were compared on a solvent-free basis in order to

compare the recovered extractives as a percentage of the entire sample. The numbers give a rough comparison; a more accurate analysis could be completed by creating a calibration curve for each extractive component. This would be a time-consuming process, however, and not provide much additional information for our purposes.

Table E.1: Extractive components recovered from wood chips pretreated with GX-MeOH (40 °C, 17.4 bar, 3 days), MeOH only (ambient temperature and pressure, 3 days) and GX-MeOH (40 °C, 17.4 bar, 24 hours).

Component	Structure	% in GX-sample (solvent free basis) 3 days	% in BT sample (solvent free basis) 3 days	Average % in GX- sample 1 hr (solvent free basis)
a-pinene		1.2	3.6	0.5
b-pinene		0.3	1.5	0.2
octanoic acid (caprylic acid)		1.1	0.9	0.6
verbenone		0.5	0.5	0.3
nonanoic acid	 HO <sub>2</sub> C-(CH <sub>2</sub> ) <sub>7</sub> -Me	1.1	1.1	1.0
vanillin		0.2	N/A	0.4
tetradecanoic acid	HO <sub>2</sub> C-(CH <sub>2</sub> ) <sub>12</sub> -Me	0.2	N/A	0.7
hexadecanoic acid (palmitic acid)	HO <sub>2</sub> C-(CH <sub>2</sub> ) <sub>14</sub> -Me	5.0	5.6	4.2
9-octadenoic acid (oleic acid)	CH <sub>3</sub> (CH <sub>2</sub> ) <sub>7</sub> CH=CH(CH <sub>2</sub> ) <sub>7</sub> CO OH	9.9	11.5	9.0
resins*		31.6	24.7	14.2

Several of the recovered extractives have value. Two of the fatty acids, palmitic and oleic acids, are value-added products and can be used as, or to create, surfactants or lubricants.<sup>14, 15</sup> They could also be potential feedstocks for biodiesel or diesel additives.<sup>16</sup> Resin acids, such as those identified, are known to be toxic in pulp and paper waste streams.<sup>17</sup> Removing them via pretreatment, and possibly selling them for use in pesticides, could improve profits in a biorefinery. Other extractives, such as vanillin and pinenes, have value as flavoring agents and could also be sold.<sup>18</sup>

Comparing the actual percentages recovered suggest that GX-MeOH does not offer any advantages over just MeOH. Vanillin and tetradecanoic acid were not found in the MeOH only samples, while the pinenes had a higher concentration in the GX-MeOH samples. The other numbers are similar and are probably within experimental error. The qualitative amounts of extractives after only one hour of GX-MeOH pretreatment are also similar, with the exception of the resins. A closer look at the effect of the pretreatment over time is offered in Figure E.3. As can be seen, the percent of most extractives leveled off after only a few hours of pretreatment. This suggests that an effective pretreatment method could be developed that only requires a short amount of time, which could significantly lower processing costs in an industrial process.

<sup>1</sup>H-NMR samples of the extractives were also prepared in deuterated water. The samples were run by the Ragauskas lab, and the resulting spectra were returned to us without being analyzed. The spectra (not shown) had many peaks overlapping and provided little useful information. The lack of peaks in areas of the spectra, however, revealed that no aldehydes, aromatics, simple straight-chain alkanes, or cyclic alkanes were extracted from the biomass.



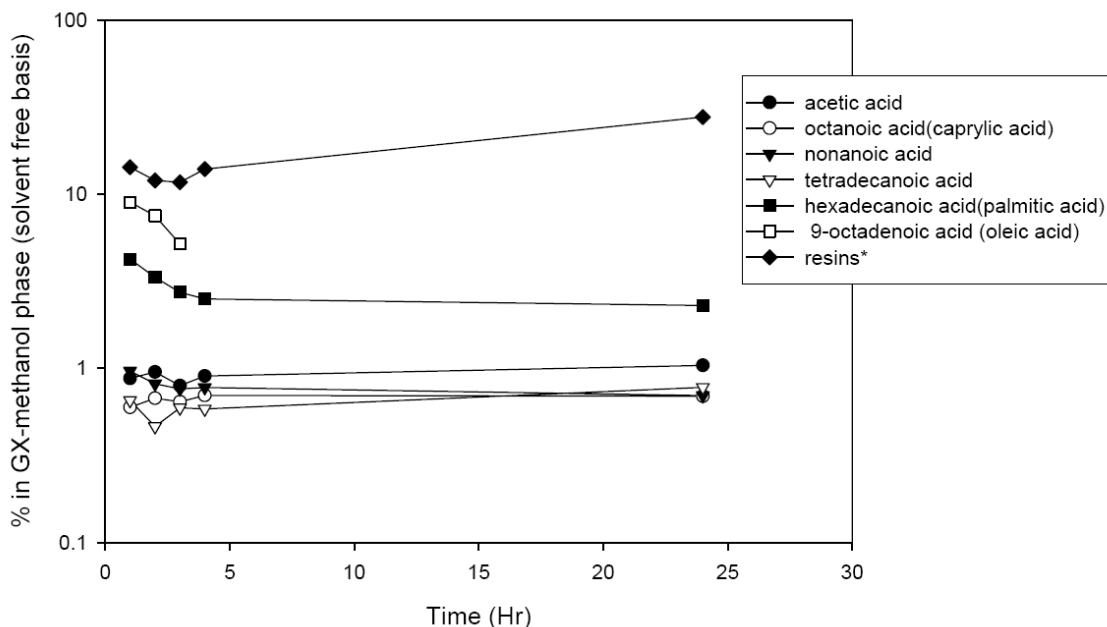


Figure E.3: Percentage of components over time extracted from wood chips by GX-MeOH (40 °C, 26.6 bar).

## Biomass Pretreatments

### Determination of Mass Loss

The mass percent lost during GX-MeOH pretreatment is shown in Figure E.4. These mass percents, however, were calculated by the initial weight of the biomass samples (not dried). This means that some mass removed is probably water existing within the lignocellulosic matrix. Thus it is difficult to understand from these results whether water, extractives, carbohydrates, or lignin were affected by the pretreatment methods. The significantly lower percentage of mass removed from the wood chips, however, may be due to the higher lignin content, which makes penetration more difficult. The compositional analysis of the residual solid biomass was determined by the methods described earlier to better delineate the mass results.

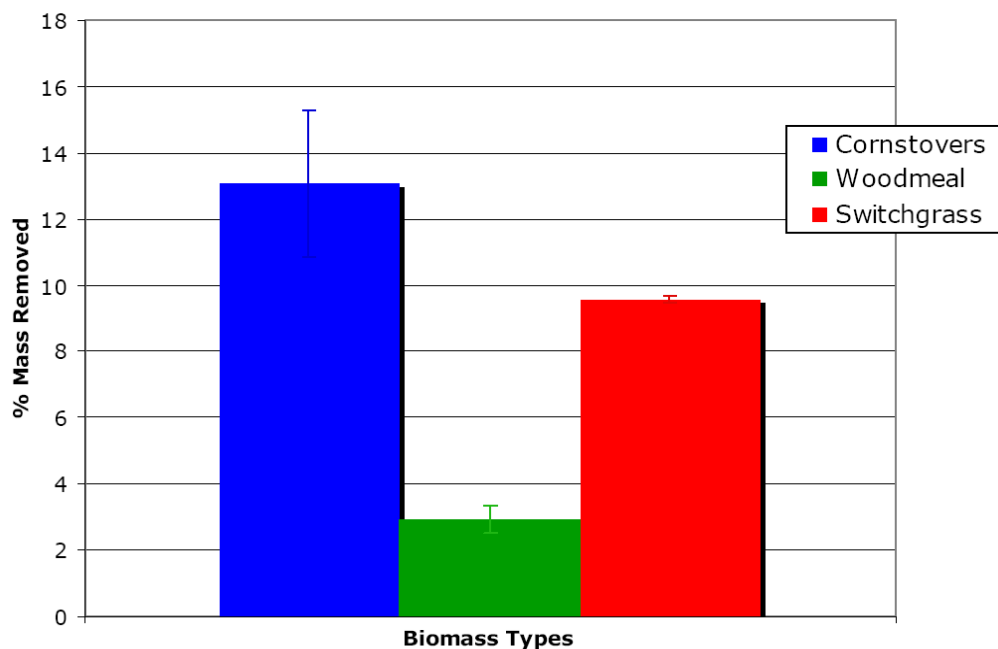


Figure E.4: Mass percent removed by GX-MeOH pretreatment for wood chips, corn stover, and switchgrass (60 °C, 30 bar, 24 h).

### Biomass Composition Determination

The results of the polymeric biomass compositions after no treatment, treatment with GX-MeOH (60 °C, 30 bar, 24 hours), and treatment with GX-MeOH (30 °C, 40 bar, 3 hours) are shown in Figures E.5 - E.7. The first important finding is that this chemical analysis method yields drastically different component percentages than those reported by Mosier et al., which are shown in Table E.2.

Table E.2: Dry weight composition (%) of selected lignocellulosic biomass feedstock as reported by Mosier et al.<sup>19</sup> *Note:* Numbers do not sum to 100% because minor components are not listed.

<b>Feedstock</b>	<b>Cellulose</b>	<b>Hemicellulose</b>	<b>Lignin</b>
Corn stover	37.5	22.4	17.6
Pine wood	46.4	8.8	29.4
Switchgrass	31.0	20.4	17.6

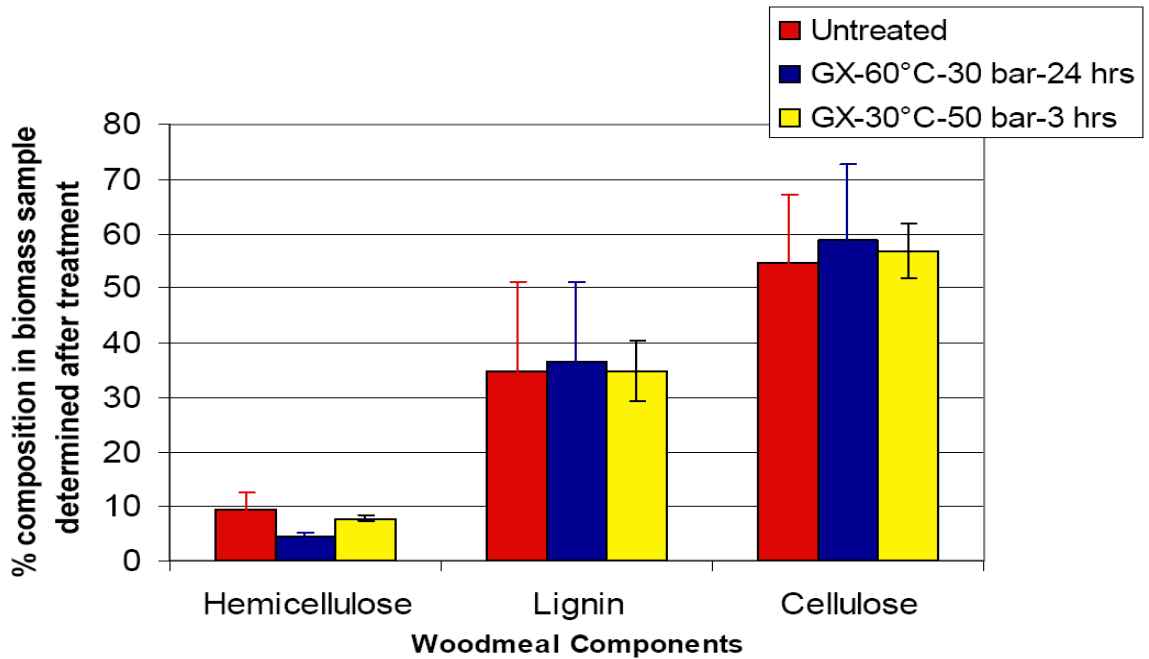


Figure E.5: Solid wood chip composition after no treatment, treatment with GX-MeOH (60 °C, 30 bar, 24 hours), and treatment with GX-MeOH (30 °C, 40 bar, 3 hours).

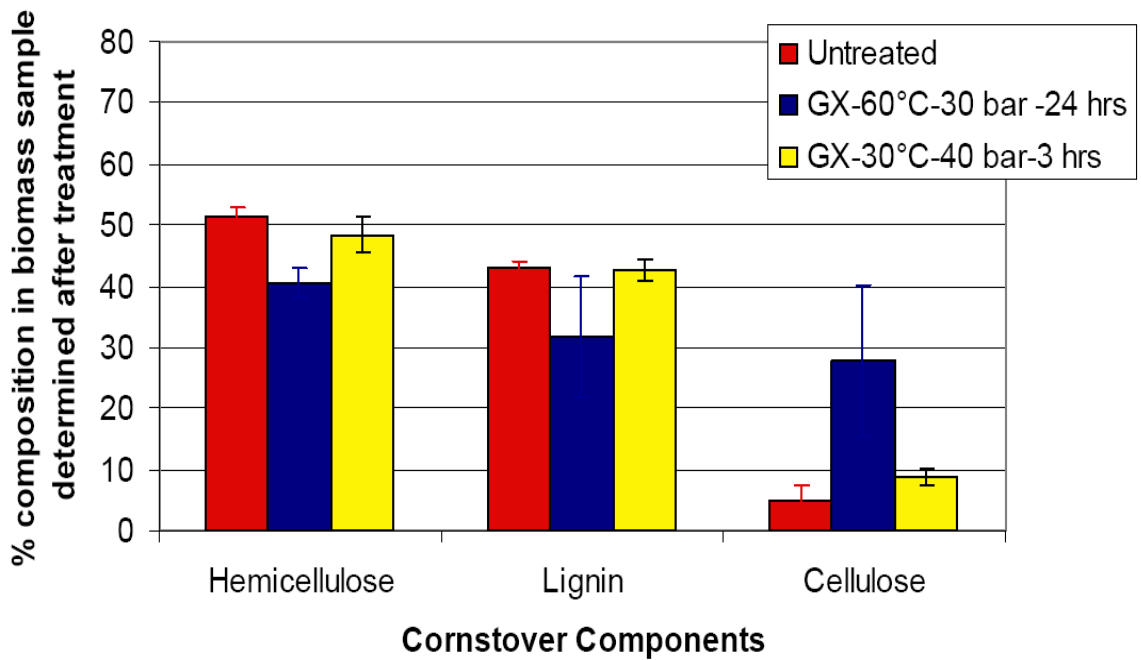


Figure E.6: Solid corn stover composition after no treatment, treatment with GX-MeOH (60 °C, 30 bar, 24 hours), and treatment with GX-MeOH (30 °C, 40 bar, 3 hours).

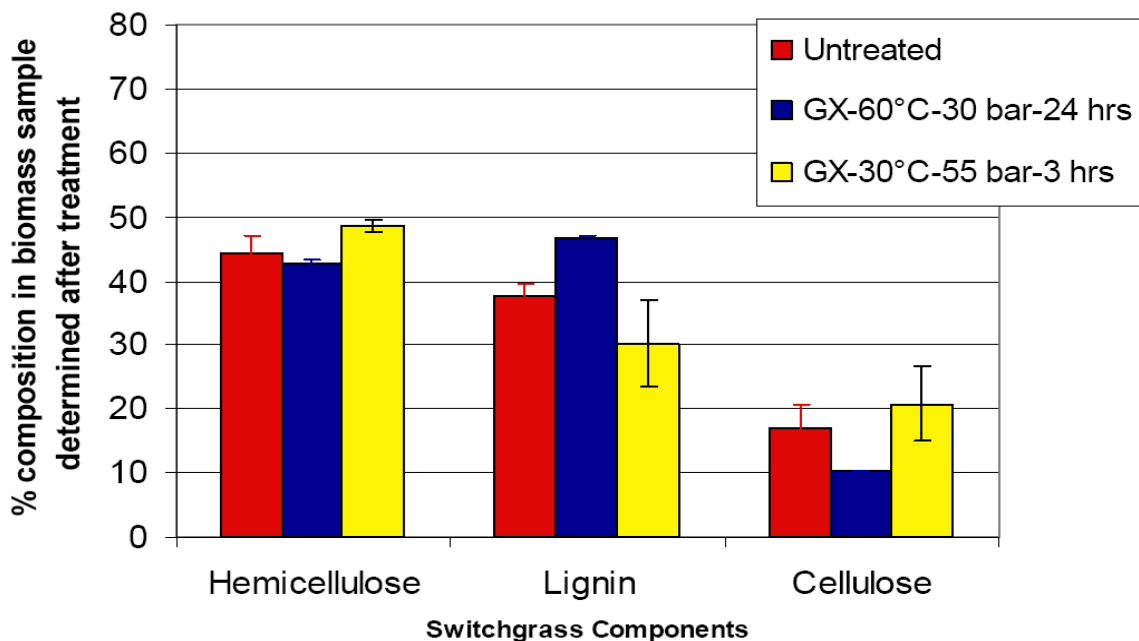


Figure E.7: Solid switchgrass composition after no treatment, treatment with GX-MeOH (60 °C, 30 bar, 24 hours), and treatment with GX-MeOH (30 °C, 40 bar, 3 hours).

A closer examination reveals a few reasons why these discrepancies occurred. The extractive percentages, which are not depicted in the above graphs, are vastly different from the literature values. A comparison of these numbers is shown in Table E.3: Comparison of extractive composition as reported in literature and compared to chemical analysis completed in lab for three different treatments. Table E.3. This is probably due to the procedure detailed in Yang et al.<sup>13</sup> Their reflux time of 3 hours is significantly shorter than most common analytical methods (NREL and TAPPI). For a more accurate comparison to other data, future analytical work done in our lab should follow the longer reflux times commonly used by others. Additionally, the literature values are for extractives and minor components, so the minor components might not have been extracted during the Soxhlet procedure.

The vast differences between our compositions and the literature values, however, most likely occurred because the chemical analysis is less rigorous than the multi-step processes outlined by NREL. Biomass is a highly complicated feedstock, and the use of HPLC methods and UV detection make the NREL methods more likely accurate than merely determining weight loss from different reactions. While the different chemical steps used by Yang et al. do provide a rough estimation, it is doubtful that these results can be taken as absolute fact.

Table E.3: Comparison of extractive composition as reported in literature and compared to chemical analysis completed in lab for three different treatments.

<b>Feedstock</b>	<b>Literature</b>	<b>No Treatment</b>	<b>GX-MeOH (60 °C, 30 bar, 24 h)</b>	<b>GX-MeOH (30 °C, 40 bar, 3 h)</b>
Corn stover	22.5	0.38	0.04	0.37
Pine wood	15.4	0.46	0.03	0.61
Switchgrass	31	0.39	0.04	0.32

Although the compositions determined by chemical analysis are greatly different compared to those reported in literature, the results are fairly consistent between our pretreatment methods. The fact that GX-MeOH provides similar results to MeOH alone suggests that methylcarbonic acid is not acidic enough to promote acid-catalyzed hydrolysis of the biopolymers. Additionally, our results show that the higher CO<sub>2</sub> pressures had no effect, suggesting that either the lignocellulosic matrix is already being penetrated, or even these moderate CO<sub>2</sub> pressures are not enough to allow penetration.

## CONCLUSIONS AND RECOMMENDATIONS

This appendix examined the use of GX-MeOH as a process to not only remove extractives from lignocellulosic biomass, but also to hydrolyze the biopolymers via the in-situ acid methylcarbonic acid. Three types of biomass (wood chips, corn stover, and switchgrass) were treated with only MeOH, and with GX-MeOH, to determine the value of adding CO<sub>2</sub>. The pretreatment results suggest that GX-MeOH is not a viable lignocellulosic biomass pretreatment option. Overall, only 10% of the total mass was removed by pretreatment, which is significantly less than other pretreatments detailed in Chapter II. Additionally, the differences between MeOH and GX-MeOH were minimal. Thus we can conclude that GX-MeOH does not create a strong enough acid to be useful in biomass pretreatment. It is also important to note that using a pressurized pretreatment system can significantly increase the cost of the process. The benefits of a GXL would need to outweigh the difference in MOC costs.

Many extractives were recovered from the biomass when treated with both MeOH and GX-MeOH. Although the total amount did not change much, the percentages of certain extractives differed depending on whether MeOH or GX-MeOH was used. If any known extractives were targeted, it could be possible to tune the properties of the GX-MeOH to remove preferentially that targeted compound. More detailed studies would need to be run in order to definitively determine whether or not GX-MeOH could be a useful extraction method. The high cost of adding another processing step, however, probably prohibits the use of GX-MeOH in industry.

This project also revealed that the methods used by NREL and TAPPI should be the ones followed by our lab for all future projects. This is true for two reasons. One motivation is that the more facile chemical analysis method outlined by Yang et al. was not accurate enough for us to determine for certain whether GX-MeOH was an effective biomass pretreatment options. The second motive for switching to the NREL and TAPPI methods is that our results can be better compared to other published results, which also tend to use these methods. For these reasons, NREL methods were used for all studies detailed in Chapter 2.

## REFERENCES

1. A. Kordikowski, A. P. Schenk, R. M. Van Nielen and C. J. Peters, *The Journal of Supercritical Fluids*, 1995, **8**, 205-216.
2. C. J. Chang, *Journal of Chemical Engineering Japan*, 1992, **25**, 164-169.
3. J. C. de la Fuente Badilla, C. J. Peters and J. de Swaan Arons, *The Journal of Supercritical Fluids*, 2000, **17**, 13-23.
4. E. M. Hill, J. M. Broering, J. P. Hallett, A. S. Bommarius, C. L. Liotta and C. A. Eckert, *Green Chemistry*, 2007, **9**, 888-893.
5. J. W. Ford, J. Lu, C. L. Liotta and C. A. Eckert, *Ind. Eng. Chem. Res.*, 2008, **47**, 632-637.
6. J. Lu, J. Lazzaroni, J. P. Hallett, A. S. Bommarius, C. L. Liotta and C. A. Eckert, *Industrial & Engineering Chemistry Research*, 2004, **43**, 1586-1590.
7. R. R. Weikel, J. P. Hallett, C. L. Liotta and C. A. Eckert, *Topics in Catalysis*, 2006, **37**, 75-80.
8. C. Schuerch, *Journal of the American Chemical Society*, 1952, **74**, 5061-5067.
9. C. Eckert, C. Liotta, A. Ragauskas, J. Hallett, C. Kitchens, E. Hill and L. Draucker, *Green Chemistry*, 2007, **9**, 545-548.
10. M. Wei, G. T. Musie, D. H. Busch and B. Subramaniam, *Green Chemistry*, 2004, **6**, 387-393.
11. S.-F. Chen, R. A. Mowery, C. J. Scarlata and C. K. Chambliss, *J. Agric. Food Chem.*, 2007, **55**, 5912-5918.

12. K. Thammasouk, D. Tandjo and M. H. Penner, *Journal of Agricultural and Food Chemistry*, 1997, **45**, 437-443.
13. H. Yang, R. Yan, H. Chen, C. Zheng, D. H. Lee and D. T. Liang, *Energy Fuels*, 2006, **20**, 388-393.
14. P. Gallezot, *Green Chemistry*, 2007, **9**, 295-302.
15. O. Falk and R. Meyer-Pittroff, *European Journal of Lipid Science and Technology*, 2004, **106**, 837-843.
16. J. M. Marchetti, V. U. Miguel and A. F. Errazu, *Fuel*, 2007, **86**, 906-910.
17. S. Ledakowicz, M. Michniewicz, A. Jagiella, J. Stufka-Olczyk and M. Martynelis, *Water Research*, 2006, **40**, 3439-3446.
18. L. Draucker, in *School of Chemical and Biomolecular Engineering*, Georgia Institute of Technology, Atlanta, 2007.
19. N. Mosier, C. Wyman, B. Dale, R. Elander, Y. Y. Lee, M. Holtzapple and M. Ladisch, *Bioresource Technology*, 2005, **96**, 673-686.



## **APPENDIX F: ACID-CATALYZED BIODIESEL PRODUCTION USING GAS-EXPANDED LIQUIDS**

### **INTRODUCTION**

Ethanol is only one of many biofuels being studied extensively as an alternative transportation fuel. One of the other most popular options is biodiesel, which is made from the transesterification of fatty acid esters from oils with an alcohol (usually methanol or ethanol). Biodiesel has many properties similar to standard diesel fuel, making it an attractive option. Although it can technically be made from waste oil, such as used cooking oil, there are a number of complications associated with using feedstock that is not pure. The biggest challenge is the presence of free fatty acids, which interfere with the traditional base-catalysis process of making biodiesel. The acid-catalyzed route can accommodate free fatty acids, but the required neutralization adds significant cost.

This appendix examines the possibility of using methylcarbonic acid, the in-situ acid formed in CO<sub>2</sub>-expanded methanol. Gas-expanded methanol (GX-MeOH) is an attractive solvent for this process because one of the transesterification reactants (MeOH) is also the solvent. Additionally, the downstream neutralization is facile because it just requires depressurization of the CO<sub>2</sub>.

## BACKGROUND

Obtaining alternate fuel sources has been a major research drive during the past decade. One of the most popular alternative fuels is biodiesel, the common name associated with a number of fatty acid esters. These fatty acid esters are usually achieved by the transesterification of triglycerides with a monobasic alcohol, most commonly either methanol or ethanol. The formation of glycerol, from the glyceride backbone, is the major byproduct of the reaction.<sup>1</sup> The transesterification can be accomplished through two chemical catalysis methods: base and acid. There is also an enzymatic pathway, although it is not currently considered an industrially-feasible process.<sup>2</sup>

Base-catalyzed transesterification is the current preferred industrial method for the production of biodiesel for multiple reasons.<sup>1</sup> First of all, the wide availability and low cost of both KOH and NaOH, the two bases most commonly utilized, make it an attractive process. Additionally, the reaction time is much faster than the other two methods. Some sources have suggested that the base-catalyzed transesterification occurs at a rate up to 4000 times faster than its acid counterpart. The reaction also occurs under mild conditions: with 1% base, nearly complete biodiesel was produced in 30 minutes from sunflower oil at 25 °C and ambient temperature.<sup>3</sup> Despite these advantages, the process of alkali-catalyzed transesterification of triglycerides does have several drawbacks which economically limit the production of biodiesel. Its major limitation is the feedstock must be of sufficient quality to contain less than 0.5 wt % free-fatty acids (FFAs), which translates to a high cost of starting material. FFA concentration must be

minimized because the presence of FFAs leads to the soap formation, resulting not only in a higher viscosity for the biodiesel product, but also giving it a tendency to form gels.<sup>4</sup>

The high-quality oil required as feedstock for the alkali-catalyzed transesterification is currently the limiting economic factor in biodiesel production. The ability to use lower grade feedstock would have a profound favorable effect on the economics of biodiesel processing, bringing it closer in cost to the production of petroleum diesel.<sup>5</sup> Due to the stringent requirements of the starting material for the base-catalyzed process, it is unlikely that low grade oil will be a reasonable option in the foreseeable future. The acid-catalyzed process, however, has no such restrictions on the FFA concentration of the feedstock because the both the esterification and transesterification reactions are completed. This means the adoption of an acid-catalyzed process in industry would allow for a low grade oil feedstock.

There have been a variety of groups who have tried to utilize the advantages of both acid and alkali-catalyzed reactions by doing an acid-catalyzed pretreatment to remove the FFAs, then running the product through the base-catalyzed transesterification.<sup>6, 7</sup> This approach has had success, but multiple-stage processes rarely match the economic advantage of a single-stage method. With this in mind, and since the acid-catalyzed transesterification method can tolerate sub-par, inexpensive feedstock, much effort has gone into understanding the process and improving reaction rates.

Various approaches have been taken to try to improve the transesterification rates. The substitution of heavier alcohols, such as butanol, increases the solubility of oil in the alcohol, reducing mass-transfer limitations and thus increasing the reaction rate. Multiple catalysts have been tried, including HCl, H<sub>2</sub>SO<sub>4</sub>, and Lewis acids.<sup>3</sup> While each catalyst

was successful, no current acid-catalyst is able to compare to the alkali-catalyzed rates. Some other work has focused on utilizing supercritical methanol, a process that is “catalyst-free.”<sup>8</sup> The high temperature and pressure requirements of supercritical methanol (350 °C and 45 MPa) are a deterrent, but the concept provides a framework for other possible techniques.

The basis behind using supercritical methanol is that certain properties such as viscosity, dielectric constant, specific gravity, and polarity can be influenced by changing the reactor pressure and temperature. Supercritical fluids have excellent transport properties, but limited solubility of substrates. Another tunable approach to process design is the use of gas-expanded liquids (GXLs), which have nearly as outstanding transport properties, with better solubility, than supercritical fluids. By manipulating the solvent properties, in this case methanol, it is often possible to improve reaction rates. For this application, it was decided to add CO<sub>2</sub> to methanol, creating methylcarbonic acid, and thus use the solvent as the catalyst. Methanol was chosen due to its abundance, inexpensive cost, and low volatility. Not only is methanol the most common alcohol used in the current biodiesel industry, but also methyl carbonic acid is the strongest acid made from the addition of CO<sub>2</sub> to a monobasic alcohol.

This project focused on the effects various pressures of CO<sub>2</sub> had on the transesterification rate. As triglycerides are expensive and difficult to purify, a model system was designed using vinyl palmitate as the substrate. The goal was to establish the conversion of vinyl palmitate to methyl palmitate under various experimental conditions. The reaction rates using gas-expanded methanol (GX-MeOH) were compared to those using neat methanol.

## **EXPERIMENTAL**

### **Materials**

Methanol (anhydrous, 99.8%) was purchased from Sigma-Aldrich, but the rubber septa was removed prior to the beginning of this project. Vinyl palmitate, or palmitic acid vinyl ester (stabilized with MEHQ), was purchased from TGI Chemicals. Ethyl palmitate ( $\geq 99\%$ ) was purchased from Sigma-Aldrich. Carbon dioxide gas (SFC grade, 99.99%) was purchased from Air Gas. For analytical purposes, acetonitrile (ReagentPlus, 99%) and deuterated chloroform (99.8 atom % d) were respectively purchased from Sigma-Aldrich and Aldrich. Except where mentioned, all chemicals were used as received.

### **Methods**

Vinyl palmitate was weighed and placed in a saturator reactor. The appropriate molar ratio of methanol was added to the reactor (see Table F.1) along with a stir bar. The saturator was sealed using a nitrile rubber o-ring and placed on a stir plate set at 400 rpm. A heating jacket run by a temperature controller was used to bring the saturator up to reaction temperature, and then control it for the duration of the experiment. For experiments that used CO<sub>2</sub>, the gas was added by an Isco pump (set at constant pressure) after the saturator had reached the appropriate experimental temperature. Once the saturator reached temperature, experimental time began. After leaving the reactor running for the appropriate amount of the time, the heating jacket was turned off and the entire apparatus was left to cool for 45 minutes. The reactor contents were then transferred to a vial. Upon settling, the fluid in the vial was biphasic in nature.

For the  $^1\text{H}$  NMR analysis, a small sample was taken from the bottom phase and added to deuterated chloroform ( $\text{CDCl}_3$ ). Before analysis via GC-MS, 5 mL of acetonitrile and 1 mL rinse acetone were added to the vial, making the mixture homogeneous and allowing the reaction to be analyzed accurately. A small sample from the vial was dissolved in rinse acetone and run through the GC-MS. The resulting peaks were compared to standards of known concentration of the starting material, vinyl palmitate. Error calculations were done by assessing the results of experiments done either in duplicate or triplicate.

Table F.1: Reaction conditions for each set of experiments.

Ratio Methanol to Vinyl Palmitate (Molar)	Temperature ( $^{\circ}\text{C}$ )	Time (h)	$\text{CO}_2$ Pressure (psi)	Agitation (rpm)	Reactor
20:1	250	24	0	None	Ti Tube
15:1	75	48	0, 200, 1000	400	Saturator
15:1	75	4	0, 200, 500	400	Saturator
30:1	75	4	0, 200	400	Saturator
15:1	40	24	0, 200	400	Saturator

## RESULTS AND DISCUSSION

Several experimental factors needed to be taken into consideration when designing this experiment. Different variable conditions include starting ratio of methanol to oil, temperature, reaction time, agitation speed, and pressure. While higher ratios of methanol to oil are known to increase conversion, as well as higher reaction temperatures, it is not economically favorable to use these conditions. According to the academic research, most methanolysis reactions are run at about  $75\text{ }^{\circ}\text{C}$  and with methanol

to oil ratios ranging from 6:1 to 250:1.<sup>3, 4</sup> For the pressure experiments, an initial methanol to vinyl palmitate molar ratio of 15:1 was chosen, as well as a 48 hour reaction duration time.

Before running the pressure experiments, initial tests were performed to ensure that the vinyl palmitate would undergo methanolysis in neat methanol. An extreme temperature of 250 °C was chosen, and the reaction allowed to run for 24 hours. In the GC-MS analysis, all starting material disappeared when the reaction occurred at 250 °C. The resulting product peak was assumed to be methyl palmitate due to its retention time and molecular weight. This product peak was used as the standard methyl palmitate peak for all subsequent GC-MS analysis of experimental runs. An analogous experiment involving the conversion of ethyl palmitate to methyl palmitate was also run with no conversion occurring in neat methanol, even at extreme temperatures.

The initial temperature chosen to study the effects of CO<sub>2</sub> on the methanolysis of vinyl palmitate was 75 °C. Reactions were allowed to run for 48 hours with no CO<sub>2</sub>, 200 psi CO<sub>2</sub>, and 1000 psi CO<sub>2</sub> added. As illustrated in Figure F.1, no conversion was detected at 1000 psi CO<sub>2</sub> and limited conversion at 500 psi CO<sub>2</sub>. From these results, it seems the addition of CO<sub>2</sub> does not improve the conversion; conversely, it actually appears to hinder the desired reaction.

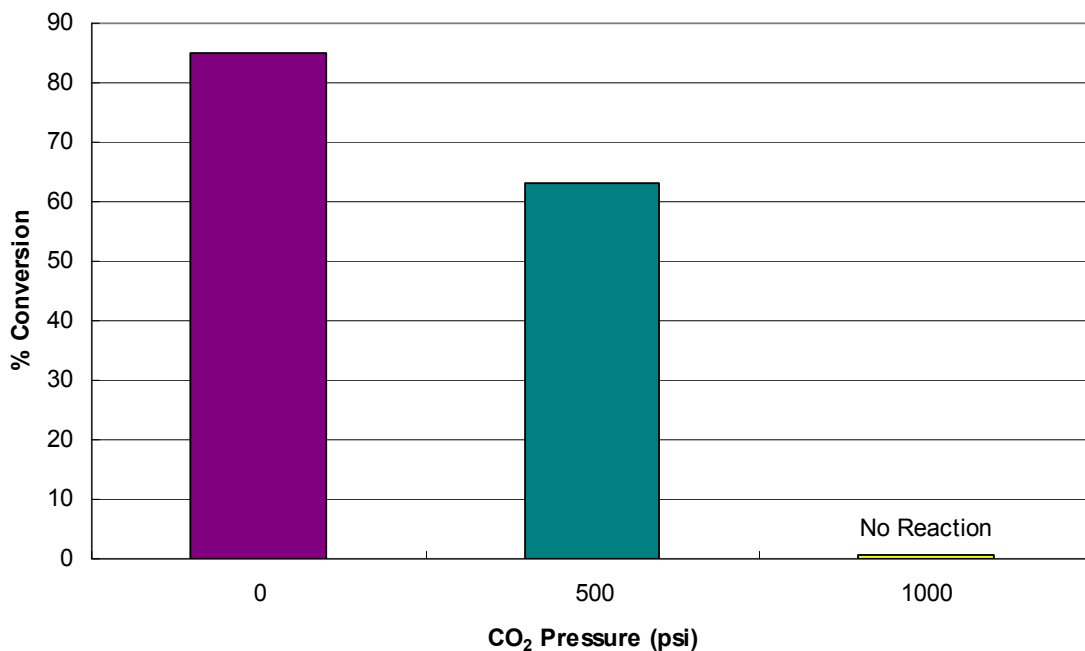


Figure F.1: Percent conversion of vinyl palmitate to methyl palmitate after 48 hours using differing amounts of CO<sub>2</sub> (75 °C, 15:1 molar ratio methanol to vinyl palmitate).

Previous research in our lab has suggested that the addition of CO<sub>2</sub> increases reaction rates by the optimization of two competing effects. One is the driving effect of high CO<sub>2</sub> concentrations on the equilibrium, causing more acid formation. The increased CO<sub>2</sub> concentration, however, will also lower the polarity of the solvent.<sup>9</sup> In several instances, a total pressure of 200 psi CO<sub>2</sub> was observed as the best pressure to optimize the counteracting influences of the driving effect and decreased solvent polarity. The experiments were repeated over a shorter duration (4 hours) in neat methanol (no CO<sub>2</sub>, as well as GX-MeOH with both 200 and 500 psi CO<sub>2</sub> added. The results depicted in Figure F.2 show that even moderate pressures of CO<sub>2</sub> hinder the methanolysis of vinyl palmitate.



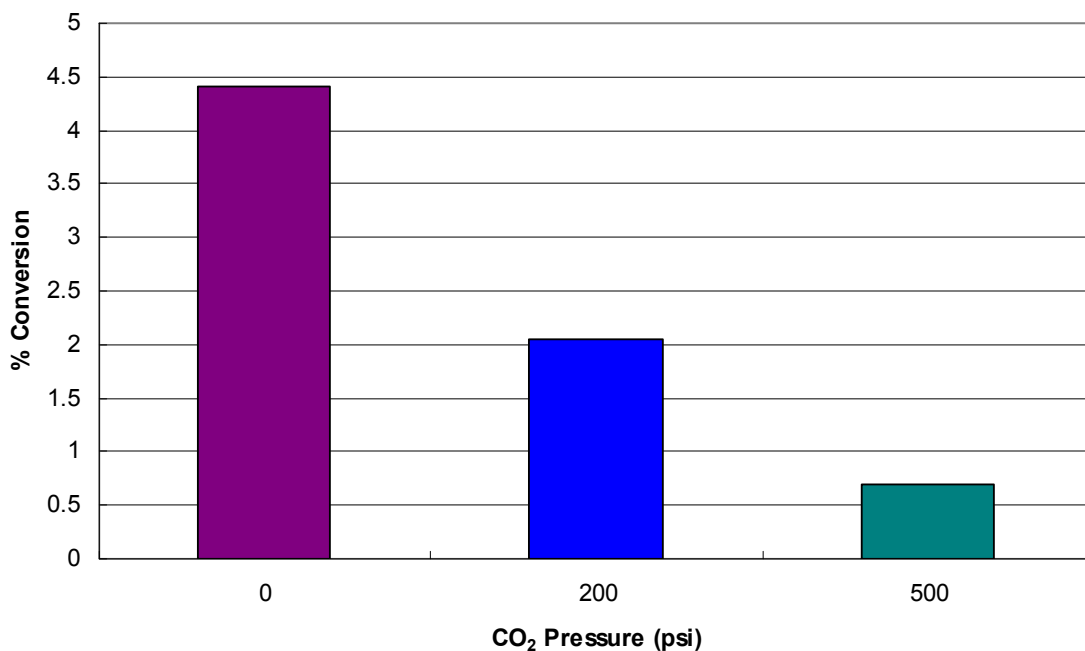


Figure F.2: Percent conversion of vinyl palmitate to methyl palmitate after 4 hours using differing amounts of CO<sub>2</sub> (75 °C, 15:1 molar ratio methanol to vinyl palmitate).

The results of these experiments strongly suggest that any moderate addition of CO<sub>2</sub> at 75 °C with a 15:1 molar ratio of reactants limits the transesterification reaction. As there are several experimental variables that can be altered, the next few sets of experiments focused on trying different reaction conditions. Reactions were run at different temperatures (40 °C) and molar ratios (30:1 molar ratio methanol to vinyl palmitate). Agitation speeds were never varied because previous research suggests that agitation speed, when varied between 100-600 rpm, has little impact on biodiesel transesterification reactions.<sup>5</sup> Regardless of changes to experimental parameters (temperature, molar ratio, and time), every set of experiments showed the addition of CO<sub>2</sub> hinders the transesterification of vinyl palmitate to methyl palmitate.

## CONCLUSIONS AND RECOMMENDATIONS

The results from these experiments suggest that methylcarbonic acid has no additional effect on the transesterification rate of a triglyceride with MeOH. In fact, it seems that the addition of pressurized CO<sub>2</sub> is actually hindering the transesterification rate, possibly due to enhanced steric hinderance. The project was dropped after the experimental results were analyzed, and there is no path forward.

## REFERENCES

1. M. Di Serio, M. Ledda, M. Cozzolino, G. Minutillo, R. Tesser and E. Santacesaria, *Industrial & Engineering Chemistry Research*, 2006, **45**, 3009-3014.
2. National Biodiesel Board - [www.biodiesel.org](http://www.biodiesel.org) - [www.nbb.org](http://www.nbb.org), <http://www.biodiesel.org/>.
3. M. G. Kulkarni and A. K. Dalai, *Industrial & Engineering Chemistry Research*, 2006, **45**, 2901-2913.
4. E. Lotero, Y. J. Liu, D. E. Lopez, K. Suwannakarn, D. A. Bruce and J. G. Goodwin, *Industrial & Engineering Chemistry Research*, 2005, **44**, 5353-5363.
5. S. Zheng, M. Kates, M. A. Dube and D. D. McLean, *Biomass & Bioenergy*, 2006, **30**, 267-272.
6. Y. Wang, S. Y. Ou, P. Z. Liu and Z. S. Zhang, *Energy Conversion and Management*, 2007, **48**, 184-188.
7. M. Canakci and J. Van Gerpen, *Transactions of the Asae*, 2001, **44**, 1429-1436.
8. S. Saka, D. Kusdiana and E. Minami, *Journal of Scientific & Industrial Research*, 2006, **65**, 420-425.
9. R. R. Weikel, J. P. Hallett, C. L. Liotta and C. A. Eckert, *Topics in Catalysis*, 2006, **37**, 75-80.

## VITA

Michelle Kimberly Kassner was born on April 5, 1981 in Scottsdale, AZ to Diane and Rick Kassner. She graduated from Scottsdale's Saguaro High School in 1999 in the top one percent of her class. Michelle attended the University of Arizona in Tucson, where she graduated *magna cum laude* in 2003 after earning a B.S.E. in Chemical Engineering and a B.S. in Biochemistry (both With Honors). She began her graduate studies at Princeton University, and received a M.S.E. in Chemical Engineering in 2005 after completing research in the laboratory of Dr. David Wood. Michelle decided to pursue a Ph.D. in Chemical Engineering at the Georgia Institute of Technology under the guidance of Dr. Charles Eckert and Dr. Charles Liotta. After finishing her Ph.D. in December 2008, she is moving to Houston, TX to begin biofuels research with Chevron. She and her fiancé Jimmy Young will be married in May 2009.